

**ANALYSIS OF DYNAMIC STRESS PROPAGATION OF A VIBRATING SUBSEA
STRUCTURE IN A PRESSURIZED ENVIRONMENT**

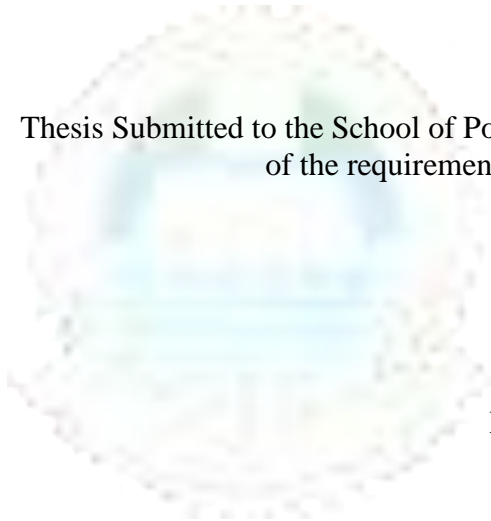
by

OGUNMOLA, Ogunbayo Yemisi

(MATRICULATION NUMBER: 890404031)

B.Sc. (Hons), M.Sc. Lagos

Thesis Submitted to the School of Postgraduate Studies, University of Lagos in partial fulfilment
of the requirements for the degree of Doctor of philosophy



UNIVERSITY
OF LAGOS

in

Engineering Mechanics

Department of Mechanical Engineering
Faculty of Engineering
University of Lagos, Nigeria
August, 2011

**SCHOOL OF POST-GRADUATE STUDIES
UNIVERSITY OF LAGOS, AKOKA, LAGOS
*CERTIFICATION***

This is to certify that the thesis

**“ANALYSIS OF DYNAMIC STRESS PROPAGATION OF A VIBRATING SUBSEA
STRUCTURE IN A PRESSURIZED ENVIRONMENT”**

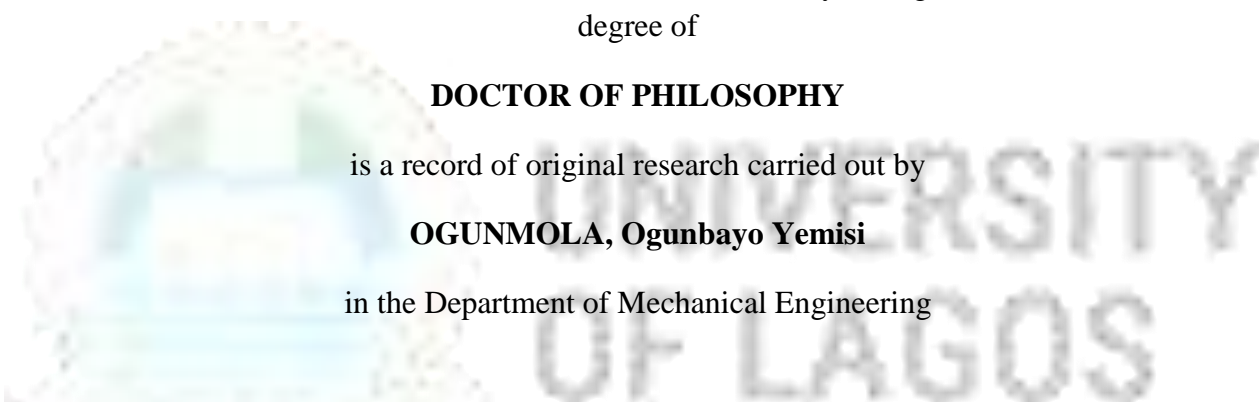
Submitted to the School of Post-Graduate Studies University of Lagos for the award of the
degree of

DOCTOR OF PHILOSOPHY

is a record of original research carried out by

OGUNMOLA, Ogunbayo Yemisi

in the Department of Mechanical Engineering



Author's Name	Signature	Date
First Supervisor's Name	Signature	Date
Second Supervisor's Name	Signature	Date
Third Supervisor's Name	Signature	Date
External Examiner's Name	Signature	Date
Internal Examiner's Name	Signature	Date

Internal Examiner's Name

Signature

Date

SPGS Representative

Signature

Date

DEDICATION

in
Loving Memory of my Late Father
(Pa Joseph Ogunmola Oguntobi)

and to my
Mother, Wife, Siblings and Teachers

and to
The Almighty God



UNIVERSITY
OF LAGOS

ABSTRACT

Offshore pipeline and flow line systems define a variety of subsea architectures associated with Floating Production Storage and Offloading units (FPSOs) or Floating Storage and Offloading units (FSOs) that are usually employed for oil and gas production in deep and ultra deep waters. The design of such transmission facilities, must satisfactorily account for various phenomena such as hydrodynamic wave loading, fluid transport velocity, operating pressure and temperature of the internal fluid as well as limitations imposed by the seabed subsoil layer geotechnical properties. In fact the transverse and longitudinal dynamic responses of these pipeline and flow line systems are strongly modulated by these effects. Subsea pipelines are on the high demand to function at high temperatures and pressures. The natural behavior of a pipeline is to relieve the attendant high axial stress in the pipe-wall by buckling. Such uncontrolled buckling can have serious implication on the integrity of a pipeline. Hence, the usual practice to date, in the industry is to restrain pipelines by trenching and burying, or relieving the stress with inline expansion spools. In this work, the effect of transverse and longitudinal vibrations on the dynamic stresses induced by the fluid flow was studied with special reference to onset of buckling or bursting of such pipes. For this purpose, an offshore pipeline was idealized as a fluid conveying elastic beam on an elastic foundation and the corresponding set of equations governing the transverse and longitudinal motion of the pipe were formulated. Particularly, by employing integral transforms, an analytic solution for the induced stresses was computed and simulated for design applications while comparison with corresponding formulae currently in use in the field was also carried out. Furthermore, the earlier work was extended to capture the effect of deliberate or natural sediment covering of pipe that occurs over a long period of time, by examining the dynamic stress propagation through a partially or fully buried offshore pipeline. For this problem a boundary valued partial differential equation for the fluid- structure- soil interaction mechanics was formulated. In particular, by employing operational methods, the burst and buckling pressure profiles as modulated by the seabed sediment layer history were reported for design analysis and applications. Lastly this research reported an analytic solution for the induced stresses in polar coordinates coupled with von Mises yield criterion in conjunction with the corresponding set of equations governing the transverse and longitudinal motions of an offshore pipeline on an elastic foundation. Interesting results were simulated for practical analysis and applications.

ACKNOWLEDGEMENT

Foremost, I am greatly thankful to God Almighty for His divine intervention and mercy throughout my academic pursuit. My tremendous gratitude goes to my supervisors, Distinguished Professor V.OS. Olunloyo NNOM, Dr. O. Damisa and Dr. C.A. Osheku for their exemplary, moral and intellectual commitment both in the problems formulation and analytical methodology. Besides, their efforts throughout the pursuit of this research are highly appreciated.

I give many thanks to Dr. A. Oyediran of AYT Corporation, USA for putting me through the rudiments of the problems formulation at the initial stage of this research.

My warmest regard to my loving wife, Toyin and our dearest daughter Kikelomo for their patience in my absence in their midst while this research lasted.

Also, my sincere appreciation goes to my mother, brothers and sisters for their prayers and moral supports throughout the period of this work.

The Dean, Professor M.A. Salau, of the faculty of Engineering, University of Lagos, is highly thanked for his invaluable support during the series of my seminars and words of encouragement.

I acknowledge the support of my Acting Head, Dr. J.S. Ajiboye for his moral and physical encouragement. The academic staff of Mechanical and Systems Engineering Departments are well acknowledged for standing by me in the course of this research.

My acknowledgement is not complete without mentioning those that we pursued research together under the same Professor at the same period, i.e. Engr. A.O. Adelaja, Engr. O.A. Alli and Engr. Mrs. S.I. Kuye. The encouragement and contribution of one another is highly commendable and appreciated.

Finally, I express my profound gratitude to the experts and earlier workers in the field of offshore engineering.

TABLE OF CONTENTS

	Pages
Title Page	i
Certification	ii
Dedication	iii
Abstract	iv
Acknowledgement	v
Table of Contents	vi
List of Figures	ix
List of Tables	xiv
Notations	xv
CHAPTER 1 INTRODUCTION	1
1.1 Brief introduction	1
1.2 Motivation for the present work	2
1.3 Establishment of background to the Study	3
1.4 Statement of Problem	4
1.5 Objective of Study	4
1.6 Scope and Limitation	5
1.6 Significance of the Study	5
1.7 Overview of Thesis	6
CHAPTER 2 LITERATURE REVIEW	7
2.1 Historical Development of Pipe Dynamics	7
2.2 Studies on Pipe Dynamic Stability	7
2.3 Non-Linear Vibrations of Pipe Conveying Fluid	10
2.4 Further Review Concerning the Pipelines with Internal Fluid Velocity	11
2.5 Pipeline Design	13
2.6 Pipe Buckling & Bursting	14
CHAPTER 3 ANALYSIS OF DYNAMIC STRESS PROPAGATION IN SUBSEA PIPELINE AND FLOW LINE SYSTEMS	16

3.1	Problem Fundamentals and Governing Differential Equation	16
3.2	Governing Differential Equations	17
3.3	Analysis of Transverse Vibration Problem	19
3.4	Analysis of Longitudinal Vibration Problem	21
3.5	Analysis of Dynamic Stress Propagation	25
3.5.1	Case 1: Maximum Bending Stress	25
3.5.2	Case 2: Maximum Shear Stress	26
3.5.3	Computation of Dynamic Stresses	26
3.6	Analysis of Burst Pressure Induced by Vibration	29
3.6.1	Computation of Burst Pressure for the Pipe under investigation	30
3.7	Computation of Buckling Pressure for the Pipe under investigation	31
3.8	Computation of Burst Equation with Barlow's Equation	31
3.9	Analysis and Discussion of Results	32
CHAPTER 4 THE EFFECT OF FLUID PIPELINE SOIL INTERACTION ON DYNAMIC STRESS PROPAGATION AT SEABED		53
4.1	Problem Fundamentals and Governing Differential Equation	53
4.2	Analysis of Transverse Vibration Problem	55
4.3	Analytic Solution for \bar{w} via Integral Transforms Method	56
4.4	Analysis of Longitudinal Vibration Problem	59
4.5	Computation of Burst Pressure	63
4.6	Computation of buckling pressure for the pipe	64
4.7	Discussion of Results	65
CHAPTER 5 CONCERNING DYNAMIC STRESS PROPAGATION IN AN OFFSHORE PIPELINE AT THE SEABED FOR DESIGN APPLICATION		76
5.1	Problem Fundamentals and Governing Differential Equation	76
5.2	Failure Analysis	77
5.3	Discussion of the Results	81
CHAPTER 6 CONCLUSION		85
6.1	Summary and Findings for Model Problems	85
6.2	Contributions to knowledge	86
6.3	Recommendations	86
REFERENCES		87
APPENDICES		94

APPENDIX A GENERALIZED GOVERNING DIFFERENTIAL EQUATION FOR MODEL PROBLEM CONCERNING DYNAMIC STRESSES OF SUBSEA PIPELINE	94
APPENDIX B GENERALIZED GOVERNING DIFFERENTIAL EQUATION FOR MODEL PROBLEM CONCERNING VIBRATION OF SUBSEA PIPELINE	98
B.1 Model formulation	98
B.2 Procedural analysis	100
APPENDIX C BURST PRESSURE FORMULATION IN CYLINDRICAL POLAR COORDINATES	108
APPENDIX D MATLAB PROGRAMS	113
D.1 Matlab Program for Pipe Sitting on the Seabed	113
D.2 Matlab Program for Pipe Partially/Fully Buried on the Seabed	136
D.3 Matlab Program for Pipe Sitting on the Seabed	150

LIST OF FIGURES

	Pages
Figure 1.0: Offshore field development components	2
Figure 3.0: A model of the elastic beam approximation with upper and lower layers	16
Figure 3.1a: The flow geometry of the dynamic interaction of pipeline on sea bed when γ is zero	17
Figure 3.1b: The flow geometry of the dynamic interaction of pipeline on seabed when γ is 0.02	17
Figure 3.2: Steady state burst pressure profile at the upper layer of the pipe on a soft sea bed for the case $n = 1; \bar{x} = 0.5; \bar{z} = 1; \bar{K}_b = 800$	36
Figure 3.3: Steady state burst pressure profile at the upper layer of the pipe on a hard sea bed for the case $n = 1; \bar{x} = 0.5; \bar{z} = 1; \bar{K}_b = 800$	36
Figure 3.4: Steady state burst pressure profile at the upper layer of the pipe on a soft sea bed for the case $n = 2; \bar{x} = 0.5; \bar{z} = 1; \bar{K}_b = 8$	37
Figure 3.5: Steady state burst pressure profile at the upper layer of the pipe on a hard sea bed for the case $n = 2; \bar{x} = 0.5; \bar{z} = 1; \bar{K}_b = 800$	37
Figure 3.6: Steady state burst pressure profile at the upper layer of the pipe on a soft sea bed for the case $n = 4; \bar{x} = 0.5; \bar{z} = 1; \bar{K}_b = 8$	38
Figure 3.7: Steady state burst pressure profile at the upper layer of the pipe on a hard sea bed for the case $n = 4; \bar{x} = 0.5; \bar{z} = 1; \bar{K}_b = 800$	38
Figure 3.8: Steady state burst pressure profile at the upper layer of the pipe on a soft sea bed for the case <i>normalized pipe thickness</i> = 0.1; $\bar{U} = 0.5; \bar{z} = 1; \bar{K}_b = 8$	39
Figure 3.9: Steady state burst pressure profile at the upper layer of the pipe on a soft sea bed for the case <i>normalized pipe thickness</i> = 0.1; $\bar{U} = 0.5; \bar{z} = 1; \bar{K}_b = 8$	39
Figure 3.10: Steady state burst pressure profile at the upper layer of the pipe on a hard sea bed for the <i>normalized pipe thickness</i> = 0.1; $\bar{U} = 0.5; \bar{z} = 1; \bar{K}_b = 800$	40
Figure.3.11: Steady state burst pressure profile at the upper layer of the pipe on a hard sea bed for the case <i>normalized pipe thickness</i> = 0.1; $\bar{U} = 0.5; \bar{z} = 1; \bar{K}_b = 800$	40
Figure 3.12: Steady state pressure profile at the upper layer of the pipe on a soft sea bed for the case	

- normalized pipe thickness* = 0.1; $n = 1$; $\bar{U} = 5$; $\bar{z} = 1$; $\bar{K}_b = 8$ 41
- Figure 3.13: Steady state pressure profile at the upper layer of the pipe on a hard sea bed for the case *normalized pipe thickness* = 0.1; $n = 1$; $\bar{U} = 5$; $\bar{z} = 1$; $\bar{K}_b = 800$ 41
- Figure 3.14: Steady state pressure profile at the upper layer of the pipe on a soft sea bed for the case *normalized pipe thickness* = 0.1; $n = 2$; $\bar{U} = 5$; $\bar{z} = 1$; $\bar{K}_b = 8$ 42
- Figure 3.15: Steady state pressure profile at the upper layer of the pipe on a hard sea bed for the case *normalized pipe thickness* = 0.1; $n = 2$; $\bar{U} = 5$; $\bar{z} = 1$; $\bar{K}_b = 800$ 42
- Figure 3.16: Steady state burst pressure profile at the lower layer of the pipe on a soft sea bed for the case *normalized pipe thickness* = 0.1; $\bar{x} = 0$; $n = 1$; $\bar{U} = 5$; $\bar{K}_b = 8$ 43
- Figure 3.17: Steady state burst pressure profile at the lower layer of the pipe on a hard sea bed for the case *normalized pipe thickness* = 0.1; $\bar{x} = 0$; $n = 1$; $\bar{U} = 5$; $\bar{K}_b = 800$ 43
- Figure 3.18: Steady state burst pressure profile at the upper layer of the pipe on a soft sea bed for the case *normalized pipe thickness* = 0.1; $\bar{x} = 0$; $n = 2$; $\bar{U} = 5$; $\bar{K}_b = 8$ 44
- Figure 3.19: Steady state burst pressure profile at the upper layer of the pipe on a soft sea bed for the case *normalized pipe thickness* = 0.1; $\bar{x} = 0$; $n = 2$; $\bar{U} = 5$; $\bar{K}_b = 8$ 44
- Figure 3.20: Steady state burst pressure profile at the upper layer of the pipe on a soft sea bed for the case *normalized pipe thickness* = 0.1; $\bar{x} = 0.5$; $n = 1$; $\bar{U} = 5$; $\bar{K}_b = 8$ 45
- Figure 3.21: Steady state burst pressure profile at the upper layer of the pipe on a hard sea bed for the case *normalized pipe thickness* = 0.1; $\bar{x} = 0.5$; $n = 1$; $\bar{U} = 5$; $\bar{K}_b = 800$ 45
- Figure 3.22: Steady state burst pressure profile at the upper layer of the pipe on a soft sea bed for the case *normalized pipe thickness* = 0.1; $\bar{x} = 0.5$; $n = 2$; $\bar{U} = 5$; $\bar{K}_b = 8$ 46
- Figure 3.23: Steady state burst pressure profile at the upper layer of the pipe on a hard sea bed for the case *normalized pipe thickness* = 0.1; $\bar{x} = 0.5$; $n = 2$; $\bar{U} = 5$; $\bar{K}_b = 800$ 46
- Figure 3.24: Ratio of steady state burst/buckling pressure profile at the upper layer of the pipe on a hard sea bed for the case $\bar{x} = 0$; $\bar{z} = 1$; $\bar{K}_b = 800$ 47
- Figure 3.25: Ratio of steady state burst/buckling pressure profile at the upper layer of the pipe on a soft sea bed for the case $\bar{x} = 0$; $\bar{z} = 1$; $\bar{K}_b = 8$ 47
- Figure 3.26: Steady state burst pressure profile at the upper layer of the pipe on a soft sea bed for the case $\bar{x} = 0.5$; $z = 1$, $L = 6km$, $\bar{U} = 0.5$; $\bar{K}_b = 8$ 48
- Figure 3.27: Steady state burst pressure profile at the upper layer of the pipe on a soft sea bed for the case $\bar{x} = 0.5$; $z = 1$, $L = 6m$, $\bar{U} = 0.5$; $\bar{K}_b = 8$ 48
- Figure 3.28: Steady state burst pressure profile at the upper layer of the pipe on a hard sea bed for

the case $\bar{x} = 0.5; z = 1, L = 6m, \bar{U} = 0.5; \bar{K}_b = 800$	49
Figure 3.29: Steady state burst pressure profile at the upper layer of the pipe on a soft sea bed for the case $\bar{x} = 0.5; z = 1, L = 6km, \bar{U} = 0.5; \bar{K}_b = 8$	49
Figure 3.30: Steady state burst pressure profile at the upper layer of the pipe on a hard sea bed for the case $\bar{x} = 0.5; z = 1, L = 6km, \bar{U} = 0.5; \bar{K}_b = 800$	50
Figure 3.31: Steady state burst pressure profile at the upper layer of the pipe on a soft sea bed for the case $\bar{x} = 0.5; z = 1, L = 6m, \bar{U} = 0.5; \bar{K}_b = 8$	50
Figure 3.32: Steady state burst pressure profile at the upper layer of the pipe on a hard sea bed for the case $\bar{x} = 0.5; z = 1, L = 6m, \bar{U} = 0.5; \bar{K}_b = 800$	51
Figure 3.33: Steady state burst pressure profile at the upper layer of the pipe on a soft sea bed for the case $\bar{x} = 0.5; z = 1, L = 6km, \bar{U} = 0.5; \bar{K}_b = 8$	51
Figure 3.34: Steady state burst pressure profile at the upper layer of the pipe on a hard sea bed for the case $\bar{x} = 0.5; z = 1, L = 6km, \bar{U} = 0.5; \bar{K}_b = 800$	52
Figure 4.0: The flow geometry of the dynamic interaction of a partially buried offshore pipeline.	54
Figure 4.1: Steady state burst pressure profile of the pipe on a hard sea bed for the case $n = 1; U = 5m/s; \bar{t} = 1; \bar{z} = 1; k_b = 800; \bar{\delta}_s = 0.5; L = 6m$	68
Figure 4.2: Steady state burst pressure profile of the pipe on a hard sea bed for the case $n = 1; U = 5m/s; \bar{t} = 1; \bar{z} = 1; k_b = 800; \bar{\delta}_s = 0.5; L = 60m$	68
Figure 4.3: Steady state buckling pressure profile of the pipe on a hard sea bed for the case $n = 1; U = 5m/s; \bar{t} = 1; \bar{z} = 1; k_b = 800; \bar{\delta}_s = 0.5; L = 6m$	69
Figure 4.4: Steady state buckling pressure profile of the pipe on a hard sea bed for the case $n = 1; U = 5m/s; \bar{t} = 1; \bar{z} = 1; k_b = 800; \bar{\delta}_s = 0.5; L = 60m$	69
Figure 4.5: Steady state burst pressure profile of the pipe on a hard sea bed for the case $n = 1; U = 5m/s; \bar{t} = 1; \bar{z} = 1; k_b = 800; \bar{\delta}_s = 0.5; L = 6m$	70
Figure 4.6: Steady state burst pressure profile of the pipe on a hard sea bed for the case $n = 1; \bar{t} = 1; \bar{z} = 1; k_b = 800; \bar{\delta}_s = 0.5; L = 6m$	70
Figure 4.7: Steady state burst pressure profile of the pipe on a hard sea bed for the case (orthogonal axis) $n = 1; \bar{t} = 1; \bar{z} = 1; k_b = 800; \bar{\delta}_s = 0.5; L = 6m$	71
Figure 4.8: Transient burst pressure response profile of the pipe on a hard sea bed for the case $n = 1; U = 5m/s; \bar{x} = 1; \bar{z} = 1; k_b = 800; \bar{\delta}_s = 0.5; L = 6m$	71

Figure 4. 9: Steady state burst pressure profile of the pipe on a hard sea bed for the case	
$n = 1; U = 5m/s; \bar{t} = 1; \bar{x} = 0.5; \bar{z} = 1; k_b = 800; L = 6m$	72
Figure 4.10: Steady state burst pressure profile of the pipe on a hard sea bed for the case	
$n = 1; U = 5m/s; \bar{t} = 1; \bar{x} = 0.5; \bar{z} = 1; k_b = 800; \bar{\delta}_s = 0.5; L = 6m$	72
Figure 4.11: Steady state burst pressure profile of the pipe on a hard sea bed for the case	
$n = 1; U = 5m/s; \bar{t} = 1; \bar{z} = 1; k_b = 800; \bar{\delta}_s = 0.5; L = 6m$	73
Figure 4.12: Steady state burst pressure profile of the pipe on a hard sea bed for the case	
$U = 5m/s; \bar{t} = 1; \bar{z} = 1; k_b = 800; \bar{\delta}_s = 0.5; L = 6m$	73
Figure 4.13: Steady state burst pressure profile of the pipe on a hard sea bed for the case	
$n = 1; U = 5m/s; \bar{t} = 1; \bar{z} = 1; k_b = 800; \bar{\delta}_s = 0.5; L = 6m$	74
Figure 4.14: Steady state burst pressure profile of the pipe on a hard sea bed for the case	
$n = 1; \bar{U} = 5; \bar{z} = 1; k_b = 800; \bar{\delta}_s = 0.5; L = 6m$	74
Figure 4.15: Steady state burst pressure profile of the pipe on a hard sea bed for the case	
$n = 1; \bar{U} = 5; \bar{z} = 1; k_b = 800; \bar{\delta}_s = 0.5; L = 6m$	75
Figure 5.0: The flow geometry of the model at the seabed	77
Figure 5.1: Burst pressure profile for the case	
$n = 1; \bar{U} = 5; \bar{x} = 1; k_b = 8000; L = 2km, h = 1500m$	82
Figure 5.2: Burst pressure profile with different modes for the case	
$\bar{U} = 5; \bar{x} = 1; k_b = 8000; \bar{\delta}_s = 0.5; L = 2km, h = 1500m$	82
Fig. 5.3: Burst pressure profile for the case	
$n = 1; \bar{U} = 5; k_b = 8000; \bar{\delta}_s = 0.5; L = 2km, h = 1500m$	83
Figure 5.4: Burst pressure profile for the against normalized pipe thickness	83
Figure 5.5: Burst pressure profile with different pipe thicknesses for the case	
$n = 1; \bar{U} = 5; \bar{x} = 1; k_b = 8000; \bar{\delta}_s = 0.5; L = 2km, h = 1500m$	84
Figure 5.6 Burst pressure profile with different flow velocities for the case	
$n = 1; k_b = 8000; \bar{x} = 0.5; L = 2km, h = 1500m$	84
Figure A1a: Pre-deformed free body diagram	94
Figure A1b: Free body diagram of the elastic beam approximation with upper and lower layers	94
Figure B1: Fluid and pipe elements model diagram	98
Figure B2: Right angle triangle for the Strain	101
Figure C1: Stress Components on a sector-shaped element ABCD of an axisymmetric pipe	108

LIST OF TABLES

	pages
Table 3.1: Parametric Values Used For Simulation	35
Table 4.1: Parametric Values Used For Simulation	67



UNIVERSITY
OF LAGOS

NOTATION

A pipe cross sectional area after deformation

A_o original cross sectional area of pipe

A_p surface area of pipe

A' change in the surface area of the pipe

C_1 damping force per unit velocity in the transverse direction

C_2 damping force per unit velocity in the axial direction

C_D hydrodynamic drag coefficient

E Young modulus of elasticity

$F_1(t)$ external force in the transverse direction

$F_2(t)$ external force in the longitudinal direction

g acceleration due to gravity

h depth of pipe below sea level

I moment of inertia

k_b stiffness of the sea bed

L length of pipe

m sum of the masses of pipe and fluid

m_f	mass of flowing fluid in side the pipe
m_w	mass of sea water displaced by pipe
M	sum of masses of pipe, fluid in pipe and external water displaced by pipe
pA	pressurization effect
P_h	hydrodynamic effect of the ocean
p_o	pressure at entry
T_o	tension in pipe
t	time
u	longitudinal displacement
U	velocity of fluid flowing inside pipe
U'	differential of velocity with respect to x
\dot{U}	differential of fluid velocity with respect to time
\tilde{u}	longitudinal response in Laplace plane
u^F	longitudinal response in Fourier plane
\tilde{u}^F	longitudinal response in Fourier-Laplace plane
w	transverse displacement
\tilde{w}	transverse response in Laplace plane
w^F	transverse response in Fourier plane
\tilde{w}^F	transverse response in Fourier-Laplace plane
x	axial displacement coordinate
z	transverse displacement coordinate

r_i internal radius of pipe

r_o external radius of pipe

B_r = the body force in the r direction

\bar{a}_r = the acceleration in the r direction

Greek letters

α coefficient of thermal expansivity

γ coefficient of area deformation

$\Delta\Theta$ temperature change from inlet to outlet

Δp pressure change from inlet to outlet

Θ temperature of the flowing fluid

Θ' temperature gradient

μ coefficient of sliding friction

∇^2 Laplacian operator

∇ gradient operator

ρ_w density of water

Φ velocity potential

σ_y transverse bending stress

σ_x axial bending stress

σ_r radial bending stress

σ_θ Hoop stress

$\tau_{\theta r}, \tau_{r\theta}$ radial shear stresses

$\tau_{(xz)1}$, shear stress on the upper layer

$\tau_{(xz)2}$, shear stress on the lower layer

δ_s sediment layer

CHAPTER 1

INTRODUCTION

1.1 Brief Introduction

Producing oil and gas from offshore and deepwater by means of pipeline has gained a tremendous momentum in the energy industry in the past few decades. Presently, the pipeline technology has been successfully used in areas with water depths greater than 1500 m.

The first pipeline was built in the United States in 1859 to transport crude oil, Wolbert (1952). For the one-and a half century of pipeline operating practice, it was reported by Boyun et al (2005) that the petroleum industry has proven that pipelines are by far the most economical means of large scale overland transportation for crude oil, natural gas and their products, clearly superior to rail and truck transportation over competing routes, given large quantities to be moved on a regular basis.

Transporting petroleum fluids with pipelines is a continuous and reliable operation. Thus pipelines have demonstrated an ability to adapt to a wide variety of environments including remote areas and hostile environments.

Man's inexorable demand for petroleum products intensified the search for oil in the offshore regions of the world as early as 1897, when the offshore oil exploration and production started from the Summerland, California, Leffler et al (2003). The first offshore pipeline was built in the Summerland, just southeast of Santa Barbara. Since then, the offshore pipeline has become the unique means of efficiently transporting offshore fluids, i.e., oil, gas and water.

Offshore pipelines can be classified as follows:

- Flowlines transporting oil and gas from satellite subsea wells to subsea manifolds;
- Flowlines oil and gas from subsea, manifolds to production facility platforms;

- Infield flowlines transporting oil and gas between production facility platforms;
- Export pipelines transporting oil and gas from production facility platforms to shore; and
- Flowlines transporting water or chemicals from production facility platforms, through subsea injection manifolds, to injection wellheads.

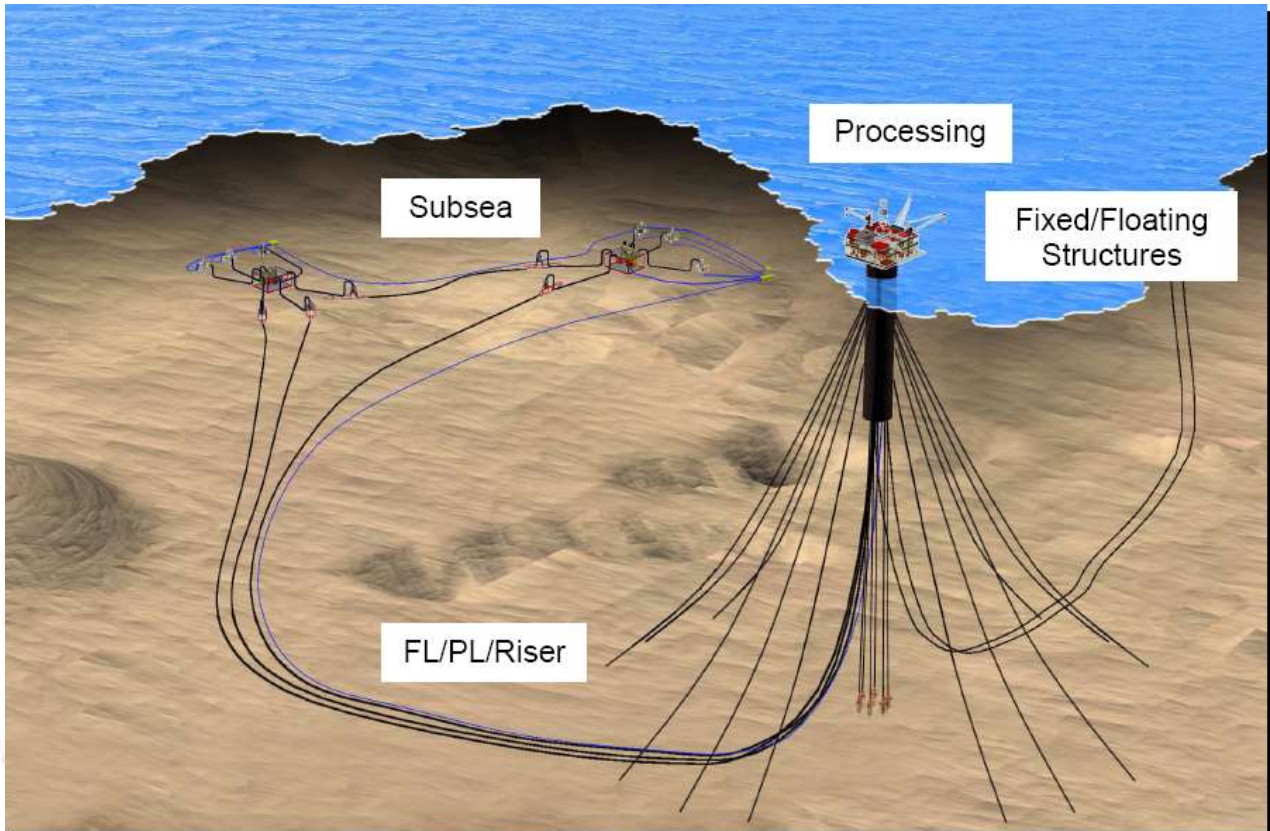


Figure 1.0 Offshore Field Development Components

Source :Jaeyoung Lee, P.E. “ Introduction to Offshore pipelines and Risers”; Houston, Texas; (2008) p10

1.2 Motivation for the present work

Pipelines affect daily lives in most of the world. As such, modern people’s lives are dependent on an environment in which energy plays a vital significance. Oil and gas are major factors in the supply of energy, thus pipelines are the primary modes of their transportation. Also, it is pertinent to know that an extensive pipeline network goes hand-in-hand with a high standard of living and technological progress.

Furthermore, oil and gas are important to generation of electrical power worldwide. The electricity/oil and gas directly are employed domestically for heating the houses, cooking meals

and for living comfortably. Petrochemical processes equally use oil and gas to make useful products.

In order to meet the oil and gas demand for the aforementioned, pipelines are employed to transport the supply from their source. These facilities are normally buried and function without creating nuisance to the human comfort. They transport large volumes of natural gas, crude oil and other products in continuous streams. It is therefore necessary to safeguard the pipelines and ensure minimal damage to the offshore facilities at all time.

1.3 Background to the Study

The problem of meeting energy demands globally in the present dispensation has necessitated challenges of looking inward for new fossil deposits hence, the need for new technology in the quest for oil and gas prospecting. In respect of fossil deposits, this has intensified interests and activities of oil and gas exploration companies for offshore hydrocarbon deposits even though, such offshore prospecting in deep waters, has its challenges as there are additional problems to contend with especially the hazards attributed to environmental forces such as, currents, winds, waves, etc., to which the engineering structures are now exposed, Olunloyo et al (2007).

In the last few years, the price of crude oil has been on the increase, as a result of high demand for energy consumption worldwide, though of recent, the price has been fluctuating due to financial crisis in the economy of the super nation (USA) that controls the international market forces. In Nigeria, prospecting and oil exploration in the Niger-Delta region has become a big challenge as on-shore exploration in this area is fraught with security problems including sabotage, vandalism and social unrest. The losses presently to the country are very tremendous.

The Niger-Delta region of Nigeria is one area where the discovery of offshore hydrocarbon deposits has intensified the awareness and activities of oil prospecting companies in areas such as the Bonga oil field etc. Besides, the risk of deep sea oil spillage is real especially, in the process of its conveyance from the seabed to the Production Storage facilities; such consideration is particularly important in the regions that have been geologically active.

Furthermore, exploited hydrocarbon resources from under the seabed are transported via transmission pipelines from the oil fields production storage facilities, the hydrodynamic forces

to which these pipelines are subjected and their overall effects on the longevity of these pipelines is an area that is yet to be fully explored. Hence, the lifespan of such pipelines depends on various factors namely, the characteristics of the pipeline materials, water depth, ground motion and seabed integrity in relation to geological and geo-mechanical properties etc, Osheku (2005).

Suffice to mention, oil spills are detrimental environmentally to both terrestrial and aquatic lives which happen via pipeline rupture. Notwithstanding, such transmission pipelines vibrate transversely and longitudinally due to the conveyance of fluid through the pipe, thus subjecting such piping to stress distributions.

1.4 Statement of Problem

There are millions of kilometres of transmission pipelines around the world. In Nigeria alone, the oil and gas transmission system is over several kilometres in length. These pipes conveying fluids are generally under the influence of both natural vibration and pipe deformation. Presently, the functional oil and gas pipelines are increasingly being subjected to high temperatures and pressures which occasionally lead to:

- Euler buckling (upheaval or lateral) when under constraint;
- Pipe walking i.e. pipe elongation in the axial direction, if unconstrained and
- Pipe burst due to material failure under constraint.

Most significantly, are the phenomena of pipe bursting and buckling that continue to receive special attention as they affect the integrity and reliability of conveyance networks.

To fully understand the study of the fluid conveying pipelines both in the offshore and onshore environments, the following factors are taken into cognizance viz:

- The flow velocity of oil/gas within pipeline
- Temperature and temperature gradient
- Oscillatory strain due to pipe vibration
- Geology characteristics of the seabed and
- Size of the pipeline.

1.5 Aim and Objective of Study

The aim is to model and investigate the problem of dynamic stress propagation of a subsea pipeline during the transportation of crude oil from one location to the other in exploration. The

issue of pipeline failure is a very significant interest with regard to the safety of oil facility, especially under the depth of sea. Thus, this research work attempts to develop a comprehensive and pro-active model to quantitatively and qualitatively address the problems of pipe bursting and buckling in an offshore environment. Hence, this research work presents a model of dynamic stress propagation of subsea pipeline which will be of practicable design analysis to take care of the pipeline integrity and ensuring its lifespan. This model differs from the existing ones by the incorporation of dynamic vibration in this analysis.

The objectives of this research work are:

- To establish the generalised governing differential equations for the transverse and longitudinal vibrations of an offshore pipeline by using the modified version of Gorman et al approach;
- To formulate the dynamic stresses concerning the bursting and buckling of fluid conveyance pipeline in offshore environment based on some criteria ;
- To solve the equations obtained analytically by employing double-integral transforms approach and
- To do computer simulation of the model analysis with some parameters and validate it by comparing this model with existing conservative model in oil and gas industries.

1.6 Scope and Limitation of Study

The study is limited to:

- pipelines lying horizontally on seabed
- Newtonian fluids as applicable to crude oil and gas
- Traditional steel pipes without defects

1.7 Significance of the Study

Pipeline failure (either onshore or offshore) is always detrimental to human lives, properties and facilities. The attendant losses are often colossal. The significance of this study is based on the interest in the oil/gas exploration, where the demand for the energy accruable is on the rise globally. Because of the high pressure and temperature involved in the pumping of crude oil through the pipeline, there is need to fathom a way of safeguarding the subsea facilities from severe damage or failure which can lead to environmental hazard, such as the recent Gulf of

Mexico pipeline burst and its aftermath. Thus, transportation of crude from the seabed has to be accomplished in a safer and crisis free manner. Only appropriate design analysis can bring this situation.

1.8 Overview of Thesis

This research work presents the problem of fluid-pipe-soil dynamic interaction concerning conveyance of oil and gas through subsea pipelines. The focus here is to formulate the dynamic stresses in conjunction with the vibration of the pipe to enable us eventually obtain practical design analysis of onset of pipe bursting and buckling pressures. These are achieved via the following overviews:

Chapter 1 presents brief introduction of the problem, the motivation and establishment of our study. Also, it highlights the statement and objectives of the research matters as well as the significance of the study.

In chapter 2, detailed literature studies of the existing past and recent works on pipe vibration, pipe bursting and buckling phenomena are enumerated.

Next is chapter 3, where the analysis of dynamic stress propagation of an offshore pipeline sitting on a seabed is reported.

Similarly, chapter 4 considered the phenomena in chapter 3, but here, the pipe is considered partially or fully buried.

Furthermore, in chapter 5, another model for the pipe bursting and buckling pressures using polar coordinates method in conjunction with von Misses yield criterion is presented.

The last but not the least is chapter 6, where summary of findings, contributions and future works are discussed.

CHAPTER 2

LITERATURE REVIEW

2.1 Historical Development of Pipe Dynamics

Whereas the installation of pipelines for the transportation of liquids over land may be traced back to antiquity, the establishment of marine pipelines is a more recent development of the latter part of the twentieth century. The fuel line installed across the English channel in 1944 to supply the allied troops during the Normandy landings is often cited as the first example. In fact, before the war small diameter oil export lines had already been installed in shallow waters off the US Gulf coast, and possibly also in Caddo Lake (Louisiana), off California and in the Caspian Sea, where offshore hydrocarbon exploration began.

The first oil-producing well 'out of sight of land' (in the Mexican Gulf) was drilled in 1947, the first pipelay barge commissioned in 1952, and the first pipeline laid on the seabed in 1954. Separate tallying of offshore pipelines did not start until 1968, but during following three decades it is estimated that close to 90000 km of marine pipelines were installed for the transportation of hydrocarbons, with approximately 5000 km being added each year. The majority of the pipeline systems are located in the heavily developed regions of the Arabian Gulf, the Gulf of Mexico and the North Sea, Andersen *et al.* (2005).

2.2 Studies on Pipe Dynamic Stability

An extensive review of the dynamics and stability of pipes transporting fluid, where the flow velocity is either entirely constant, or with a small harmonic component superposed is given here. Concerning constant flow velocity, Paidoussis and Issid (1973) observed that, the dynamics of the system in a general form showed that conservative systems are subjected not only to buckling (divergence) at sufficiently highly flow velocities, but also flutter (oscillatory instabilities) at high transport velocity. The co-workers stated further that, for harmonically varying flow velocity, the extent of the instability regions increases with fluid velocity for clamped-clamped and pinned-pinned pipes, while a more complex behaviour occurs for cantilevered pipes.

Experimentally, Aitken (1876) worked extensively on travelling chains and elastic cords, showing the balance between motion-induced tensile and centrifugal forces, as pertinent to the

study of dynamics of flexible pipes conveying fluid. Marcel Brillouin, in 1885, was first to recognize a self-excited oscillation of spontaneous motions imparted to the free end of a rubber pipe by a sufficiently high flow rate, but his work on the subject is hitherto unpublished.

Meanwhile, Bourrieres (1939) who was one of Brillouin's students made the first attempt to investigate serious study on the dynamics of flexible pipes conveying fluid. He reported in his remarkable paper published in that year, the oscillatory instability of cantilevered pipes conveying fluid, both theoretically and experimentally. Though he derived the correct equation of motion, he failed to obtain analytically the critical flow velocity for the onset of motion; he however, achieved most of the vital features of the phenomenon. Sadly, this important paper was evidently "lost" in the sense of being unknown to those who have since undertaken research in this area.

Interestingly, the subject was reactivated by Ashley and Haviland (1950) in connection with the study of vibration of the Trans-Arabian pipeline. Later, Feodos'ev (1951) derived the full equation of motion for a pipe conveying fluid and analysed the case of a pipe with simply-supported ends. Independently, Housener (1952) studied the same problem by using a different method. Both workers found that for sufficiently high flow velocities, the pipe may buckle if it is loaded axially. Niordson (1953) subsequently, obtained a more general and elegant investigation which led to the same equation of motion and concluded in the same way regarding stability of pipes with simply-supported ends.

Furthermore, Long (1955) was the first after Bourrieres (1939), to consider cantilevered pipes transporting fluid with another set of boundary conditions. His analysis dealt with relatively small flow velocities, appreciably below the threshold of oscillatory instability, the existence of which he seemed to be unaware. Notwithstanding, he observed and confirmed experimentally that, contrarily, to those of simply-supported pipes, forced vibrations of cantilevered pipes are damped by internal flow in the range of flow velocities investigated.

An analytical method in which the character of the eigenvalues of the problem is obtained from the structure of the differential equation of motion without finding specific solutions was presented by Handelman (1955). Besides, Heinrich (1956), Bolotin (1956) as well as Hu and Tsoon (1957) investigated various aspects of the problem. Later, Movchan (1965) recovered the

condition of stability for a simply-supported pipe conveying fluid by means of Liapunov's direct method.

Prior to 1963, apart from Bourrieres, the only form of instability known was buckling in all the above studies. In 1963, Gregory and Paidoussis (1966a, b) showed theoretically and experimentally that, at sufficiently high flow velocities, cantilevered pipes are subject to oscillatory instabilities (flutter) rather than buckling (divergence). However, Benjamin (1961a, b) observed fully the existence of oscillatory instabilities in his two outstanding papers. He was the first worker to discover that the dynamical problem is independent of fluid friction, and forecast analytically the existence of oscillatory instability of cantilevered pipes conveying fluid. These effects were confirmed by Gregory and Paidoussis' work.

Benjamin (1961a) further found that buckling instability is possible in the case of a vertical cantilevered system, where gravity is functional, if the fluid is sufficiently heavy; on the other hand, Paidoussis (1970) discovered that, vertical continuously flexible pipes are never subject to buckling. However, Paidoussis and Deksnis (1970) gave a clarification of this controversy.

Further study on the stability of tubular cantilevers conveying fluid was reported by Nemat-Nasser *et al.* (1966) where they neglected the gravity forces. Their emphasis was on the effect on stability of velocity-dependent forces, such as dissipative and Coriolis forces; they showed that such forces may destabilize the system, which corroborated Gregory and Paidoussis (1966a, b) earlier discovery. Subsequent publications by Herrmann (1967), Herrmann and Nemat-Nasser (1967) emphasised the connection between the problem of instability of a cantilever conveying fluid and the more encompassing problem of instability of a cantilever subjected to a "follower"-type force at the free end. Wiley and Furkert (1972) studied the problem of a beam subjected to a follower force acting within the span, where the force is caused by a fluid jet attached to the beam and fed by an infinitely flexible supply line. They concluded that either buckling or oscillatory instabilities, or both, may exist, based on the boundary conditions.

A correction to the equation of motion as earlier formulated in some of the investigations aforementioned was given by Stein and Torbiner (1970) with regards to the infinitely long pipes conveying fluid. The correction was first noticed by Heinrich (1956) and by Hu and Tsoon (1957) separately, and had been observed in a slightly different nature by Haringx (1952) much earlier. This correction emanates from the effect of internal pressure and may become significant

for sufficiently high pressures. The experimental and theoretical aspect of the problem was considered by Naguleswaran and Williams (1968). Interestingly, pipes with both ends supported may buckle even at very small fluid velocities due to internal pressure.

Another remarkable work on non-linear analysis for a pipe with simply-supported ends conveying fluid was done by Thurman and Mote (1969). Here they used perturbation technique to determine natural frequencies of the system and found that, the significance of non-linear terms increases with flow velocity, so that the range of applicability of linear theory becomes more restricted as the flow velocity increases. Chen (1971) in a related study observed that buckling and oscillatory instabilities are possible in the vibration of a pipe transporting fluid with the upstream end clamped and the downstream end constrained by a linear spring. The boundary conditions here are intermediate between clamped-free and clamped-pinned.

In Paidoussis and Denise (1971, 1972) work, the dynamics of cantilevered pipes and pipes with clamped ends were investigated. They discovered that thin pipes with clamped ends are subject to buckling as well as coupled-mode flutter which was confirmed experimentally by the duo. Later, Weaver and Unny (1973) achieved similar theoretical results by using a different analytical technique for simply-supported shells.

In all the investigations mentioned above, the fluid velocity was considered uniform. A striking study was done by Chen (1971), where he examined the stability of simply-supported pipes conveying fluid with a flow velocity U that is harmonically changing at the same time superposed on the steady velocity, U_0 . He expressed U as $U = U_0(1 + \mu \cos \omega t)$. He concluded that, parametric instabilities are possible in such cases and found the boundaries of stability-instability regions. Also, he confirmed the combination of resonances.

2.3 Non-Linear Vibrations of Pipe Conveying Fluid

Extensive reviews of flow-induced vibrations are highlighted here. Leissa (1973) reported on large-amplitude vibrations of circular cylindrical shells. Other workers in this area are Amabili *et al.* (1998), Paidoussis (2003) as well as Kubenko and Koval'chuk (1998). In their various reviews, they all agreed that instabilities may be achieved by increasing the flow velocity in the axial direction of pipe conveying fluid.

Evensen (2000) in his publication, originally written in 1968, studied the influence of pressure and axial loading on large-amplitude vibrations of circular cylindrical shells. He assumed mode shapes which were derived in agreement with the experimental observation. This method was first introduced to study buckling of circular cylindrical shell. Also, Amabili *et al.* (1999, 2000) showed that at least the first and third axisymmetric modes (axisymmetric modes with an even number of longitudinal half-waves are insignificant) must be incorporated in the mode expansion (for modes with a single longitudinal half-wave), as well as using both the driven and companion modes, to correctly predict the trend of nonlinearity with sufficiently good accuracy.

Raouf and Palazotto (1991) adopted an asymptotic method to get the nonlinear equations of motion governing the forced dynamic response of a laminated circular cylindrical panel in cylindrical bending. The expansion is valid for near-resonant external excitation and in the presence of a two-to-one internal resonance. Raouf and Palazotto (1992) further extended the work by using the formulations developed earlier (1991) with a single-mode expansion. Their results showed that the response of panels simply supported on the straight edges (no deformation arises along the longitudinal axis) is of hardening type. Besides, Raouf (1993) and Raouf and Palazotto (1994) investigated the nonlinear free vibrations of curved orthotropic panels. They combined the Galerkin method with perturbation method in a single-mode analysis that was studied. In particular, Raouf (1993) observed that, thin circular cylindrical pipes display softening nonlinearity when the ratio between the radius and length (R/L) of the pipe is smaller than 1.25 or 1.5, for the orthotropic composite material used, but display a hardening nonlinearity for R/L too close to zero.

2.4 Further Review Concerning the Pipelines with Internal Fluid Velocity

In this context, there are several media transporting fluid internally at high velocity and pressure under time-varying being influenced by pump and valve operations. These include: the anchored pipelines arrays above ground level, pipeline arrays in a steam generator, oil pipelines, pump discharge lines, propellant fluid lines of liquid-filled rockets and human circulatory system as pointed out by Lee *et al.* (2004). In their study, they found out that generally, when a pipeline transporting fluid vibrates, the internal fluid interacts with the pipe wall and influences the dynamic characteristics of the pipeline system, which may lead to catastrophic structural imbalance.

Paidoussis and Li (1993) gave extensive review on the modelling and analysis of the flow-induced vibrations of pipeline systems covering over six decades. It is worthy of mentioning that, Ashley and Haviland (1950) were the first workers to consider the internal flow-induced transverse vibration of a pipeline. Later, their work was revised by Housner (1952) where he included the inertia force concerning coriolis acceleration of internal fluid. Following this revision, there have been various modifications to the earlier studies on pipe-dynamic analysis which are available in the literature.

Among these are the linear theories of the following researchers viz: Nemat-Nasser *et al.* (1966), Stein and Tobriner (1970), Chen (1971), Hill and Davis (1974), Paidoussis *et al.* (1986) and Lesmez *et al.* (1990). On the other hand, Semler *et al.* (1994), Lin and Tsai (1997), Jensen (1997), Zhang *et al.* (1999), Öz (2001), Lee and Chung (2002) did extensive studies on the non-linear theories of pipe dynamics.

Impressively, most available pipe-dynamic analyses considered the structural vibration of pipeline only without the dynamics of internal fluid in conjunction with the vibration of pipeline. To correct this serious anomaly, Lee *et al.* (1995) formulated a set of coupled pipe-dynamic equations for the longitudinal, radial and transverse vibrations of pipeline and also for the transients of unsteady internal fluid pressure and velocity. The work of Lee *et al.* (1995) was further extended by Lee and Kim (1999). They generalized the governing differential equations by adding the circumferential strain effect due to the internal fluid pressure. Subsequently, Gorman *et al.* (2000) included radial shell vibration and initial axial tension to the work of Lee and Kim (1999).

There are equally contributions from Paidoussis and his co-workers (1974, 1976, 1986 and 1994), where their studies were based on both the Euler-Bernoulli beam theory and the Timoshenko beam theory. Others that also employed these theories in their investigations included Pramila and Laukkanen (1991), Chu and Lin (1995), Lin and Tsai (1997), Zhang *et al.* (1999) and Lee and Oh (2003). Reddy and Wang (2004) too presented a paper with complete derivation of the equations of fluid-conveying pipes with small strains but moderate rotations. In their studies, they made use of the Euler-Bernoulli beam theory and the Timoshenko beam theory based on energy considerations. They included contributions of fluid velocity to the

kinetic energy as well as to the body forces. Their non-linear formulations were in agreement with those of Semler *et al.* (1994).

Furthermore, Ibrahim (2010) in his articles presented a comprehensive overview of mechanics of pipes conveying fluid and related problems concerning the fluid-elastic instability under conditions of turbulence in nuclear power plants. He articulated many areas involving different types of modelling, dynamic analysis and stability regimes of pipes conveying fluid restrained by elastic or inelastic barriers subject to the dynamic and stability behaviours of pinned-pinned, clamped-clamped and cantilevered pipes transporting fluid.

In particular, Osheku (2005) made useful contributions to the study of a conveyance of fluid in pipes laid on or buried under the sea floor. In his investigations, he considered the pipeline as a hollow beam vibrating on an elastic foundation by using analytic methods that involved doubled integral transforms. He however, solved for the transverse vibration only. There are avalanche of studies from Olunloyo *et al.* in recent time concerning the problems of offshore pipeline. Olunloyo *et al.* (2007a, 2007b) reported the cases of transverse and longitudinal vibrations of a fluid conveying beam and the pipe walking phenomenon as well as the dynamics and stability of a fluid conveying vertical beam. The studies were extended to the dynamics and stability of a viscoelastic pipe conveying a non-Newtonian fluid by Olunloyo *et al.* (2009). Besides, Olunloyo *et al.* (2010a, 2010b,) and Osheku *et al.* (2010) further their investigations concerning the Mechanics of gas pipeline vibrations, vibration and stability behaviour of sandwiched viscoelastic pipe conveying a non-Newtonian fluid and the mechanics of pipe walking of buried pipeline.

2.5 Pipeline Design

The objective of a subsea pipeline is to transport a medium from one location to another. Many different parameters – economic, technical, environmental, etc. - determine whether or not a subsea pipeline system will be installed. The justification may not rely solely on assessments of cost estimates and transportation requirements. Decisions may also be influenced by technically less tangible aspects such as societal expectations of security of supply, requiring sufficient redundancy in pipeline networks, or the political objectives of opening up new oil or gas provinces for economic or strategic reasons.

The bases for design consist of the basic requirements to functionality, as well as a description of the environment into which the pipeline will be placed, leading to the selection of pipeline dimension and routing. Also, the requirements included in the bases for design are the ; physical pipe properties, such as diameter, steel grade options and line-pipe specification details, including supplementary requirements to codes and guidelines. Central also are the parameters regarding flow assurance and pressure containment, i.e. design temperature and pressure, maximum and minimum operating temperatures, maximum operating pressure, and details of incidental operation.

The subsea pipeline system design and installation covers the marine pipeline proper, platform risers, tie-in and spool connection parts, hydrostatic testing, possible subsea valve or branch assemblies, the corresponding protection works, as well as the activities conducted in association with start-up of production. The construction of subsea pipelines took off in the 1970s, and literature on the technology started to appear in the next decade, prominent workers in this area are, Mouselli (1981), who contributed immensely to the analysis and method of Offshore pipeline design; while a few years later, in 1985, de la Mare (1985), published a scientific work on Advances in Offshore Oil and Gas pipeline technology.

Yong Bai (2001), gave a comprehensive overview of design methods based upon two decades of research and teaching experience on Pipelines and Risers. Also, Palmer and King (2004), reported extensively on the Subsea pipeline, but have less emphasis on practical construction issues.

2.6 Pipe Buckling & Bursting

Pipe buckling and bursting in the oil and gas industry are phenomena that generally cannot be overlooked. Rather, holistic approach has to be adopted in order to protect the integrity of the pipe installations in the deep sea and ultra deep sea. In this regard, analytical and numerical modellings of the upheaval buckling response of offshore pipelines have progressed rapidly over the last few years, Rafael *et al.* (2004). This is viewed globally from the classical analysis by Hobbs (1974), Hobbs and Liang (1989), to one covering initial imperfections as reported by Taylor and Gan (1986), Ju and Kyriakides (1988), to one additionally including large pipe displacement and associated cover non-linearity in the work of Pedersen and Jensen (1988). Besides, Palmer *et al.* (1988) used a design method based on the application of the computer

program while, a finite-element models were developed to carry out analysis of pipeline upheaval buckling by Croll (1997) and Palmer *et al.* (1990).

Furthermore, Olunloyo *et al.* (2008) contributed immensely to the field of pipeline analysis by reporting the sets of dynamic stresses in conjunction with the buckling and burst pressures phenomena.

In general, earlier researcher in this offshore field, such as Paidoussis and Issid (1974), Semler *et al.* (1994) and Gorman *et al.* (2000) studied the instability and pipe dynamics of offshore vibrating pipelines without investigating the related dynamic stress. Olunloyo *et al.* (2007a, 2007b) equally did excellent works concerning the transverse and longitudinal motions of the offshore vibrating pipeline. On the other hand, Oshoku (2005) mainly investigated the transverse motion of the pipeline. Their studies however, did not account for the dynamic stress and the phenomena of pipe buckling and bursting pressures.

Hence, this work will attempt to account for the pipe dynamics, dynamic stresses and the attendant pipe bursting and buckling pressures of a vibrating subsea pipeline.

CHAPTER 3

ANALYSIS OF DYNAMIC STRESS PROPAGATION IN SUBSEA PIPELINE AND FLOW LINE SYSTEMS

3.1 Problem Fundamentals and Governing Differential Equation

The problem of dynamic stress propagation concerning the vibration of a pre-stressed high pressure and high temperature subsea pipe that is transporting a fluid, resting on the seabed is considered here. To study this, we look at the problems viz:

- (a) The dynamic stresses and
- (b) The vibrations of the pipe in transverse and longitudinal perspectives.

For the dynamic stresses, underlying assumptions in the formulation of the governing dynamic stress equations are as follows:

- (i) the fluid conveying pipe is idealised as an elastic beam with the neutral plane lying along the geometric centre or mid plane where the internal transport velocity is maximum.
- (ii) the deflection of the beam is small compared with the span of the beam.
- (iii) during bending the elastic beam has two (upper and lower) layers such that each has its neutral plane which may not necessarily coincide with the geometric mid plane of the beam.
- (iv) these neutral planes are located at $z_1 = \frac{\alpha(x)R_i}{2}$ and $z_2 = -\frac{\alpha(x)R_i}{2}$ where $\alpha(x)$ is a function of x as illustrated in Figure 3.
- (v) the approximations involved in the foregoing beam theory are such that the field variables are expressible in terms of derivatives of the deflection $w(x)$ which is taken to be same for both layers.

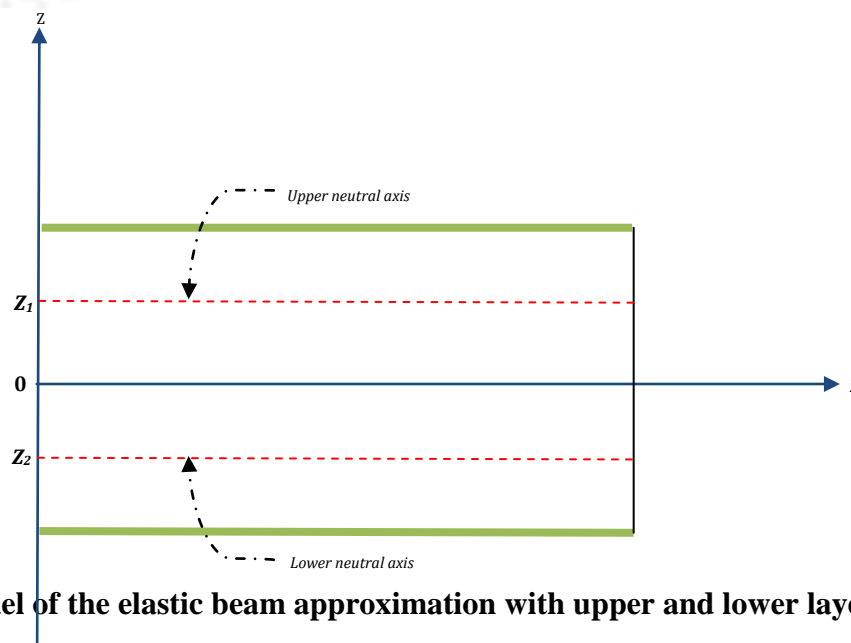


Figure. 3.0: A model of the elastic beam approximation with upper and lower layers.

Following the foregoing assumptions, the formulated dynamic stress propagation equations of the subsea pipeline have been derived in equations (A.11, A.13, A.16, A.17, A.20 and A.21) as

$$\tau_{(zx)_1} = \frac{E}{2} (Z^2 - R_i Z) \frac{\partial^3 \bar{w}}{\partial \bar{x}^3} - \frac{z \tau_{max}}{R_i} \quad (3.1)$$

$$\tau_{(zx)_2} = \frac{E}{2} (Z^2 + R_i Z) \frac{\partial^3 w}{\partial x^3} - z \frac{\tau_{max}}{R_i} \quad (3.2)$$

$$\sigma_{(x)_1} = -\frac{E}{2} (2Z - R_i) \frac{\partial^2 w}{\partial x^2} + x \frac{\tau_{max}}{R_i} + x(\rho + \rho_f) \frac{\partial^2 u}{\partial t^2} \quad (3.3)$$

$$\sigma_{(x)_2} = -\frac{E}{2} (2Z + R_i) \frac{\partial^2 w}{\partial x^2} + x \frac{\tau_{max}}{R_i} + x(\rho + \rho_f) \frac{\partial^2 u}{\partial t^2} \quad (3.4)$$

while

$$\sigma_{z_1} = \frac{F_{im} - C_{st} \frac{\partial w}{\partial t}}{2\pi R_o L} - P_f - \frac{E}{2} \left[\frac{1}{3} (Z^3 - R_o^3) - \frac{1}{2} (R_i Z^2 - R_i R_o^2) \right] \frac{\partial^4 w}{\partial x^4} + (Z - R_o)(\rho + \rho_f) \frac{\partial^2 w}{\partial t^2} \quad (3.5)$$

Similarly,

$$\begin{aligned} \sigma_{z_2} = & \frac{1}{2\pi R_o L} \left(F_{im} - (c_{st} - c_o) \frac{\partial w}{\partial t} - K_{soil} w - c_{soil} \frac{\partial w}{\partial t} \right) + P_f \\ & - \frac{E}{2} \left[\frac{1}{3} (Z^3 + R_o^3) + \frac{1}{2} (R_i Z^2 + R_i R_o^2) \right] \frac{\partial^4 w}{\partial x^4} + (Z + R_o)(\rho + \rho_f) \frac{\partial^2 w}{\partial t^2} \end{aligned} \quad (3.6)$$

3.2 Governing Differential Equations

Following Olunloyo et al (2007), the physical problem under investigation consists of a pre-stressed pipe and pressurized hot fluid conveying pipeline that is resting on the seabed. The pre- and post- deformation fluid flow geometries of the boundary value problem are posed in Figures 3.1a and 3.1b.

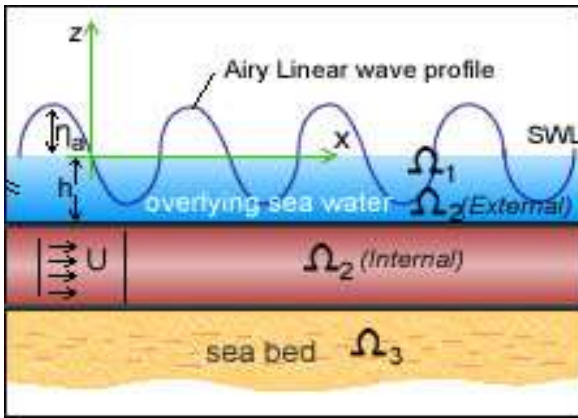


Fig. 3.1a: The flow geometry of the dynamic interaction of pipeline on sea bed when γ is zero

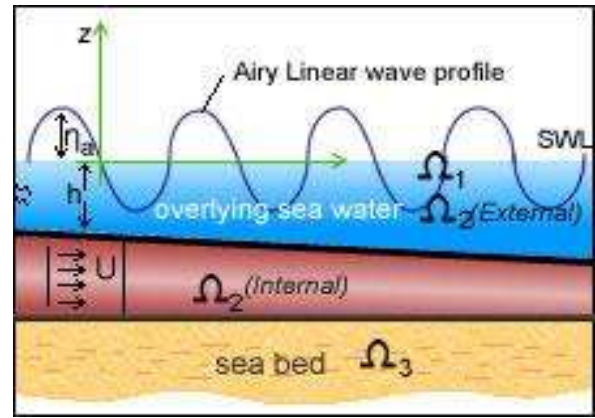


Fig. 3.1b: The flow geometry of the dynamic interaction of pipeline on seabed when γ is 0.02

The underlying theory employs the following hypotheses namely:

- (i) the pre-stressed pipeline is idealised as an elastic beam on a subsoil layer that is considered to be a homogenous semi-infinite elastic continuum with non-retarded geo-mechanical properties.
- (ii) a fully developed incompressible viscous Newtonian pressurised hot fluid is flowing through the pipeline.
- (iii) the contrived dynamic system is under the influence of hydrodynamic and bending loads, internal fluid transverse and longitudinal transmission forces, seabed subsoil layer and overlying sea water pipeline interfaces frictional and drag forces.
- (iv) the elastically deforming pre-stressed hot fluid conveying pipeline is subjected to both non linear infinitesimal strains of Semler et al or Reddy and Wang.
- (v) the temperature differential between the external and internal walls of the pipeline results in thermal strain with attendant cross sectional area change.
- (vi) a linear Airy wave profile propagates uniformly above the still water level (SWL).

Under these assumptions, the generalised governing differential equations for the case of a vibrating horizontal fluid conveying pipe sitting on the ocean floor in transverse and longitudinal directions as reported in equations (B.48) and (B.49) read

$$\begin{aligned}
 m\ddot{w} + (C_1 + C_D)\dot{w} + Kw + 2m_f U\dot{w}' + m_f \dot{U}w' + m_f UU'w' + m_f U^2w'' - [T_o - PA - \alpha EA\Theta]w'' + EIw'^v \\
 + [T_o - EA - PA - \alpha EA\Theta] \left[w''u' + w'u'' + \frac{3}{2}w'^2w'' \right] + [P'A + PA' - \alpha EA' - \alpha EA\Theta'] \left[w' - u'w' - \frac{w'^3}{2} \right] \\
 - EI \left[4w'^v u'' + 3w''u''' - 2w'^v u' - w'u'^v \right] - [EA'] \left[u'w' + \frac{w'^3}{2} \right] + mg = P_h(t)A_p
 \end{aligned} \tag{3.7}$$

and

$$\begin{aligned}
 m\ddot{u} + (C_2 + C_D)\dot{u} + 2m_f U\dot{u}' + m_f \dot{U}u' + m_f \dot{U}u' + m_f UU' + m_f UU'u' + m_f U^2u'' \\
 - EAu'' - EA' \left(u' + \frac{w'^2}{2} \right) + \alpha EA'\Theta + \alpha EA\Theta' - \alpha EA'\Theta \frac{w'^2}{2} - \alpha EA\Theta' \frac{w'^2}{2} - EI[w''w''' + w'w'^v] \\
 - \alpha EA'\Theta \frac{w'^2}{2} - \alpha EA\Theta' \frac{w'^2}{2} - EI[w''w''' + w'w'^v] + \left[P'A + PA' - \frac{P'A}{2}w'^2 - \frac{PA'}{2}w'^2 - PAw'w'' \right] \\
 + [T_o - EA - \alpha EA\Theta]w'w'' = -\mu mg
 \end{aligned} \tag{3.8}$$

The linearised form of equations (3.7) and (3.8) as special cases for our problem are:

$$m\dot{w} + (C_1 + C_D)\dot{w} + Kw + 2m_f U \dot{w}' - [T_o - PA - m_f U^2 w'' - \alpha EA \Theta] w'' + EI w'^v + [P'A + PA' - \alpha EA' - \alpha EA \Theta'] w' + mg = P_h(t) A_p \quad (3.9)$$

and

$$m\ddot{u} + (C_2 + C_D)\dot{u} + 2m_f U \dot{u}' - (EA - m_f U^2) u'' - EA' u' + [T_o - EA - \alpha EA \Theta] w' w'' + (P'A + PA' + \alpha EA' \Theta + \alpha EA \Theta') - \alpha EA' \Theta \frac{w'^2}{2} - \alpha EA \Theta' \frac{w'^2}{2} - [P'A + PA' + \alpha EA' \Theta + \alpha EA \Theta' + EA'] \frac{w'^2}{2} - EI[w'' w''' + w' w'^v] = -\mu mg \quad (3.10)$$

3.3 Analysis of Transverse Vibration Problem

Following Olunloyo et al (2007), it is possible to substitute for the geometric and operating flow variables in eqns.(3.7-3.8) via the following relations viz;

$$A = A_0 \left(1 - \gamma \frac{x}{L}\right) \text{ and } A' = -A_0 \frac{\gamma}{L} \text{ or using average area } A, \text{ i.e.}$$

$$A \approx A_0 \left(1 - \frac{\gamma}{2}\right); (PA)' = -PA_0 \frac{\gamma}{L} - \frac{\Delta P}{L} A_0 \left(1 - \frac{\gamma}{2}\right); \Theta' = -\frac{\Delta \Theta}{L}$$

while γ is the area deformation coefficient. Also, the hydrodynamic effect in Eq. (3.9) could be expressed, using the relation derived by Olunloyo et al (2005) i.e.

$$P_h = -\left(\frac{\partial \phi}{\partial t} + gz\right) \rho_w \quad (3.11)$$

Accordingly, equation (3.7) in non-dimensionalised form becomes

$$\varepsilon^2 \frac{\partial^4 \bar{w}}{\partial \bar{x}^4} + [3\delta \bar{U}^2 - \beta + \beta_3(1-\gamma)\bar{\theta} + \bar{P}\beta_1(1-\gamma)] \frac{\partial^2 \bar{w}}{\partial \bar{x}^2} + \frac{\partial^2 \bar{w}}{\partial \bar{t}^2} + [\bar{C}_1 + \bar{C}_D - \beta_5 \gamma \bar{\theta} - \beta_5(1-\gamma)\Delta \bar{\theta} - \bar{P}\beta_4 \gamma - \Delta \bar{P}\beta_4(1-\gamma)] \frac{\partial \bar{w}}{\partial \bar{t}} + \bar{k}_b \bar{w} = -\bar{\rho}_w \left(\frac{\partial \bar{\Phi}}{\partial \bar{t}} + \bar{g}\bar{z}\right) \bar{A}_p \beta_6 \quad (3.12)$$

where,

$$\varepsilon^2 = \frac{EI}{L^2 T} \ll 1, \quad \frac{mL^2}{\tau^2 T} = \frac{k_o L^2}{T} = 1, \quad \bar{C}_1 = \frac{C_1 L^2}{\tau T}, \quad \bar{C}_2 = \frac{C_2 L^2}{\tau T}, \quad U_o^2 = \frac{L^2}{\tau^2}, \quad \bar{C}_D = \frac{C_D L^2}{\tau T}$$

in conjunction with the following non-dimensionalised parameters namely;

$$\begin{aligned}
x &= \bar{x}L, w = \bar{w}L, \delta = \frac{m_f}{m}, t = \tau \bar{t}, \tau = L^2 \sqrt{\frac{m}{EI}}, U = \bar{U} \frac{L}{\tau_f}, \bar{P}\bar{A} = \frac{PA_0L^2}{EI}, \Delta\bar{P}\bar{A} = \frac{\Delta PA_0L^2}{EI}, \delta_1 = \frac{m_w}{M}, \\
R &= \bar{R}L, A = \bar{A}L^2, \delta_s = \delta_s L, \beta_0 = \frac{T_0L^2}{EI}, \beta_1 = \frac{EA_0L^2}{EI}, \beta_2 = \frac{\sqrt{\delta}}{U}, \beta_3 = \alpha\beta_1\beta_2\Theta, \beta_4 = \alpha\beta_1\beta_2\Delta\Theta, \beta_5 = \alpha\beta_1\Theta, \\
\beta_6 &= \alpha\beta_1\Delta\Theta, \beta_7 = \frac{\beta_1}{U}, \beta_8 = \frac{\delta_1}{L}, \bar{C}_D = \frac{C_D L^2}{\sqrt{mEI}}, \bar{C}_s = \frac{C_s L^2}{\sqrt{mEI}}, \Phi = \frac{\bar{\Phi}L^2}{\tau^2}, \bar{g} = \frac{MgL^3}{EI}, \bar{K}_b = \frac{K_b L^4}{EI}, \alpha' = \frac{L^4}{I}
\end{aligned}$$

By introducing the Laplace and Finite Fourier Sine transforms namely,

$$\begin{aligned}
\bar{(\cdot)} &= \int_0^\infty (\cdot) e^{-s\bar{t}} d\tau; (\cdot) = \frac{1}{2\pi i} \int_{\eta-i\infty}^{\eta+i\infty} \bar{(\cdot)} e^{s\bar{t}} ds; \\
&\text{and}
\end{aligned} \tag{3.13}$$

$$\bar{[.]} = \int_0^1 [.] \sin n\pi\bar{x} d\bar{x}; [.] = 2 \sum_{n=1}^{\infty} \bar{[.]} \sin n\pi\bar{x}$$

subject to the under listed pinned-pinned end boundary conditions viz;

$$\bar{w}(0, s) = \bar{w}(1, s) = \bar{w}_{xx}(0, s) = \bar{w}_{xx}(1, s) = 0; \tag{3.14}$$

Further more, noting that

$$\begin{aligned}
\mathfrak{I}_S \left\{ \tilde{\bar{w}}_{xxxx}(\bar{x}, s) \right\} &= n^4 \pi^4 \tilde{\bar{w}}^F(\lambda_n, s) - n^3 \pi^3 \left\{ \bar{w}(0, s) + (-1)^{n+1} \bar{w}(1, s) \right\} \\
&\quad + n\pi \left\{ \bar{w}_{xx}(0, s) + (-1)^{n+1} \bar{w}_{xx}(1, s) \right\}
\end{aligned} \tag{3.15a}$$

$$\begin{aligned}
\mathfrak{I}_S \left\{ \tilde{\bar{w}}_{xx}(\bar{x}, s) \right\} &= -n^2 \pi^2 \tilde{\bar{w}}^F(\lambda_n, s) \\
&\quad + n\pi \left\{ \bar{w}(0, s) - \bar{w}(1, s) (-1)^n \right\}
\end{aligned} \tag{3.15b}$$

Equation (3.12) with zero initial conditions, can be re-written as,

$$\begin{aligned}
&\varepsilon^2 n^4 \pi^4 \tilde{\bar{w}}^F(\lambda_n, s) - [3\delta\bar{U}^2 - \beta + \beta_3(1-\gamma)\bar{\theta} + \bar{P}\beta_1(1-\gamma)] n^2 \pi^2 \tilde{\bar{w}}^F(\lambda_n, s) + s^2 \tilde{\bar{w}}^F(\lambda_n, s) \\
&+ [\bar{C}_1 + \bar{C}_D - \beta_5(1-\gamma)\Delta\bar{\theta} - \beta_5\gamma\bar{\theta} - \Delta\bar{P}\beta_4(1-\gamma) - \bar{P}\beta_4\gamma] s \tilde{\bar{w}}^F(\lambda_n, s) + \bar{k}_b \tilde{\bar{w}}^F(\lambda_n, s) \\
&= -\bar{\rho}_w \left\{ [s \tilde{\Phi}^F(\lambda_n, s, \bar{z})]_{\bar{z}=-\bar{h}} + \frac{\bar{g}\bar{h}1^F}{s} \right\} \bar{A}_p \beta_6
\end{aligned} \tag{3.16}$$

Employing the procedural analysis reported in Olunloyo et al (2004), it is possible to rewrite Φ in the Fourier-Laplace transform plane as

$$\tilde{\Phi}^F = \hat{\beta} s \tilde{w}^F(\lambda_n, s), \hat{\beta} = \frac{-\bar{U}_w \cosh(\bar{k}\bar{z})}{\bar{k} \sinh(\bar{k}\bar{h})}, \bar{k} = \frac{n\pi}{\bar{\lambda}} \text{ and } h = \bar{h}L \tag{3.17}$$

Hence, a closed form solution for the transverse dynamic response can be computed as,

$$\bar{w}^F(\bar{\lambda}_n, s) = \frac{\bar{\rho}_w \bar{g} \bar{h} \bar{A}_p \beta_6 \bar{I}^F}{(1 + \bar{\rho}_w \bar{\beta} \bar{A}_p \beta_6) s(s^2 + \bar{\eta}_1 s + \bar{\eta}^2)} \quad (3.18)$$

where,

$$\bar{\beta} = \frac{-U_w \coth(k\bar{h})}{\bar{k}} \quad (3.19)$$

$$\bar{I}^F = \int_0^1 \sin n\pi \bar{x} d\bar{x} = \frac{(1 + (-1)^{n+1})}{n\pi} \quad (3.20)$$

while,

$$\bar{\eta}_1 = \frac{\bar{C}_1 + \bar{C}_D - \beta_5(1-\gamma)\Delta\bar{\theta} - \beta_3\gamma\bar{\theta} - \Delta\bar{P}\beta_4(1-\gamma) - \bar{P}\beta_4\gamma}{1 + \bar{\rho}_w \bar{\beta} \bar{A}_p \beta_6} \quad (3.21)$$

and,

$$\bar{\eta}^2 = \left(\frac{\varepsilon^2 n^4 \pi^4 - (3\delta\bar{U}^2 - \beta + \beta_3(1-\gamma)\bar{\theta} + \bar{P}\beta_1(1-\gamma))n^2 \pi^2 + \bar{k}_b}{1 + \bar{\rho}_w \bar{\beta} \bar{A}_p \beta_6} \right) \quad (3.22)$$

From the Fourier-Laplace inversion, the solution of equation (3.18) now gives,

$$\bar{w}(\bar{x}, \bar{t}) = \sum_{n=1}^{\infty} \frac{\bar{\rho}_w \bar{g} \bar{h} \bar{A}_p \beta_6}{1 + \bar{\rho}_w \bar{\beta} \bar{A}_p \beta_6} \frac{\bar{F}(\bar{t}) (1 + (-1)^{n+1}) \sin n\pi \bar{x}}{n\pi} \quad (3.23)$$

where,

$$\bar{F}(\bar{t}) = \left(\frac{1}{\bar{\alpha}_1 \bar{\alpha}_2} + \frac{1}{\bar{\alpha}_1 \bar{\alpha}_2 (\bar{\alpha}_2 - \bar{\alpha}_1)} (\bar{\alpha}_1 e^{-\bar{\alpha}_2 \bar{t}} - \bar{\alpha}_2 e^{-\bar{\alpha}_1 \bar{t}}) \right) \quad (3.24)$$

and,

$$\bar{\alpha}_1 = \frac{\bar{\eta}_1}{2} + i \sqrt{\bar{\eta}^2 - \frac{\bar{\eta}_1^2}{4}} \quad (3.25)$$

$$\bar{\alpha}_2 = \frac{\bar{\eta}_1}{2} - i \sqrt{\bar{\eta}^2 - \frac{\bar{\eta}_1^2}{4}} \quad (3.26)$$

3.4 Analysis of Longitudinal Vibration Problem

By following the same method used above for the transverse problem, equation (3.8) is rewritten as

$$\begin{aligned}
& \frac{\partial^2 \bar{u}}{\partial \bar{t}^2} + (\bar{C}_2 + \bar{C}_D) \frac{\partial \bar{u}}{\partial \bar{t}} + (3\delta \bar{U}^2 - (1-\gamma)\beta_2) \frac{\partial^2 \bar{u}}{\partial \bar{x}^2} = \varepsilon^2 \left(\frac{\partial^4 \bar{w}}{\partial \bar{x}^4} \frac{\partial \bar{w}}{\partial \bar{x}} + \frac{\partial^2 \bar{w}}{\partial \bar{x}^2} \frac{\partial^3 \bar{w}}{\partial \bar{x}^3} \right) \\
& - [\beta - (1-\gamma)\beta_2 - \bar{P}(1-\gamma)\beta_1 - (1-\gamma)\bar{\theta}\beta_3] \frac{\partial \bar{w}}{\partial \bar{x}} \frac{\partial^2 \bar{w}}{\partial \bar{x}^2} - \frac{1}{2} [\Delta \bar{P}\beta_1(1-\gamma) + \Delta \bar{\theta}\beta_3(1-\gamma)] \left(\frac{\partial \bar{w}}{\partial \bar{x}} \right)^2 \\
& + [\Delta \bar{P}\beta_1(1-\gamma) + \bar{P}\gamma\beta_1 + \Delta \bar{\theta}\beta_3(1-\gamma) + \gamma\bar{\theta}\beta_3 - \mu \bar{g}]
\end{aligned} \tag{3.27}$$

Substituting the result of equation (3.23) into (3.27), then gives

$$\begin{aligned}
& \frac{\partial^2 \bar{u}}{\partial \bar{t}^2} + (\bar{C}_2 + \bar{C}_D) \frac{\partial \bar{u}}{\partial \bar{t}} + (3\delta \bar{U}^2 - (1-\gamma)\beta_2) \frac{\partial^2 \bar{u}}{\partial \bar{x}^2} = \varepsilon^2 \left[\sum_{n=1}^{\infty} \left(\frac{\bar{\rho}_w \bar{g} \bar{h} \bar{A}_p \beta_6}{1 + \bar{\rho}_w \bar{\beta} \bar{A}_p \beta_6} \right)^2 \bar{\Lambda}(\bar{t}) (1 + (-1)^{n+1})^2 \frac{\sin 2n\pi \bar{x}}{2} \right] n^3 \pi^3 \\
& - [\beta - (1-\gamma)\beta_2 - \bar{P}(1-\gamma)\beta_1 - (1-\gamma)\bar{\theta}\beta_3] \left[\sum_{n=1}^{\infty} \left(\frac{\bar{\rho}_w \bar{g} \bar{h} \bar{A}_p \beta_6}{1 + \bar{\rho}_w \bar{\beta} \bar{A}_p \beta_6} \right)^2 \bar{\Lambda}(\bar{t}) (1 + (-1)^{n+1})^2 \frac{\sin 2n\pi \bar{x}}{2} \right] n\pi \\
& - \frac{1}{2} [\Delta \bar{P}\beta_1(1-\gamma) + \Delta \bar{\theta}\beta_3(1-\gamma)] \left[\sum_{n=1}^{\infty} \frac{\bar{\rho}_w \bar{g} \bar{h} \bar{A}_p \beta_6}{1 + \bar{\rho}_w \bar{\beta} \bar{A}_p \beta_6} \right]^2 \bar{\Lambda}(\bar{t}) (1 + (-1)^{n+1})^2 \cos^2 n\pi \bar{x} \\
& + [\Delta \bar{P}\beta_1(1-\gamma) + \bar{P}\gamma\beta_1 + \Delta \bar{\theta}\beta_3(1-\gamma) + \gamma\bar{\theta}\beta_3 - \mu \bar{g}]
\end{aligned} \tag{3.28}$$

where,

$$\begin{aligned}
\bar{\Lambda}(\bar{t}) = & \left(\frac{1}{\bar{\alpha}_1^2 \bar{\alpha}_2^2} + \frac{2}{\bar{\alpha}_1^2 \bar{\alpha}_2^2 (\bar{\alpha}_2 - \bar{\alpha}_1)} (\bar{\alpha}_1 e^{-\bar{\alpha}_1 \bar{t}} - \bar{\alpha}_2 e^{-\bar{\alpha}_2 \bar{t}}) \right) \\
& + \frac{1}{\bar{\alpha}_1^2 \bar{\alpha}_2^2 (\bar{\alpha}_2 - \bar{\alpha}_1)^2} (\bar{\alpha}_2^2 e^{-2\bar{\alpha}_1 \bar{t}} - 2\bar{\alpha}_2 \bar{\alpha}_1 e^{-(\bar{\alpha}_1 + \bar{\alpha}_2) \bar{t}} + \bar{\alpha}_1^2 e^{-\bar{\alpha}_2 \bar{t}})
\end{aligned} \tag{3.29}$$

Equation (3.28) in the Fourier-Laplace plane, subject to the boundary conditions

$$\tilde{\bar{u}}(0, \infty) = \tilde{\bar{u}}(1, \infty) = 0 \tag{3.30}$$

gives

$$\begin{aligned}
& (s^2 \tilde{u}^F(\bar{\lambda}_n, s) - s \tilde{u}(\bar{x}, 0) - \tilde{u}_1(\bar{x}, 0)) + (\bar{C}_2 + \bar{C}_D) (s \tilde{u}^F(\bar{\lambda}_n, s) - \tilde{u}(\bar{x}, 0)) \\
& - (3\delta \bar{U}^2 - (1-\gamma)\beta_2) n^2 \pi^2 \tilde{u}^F(\bar{\lambda}_n, s) = \\
& - \frac{1}{2} [\Delta \bar{P} \beta_1 (1-\gamma) + \Delta \bar{\theta} \beta_3 (1-\gamma)] \left(\frac{\bar{\rho}_w \bar{g} \bar{h} \bar{A}_p \beta_6}{1 + \bar{\rho}_w \bar{\beta} \bar{A}_p \beta_6} \right)^2 \sum_{n=1}^{\infty} \left(\frac{4}{3n\pi} + \frac{4(-1)^{n+1}}{3n\pi} \right) \tilde{\Lambda}(s) \\
& + \left[\frac{\Delta \bar{P} \beta_1 (1-\gamma) + \bar{P} \gamma \beta_1 + \Delta \bar{\theta} \beta_3 (1-\gamma) + \gamma \bar{\theta} \beta_3 - \mu \bar{g}}{s} \right] 1^F
\end{aligned} \tag{3.31}$$

where

$$\bar{\lambda}_n = n\pi; \quad \bar{1}^F = \left(\frac{1 + (-1)^{n+1}}{n\pi} \right) \tag{3.32}$$

with zero initial conditions, equation (3.31) now becomes,

$$\begin{aligned}
\tilde{u}^F(\lambda_n, s) = & \Gamma \left(\frac{\bar{\rho}_w \bar{g} \bar{h} \bar{A}_p \beta_6}{1 + \bar{\rho}_w \bar{\beta} \bar{A}_p \beta_6} \right)^2 \sum_{n=1}^{\infty} \left(\frac{4}{3n\pi} + \frac{4(-1)^{n+1}}{3n\pi} \right) \frac{\bar{\Lambda}(s)}{(s + \bar{\chi}_1)(s + \bar{\chi}_2)} \\
& + \frac{\Gamma + \bar{P} \gamma \beta_1 + \gamma \bar{\theta} \beta_3 - \mu \bar{g}}{s(s + \bar{\chi}_1)(s + \bar{\chi}_2)} 1^F
\end{aligned} \tag{3.33}$$

where,

$$\Gamma = \beta_1 \Delta \bar{P} (1-\gamma) + \beta_3 \Delta \bar{\theta} (1-\gamma) \tag{3.34}$$

and

$$\tilde{\Lambda}(s) = \left(\begin{aligned} & \frac{1}{\bar{\alpha}_1^2 \bar{\alpha}_2^2} - \frac{2}{\bar{\alpha}_1^2 \bar{\alpha}_2^2 (\bar{\alpha}_2 - \bar{\alpha}_1)} \left(\frac{\bar{\alpha}_1}{(s + \bar{\alpha}_2)} - \frac{\bar{\alpha}_{2s}}{\bar{\alpha}_2 (s + \bar{\alpha}_1)} \right) \\ & - \frac{1}{\bar{\alpha}_1^2 \bar{\alpha}_2^2 (\bar{\alpha}_2 - \bar{\alpha}_1)^2} \left(\frac{\bar{\alpha}_2^2}{(s + 2\bar{\alpha}_1)} - \frac{2\bar{\alpha}_1 \bar{\alpha}_2}{s + (\bar{\alpha}_1 + \bar{\alpha}_2)} + \frac{\bar{\alpha}_1^2}{(s + 2\bar{\alpha}_2)} \right) \end{aligned} \right) \tag{3.35}$$

while

$$\bar{\chi}_1 = \left(\frac{\bar{C}_2 + \bar{C}_D}{2} \right) - \sqrt{\left(\frac{\bar{C}_2 + \bar{C}_D}{2} \right)^2 - [3\delta \bar{U}^2 - (1-\gamma)\beta_2] n^2 \pi^2} \tag{3.36}$$

and

$$\bar{\chi}_2 = \left(\frac{\bar{C}_2 + \bar{C}_D}{2} \right) + \sqrt{\left(\frac{\bar{C}_2 + \bar{C}_D}{2} \right)^2 - [3\delta \bar{U}^2 - (1-\gamma)\beta_2] n^2 \pi^2} \tag{3.37}$$

From the Fourier-Laplace inversion, the axial displacement is now obtained as,

$$\bar{u}(\bar{x}, \bar{t}) = \left\{ \begin{aligned} & \Gamma \left(\frac{\bar{\rho}_w \bar{g} h \bar{A}_p \beta_6}{1 + \bar{\rho}_w \bar{\beta} \bar{A}_p \beta_6} \right)^2 \bar{H}_1(\bar{t}) \sum_{n=1}^{\infty} \left(\frac{4}{3n\pi} + \frac{4(-1)^{n+1}}{3n\pi} \right) \sin n\pi\bar{x} \\ & (\Gamma + \bar{P} \gamma \beta_1 + \gamma \bar{\theta} \beta_3 - \mu \bar{g}) \bar{H}_2(\bar{t}) \sum_{n=1}^{\infty} \frac{\sin n\pi\bar{x}}{n\pi} \end{aligned} \right\} \quad (3.38)$$

where,

$$\bar{H}_1(\bar{t}) = \left\{ \begin{aligned} & \frac{1}{\bar{\alpha}_1^2 \bar{\alpha}_2^2} - \frac{2}{\bar{\alpha}_1(\bar{\alpha}_2 - \bar{\alpha}_1)} \bar{\Pi}_1(\bar{t}) - \frac{2}{\bar{\alpha}_1(\bar{\alpha}_2 - \bar{\alpha}_1)} \bar{\Pi}_2(\bar{t}) \\ & + \frac{2}{\bar{\alpha}_2(\bar{\alpha}_2 - \bar{\alpha}_1)} \bar{\Pi}_3(\bar{t}) - \frac{1}{(\bar{\alpha}_2 - \bar{\alpha}_1)^2} \bar{\Pi}_4(\bar{t}) \end{aligned} \right\} \quad (3.39)$$

$$\begin{aligned} \bar{\Pi}_1(\bar{t}) &= \left(\frac{1}{\bar{\chi} \bar{\chi}_2} - \frac{e^{-\bar{\chi}_1 \bar{t}}}{\bar{\chi}_1 \bar{\chi}_2 - \bar{\chi}_1^2} + \frac{e^{-\bar{\chi}_2 \bar{t}}}{\bar{\chi}_2^2 - \bar{\chi}_1 \bar{\chi}_2} \right) \\ \bar{\Pi}_2(\bar{t}) &= \left(\begin{aligned} & \frac{e^{-\bar{\alpha}_1 \bar{t}}}{\bar{\chi}_1 \bar{\chi}_2 - \bar{\alpha}_1 \bar{\chi}_2 - \bar{\alpha}_2 \bar{\chi}_1 + \bar{\alpha}_1^2} - \frac{e^{-\bar{\chi}_1 \bar{t}}}{\bar{\chi}_1 \bar{\chi}_2 - \bar{\alpha}_1 \bar{\chi}_2 - \bar{\chi}_1^2 + \bar{\alpha}_1 \bar{\chi}_1} \\ & + \frac{e^{-\bar{\chi}_2 \bar{t}}}{-\bar{\chi}_1 \bar{\chi}_2 + \bar{\alpha}_1 \bar{\chi}_1 + \bar{\chi}_2^2 - \bar{\alpha}_1 \bar{\chi}_2} \end{aligned} \right) \\ \bar{\Pi}_3(\bar{t}) &= \left(\begin{aligned} & \frac{e^{-\bar{\alpha}_2 \bar{t}}}{\bar{\chi}_1 \bar{\chi}_2 - \bar{\alpha}_1 \bar{\chi}_2 - \bar{\alpha}_2 \bar{\chi}_1 + \bar{\chi}_1^2} - \frac{e^{-\bar{\chi}_1 \bar{t}}}{\bar{\chi}_1 \bar{\chi}_2 - \bar{\alpha}_2 \bar{\chi}_2 - \bar{\chi}_1^2 + \bar{\alpha}_2 \bar{\chi}_1} \\ & + \frac{e^{-\bar{\chi}_2 \bar{t}}}{-\bar{\chi}_1 \bar{\chi}_2 + \bar{\alpha}_1 \bar{\chi}_1 + \bar{\chi}_2^2 - \bar{\alpha}_2 \bar{\chi}_2} \end{aligned} \right) \end{aligned} \quad (3.40)$$

$$\bar{\Pi}_4(\bar{t}) = \left\{ \begin{aligned} & \bar{\alpha}_2^2 \left(\begin{aligned} & \frac{e^{-2\bar{\alpha}_1 \bar{t}}}{\bar{\chi}_1 \bar{\chi}_2 - 2\bar{\alpha}_1 \bar{\chi}_2 - 2\bar{\alpha}_1 \bar{\chi}_1 + 4\bar{\alpha}_1^2} - \frac{e^{-\bar{\chi}_1 \bar{t}}}{\bar{\chi}_1 \bar{\chi}_2 - 2\bar{\alpha}_1 \bar{\chi}_2 - \bar{\chi}_1^2 + 2\bar{\alpha}_1 \bar{\chi}_1} \\ & + \frac{e^{-\bar{\chi}_2 \bar{t}}}{-\bar{\chi}_1 \bar{\chi}_2 + 2\bar{\alpha}_1 \bar{\chi}_1 + \bar{\chi}_2^2 - 2\bar{\alpha}_1 \bar{\chi}_2} \end{aligned} \right) \\ & - 2\bar{\alpha}_1 \bar{\alpha}_2 \left(\begin{aligned} & \frac{e^{-(\bar{\alpha}_1 + \bar{\alpha}_2) \bar{t}}}{\bar{\chi}_1 \bar{\chi}_2 - (\bar{\alpha}_1 + \bar{\alpha}_2) \bar{\chi}_1 - (\bar{\alpha}_1 + \bar{\alpha}_2) \bar{\chi}_1 + 4(\bar{\alpha}_1 + \bar{\alpha}_2)^2} \\ & - \frac{e^{-\bar{\chi}_1 \bar{t}}}{\bar{\chi}_1 \bar{\chi}_2 - (\bar{\alpha}_1 + \bar{\alpha}_2) \bar{\chi}_2 - \bar{\chi}_1^2 + (\bar{\alpha}_1 + \bar{\alpha}_2) \bar{\chi}_1} \\ & + \frac{e^{-\bar{\chi}_2 \bar{t}}}{-\bar{\chi}_1 \bar{\chi}_2 - (\bar{\alpha}_1 + \bar{\alpha}_2) \bar{\chi}_1 - \bar{\chi}_2^2 + (\bar{\alpha}_1 + \bar{\alpha}_2) \bar{\chi}_2} \end{aligned} \right) \\ & + \bar{\alpha}_1^2 \left(\begin{aligned} & \frac{e^{-2\bar{\alpha}_2 \bar{t}}}{\bar{\chi}_1 \bar{\chi}_2 - 2\bar{\alpha}_2 \bar{\chi}_2 - 2\bar{\alpha}_2 \bar{\chi}_1 + 4\bar{\alpha}_2^2} - \frac{e^{-\bar{\chi}_1 \bar{t}}}{\bar{\chi}_1 \bar{\chi}_2 - 2\bar{\alpha}_2 \bar{\chi}_2 - \bar{\chi}_2^2 + 2\bar{\alpha}_2 \bar{\chi}_1} \\ & + \frac{e^{-\bar{\chi}_2 \bar{t}}}{-\bar{\chi}_1 \bar{\chi}_2 + 2\bar{\alpha}_1 \bar{\chi}_1 + \bar{\chi}_2^2 - 2\bar{\alpha}_2 \bar{\chi}_2} \end{aligned} \right) \end{aligned} \right\} \quad (3.41)$$

and,

$$\bar{H}_2(\bar{t}) = \left(\frac{1}{\bar{\chi}_1 \bar{\chi}_2} - \frac{e^{-\bar{\chi}_1 \bar{t}}}{\bar{\chi}_1 \bar{\chi}_2 - \bar{\chi}_1^2} + \frac{e^{-\bar{\chi}_2 \bar{t}}}{\bar{\chi}_2^2 - \bar{\chi}_1 \bar{\chi}_2} \right) \quad (3.42)$$

3.5 Analysis of Dynamic Stress Propagation

The non-dimensionalised equations of stresses as can be recalled from equations (3.1 - 3.6) are:

$$\bar{\tau}_{(\bar{z} \bar{x})_1} = \frac{\acute{\alpha}}{2} (\bar{z}^2 - \bar{R}_i \bar{z}) \frac{\partial^3 \bar{w}}{\partial \bar{x}^3} - \bar{z} \frac{\bar{\tau}_{max}}{\bar{R}_i} \quad (3.43)$$

$$\bar{\tau}_{(\bar{z} \bar{x})_2} = \frac{\acute{\alpha}}{2} (\bar{z}^2 + \bar{R}_i \bar{z}) \frac{\partial^3 \bar{w}}{\partial \bar{x}^3} - \bar{z} \frac{\bar{\tau}_{max}}{\bar{R}_i} \quad (3.44)$$

$$\bar{\sigma}_{\bar{x}_1} = -\frac{\acute{\alpha}}{2} (2\bar{z} - \bar{R}_i) \frac{\partial^2 \bar{w}}{\partial \bar{x}^2} + \bar{x} \frac{\bar{\tau}_{max}}{\bar{R}_i} + \bar{x}(1 + \delta) \frac{\partial^2 \bar{u}}{\partial \bar{t}^2} \quad (3.45)$$

$$\bar{\sigma}_{\bar{x}_2} = -\frac{\acute{\alpha}}{2} (2\bar{z} + \bar{R}_i) \frac{\partial^2 \bar{w}}{\partial \bar{x}^2} + \bar{x} \frac{\bar{\tau}_{max}}{\bar{R}_i} + \bar{x}(1 + \delta) \frac{\partial^2 \bar{u}}{\partial \bar{t}^2} \quad (3.46)$$

$$\bar{\sigma}_{\bar{z}_1} = -\frac{\acute{\alpha}}{2} \left[\frac{1}{3} (\bar{z}^3 - \bar{R}_0^3) - \frac{1}{2} (\bar{R}_i \bar{z}^2 - \bar{R}_i \bar{R}_0^2) \right] \frac{\partial^4 \bar{w}}{\partial \bar{x}^4} + \frac{\bar{F} - \bar{C}_{st} \frac{\partial \bar{w}}{\partial \bar{t}}}{2\pi \bar{R}_0} - \bar{P}_f + (\bar{z} - \bar{R}_0)(1 + \delta) \frac{\partial^2 \bar{w}}{\partial \bar{t}^2} \quad (3.47)$$

$$\begin{aligned} \bar{\sigma}_{\bar{z}_2} = & -\frac{\acute{\alpha}}{2} \left[\frac{1}{3} (\bar{z}^3 + \bar{R}_0^3) + \frac{1}{2} (\bar{R}_i \bar{z}^2 + \bar{R}_i \bar{R}_0^2) \right] \frac{\partial^4 \bar{w}}{\partial \bar{x}^4} + \frac{\bar{F} - (\bar{C}_{st} + \bar{C}_{soil} - \bar{C}_o) \frac{\partial \bar{w}}{\partial \bar{t}} - \bar{K}_{soil} \bar{w}}{2\pi \bar{R}_0} + \bar{P}_f \\ & + (\bar{z} + \bar{R}_0)(1 + \delta) \frac{\partial^2 \bar{w}}{\partial \bar{t}^2} \end{aligned} \quad (3.48)$$

where the following dimensionless parameters have been used viz:

$$\tau_{(zx)} = \bar{\tau}_{(\bar{z} \bar{x})} P_o, \quad z = \bar{z} L, \quad R = \bar{R} L, \quad x = \bar{x} L, \quad \sigma = \bar{\sigma} P_o, \quad w = \bar{w} L, \quad u = \bar{u} L, \quad L^2 \rho / \tau^2 P_o = 1$$

$$t = \bar{t} \tau, \quad P = \bar{P} P_o, \quad F = \bar{F} P_o L^2, \quad \acute{\alpha} = E / P_o, \quad K = \bar{K} L P_o, \quad C = \bar{C} L \tau P_o, \quad \delta = \rho_f / \rho.$$

Validation Analysis

To validate the proposed flow induced dynamic stress theory, two special cases shall be demonstrated namely:

3.5.1 Case 1: Maximum Bending Stress

The maximum values of the bending stresses viz

$$\sigma_{(x)_1} = -\frac{E}{2} (2z - R_i) \frac{\partial^2 w}{\partial x^2} + x \frac{\tau_{max}}{R_i} + x(\rho + \rho_f) \frac{\partial^2 u}{\partial t^2} \quad (3.49)$$

and

$$\sigma_{(x)_2} = -\frac{E}{2} (2z + R_i) \frac{\partial^2 w}{\partial x^2} + x \frac{\tau_{max}}{R_i} + x(\rho + \rho_f) \frac{\partial^2 u}{\partial t^2} \quad (3.50)$$

occur in the mid-section of the pipe. Thus, in the absence of longitudinal vibration, for an empty pipe, the above equations reduce to the forms

$$\sigma_{(max)_1} = -\frac{E}{2}(2Z - R_i) \frac{\partial^2 w}{\partial x^2} \quad (3.51)$$

and

$$\sigma_{(max)_2} = -\frac{E}{2}(2Z + R_i) \frac{\partial^2 w}{\partial x^2} \quad (3.52)$$

which sum up to give

$$\sigma_{(max)} = \sigma_{(max)_1} + \sigma_{(max)_2} = -EZ \frac{\partial^2 w}{\partial x^2} \quad \forall x = \frac{L}{2} \quad (3.53)$$

Now on substituting $R_i = \frac{d}{2}$, where d, is the internal diameter of the pipe, for this case the result below is obtained:

$$\sigma_{(max)} = -ER_i \frac{\partial^2 w}{\partial x^2} = -E \frac{d}{2} \frac{\partial^2 w}{\partial x^2} \quad \forall x = \frac{L}{2} \quad (3.54)$$

which agrees with the value reported for a circular hollow beam by Ephraim (1997).

3.5.2 Case 2: Maximum Shear Stress

For any fluid flowing through a pipe, the maximum shear stress occurs at the wall of the pipe, cf equations (3.43) and (3.44) namely;

$$\bar{\tau}_{(\bar{z} \bar{x})_1} = \frac{\acute{\alpha}}{2} (\bar{z}^2 - \bar{R}_i \bar{z}) \frac{\partial^3 \bar{w}}{\partial \bar{x}^3} - \frac{\bar{z}}{\bar{R}_i} \bar{\tau}_{max}$$

and

$$\bar{\tau}_{(\bar{z} \bar{x})_2} = \frac{\acute{\alpha}}{2} (\bar{z}^2 + \bar{R}_i \bar{z}) \frac{\partial^3 \bar{w}}{\partial \bar{x}^3} - \frac{\bar{z}}{\bar{R}_i} \bar{\tau}_{max}$$

In fact in the absence of transverse vibration, the bending terms

$\frac{\acute{\alpha}}{2} (\bar{z}^2 - \bar{R}_i \bar{z}) \frac{\partial^3 \bar{w}}{\partial \bar{x}^3}$ and $\frac{\acute{\alpha}}{2} (\bar{z}^2 + \bar{R}_i \bar{z}) \frac{\partial^3 \bar{w}}{\partial \bar{x}^3}$ are negligible. Under this restriction, we can set $\bar{z} = \pm \bar{R}$ at the lower and upper walls of the pipe to obtain the well known maximum shear stresses reported in the literature of fluid mechanics namely;

$$\bar{\tau}_{(\bar{z} \bar{x})_1}(max) = -\bar{\tau}_{max} \quad \text{and} \quad \bar{\tau}_{(\bar{z} \bar{x})_2}(max) = \bar{\tau}_{max} \quad (3.55)$$

3.5.3 Computation of Dynamic Stresses

Now in the Laplace transform domain, equations (3.43) through (3.48) become

$$\bar{\tau}_{(\bar{z} \bar{x})_1}(\bar{x}, \bar{z}, s) = \frac{\acute{\alpha}}{2} (\bar{z}^2 - \bar{R}_i \bar{z}) \frac{d^3 \bar{w}}{d\bar{x}^3}(\bar{x}, s) - \frac{\bar{z}}{\bar{R}_i} \frac{\bar{\tau}_{max}}{s} \quad (3.56)$$

$$\tilde{\tau}_{(\bar{z}\bar{x})_2}(\bar{x}, \bar{z}, s) = \frac{\acute{a}}{2}(\bar{z}^2 + \bar{R}_i\bar{z})\frac{d^3\tilde{w}}{d\bar{x}^3}(\bar{x}, s) - \frac{\bar{z}}{\bar{R}_i}\frac{\bar{\tau}_{max}}{s} \quad (3.57)$$

$$\begin{aligned} \tilde{\sigma}_{\bar{x}_1}(\bar{x}, \bar{z}, s) = & -\frac{\acute{a}}{2}(2\bar{z} - \bar{R}_i)\frac{d^2\bar{w}}{d\bar{x}^2}(\bar{x}, s) + \frac{\bar{x}}{\bar{R}_i}\frac{\bar{\tau}_{max}}{s} + \\ & \bar{x}(1 + \delta)[s^2\tilde{u}(\bar{x}, s) - s\bar{u}(\bar{x}, o) - \dot{\bar{u}}(\bar{x}, o)] \end{aligned} \quad (3.58)$$

$$\begin{aligned} \tilde{\sigma}_{\bar{x}_2}(\bar{x}, \bar{z}, s) = & -\frac{\acute{a}}{2}(2\bar{z} + \bar{R}_i)\frac{d^2\bar{w}}{d\bar{x}^2}(\bar{x}, s) + \frac{\bar{x}}{\bar{R}_i}\frac{\bar{\tau}_{max}}{s} \\ & + \bar{x}(1 + \delta)[s^2\tilde{u}(\bar{x}, s) - s\bar{u}(\bar{x}, o) - \dot{\bar{u}}(\bar{x}, o)] \end{aligned} \quad (3.59)$$

$$\begin{aligned} \tilde{\sigma}_{\bar{z}_1}(\bar{x}, \bar{z}, s) = & -\frac{\acute{a}}{2}\left[\frac{1}{3}(\bar{z}^3 - \bar{R}_o^3) - \frac{1}{2}(\bar{R}_i\bar{z}^2 - \bar{R}_i\bar{R}_o^2)\right]\frac{d^4\tilde{w}}{d\bar{x}^4}(\bar{x}, s) \\ & + \frac{\bar{F}}{2\pi\bar{R}_o s} - \frac{\bar{c}_{st}}{2\pi\bar{R}_o}\left(s\tilde{w}(\bar{x}, s) - s\bar{w}(\bar{x}, o)\right) - \frac{\bar{P}_f}{s} \\ & + (\bar{z} - \bar{R}_o)(1 + \delta)[s^2\tilde{w}(\bar{x}, s) - s\bar{w}(\bar{x}, o) - \dot{\bar{w}}(\bar{x}, o)] \end{aligned} \quad (3.60)$$

$$\begin{aligned} \tilde{\sigma}_{\bar{z}_2}(\bar{x}, \bar{z}, s) = & -\frac{\acute{a}}{2}\left[\frac{1}{3}(\bar{z}^3 + \bar{R}_o^3) - \frac{1}{2}(\bar{R}_i\bar{z}^2 + \bar{R}_i\bar{R}_o^2)\right]\frac{d^4\tilde{w}}{d\bar{x}^4}(\bar{x}, s) \\ & + \frac{\bar{F}}{2\pi\bar{R}_o s} - \frac{(\bar{C}_{st} + \bar{C}_{soil} - \bar{C}_o)}{2\pi\bar{R}_o}\left(s\tilde{w}(\bar{x}, s) - s\bar{w}(\bar{x}, o)\right) - \frac{\bar{K}_{soil}\tilde{w}(\bar{x}, s)}{2\pi\bar{R}_o} \\ & + \frac{\bar{P}_f}{s} + (\bar{z} - \bar{R}_o)(1 + \delta)[s^2\tilde{w}(\bar{x}, s) - s\bar{w}(\bar{x}, o) - \dot{\bar{w}}(\bar{x}, o)] \end{aligned} \quad (3.61)$$

At the same time the initial boundary conditions of simply supported beam at $\bar{x} = (0, L)$; in the Laplace transform plane give

$$\tilde{w}(0, s) = \tilde{w}(L, s) = 0 \quad (3.62)$$

$$\tilde{w}_{xx}(0, s) = \tilde{w}_{xx}(L, s) = 0 \quad (3.63)$$

Equations (3.56) through (3.61) via equations (3.62-3.63) can now be re-written as follows:

$$\tilde{\tau}_{(\bar{z}\bar{x})_1}(\bar{x}, \bar{z}, s) = \frac{\acute{a}}{2}(\bar{z}^2 - \bar{R}_i\bar{z})\frac{d^3\tilde{w}}{d\bar{x}^3}(\bar{x}, s) - \frac{\bar{z}}{\bar{R}_i}\frac{\bar{\tau}_{max}}{s} \quad (3.64)$$

$$\tilde{\tau}_{(\bar{z}\bar{x})_2}(\bar{x}, \bar{z}, s) = \frac{\acute{a}}{2}(\bar{z}^2 + \bar{R}_i\bar{z})\frac{d^3\tilde{w}}{d\bar{x}^3}(\bar{x}, s) - \frac{\bar{z}}{\bar{R}_i}\frac{\bar{\tau}_{max}}{s} \quad (3.65)$$

$$\tilde{\sigma}_{\bar{x}_1}(\bar{x}, \bar{z}, s) = -\frac{\acute{a}}{2}(2\bar{z} - \bar{R}_i)\frac{d^2\bar{w}}{d\bar{x}^2}(\bar{x}, s) + \frac{\bar{x}}{\bar{R}_i}\frac{\bar{\tau}_{max}}{s} + \bar{x}(1 + \delta)s^2\tilde{u}(\bar{x}, s) \quad (3.66)$$

$$\tilde{\sigma}_{\bar{x}_2}(\bar{x}, \bar{z}, s) = -\frac{\acute{a}}{2}(2\bar{z} + \bar{R}_i)\frac{d^2\bar{w}}{d\bar{x}^2}(\bar{x}, s) + \frac{\bar{x}}{\bar{R}_i}\frac{\bar{\tau}_{max}}{s} + \bar{x}(1 + \delta)s^2\tilde{u}(\bar{x}, s) \quad (3.67)$$

$$\tilde{\sigma}_{\bar{z}_1}(\bar{x}, \bar{z}, s) = -\frac{\acute{a}}{2}\left[\frac{1}{3}(\bar{z}^3 - \bar{R}_o^3) - \frac{1}{2}(\bar{R}_i\bar{z}^2 - \bar{R}_i\bar{R}_o^2)\right]\frac{d^4\tilde{w}}{d\bar{x}^4}(\bar{x}, s)$$

$$+ \frac{\bar{F}}{2\pi\bar{R}_o s} - \frac{\bar{C}_{st}}{2\pi\bar{R}_o} s \tilde{w}(\bar{x}, s) - \frac{\bar{P}_f}{s} + (\bar{z} - \bar{R}_o)(1 + \delta) s^2 \tilde{w}(\bar{x}, s) \quad (3.68)$$

$$\begin{aligned} \tilde{\sigma}_{\bar{z}_2}(\bar{x}, \bar{z}, s) = & -\frac{\dot{a}}{2} \left[\frac{1}{3} (\bar{z}^3 + \bar{R}_o^3) - \frac{1}{2} (\bar{R}_i \bar{z}^2 + \bar{R}_i \bar{R}_o^2) \right] \frac{d^4 \tilde{w}}{d\bar{x}^4}(\bar{x}, s) + \frac{\bar{F}}{2\pi\bar{R}_o s} - \frac{(\bar{C}_{st} + \bar{C}_{soil} - \bar{C}_o)}{2\pi\bar{R}_o} s \tilde{w}(\bar{x}, s) \\ & - \frac{\bar{K}_{soil} \tilde{w}(\bar{x}, s)}{2\pi\bar{R}_o} + \frac{\bar{P}_f}{s} + (\bar{z} - \bar{R}_o)(1 + \delta) s^2 \tilde{w}(\bar{x}, s) \end{aligned} \quad (3.69)$$

In view of expressions for $\tilde{w}(\bar{x}, s)$ and $\tilde{u}(\bar{x}, s)$, equations (3.64) to (3.69) are recast as follows:

$$\tilde{t}_{(\bar{z}\bar{x})_1}(\bar{x}, \bar{z}, s) = \frac{\dot{a}}{2} (\bar{z}^2 - \bar{R}_i \bar{z}) \sum_{n=1}^{\infty} n^2 \pi^2 K \left(\frac{1+(-1)^{n+1}}{s(s^2 + \bar{\eta}_1 s + \bar{\eta}^2)} \right) \cos n\pi \bar{x} - \frac{\bar{z} \bar{\tau}_{max}}{\bar{R}_i s} \quad (3.70)$$

$$\tilde{t}_{(\bar{z}\bar{x})_2}(\bar{x}, \bar{z}, s) = \frac{\dot{a}}{2} (\bar{z}^2 + \bar{R}_i \bar{z}) \sum_{n=1}^{\infty} n^2 \pi^2 K \left(\frac{1+(-1)^{n+1}}{s(s^2 + \bar{\eta}_1 s + \bar{\eta}^2)} \right) \cos n\pi \bar{x} - \frac{\bar{z} \bar{\tau}_{max}}{\bar{R}_i s} \quad (3.71)$$

$$\begin{aligned} \tilde{\sigma}_{\bar{x}_1}(\bar{x}, \bar{z}, s) = & \frac{\dot{a}}{2} (2\bar{z} - \bar{R}_i) \sum_{n=1}^{\infty} n\pi K \left(\frac{1+(-1)^{n+1}}{s(s^2 + \bar{\eta}_1 s + \bar{\eta}^2)} \right) \sin n\pi \bar{x} + \frac{\bar{x} \bar{\tau}_{max}}{\bar{R}_i s} \\ & + \bar{x}(1 + \delta) s^2 \left[K_1 \tilde{H}_1(s) \sum_{n=1}^{\infty} \left(\frac{4}{3n\pi} + \frac{4(-1)^{n+1}}{3n\pi} \right) \sin n\pi \bar{x} + \right. \\ & \left. \psi \tilde{H}_2(s) \sum_{n=1}^{\infty} \sin \frac{n\pi \bar{x}}{n\pi} \right] \end{aligned} \quad (3.72)$$

$$\begin{aligned} \tilde{\sigma}_{\bar{x}_2}(\bar{x}, \bar{z}, s) = & \frac{\dot{a}}{2} (2\bar{z} + \bar{R}_i) \sum_{n=1}^{\infty} n\pi K \left(\frac{1+(-1)^{n+1}}{s(s^2 + \bar{\eta}_1 s + \bar{\eta}^2)} \right) \sin n\pi \bar{x} + \frac{\bar{x} \bar{\tau}_{max}}{\bar{R}_i s} \\ & + \bar{x}(1 + \delta) s^2 \left[K_1 \tilde{H}_1(s) \sum_{n=1}^{\infty} \left(\frac{4}{3n\pi} + \frac{4(-1)^{n+1}}{3n\pi} \right) \sin n\pi \bar{x} + \right. \\ & \left. \psi \tilde{H}_2(s) \sum_{n=1}^{\infty} \sin \frac{n\pi \bar{x}}{n\pi} \right] \end{aligned} \quad (3.73)$$

while

$$\begin{aligned} \tilde{\sigma}_{\bar{z}_1}(\bar{x}, \bar{z}, s) = & \frac{\dot{a}}{2} \left[\frac{1}{3} (\bar{z}^3 - \bar{R}_o^3) - \right. \\ & \left. \frac{1}{2} (\bar{R}_i \bar{z}^2 - \bar{R}_i \bar{R}_o^2) \right] \sum_{n=1}^{\infty} n^3 \pi^3 K \left(\frac{1+(-1)^{n+1}}{s(s^2 + \bar{\eta}_1 s + \bar{\eta}^2)} \right) \sin n\pi \bar{x} + \frac{\bar{F}}{2\pi\bar{R}_o s} - \\ & \frac{\bar{C}_{st}}{2\pi\bar{R}_o} s \sum_{n=1}^{\infty} K \left(\frac{1+(-1)^{n+1}}{s(s^2 + \bar{\eta}_1 s + \bar{\eta}^2)} \right) \sin \frac{n\pi \bar{x}}{n\pi} - \frac{\bar{P}_f}{s} + (\bar{z} - \bar{R}_o)(1 + \\ & \delta) s^2 \sum_{n=1}^{\infty} K \left(\frac{1+(-1)^{n+1}}{s(s^2 + \bar{\eta}_1 s + \bar{\eta}^2)} \right) \sin \frac{n\pi \bar{x}}{n\pi} \end{aligned} \quad (3.74)$$

and

$$\begin{aligned}
\tilde{\sigma}_{\bar{z}_2}(\bar{x}, \bar{z}, s) = & \frac{\dot{\alpha}}{2} \left[\frac{1}{3}(\bar{z}^3 + \bar{R}_0^3) + \right] \sum_{n=1}^{\infty} n^3 \pi^3 K \left(\frac{1+(-1)^{n+1}}{s(s^2 + \bar{\eta}_1 s + \bar{\eta}^2)} \right) \sin n \pi \bar{x} + \frac{\bar{F}}{2\pi \bar{R}_0 s} + \frac{\bar{P}_f}{s} \\
& - \left[\frac{(\bar{C}_{st} + \bar{C}_{soil} - \bar{C}_o)s + \bar{K}_{soil}}{2\pi \bar{R}_0} \right] \sum_{n=1}^{\infty} K \left(\frac{1+(-1)^{n+1}}{s(s^2 + \bar{\eta}_1 s + \bar{\eta}^2)} \right) \sin \frac{n\pi \bar{x}}{n\pi} \\
& + (\bar{z} - \bar{R}_0)(1 + \delta) s^2 \sum_{n=1}^{\infty} K \left(\frac{1+(-1)^{n+1}}{s(s^2 + \bar{\eta}_1 s + \bar{\eta}^2)} \right) \sin \frac{n\pi \bar{x}}{n\pi}
\end{aligned} \quad (3.75)$$

Here,

$$K = \left(\frac{\bar{\rho}_w \bar{g} \bar{h} A_p \beta_6}{1 + \bar{\rho}_w \bar{\beta} A_p \beta_6} \right); \quad K_1 = \Gamma \left(\frac{\bar{\rho}_w \bar{g} \bar{h} A_p \beta_7}{1 + \bar{\rho}_w \bar{\beta} A_p \beta_7} \right)^2 \quad \text{and} \quad \psi = \Gamma + \mu(1 + \delta) \bar{g} \quad (3.76)$$

3.6 Analysis of Burst Pressure Induced by Vibration

We shall demonstrate an application of the derived stress relations by considering the influence of flow velocity and other operating conditions on the burst pressure of the vibrating offshore pipeline under investigation. For such an exercise, it is sufficient to invoke some well known empirical relations in the literature. As a special case and following Staat and Duc khoi vu (2006), the burst pressure for a thick-walled pipe without defect is given by the expression

$$\frac{P_b}{\sigma_u} = D \ln \frac{R_o}{R_i} = D \ln \left[1 + \left(\frac{R_o - R_i}{R_i} \right) \right] = D \left[\frac{t}{R_i} - \frac{1}{2} \left(\frac{t}{R_i} \right)^2 + \frac{1}{3} \left(\frac{t}{R_i} \right)^3 - \dots \right] \quad (3.77)$$

which realistic limit load solutions for the cracked pipe must assume asymptotically. For this case, the realistic load is fully captured via the boundary value partial differential equations as represented in equations(3.56) and (3.57). However, for a thin pipe, the approximation reduces to the form

$$\frac{P_b}{\sigma_u} = D \left(\frac{R_o - R_i}{R_i} \right) = D \left(\frac{R_o}{R_i} - 1 \right) \quad (3.78)$$

where the constraint factor D varies for yield conditions. In particular we recall

$$D = \begin{cases} 1 & \text{for Tresca,} \\ \frac{2}{\sqrt{3}} & \text{for Von Mises} \end{cases} \quad (3.79)$$

for problems of pressurized pipes without defects.

We shall next explore the aforementioned relations for the burst pressure in relation to the lower and upper shear stress as represented in equations (3.70) and (3.71).

3.6.1 Computation of Burst Pressure for the Pipe under investigation

For pipe burst, the maximum shear stress theory predicts that $\tau_{zx} = \frac{1}{2} \sigma_Y$, where σ_Y is the yield stress. Following Henry and Ronald (2004), the yield stress is related to the ultimate stress via the expression

$$\sigma_Y = \sigma_u - c\varepsilon_u \quad (3.80)$$

where ,

σ_u = ultimate stress

c = hardening modulus and

ε_u = the strain

This now allows us to redefine the maximum shear stress as

$$\tau_{zx} = \frac{1}{2}(\sigma_u - c\varepsilon_u) \quad (3.82)$$

We next set $\varepsilon_u = 0$ at yield point to rewrite equation (3.82) as

$$\tau_{zx} = \frac{1}{2} \sigma_u \quad (3.83)$$

By invoking the von Mises yield criterion, and recalling equation (3.82), we can in fact compute the burst pressure as

$$\bar{P}_{b1} = \frac{4}{\sqrt{3}} \bar{\tau}_{(zx)_1} \left[\left(\frac{\bar{R}_o - \bar{R}_i}{\bar{R}_i} \right) - \frac{1}{2} \left(\frac{\bar{R}_o - \bar{R}_i}{\bar{R}_i} \right)^2 + \frac{1}{3} \left(\frac{\bar{R}_o - \bar{R}_i}{\bar{R}_i} \right)^3 - \dots \right] \quad (3.84)$$

Equation (3.84) in view of equation (3.70) can be written in the Laplace transform plane as:

$$\begin{aligned} \tilde{P}_{b1} = \frac{2}{\sqrt{3}} \left[\dot{\alpha} (\bar{z}^2 - \bar{R}_i \bar{z}) \sum_{n=1}^{\infty} n^2 \pi^2 K \left(\frac{1 + (-1)^{n+1}}{s(s^2 + \bar{\eta}_1 s + \bar{\eta}^2)} \right) \cos n \pi \bar{x} - \frac{\bar{z}}{\bar{R}_i} \bar{\tau}_{max} \right] & \left[\left(\frac{\bar{R}_o - \bar{R}_i}{\bar{R}_i} \right) - \frac{1}{2} \left(\frac{\bar{R}_o - \bar{R}_i}{\bar{R}_i} \right)^2 + \right. \\ \left. \frac{1}{3} \left(\frac{\bar{R}_o - \bar{R}_i}{\bar{R}_i} \right)^3 - \dots \right] \end{aligned} \quad (3.85)$$

So that on invoking Laplace inversion, the burst pressure for the upper half of the pipe is

$$\begin{aligned} \bar{P}_{b1} = \frac{2}{\sqrt{3}} \dot{\alpha} \left[(\bar{z}^2 - \bar{R}_i \bar{z}) \sum_{n=1}^{\infty} n^2 \pi^2 K (1 + (-1)^{n+1}) \bar{F}_1(t) \cos n \pi \bar{x} - \frac{\bar{z}}{\bar{R}_i} \bar{\tau}_{max} \right] & \left[\left(\frac{\bar{R}_o - \bar{R}_i}{\bar{R}_i} \right) - \right. \\ \left. \frac{1}{2} \left(\frac{\bar{R}_o - \bar{R}_i}{\bar{R}_i} \right)^2 + \frac{1}{3} \left(\frac{\bar{R}_o - \bar{R}_i}{\bar{R}_i} \right)^3 - \dots \right] \end{aligned} \quad (3.86)$$

Similarly, the burst pressure for the lower half of the pipe can be expressed as:

$$\begin{aligned} \bar{P}_{b2} = \frac{2}{\sqrt{3}} \dot{\alpha} \left[(\bar{z}^2 + \bar{R}_i \bar{z}) \sum_{n=1}^{\infty} n^2 \pi^2 K (1 + (-1)^{n+1}) \bar{F}_1(t) \cos n \pi \bar{x} - \frac{\bar{z}}{\bar{R}_i} \bar{\tau}_{max} \right] & \left[\left(\frac{\bar{R}_o - \bar{R}_i}{\bar{R}_i} \right) - \right. \\ \left. \frac{1}{2} \left(\frac{\bar{R}_o - \bar{R}_i}{\bar{R}_i} \right)^2 + \frac{1}{3} \left(\frac{\bar{R}_o - \bar{R}_i}{\bar{R}_i} \right)^3 - \dots \right] \end{aligned} \quad (3.87)$$

3.7 Computation of Buckling Pressure for the Pipe under investigation

Following the analysis in section 3.6, we can in fact compute the buckling pressure via the expression

$$\bar{P}_{(buckling)1} = 2\bar{\tau}_{(zx)1} \left[\left(\frac{\bar{R}_o - \bar{R}_i}{\bar{R}_i} \right) - \frac{1}{2} \left(\frac{\bar{R}_o - \bar{R}_i}{\bar{R}_i} \right)^2 + \frac{1}{3} \left(\frac{\bar{R}_o - \bar{R}_i}{\bar{R}_i} \right)^3 - \dots \right] \quad (3.88)$$

Equation (3.88) in conjunction with equation (3.71) in the transform plane gives:

$$\begin{aligned} \tilde{\bar{P}}_{(buckling)1} = & \left[\dot{\alpha} (\bar{z}^2 - \bar{R}_i \bar{z}) \sum_{n=1}^{\infty} n^2 \pi^2 K \left(\frac{1 + (-1)^{n+1}}{s(s^2 + \bar{\eta}_1 s + \bar{\eta}^2)} \right) \cos n \pi \bar{x} - \frac{\bar{z}}{\bar{R}_i} \bar{\tau}_{max} \right] \left[\left(\frac{\bar{R}_o - \bar{R}_i}{\bar{R}_i} \right) - \right. \\ & \left. \frac{1}{2} \left(\frac{\bar{R}_o - \bar{R}_i}{\bar{R}_i} \right)^2 + \frac{1}{3} \left(\frac{\bar{R}_o - \bar{R}_i}{\bar{R}_i} \right)^3 - \dots \right] \end{aligned} \quad (3.89)$$

Laplace inversion then gives, the buckling pressure for the upper half of the pipe as

$$\begin{aligned} \bar{P}_{(buckling)1} = & \dot{\alpha} \left[(\bar{z}^2 - \bar{R}_i \bar{z}) \sum_{n=1}^{\infty} n^2 \pi^2 K (1 + (-1)^{n+1}) \bar{F}_1(t) \cos n \pi \bar{x} - \frac{\bar{z}}{\bar{R}_i} \bar{\tau}_{max} \right] \left[\left(\frac{\bar{R}_o - \bar{R}_i}{\bar{R}_i} \right) - \right. \\ & \left. \frac{1}{2} \left(\frac{\bar{R}_o - \bar{R}_i}{\bar{R}_i} \right)^2 + \frac{1}{3} \left(\frac{\bar{R}_o - \bar{R}_i}{\bar{R}_i} \right)^3 - \dots \right] \end{aligned} \quad (3.90)$$

while the corresponding buckling pressure for the lower half of the pipe is given by

$$\begin{aligned} \bar{P}_{(buckling)2} = & \dot{\alpha} \left[(\bar{z}^2 + \bar{R}_i \bar{z}) \sum_{n=1}^{\infty} n^2 \pi^2 K (1 + (-1)^{n+1}) \bar{F}_1(t) \cos n \pi \bar{x} - \frac{\bar{z}}{\bar{R}_i} \bar{\tau}_{max} \right] \left[\left(\frac{\bar{R}_o - \bar{R}_i}{\bar{R}_i} \right) - \right. \\ & \left. \frac{1}{2} \left(\frac{\bar{R}_o - \bar{R}_i}{\bar{R}_i} \right)^2 + \frac{1}{3} \left(\frac{\bar{R}_o - \bar{R}_i}{\bar{R}_i} \right)^3 - \dots \right] \end{aligned} \quad (3.91)$$

3.8 Computation of Burst Equation with Barlow's Equation

In industry, Barlow's equation is the simplest and the most widely employed conservative formula for pipelines burst pressure analysis in the absence of vibrations.

However, in this research, the effects of both longitudinal and transverse vibrations imposed by the internal fluid flow, hydrodynamic loading and excitation forces are fully captured as couched in equations (3.84) and (3.85). Nevertheless, for purpose of comparative analysis, we shall invoke the Barlow's equation as reported by Andrew and Mike (2000) viz :

$$p_f = \frac{2t\sigma_u}{(D_o - t)} \quad (3.92)$$

where the following have been defined namely;

p_f = burst pressure

D_o = external diameter

t = pipe wall thickness

σ_u = ultimate tensile strength of the pipe material

As a matter of convention, the ultimate tensile stress is not usually expressed in terms of parameters like internal fluid flow velocity, hydrodynamic loading and excitation forces; nonetheless the nondimensionnalised ultimate tensile strength of the pipe material can be written in this case as

$$\bar{\sigma}_u = \dot{\alpha}(\bar{z}^2 - \bar{R}_i\bar{z}) \frac{d^3\bar{w}}{d\bar{x}^3}(\bar{x}, s) - \frac{2\bar{z}\bar{\tau}_{max}}{\bar{R}_i s} \quad (3.93)$$

which now allow us to rewrite equation.(3.92) as

$$\bar{p}_f(\bar{x}, s) = \frac{2\bar{t}}{\bar{D}_i} \left(\dot{\alpha}(\bar{z}^2 - \bar{R}_i\bar{z}) \frac{d^3\bar{w}}{d\bar{x}^3}(\bar{x}, s) - \frac{2\bar{z}\bar{\tau}_{max}}{\bar{R}_i s} \right) \quad (3.94)$$

Since, Barlow's equation ignores the effect of vibrations, it will in this case give the Laplace inversion of equation (3.94) as

$$\bar{p}_f = -\frac{2\bar{z}\bar{t}}{\bar{R}_i^2} \bar{\tau}_{max} \quad (3.95)$$

Equation (3.95) then represents the computation of burst pressure from our theory via Barlow's equation. On the other hand, if the effect of vibrations are incorporated, the analytic expression for the case of upper layer burst pressure can be written as

$$\bar{P}_{b1} = \frac{2\dot{\alpha}\bar{t}}{\sqrt{3}\bar{R}_i} \left[(\bar{z}^2 - \bar{R}_i\bar{z}) \sum_{n=1}^{\infty} n^2 \pi^2 K(1 + (-1)^{n+1}) \bar{F}_1(t) \cos n\pi\bar{x} - \frac{2\bar{z}\bar{t}}{\bar{R}_i^2} \bar{\tau}_{max} \right] \quad (3.96)$$

which for the case n = 1(principal mode), gives

$$\bar{P}_{b1} = \frac{4\dot{\alpha}\bar{t}}{\sqrt{3}\bar{R}_i} \left[(\bar{z}^2 - \bar{R}_i\bar{z}) \pi^2 K \bar{F}_1(t) \cos\pi\bar{x} - \frac{\bar{z}\bar{t}}{\bar{R}_i^2} \bar{\tau}_{max} \right] \quad (3.97)$$

3.9 Analysis and Discussion of Results

In this work, the problem of dynamic stress propagation through a fluid conveying pipe in a generalised offshore environment is investigated. The significance of this exercise is to model stress propagation that come into play in the presence of transverse and longitudinal vibrations in a fluid conveying beam. In particular, the effect of operating parameters or variables such as hydrodynamic wave loading, fluid transport velocity, pressure and temperature of the internal fluid as well as the seabed subsoil layer geotechnical properties on the phenomena of pipe bursting and buckling are highlighted.

For the interpretation of results, simulations based on the characteristic values of some of the fluid and geo-mechanical parameters that govern this fluid-structure-soil interaction problem have been carried out. In particular some of the values used in the simulation are listed in Table 3.1 below.

Of fundamental interest are the burst and buckling pressure profiles for the fluid conveying pipeline. In particular, Figures 3.2 to 3.4 display the variation of upper layer steady state burst pressure profiles with respect to the internal flow velocity for some selected pipe thicknesses in an ocean environment. For this case, a pipe of inner radius 0.197 m and length 6m was used for the analysis which was carried out for different locations along the pipe length. Other parameters such as the cross sectional area deformation of pipe, depth of pipe from sea surface and are kept constant.

However, from Figures 3.2 and 3.3. it is observed that, for the fundamental mode and irrespective of pipe thickness or geology of the sea bed, the burst pressure increases monotonically with the fluid transport velocity; Furthermore, and as would be expected, the thicker the pipe, the higher would be the burst pressure required. However when the mode of vibration n changes, this pattern of behaviour changes. In particular, we find that when the mode is even, as for example for cases $n = 2, 4$; the burst pressure behaviour is strongly influenced by the geology of the sea bed. For example, whereas the pattern of behaviour for hard bed (Figures 3.5 and 3.7) remains the same as was earlier described, the soft bed allows the burst pressure to rise with increasing flow velocity up to a peak beyond which it gets attenuated as illustrated in Figures 3.4 and 3.6. By comparing the corresponding figures, it is also observed that the soft sea bed, will in general support a higher burst pressure than a hard sea bed at the same conveyance velocity of internal flow.

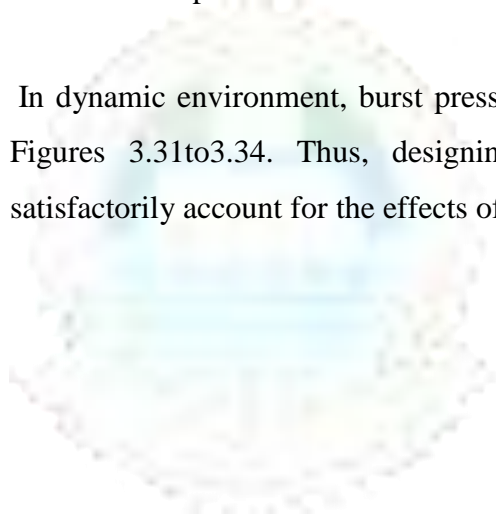
It is also noted that for a given pipe and whether it is lying on a soft sea bed (Figures 3.8 and 3.9) or hard bed (Figures 3.11 and 3.12), the even modes have higher burst pressure values than for odd modes. For a given mode and irrespective of the geology of the sea bed, the burst pressure is always greater than the buckling pressure as is clearly illustrated in Figures 3.14 and 3.15 for case $n = 2$.

Figures 3.16 and 3.17 show the stress distribution across the diameter of the pipe. It can be observed that at the inlet there is a slight asymmetry in the stress distribution with the upper half of the pipe supporting higher burst pressure values than the corresponding image. Furthermore, the burst pressure is also a function of the mass ratio of the internal fluid with the lighter fluid commanding a higher burst pressure. However, as one transcends the entry length such differences tend to be attenuated completely as shown for the situation half way through the pipe length in Figures 3.20 and 3.21.

As can be seen in the hatched zones (Figures 3.24 and 3.25), there is a tendency for the existence of regions of multiple buckles and hybrid phenomena, both for soft and hard beds. These regions are very significant and can be positively exploited for deep and ultra deep waters subsea pipeline and flow line designs.

On the other hand, Figures 3.26 to 3.32 displayed plots of upper burst pressure profiles for both soft and hard beds as computed from Barlow's equation model. In particular, Figure 3.26 to 3.30 illustrate the effects of pipe length for both soft and hard sea beds. In fact, comparison of the burst pressures from Barlow's equation and our model showed that there is a variation of about 50% for the case of a long pipeline on a hard sea bed as can be observed in Figures 3.28 to 3.30. These results showed that fluid conveyance systems are likely to burst in lower pressure range on hard seabed in comparison with soft bed.

In dynamic environment, burst pressure can be significantly affected by vibrations as shown in Figures 3.31 to 3.34. Thus, designing such fluid transmission or conveyance media must satisfactorily account for the effects of vibrations propagation.



UNIVERSITY
OF LAGOS

Table 3.1: Parametric Values Used For Simulation

S/N	DESCRIPTION	SYMBOL	VALUES USED
1	Density of pipe material	ρ	7850Kg/m ³
2	Density of sea water	ρ_w	980 kg/m ³
3	Pipeline fluid relative density	ρ_f	0.977 kg/m ³
4	Wave number	k	0.1
5	Characteristic stress	T_o	5x10 ¹⁸ N/m ²
6	Modulus of elasticity of pipe material	E	200GN/m ²
7	Acceleration due to free fall	g	9.8m/s ²
8	Height (depth) of pipeline below mean sea surface	h	1500m
9	Seabed modulus of deformation	K_b	8, 800N/m
10	Length of the pipeline	L	6m
11	External Diameter	D_o	0.4064m
12	Internal Diameter	D_i	0.394m
13	Inner Radius of the pipeline	R	$D_i/2$
14	Moment of inertia	I	1.17x10 ⁻⁵ m ⁴
15	Uniform fluid flow velocity through the pipe	U	3 m/s
16	Transverse pipe displacement	w	$w(x, t)$
17	Axial pipe displacement	u	$u(x, t)$
18	Temperature	θ	110°C
19	Temperature gradient	$\Delta\theta$	10°C
20	Pressure	P	1-5x10 ⁵ N/m
21	Tensile prestress	T	5x10 ¹⁸ N/m ²
22	Damping force/vel. in transverse and axial direction resp.	$C_1, C_2,$	1, 5
23	Normalised density of water	$\bar{\rho}_w$	1

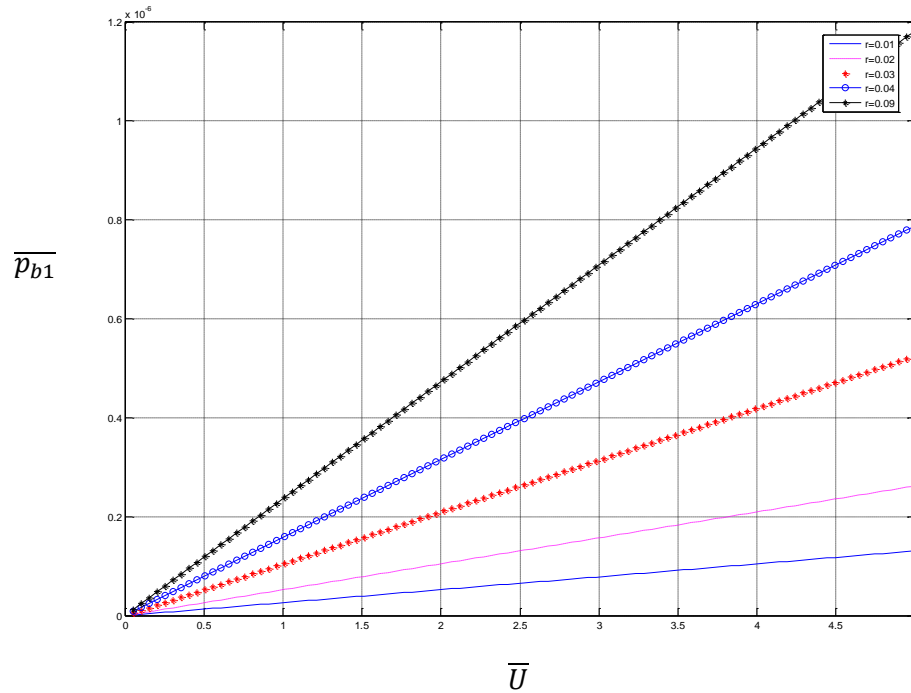


Fig. 3.2: Steady state burst pressure profile at the upper layer of the pipe on a soft sea bed for the case $n = 1; \bar{x} = 0.5; \bar{z} = 1; \bar{K}_b = 8$

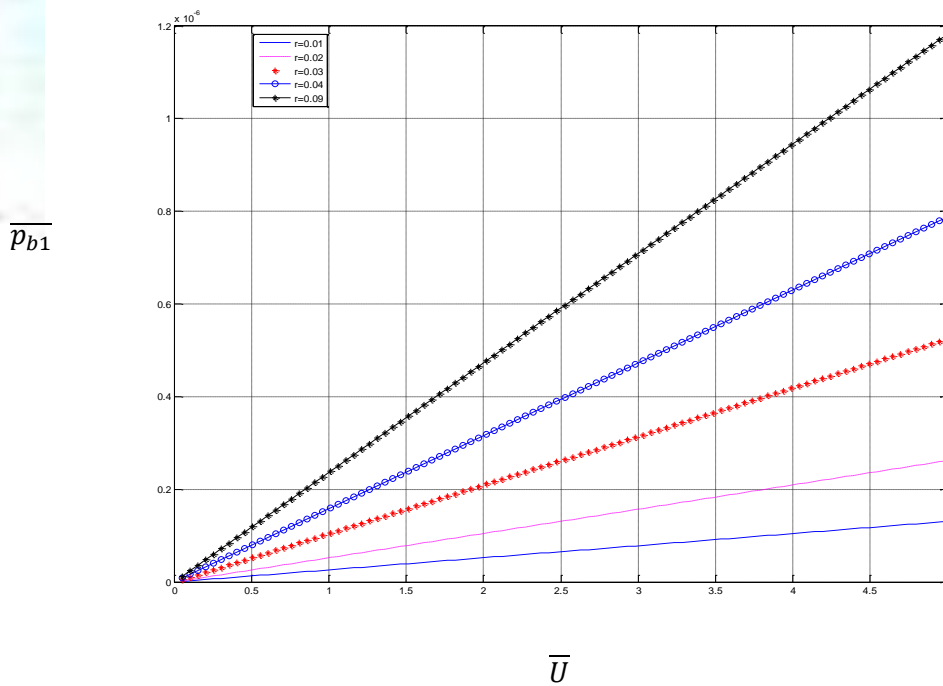


Fig. 3.3: Steady state burst pressure profile at the upper layer of the pipe on a hard sea bed for the case $n = 1; \bar{x} = 0.5; \bar{z} = 1; \bar{K}_b = 800$

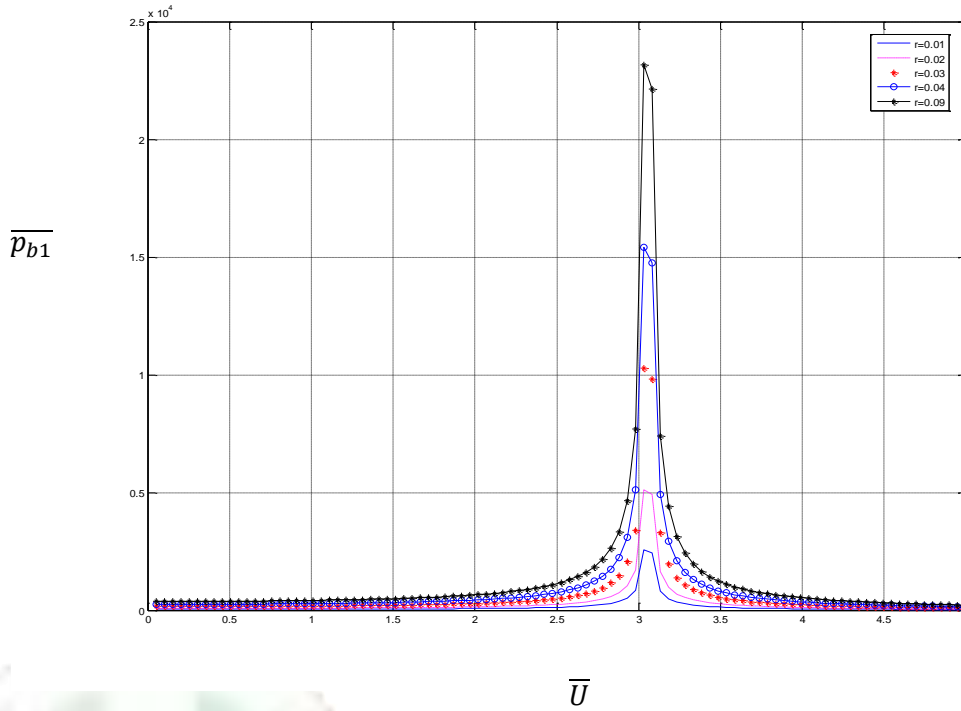


Fig. 3.4: Steady state burst pressure profile at the upper layer of the pipe on a soft sea bed for the case $n = 2$; $\bar{x} = 0.5$; $\bar{z} = 1$; $\bar{K}_b = 8$

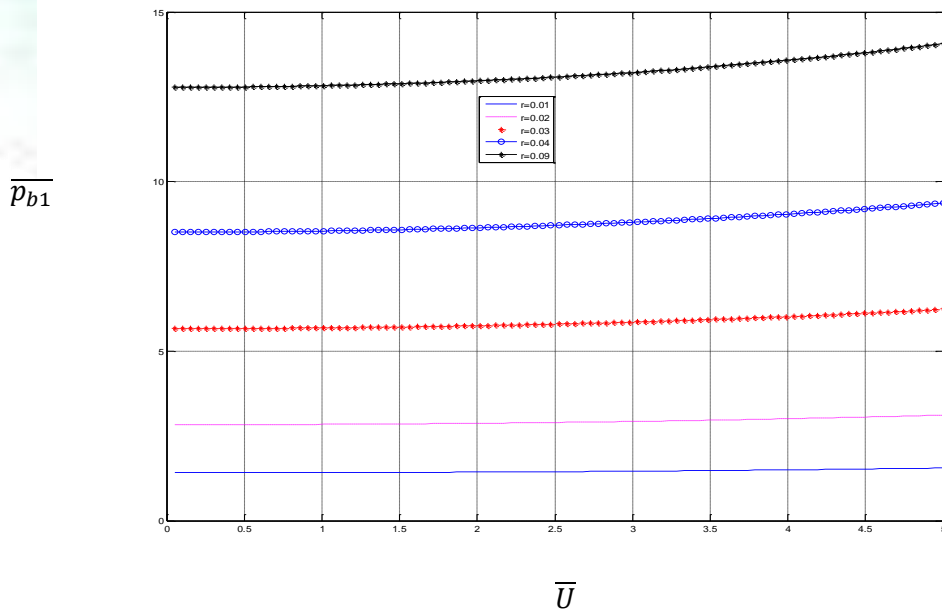


Fig. 3.5: Steady state burst pressure profile at the upper layer of the pipe on a hard sea bed for the case $n = 2$; $\bar{x} = 0.5$; $\bar{z} = 1$; $\bar{K}_b = 800$

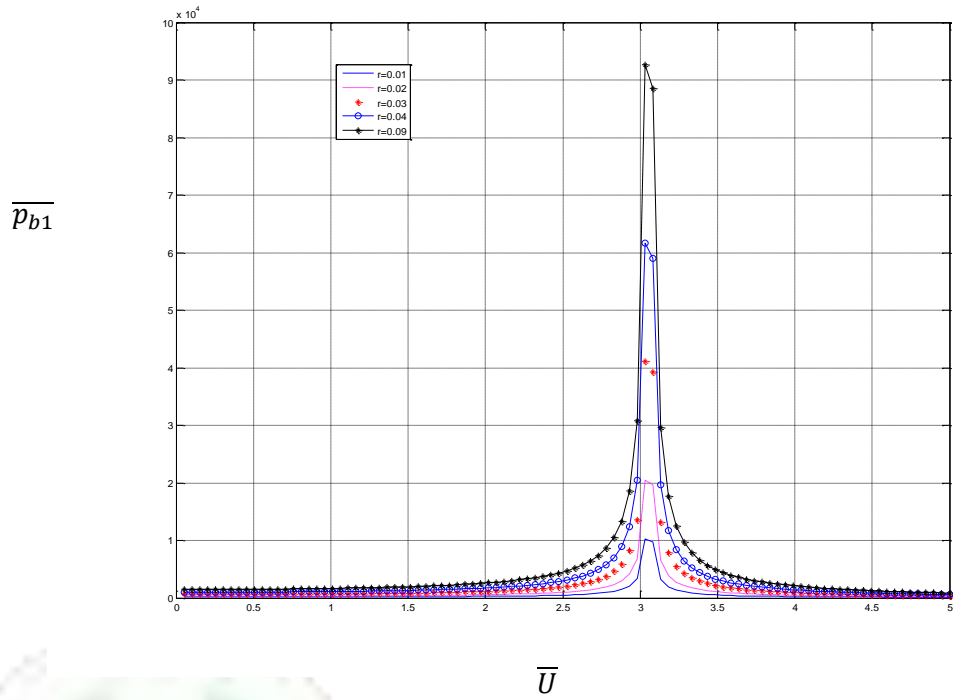


Fig. 3.6: Steady state burst pressure profile at the upper layer of the pipe on a soft sea bed for the case $n = 4; \bar{x} = 0.5; \bar{z} = 1; \bar{K}_b = 8$

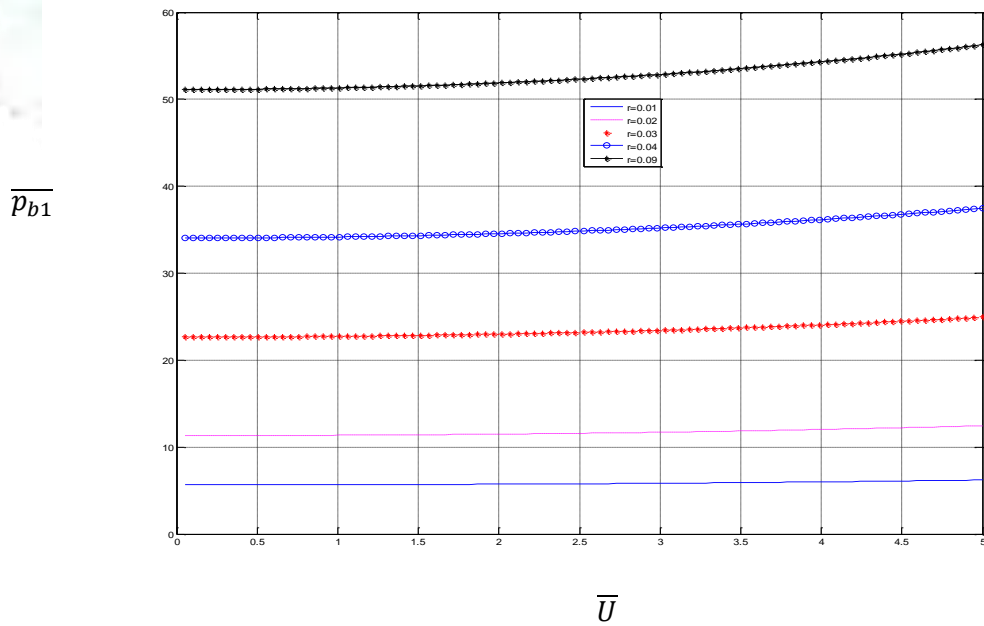


Fig. 3.7: Steady state burst pressure profile at the upper layer of the pipe on a hard sea bed for the case $n = 4; \bar{x} = 0.5; \bar{z} = 1; \bar{K}_b = 800$

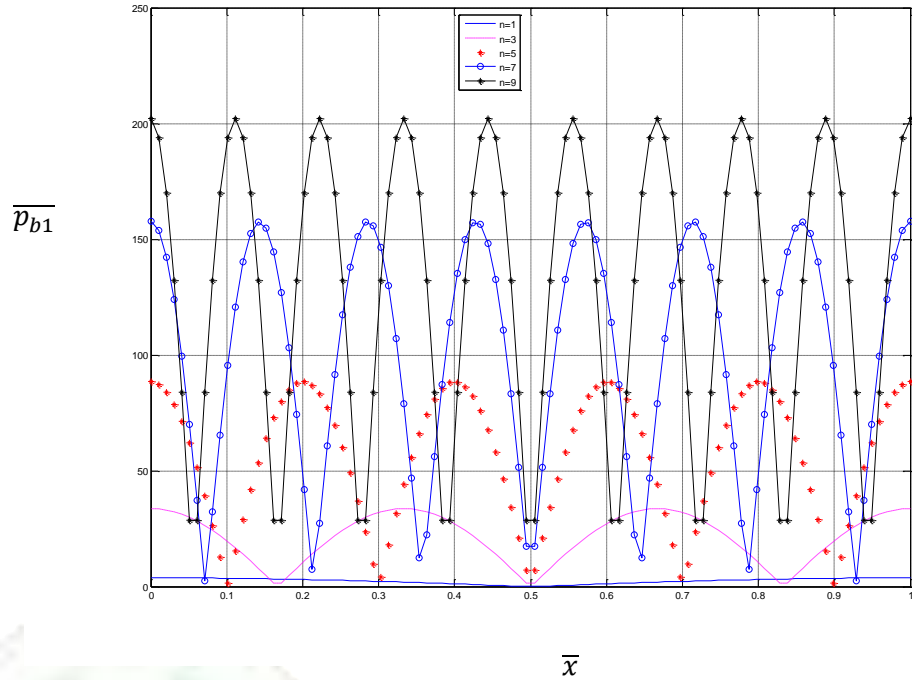


Fig.3.8: Steady state burst pressure profile at the upper layer of the pipe on a soft sea bed for the case normalized pipe thickness = 0.1; $\bar{U} = 0.5$; $\bar{z} = 1$; $\bar{K}_b = 8$

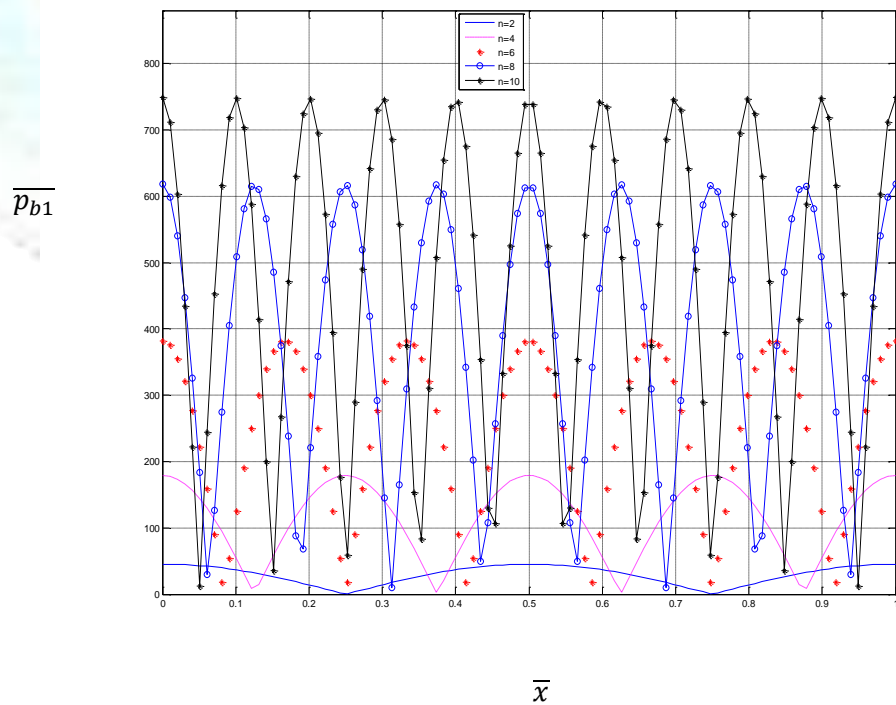


Fig. 3.9: Steady state burst pressure profile at the upper layer of the pipe on a soft sea bed for the case normalized pipe thickness = 0.1; $\bar{U} = 0.5$; $\bar{z} = 1$; $\bar{K}_b = 8$

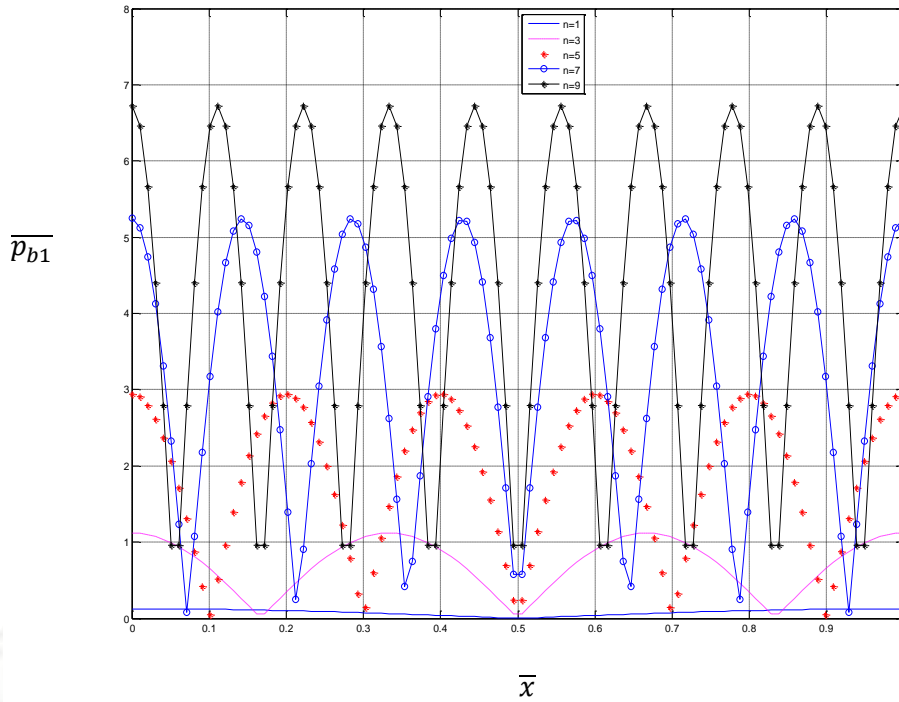


Fig.3.10: Steady state burst pressure profile at the upper layer of the pipe on a hard sea bed for the normalized pipe thickness = 0.1; $\bar{U} = 0.5$; $\bar{z} = 1$; $\bar{K}_b = 800$

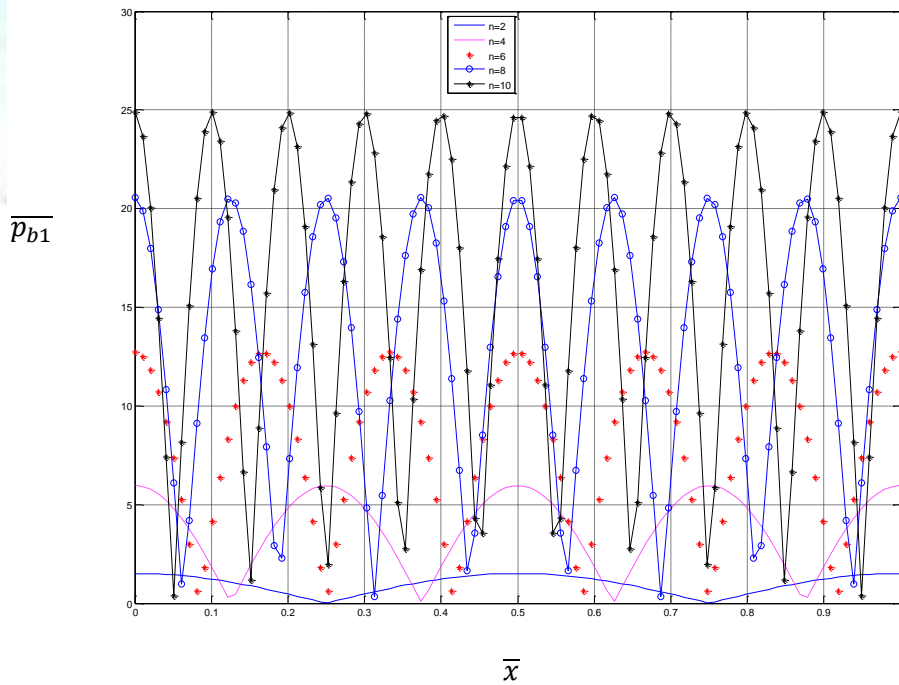


Fig.3.11: Steady state burst pressure profile at the upper layer of the pipe on a hard sea bed for the case normalized pipe thickness = 0.1; $\bar{U} = 0.5$; $\bar{z} = 1$; $\bar{K}_b = 800$

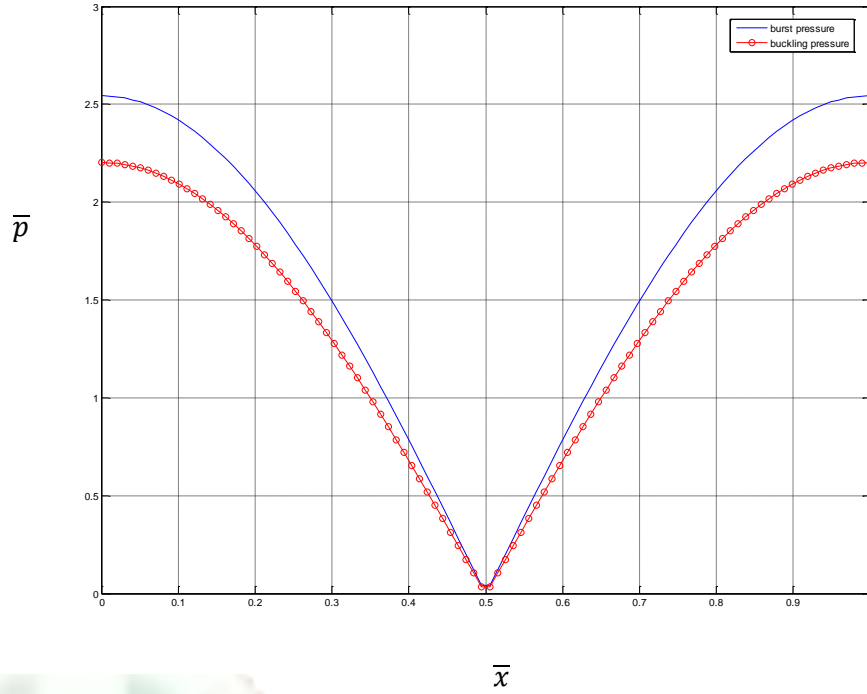


Fig.3.12: Steady state pressure profile at the upper layer of the pipe on a soft sea bed for the case
normalized pipe thickness = 0.1; $n = 1$; $\bar{U} = 5$; $\bar{z} = 1$; $\bar{K}_b = 8$

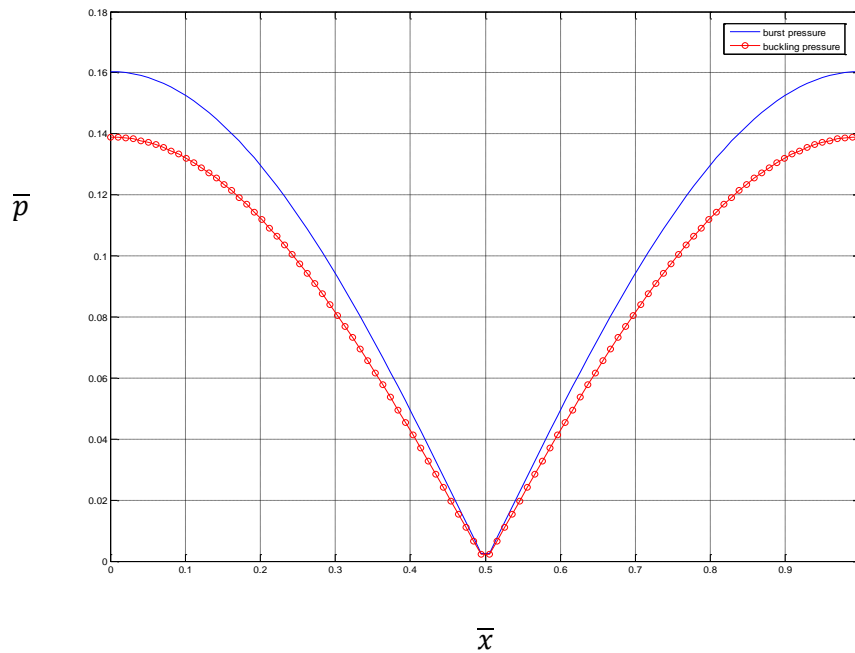


Fig.3.13: Steady state pressure profile at the upper layer of the pipe on a hard sea bed for the case
normalized pipe thickness = 0.1; $n = 1$; $\bar{U} = 5$; $\bar{z} = 1$; $\bar{K}_b = 800$

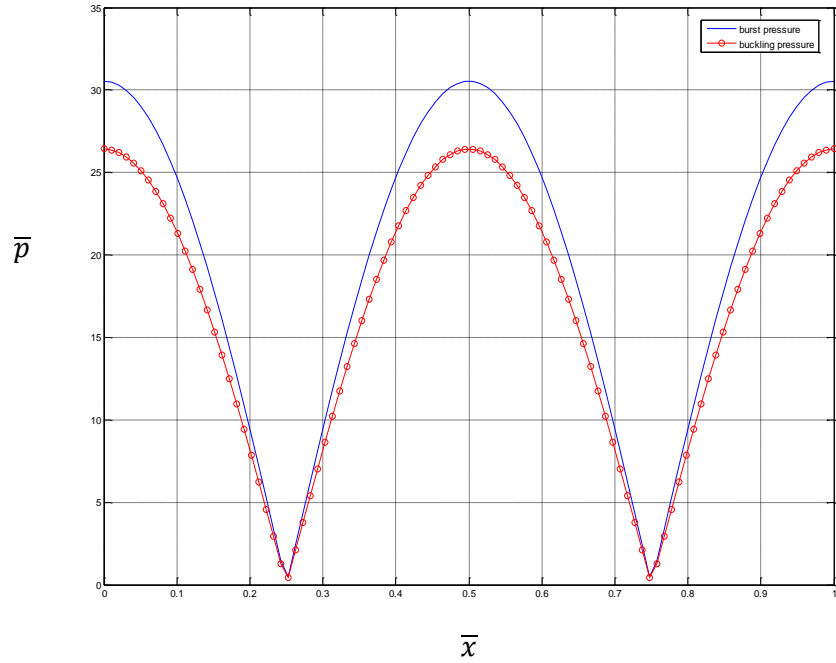


Fig.3.14: Steady state pressure profile at the upper layer of the pipe on a soft sea bed for the case *normalized pipe thickness* = 0.1; $n = 2$; $\bar{U} = 5$; $\bar{z} = 1$; $\bar{K}_b = 8$

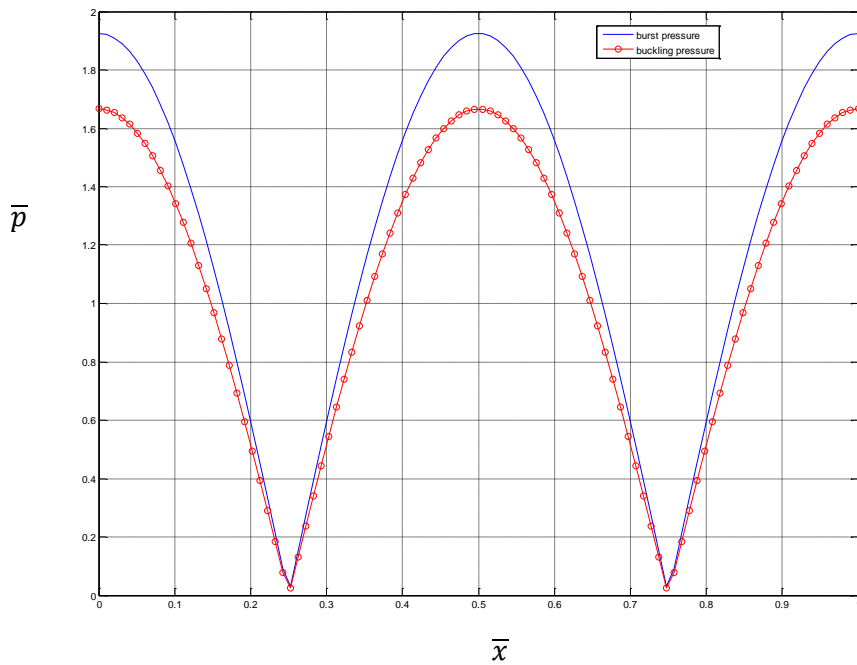


Fig.3.15: Steady state pressure profile at the upper layer of the pipe on a hard sea bed for the case *normalized pipe thickness* = 0.1; $n = 2$; $\bar{U} = 5$; $\bar{z} = 1$; $\bar{K}_b = 800$

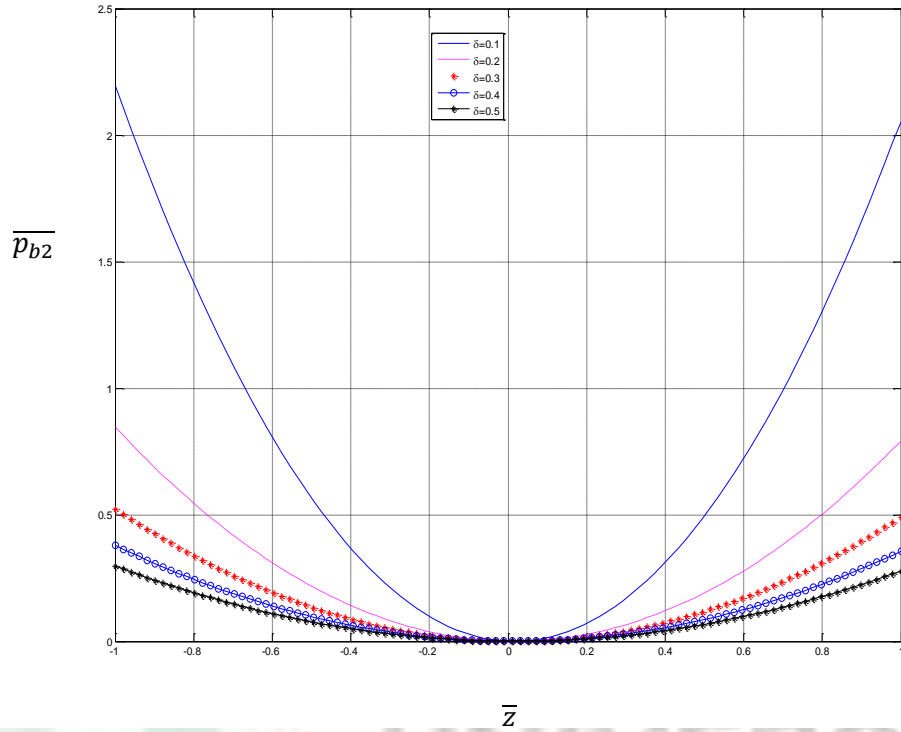


Fig.3.16: Steady state burst pressure profile at the lower layer of the pipe on a soft sea bed for the case normalized pipe thickness = 0.1; $\bar{x} = 0$; $n = 1$; $\bar{U} = 5$; $\bar{K}_b = 8$

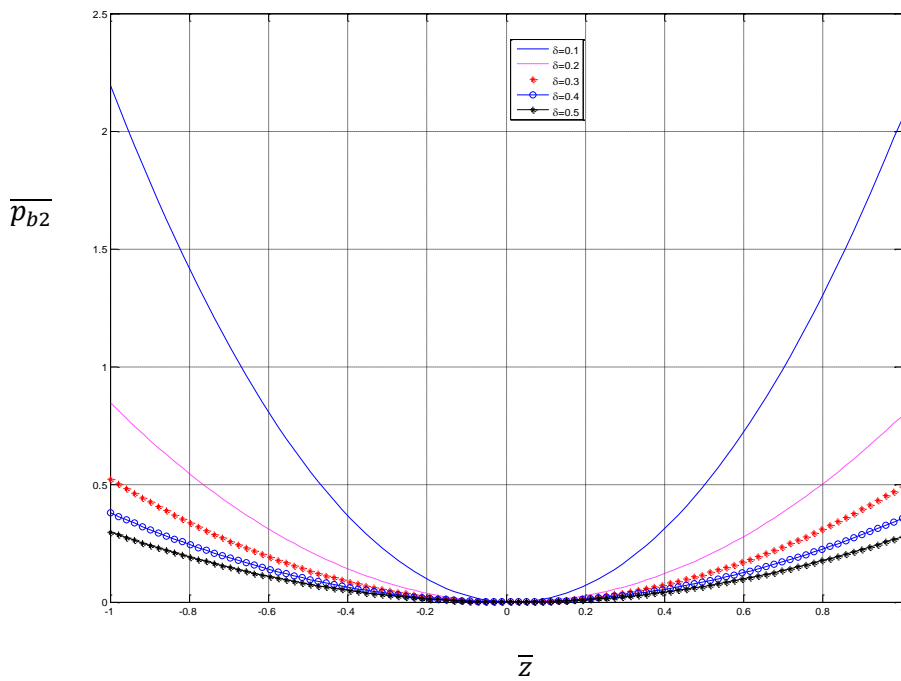


Fig.3.17: Steady state burst pressure profile at the lower layer of the pipe on a hard sea bed for the case normalized pipe thickness = 0.1; $\bar{x} = 0$; $n = 1$; $\bar{U} = 5$; $\bar{K}_b = 800$

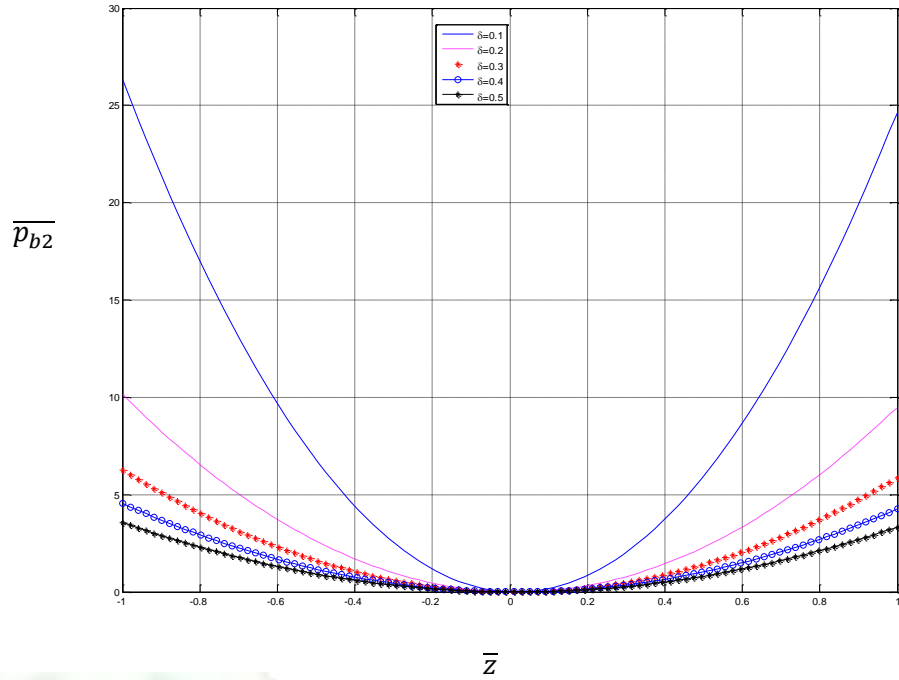


Fig.3.18: Steady state burst pressure profile at the upper layer of the pipe on a soft sea bed for the case *normalized pipe thickness* = 0.1; $\bar{x} = 0$; $n = 2$; $\bar{U} = 5$; $\bar{K}_b = 8$

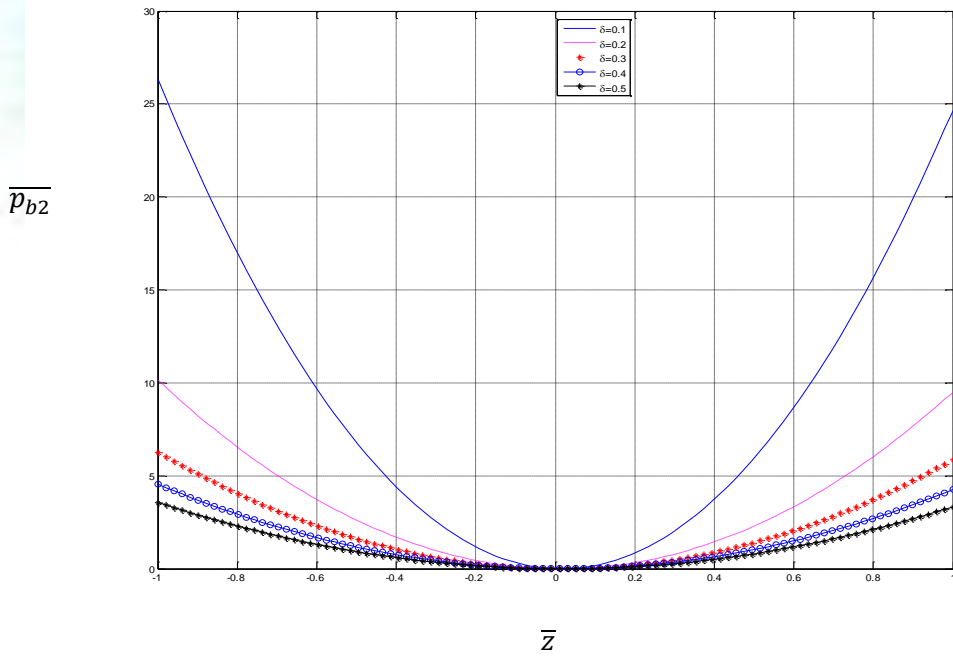


Fig. 3.19: Steady state burst pressure profile at the upper layer of the pipe on a soft sea bed for the case *normalized pipe thickness* = 0.1; $\bar{x} = 0$; $n = 2$; $\bar{U} = 5$; $\bar{K}_b = 8$

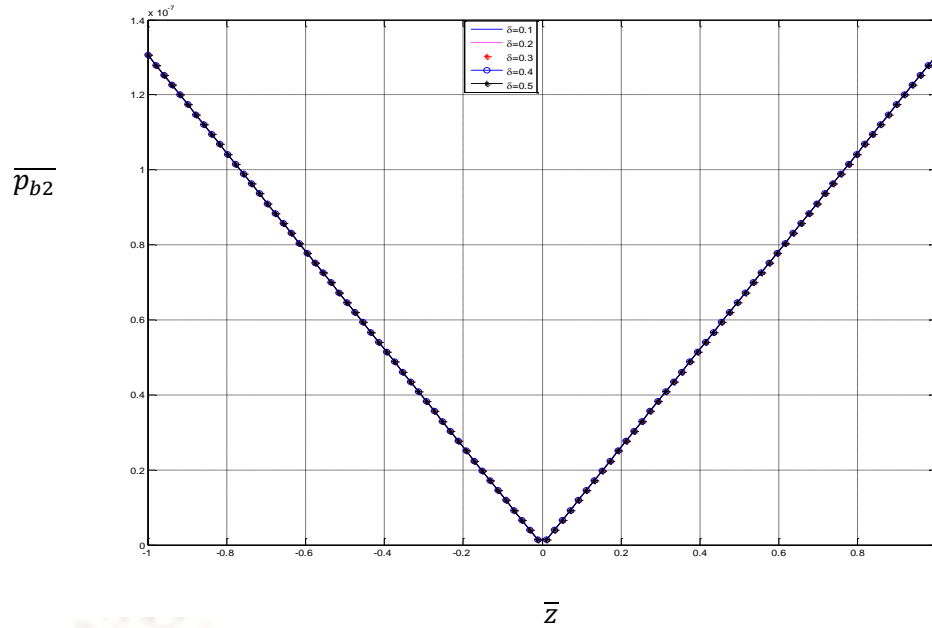


Fig. 3.20: Steady state burst pressure profile at the upper layer of the pipe on a soft sea bed for the case *normalized pipe thickness* = 0.1; $\bar{x} = 0.5$; $n = 1$; $\bar{U} = 5$; $\bar{K}_b = 8$

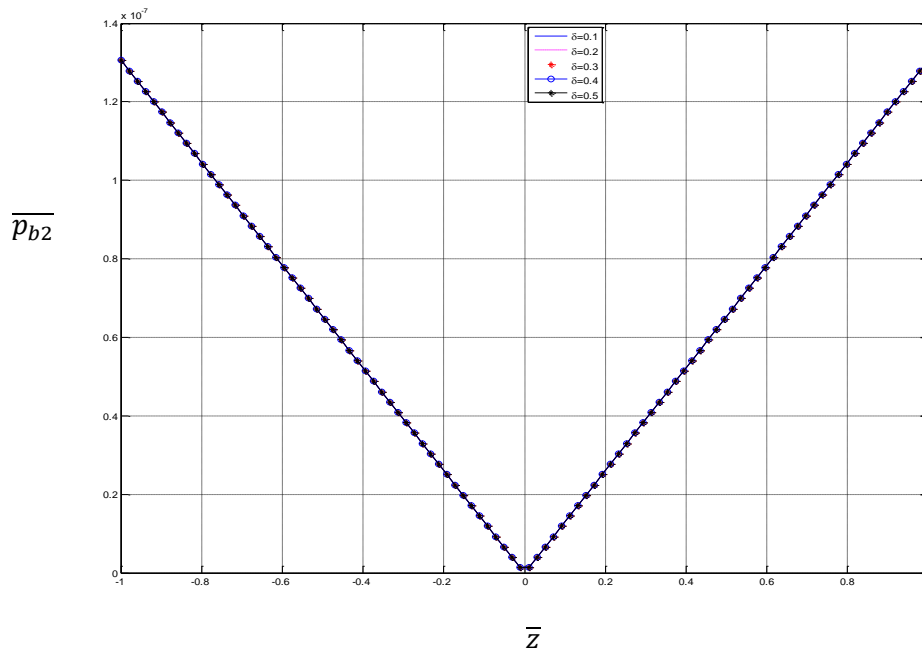


Fig.3.21: Steady state burst pressure profile at the upper layer of the pipe on a hard sea bed for the case *normalized pipe thickness* = 0.1; $\bar{x} = 0.5$; $n = 1$; $\bar{U} = 5$; $\bar{K}_b = 800$

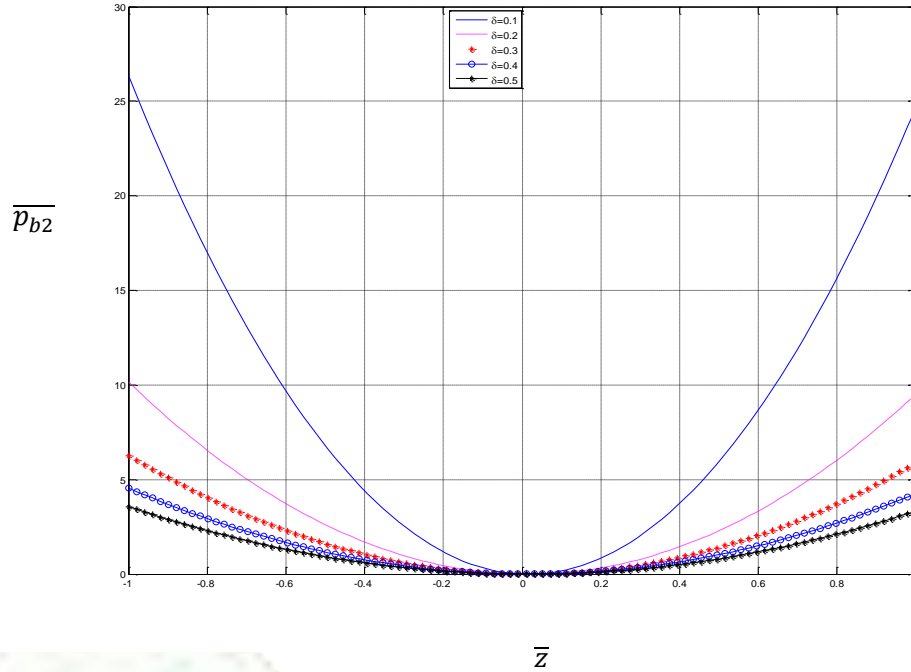


Fig.3.22: Steady state burst pressure profile at the upper layer of the pipe on a soft sea bed for the case $\text{normalized pipe thickness} = 0.1; \bar{x} = 0.5; n = 2; \bar{U} = 5; \bar{K}_b = 8$

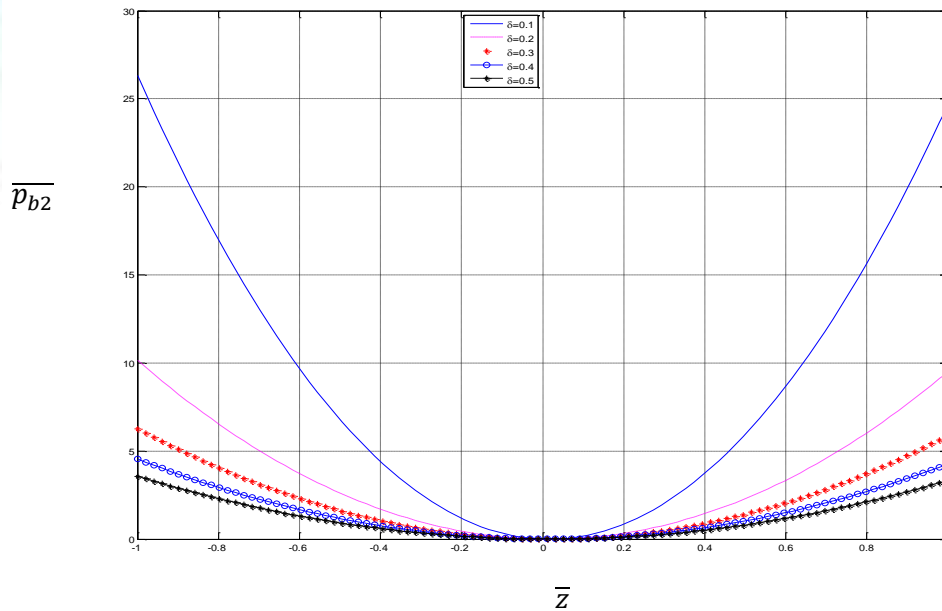


Fig.3.23: Steady state burst pressure profile at the upper layer of the pipe on a hard sea bed for the case $\text{normalized pipe thickness} = 0.1; \bar{x} = 0.5; n = 2; \bar{U} = 5; \bar{K}_b = 800$

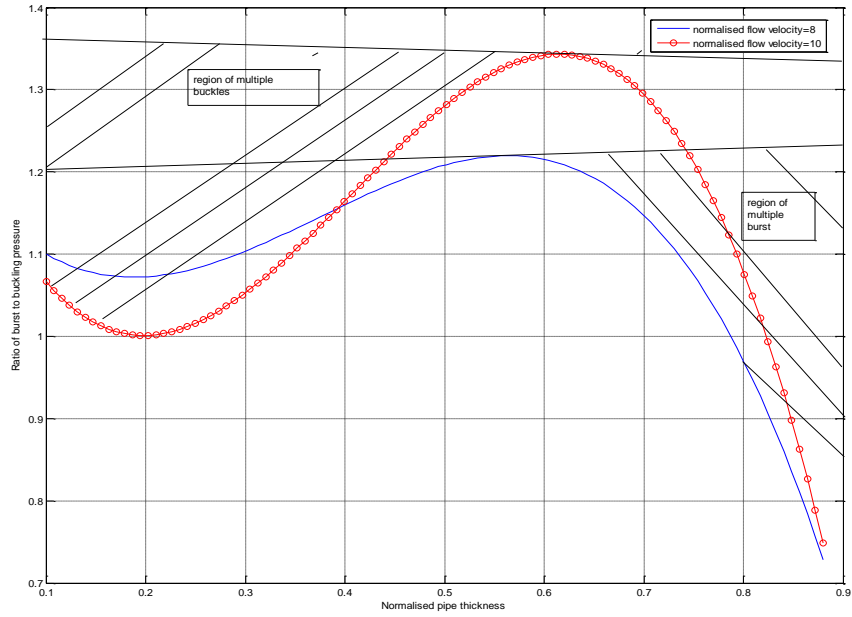


Fig.3.24: Ratio of steady state burst/buckling pressure profile at the upper layer of the pipe on a hard sea bed for the case $\bar{x} = 0$; $\bar{z} = 1$; $\bar{K}_b = 800$

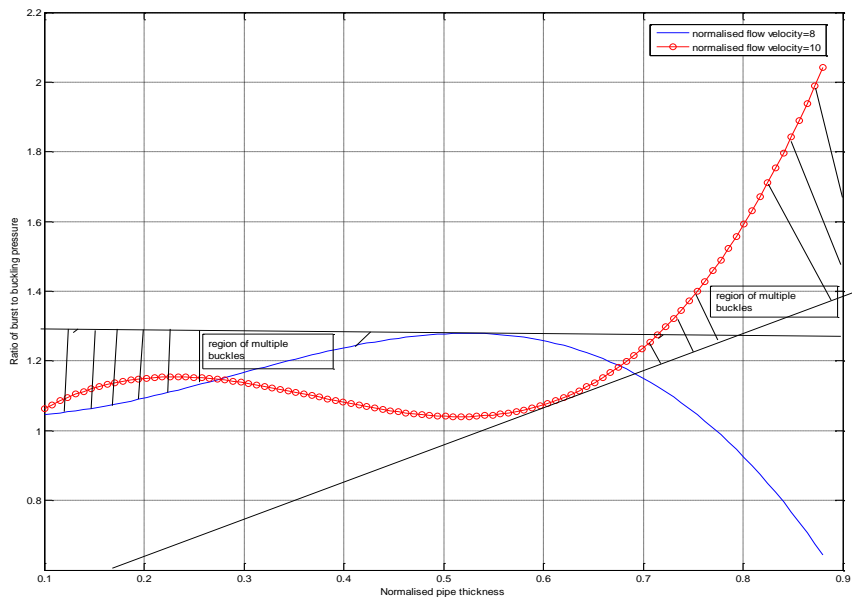


Fig.3.25: Ratio of steady state burst/buckling pressure profile at the upper layer of the pipe on a soft sea bed for the case $\bar{x} = 0$; $\bar{z} = 1$; $\bar{K}_b = 8$

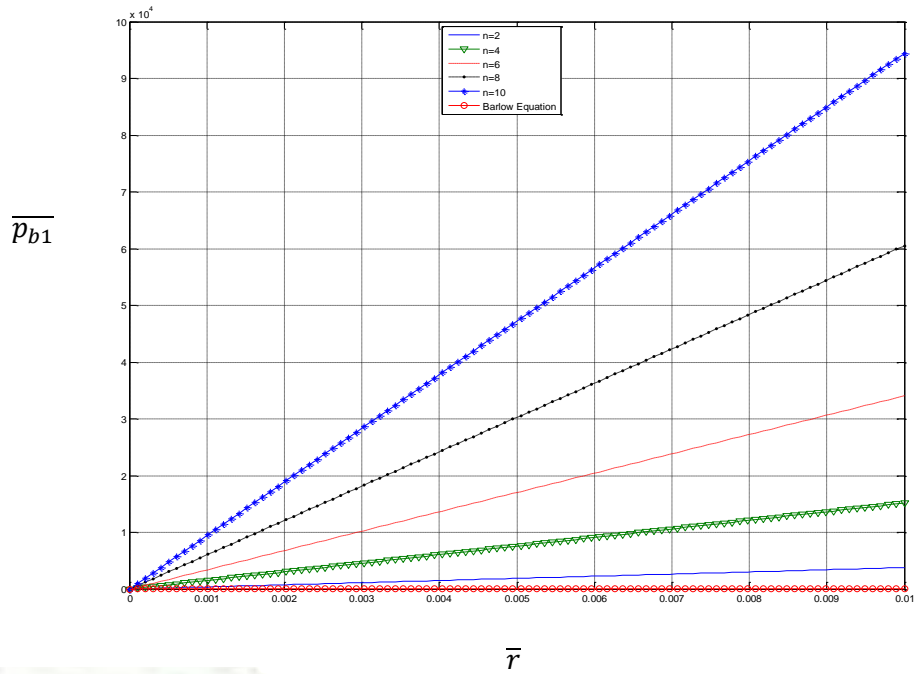


Fig.3.26: Steady state burst pressure profile at the upper layer of the pipe on a soft sea bed for the case $\bar{x} = 0.5; z = 1, L = 6km, \bar{U} = 0.5; \bar{K}_b = 8$

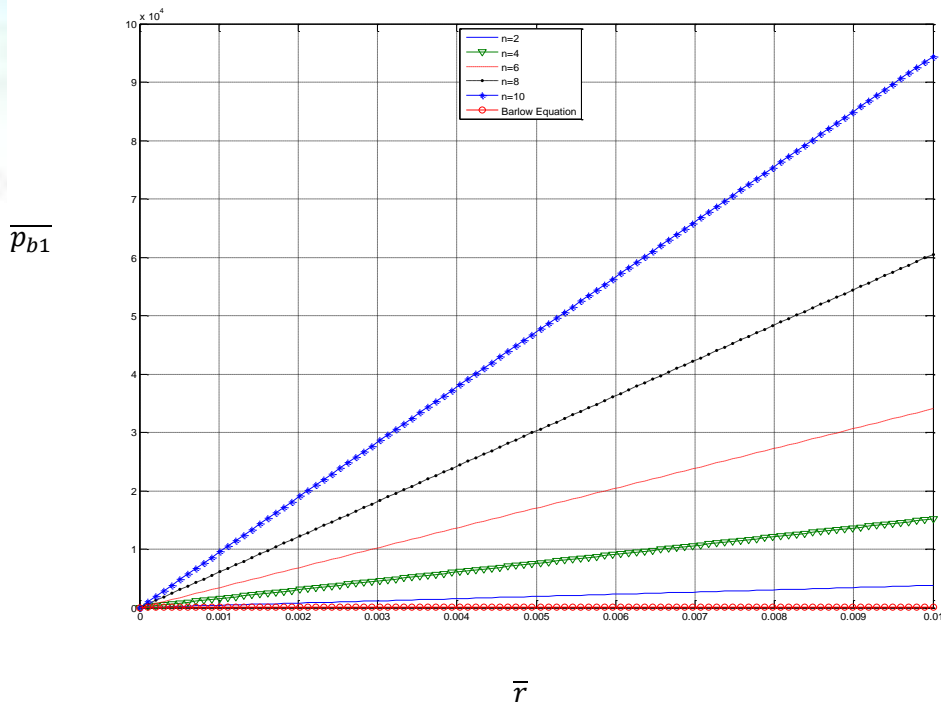


Fig.3.27: Steady state burst pressure profile at the upper layer of the pipe on a soft sea bed for the case $\bar{x} = 0.5; z = 1, L = 6m, \bar{U} = 0.5; \bar{K}_b = 8$

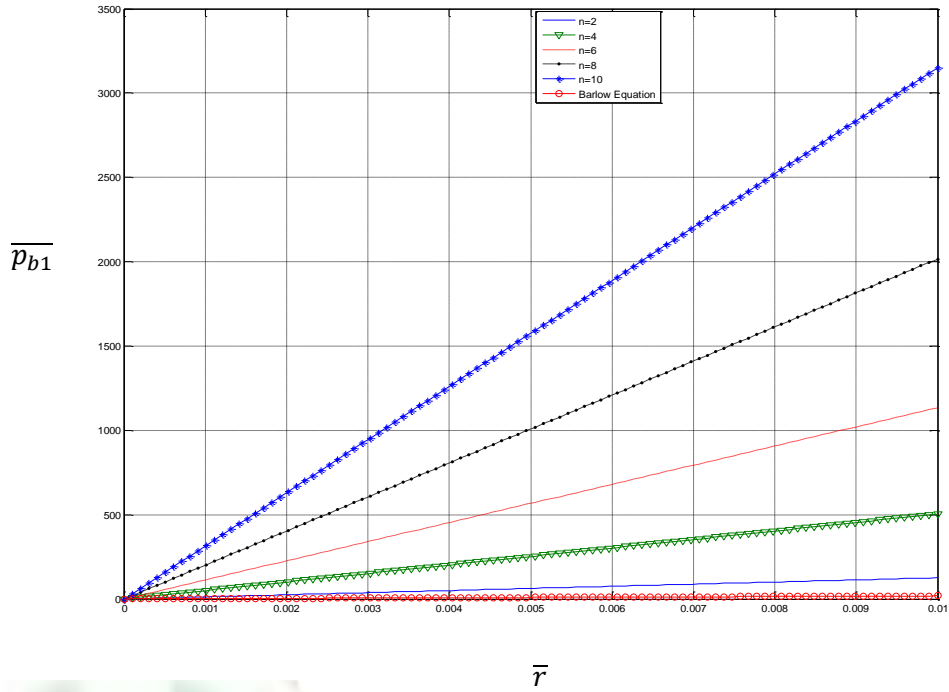


Fig.3.28: Steady state burst pressure profile at the upper layer of the pipe on a hard sea bed for the case $\bar{x} = 0.5; z = 1, L = 6m, \bar{U} = 0.5; \bar{K}_b = 800$

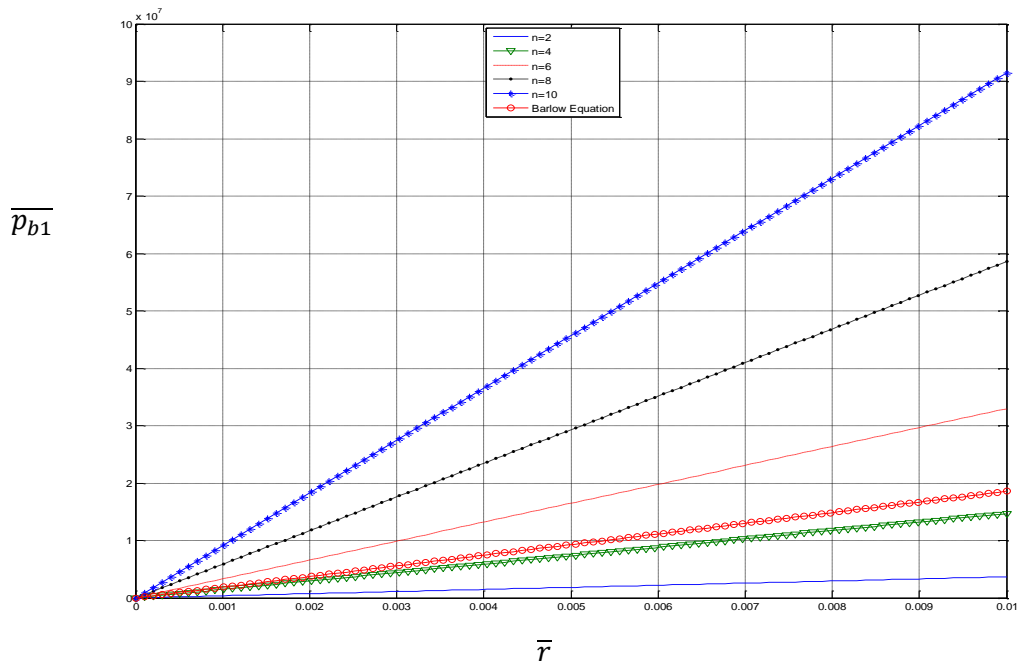


Fig.3.29: Steady state burst pressure profile at the upper layer of the pipe on a soft sea bed for the case $\bar{x} = 0.5; z = 1, L = 6km, \bar{U} = 0.5; \bar{K}_b = 8$

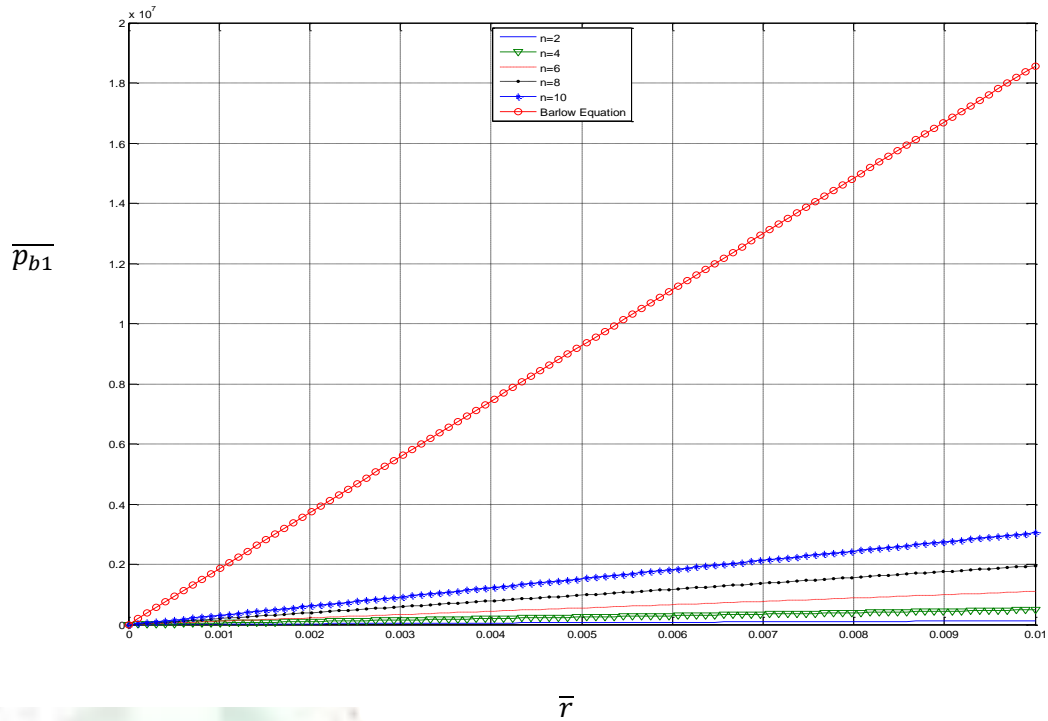


Fig.3.30: Steady state burst pressure profile at the upper layer of the pipe on a hard sea bed for the case $\bar{x} = 0.5; z = 1, L = 6km, \bar{U} = 0.5; \bar{K}_b = 800$

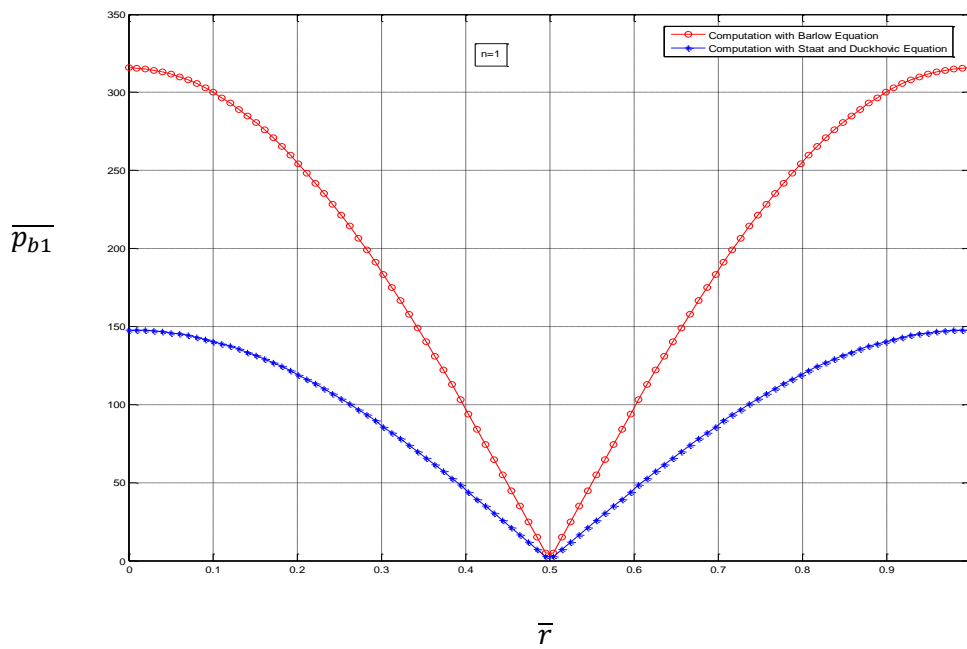


Fig.3.31: Steady state burst pressure profile at the upper layer of the pipe on a soft sea bed for the case $\bar{x} = 0.5; z = 1, L = 6m, \bar{U} = 0.5; \bar{K}_b = 8$

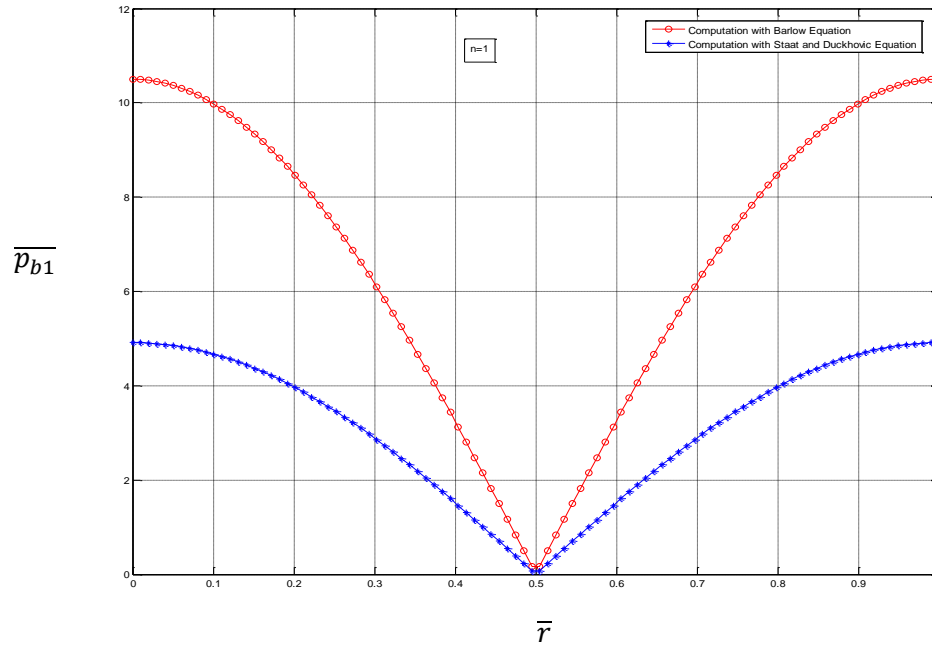


Fig.3.32: Steady state burst pressure profile at the upper layer of the pipe on a hard sea bed for the case $\bar{x} = 0.5; z = 1, L = 6m, \bar{U} = 0.5; \bar{K}_b = 800$

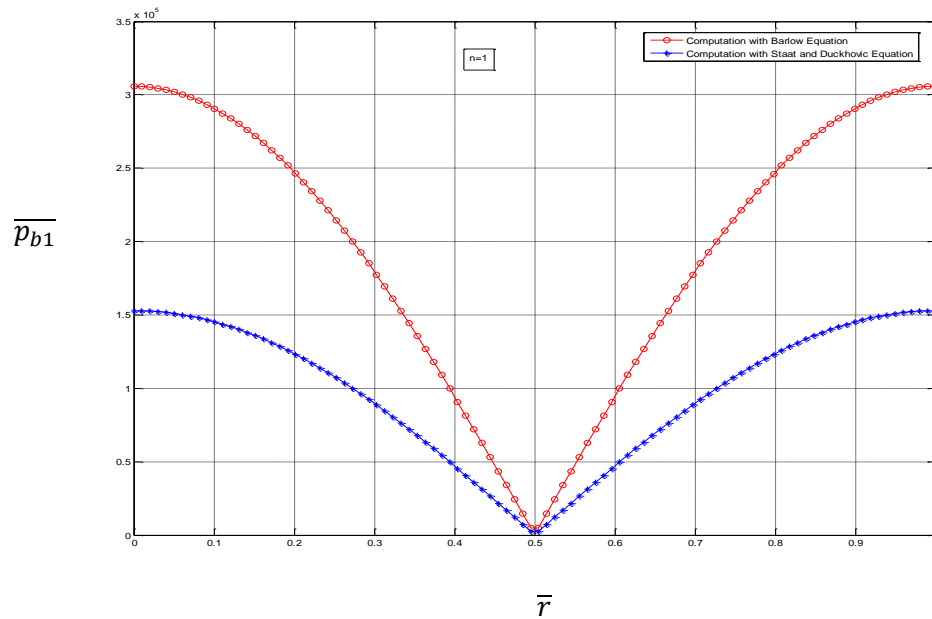


Fig.3.33: Steady state burst pressure profile at the upper layer of the pipe on a soft sea bed for the case $\bar{x} = 0.5; z = 1, L = 6km, \bar{U} = 0.5; \bar{K}_b = 8$

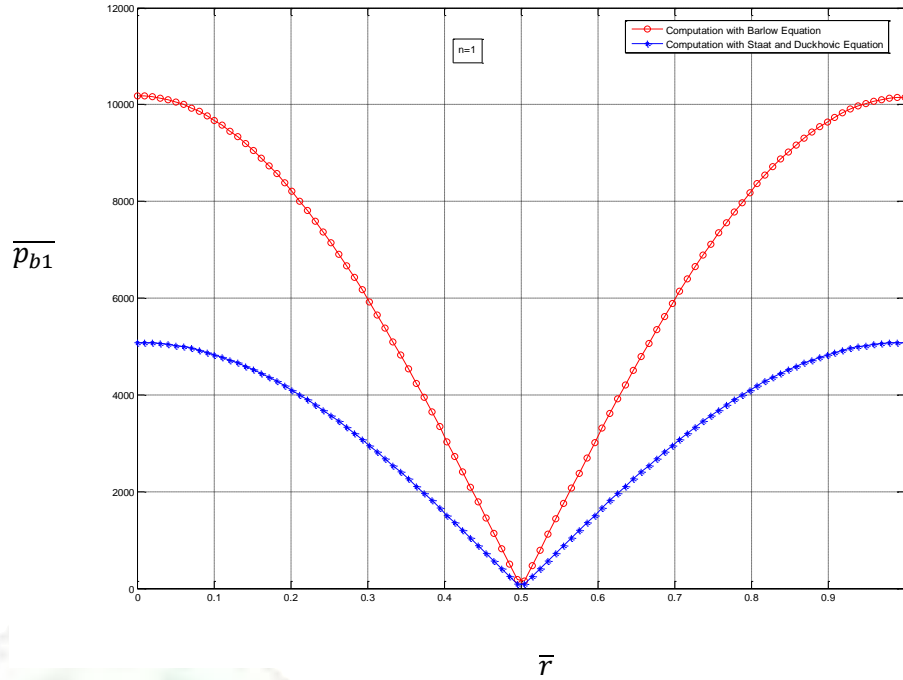


Fig.3.34: Steady state burst pressure profile at the upper layer of the pipe on a hard sea bed for the case $\bar{x} = 0.5; z = 1, L = 6km, \bar{U} = 0.5; \bar{K}_b = 800$

CHAPTER 4

THE EFFECT OF FLUID-PIPELINE-SOIL INTERACTION ON DYNAMIC STRESS PROPAGATION AT SEABED

4.1 Problem Fundamentals and Governing Differential Equation

In Chapter 3, the problem of dynamic stress propagation concerning the vibration of a pre-stressed high pressure and high temperature subsea pipe that is transporting a fluid, resting on the seabed was considered. This chapter is an attempt to extend the analysis presented in Chapter 3 to account for case of partially/fully buried pipe at seabed subject to the same operating conditions.

The focus here is to examine the effect of burial through ocean floor subsoil layer for the case of partially and fully buried offshore pipelines. For this exercise, we shall employ the modified version of Gorman's *et al.* (2000) analysis in conjunction with the recent approach of Olunloyo *et al.* (2007, 2008).

The physical problem under investigation consists of a fluid pipeline partly buried in an ocean floor or seabed. The investigation here entails the study of a fluid pipeline soil dynamic interaction boundary value problem, with the attendant fully fluid flow regime. The pipe and its position are as shown in Figure 4.0 below, while the necessary assumptions leading to the formulation of the well posed boundary value partial differential equations, governing the dynamic interaction problem under investigation are listed viz:

- (i) the pre-stressed pipeline is idealised as an elastic beam on a subsoil layer that is considered to be a homogenous semi-infinite elastic continuum with non-retarded geo-mechanical properties.
- (ii) a fully developed incompressible viscous Newtonian pressurised hot fluid is flowing through the pipeline.
- (iii) the contrived dynamic system is under the influence of hydrodynamic and bending loads, internal fluid transverse and longitudinal transmission forces, seabed subsoil layer and overlying sea water pipeline interfaces frictional and drag forces.
- (iv) the elastically deforming pre-stressed hot fluid conveying pipeline is subjected to both non-linear infinitesimal strains of Semler *et al.* (1994) or Reddy and Wang (2004).
- (v) the temperature differential between the external and internal walls of the pipeline results in the thermal strain with attendant cross sectional area change.
- (vi) a linear Airy wave profile propagates uniformly above the still water level (SWL).

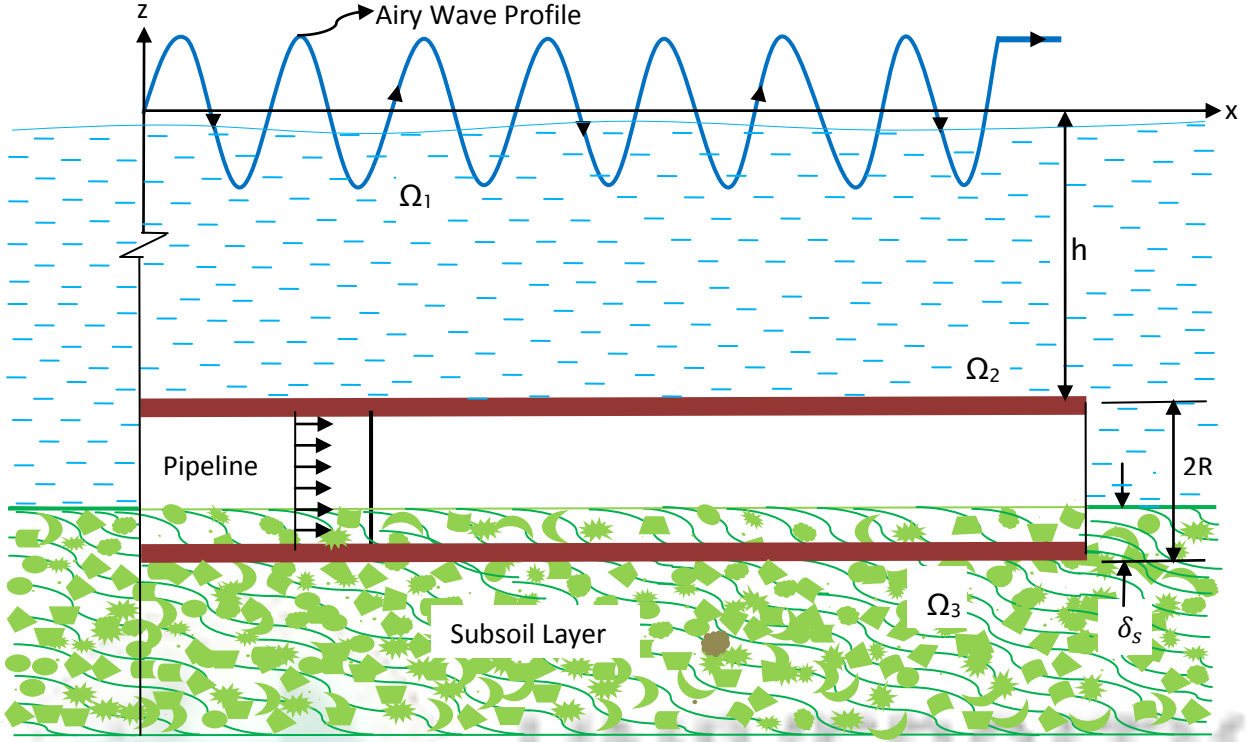


Fig. 4.0 The flow geometry of the dynamic interaction of a partially buried offshore pipeline.

By employing the foregoing assumptions, the governing non-linear partial differential equations in the transverse and longitudinal directions has been derived in equation (B.47&B.50) in the appendix as:

$$\begin{aligned}
& m\ddot{w} + (C_1 + C_D)\dot{w} + K_b w - \mu_s \pi \delta_s (R - \delta_s/2) \frac{\partial P_s}{\partial x} + 2m_f U \dot{w}' + m_f \dot{U} w' + m_f U U' w' + m_f U^2 w'' \\
& - [T_o - PA - \alpha EA \theta] w'' + EI w'''' + [T_o - EA - PA - \alpha EA \theta] \left[w'' u' + w' u'' + \frac{3}{2} w'^2 w'' \right] \\
& + [P'A + PA' - \alpha EA' \theta - \alpha EA \theta'] \left[w' - u' w' - \frac{w'^3}{2} \right] - [EA'] \left[u' w' + \frac{w'^3}{2} \right] \\
& - EI [4w'' u'' + 3w'' u'' - 2w'' u' - w' u'' - 8w' w'' w'' - 2w'' w'' - 2w''^3] = P_h \pi (2R - \delta_s)
\end{aligned} \tag{4.1}$$

and

$$\begin{aligned}
& m\ddot{u} + (C_2 + C_D)\dot{u} + 2m_f U \dot{u}' + m_f \dot{U} u' + m_f \dot{U} u' + m_f U U' u' + m_f U^2 u'' + [T_o - EA - \\
& \alpha EA \theta] w' w'' \\
& - EA u'' - EA' \left(u' + \frac{w'^2}{2} \right) + \alpha EA' \theta + \alpha EA \theta' - \alpha EA' \theta \frac{w'^2}{2} - \alpha EA \theta' \frac{w'^2}{2} - EI [w'' w'' + w' w''] \\
& + P'A + PA' - \frac{P'A}{2} w'^2 - \frac{PA'}{2} w'^2 - PA w' w'' = -2\mu_s \pi P_s (2R - \delta_s)
\end{aligned} \tag{4.2}$$

Furthermore, employing the procedural method of Olunloyo *et al.* (2007), linearised forms of equations (4.1) and (4.2) as special cases for our problem then become

$$m\ddot{w} + (C_1 + C_D)\dot{w} + K_b w - \mu_s \pi \delta_s (R - \delta_s/2) \frac{\partial P_s}{\partial x} + 2m_f U \dot{w}' - [T_o - PA - m_f U^2 - \alpha EA \theta] w'' + EI w'^v + [P'A + PA' - \alpha EA' - \alpha EA \theta'] w' = P_h \pi (2R - \delta_s) \quad (4.3)$$

and

$$m\ddot{u} + (C_2 + C_D)\dot{u} + 2m_f U \dot{u}' - [EA - m_f U^2] u'' - EA' u' + [T_o - EA - PA - \alpha EA \theta] w' w'' + [P'A + PA' + \alpha EA' \theta + \alpha EA \theta'] - [P'A + PA' + \alpha EA' \theta + \alpha EA \theta' + EA'] \frac{w'^2}{2} - EI [w'' w''' + w' w'^v] = -2\mu_s \pi P_s (2R - \delta_s) \quad (4.4)$$

4.2 Analysis of Transverse Vibration Problem

Equation (4.3) can be rewritten in the form

$$m\ddot{w} + \left[(C_1 + C_D) + \left(\frac{\alpha EA_o \left(\frac{\gamma}{L} \right) \theta - \frac{PA_o \gamma}{L} \frac{\Delta PA_o \left(1 - \frac{\gamma}{2} \right)}{U} - \alpha EA_o \frac{\Delta \theta}{L} \left(1 - \frac{\gamma}{2} \right) \right) \right] \dot{w} + K_b w - \mu_s \pi \delta_s (R - \delta_s/2) \frac{\partial P_s}{\partial x} + EI w'^v + \left(3m_f U^2 - [T_o - PA_o \left(1 - \frac{\gamma}{2} \right) - \alpha EA_o \left(1 - \frac{\gamma}{2} \right) \theta] \right) w'' = P_h \pi (2R - \delta_s) \quad (4.5)$$

where

$$A = A_o \left(1 - \gamma \frac{x}{L} \right) \text{ and } A' = -A_o \frac{\gamma}{L} \text{ or using average area } A, A \approx A_o \left(1 - \frac{\gamma}{2} \right) \\ (PA)' = -PA_o \frac{\gamma}{L} - \frac{\Delta P}{L} A_o \left(1 - \frac{\gamma}{2} \right), \quad \theta' = -\frac{\Delta \theta}{L} \text{ while } \gamma \text{ is defined as the area deformation coefficient.}$$

Equation (4.5) can now be non-dimensionalised by using the following parameters namely:

$$w = \bar{w}L, u = \bar{u}L, \delta = \frac{m_f}{m}, t = \tau \bar{t}, U = \bar{U} \frac{L}{\tau_f}, x = \bar{x}L, R = \bar{R}L, A = \bar{A}L^2, \bar{P} \bar{A} = \frac{PAL^2}{EI}, \\ \delta_1 = \frac{m_w}{M}, \Delta \bar{P} \bar{A} = \frac{\Delta PA_o L^2}{EI}, \delta_s = \bar{\delta}_s L, \frac{T_o L^2}{EI} = \beta_o, \frac{EA_{to} L^2}{EI} = \beta_1, \beta_2 = \frac{\sqrt{\delta}}{U}, \beta_3 = \alpha \beta_1 \beta_2 \theta \\ \beta_4 = \alpha \beta_1 \beta_2 \Delta \theta, \beta_5 = \alpha \beta_1 \theta, \beta_6 = \alpha \beta_1 \Delta \theta, \beta_7 = \frac{\beta_1}{U}, \beta_8 = \frac{\delta_1}{L}, \tau = L^2 \sqrt{\frac{m}{EI}}, \bar{C}_1 = \frac{C_1 L^2}{\sqrt{mEI}} \\ \bar{C}_D = \frac{C_D L^2}{\sqrt{mEI}}, \bar{g} = \frac{MgL^3}{EI}, \bar{K}_b = \frac{K_b L^4}{EI}, \Phi = \frac{L^2}{\tau^2} \bar{\Phi}, \acute{\alpha} = \frac{L^4}{I} \quad (4.6)$$

Thus, equation (4.5) becomes,

$$\begin{aligned} \frac{\partial^4 \bar{w}}{\partial \bar{x}^4} + \left[3\sqrt{\delta} \bar{U}^2 - \beta_o + \bar{P} \bar{A}_o \left(1 - \frac{\gamma}{2} \right) + \beta_5 \left(1 - \frac{\gamma}{2} \right) \right] \frac{\partial^2 \bar{w}}{\partial \bar{x}^2} + \frac{\partial^2 \bar{w}}{\partial \bar{t}^2} - \mu_s \pi \bar{\delta}_s (\bar{R} - \bar{\delta}_s / 2) \frac{\partial \bar{P}_s}{\partial \bar{x}} + \\ \left[(\bar{C}_1 + \bar{C}_D) - \beta_3 \gamma - \beta_4 \left(1 - \frac{\gamma}{2} \right) - \beta_2 \bar{P} \bar{A}_o \gamma - \Delta \bar{P} \bar{A}_o \beta_2 \left(1 - \frac{\gamma}{2} \right) \right] \frac{\partial \bar{w}}{\partial \bar{t}} + \bar{K}_b \bar{w} = P_h \pi L (2\bar{R} - \bar{\delta}_s) \frac{L^3}{EI} \end{aligned} \quad (4.7)$$

Subject to the pinned-pinned end boundary conditions viz:

$$\bar{w}(0, \bar{t}) = \bar{w}(1, \bar{t}) = 0 \text{ and } \bar{w}_{\bar{x}\bar{x}}(0, \bar{t}) = \bar{w}_{\bar{x}\bar{x}}(1, \bar{t}) = 0 \quad (4.8)$$

It is now suffice to express for P_h from the hydrodynamic effect of the overlying sea water with the assumption of Airy linear wave theory, as reported by Olunloyo et al (2007):

$$\nabla^2 \Phi = 0 \quad (4.9)$$

$$\frac{P_h}{\rho_w} + \frac{\partial \Phi}{\partial t} + gz + \frac{1}{2} |\nabla \Phi|^2 = 0 \quad (4.10)$$

In equation (4.10), P_h is obtained as,

$$P_h = -\rho_w \left(\frac{\partial \Phi}{\partial t} + gz \right) \quad (4.11)$$

Thus, the R.H.S. of equation (4.7) in view of equation (4.11) is non-dimensionalised with usual notations as in equation (4.12),

$$P_h \pi L (2\bar{R} - \bar{\delta}_s) \frac{L^3}{EI} = -\beta_8 \pi (2\bar{R} - \bar{\delta}_s) \left(\frac{\partial \bar{\Phi}}{\partial \bar{t}} + \bar{g} \bar{z} \right) \quad (4.12)$$

Using equation (4.12), equation (4.7) now becomes,

$$\begin{aligned} \frac{\partial^4 \bar{w}}{\partial \bar{x}^4} + \left[3\sqrt{\delta} \bar{U}^2 - \beta_o + \bar{P} \bar{A}_o \left(1 - \frac{\gamma}{2} \right) + \beta_5 \left(1 - \frac{\gamma}{2} \right) \right] \frac{\partial^2 \bar{w}}{\partial \bar{x}^2} + \frac{\partial^2 \bar{w}}{\partial \bar{t}^2} - \mu_s \pi \bar{\delta}_s (\bar{R} - \bar{\delta}_s / 2) \frac{\partial \bar{P}_s}{\partial \bar{x}} + \bar{K}_b \bar{w} + \\ \left[(\bar{C}_1 + \bar{C}_D) - \beta_3 \gamma - \beta_4 \left(1 - \frac{\gamma}{2} \right) - \beta_2 \bar{P} \bar{A}_o \gamma - \Delta \bar{P} \bar{A}_o \beta_2 \left(1 - \frac{\gamma}{2} \right) \right] \frac{\partial \bar{w}}{\partial \bar{t}} = -\beta_8 \left(\frac{\partial \bar{\Phi}}{\partial \bar{t}} + \bar{g} \bar{z} \right) \pi (2\bar{R} - \bar{\delta}_s) \end{aligned} \quad (4.13)$$

4.3 Analytic Solution for \bar{w} via Integral Transforms Method

Equation (4.13) is solved by employing the Laplace transform namely,

$$\overline{(\cdot)} = \int_0^\infty (\cdot) e^{-s\bar{t}} d\bar{t}; (\cdot) = \frac{1}{2\pi i} \int_0^{+i\infty} (\cdot) \int_{\eta-i\infty}^{\eta+i\infty} \overline{(\cdot)} e^{s\bar{t}} ds \quad (4.14)$$

Application of equation (4.14) to (4.13) yields:

$$\begin{aligned}
& \frac{\partial^4 \tilde{w}(\bar{x}, s)}{\partial \bar{x}^4} + \left[3\sqrt{\delta} \bar{U}^2 - \beta_o + \bar{P} \bar{A}_o \left(1 - \frac{\gamma}{2} \right) + \beta_5 \left(1 - \frac{\gamma}{2} \right) \right] \frac{\partial^2 \tilde{w}(\bar{x}, s)}{\partial \bar{x}^2} + [s^2 \tilde{w}(\bar{x}, s) - s \bar{w}(\bar{x}, 0) - \dot{\bar{w}}(\bar{x}, 0)] + \\
& \left[(\bar{C}_1 + \bar{C}_D) - \beta_3 \gamma - \beta_4 \left(1 - \frac{\gamma}{2} \right) - \beta_2 \bar{P} \bar{A}_o \gamma - \Delta \bar{P} \bar{A}_o \beta_2 \left(1 - \frac{\gamma}{2} \right) \right] [s \tilde{w}(\bar{x}, s) - \bar{w}(\bar{x}, 0)] + \tilde{w}(\bar{x}, s) \\
& - \mu_s \pi \bar{\delta}_s (\bar{R} - \bar{\delta}_s / 2) \frac{\partial \bar{P}_s}{\partial \bar{x}}(\bar{x}, s) = -\beta_8 \left[\left(s \tilde{\Phi}(\bar{x}, s) - \bar{\Phi}(\bar{x}, 0) \right) + \frac{\bar{g} \bar{z}}{s} \right] \pi (2\bar{R} - \bar{\delta}_s) \quad (4.15)
\end{aligned}$$

Next, the finite Fourier sine transform is introduced namely,

$$\overline{[.]} = \int_0^1 [.] \sin n\pi \bar{x} d\bar{x} ; [.] = 2 \sum_{n=1}^{\infty} \overline{[.]} \sin n\pi \bar{x} \quad (4.16)$$

Furthermore, noting that,

$$\begin{aligned}
\mathfrak{I}_s \{ \tilde{w}_{\bar{x}\bar{x}\bar{x}\bar{x}}(\bar{x}, s) \} &= n^4 \pi^4 \tilde{w}^F(\lambda_n, s) - n^3 \pi^3 \{ \tilde{w}(0, s) + (-1)^{n+1} \tilde{w}(1, s) \} \\
&+ n\pi \{ \tilde{w}_{\bar{x}\bar{x}}(0, s) + (-1)^{n+1} \tilde{w}_{\bar{x}\bar{x}}(1, s) \} \quad (4.17)
\end{aligned}$$

$$\mathfrak{I}_s \{ \tilde{w}_{\bar{x}\bar{x}}(\bar{x}, s) \} = -n^2 \pi^2 \tilde{w}^F(\bar{\lambda}_n, s) + n\pi \{ \tilde{w}(0, s) - \bar{w}(1, s) (-1)^n \} \quad (4.18)$$

Subject to the pipeline being idealized as simply supported at $\bar{x} = (0, 1)$, i.e.

$$\tilde{w}(0, s) = \tilde{w}(1, s) = 0 \quad (4.19)$$

$$\tilde{w}_{\bar{x}\bar{x}}(0, s) = \tilde{w}_{\bar{x}\bar{x}}(1, s) = 0 \quad (4.20)$$

Thus, equation (4.15) with zero initial conditions becomes

$$\begin{aligned}
& n^4 \pi^4 \tilde{w}^F(\bar{\lambda}_n, s) - \left[3\sqrt{\delta} \bar{U}^2 - \beta_o + \bar{P} \bar{A}_o \left(1 - \frac{\gamma}{2} \right) + \beta_5 \left(1 - \frac{\gamma}{2} \right) \right] n^2 \pi^2 \tilde{w}^F(\bar{\lambda}_n, s) + s^2 \tilde{w}^F(\bar{\lambda}_n, s) + \\
& \left[(\bar{C}_1 + \bar{C}_D) - \beta_3 \gamma - \beta_4 \left(1 - \frac{\gamma}{2} \right) - \beta_2 \bar{P} \bar{A}_o \gamma - \Delta \bar{P} \bar{A}_o \beta_2 \left(1 - \frac{\gamma}{2} \right) \right] s \tilde{w}^F(\bar{\lambda}_n, s) + \bar{K}_b \tilde{w}^F(\bar{\lambda}_n, s) \\
& - \mu_s \pi \bar{\delta}_s (\bar{R} - \bar{\delta}_s / 2) \mathfrak{I}_s \frac{\partial \bar{P}_s}{\partial \bar{x}}(\bar{x}, s) = -\beta_8 \pi (2\bar{R} - \bar{\delta}_s) \left[s \tilde{\Phi}^F(\bar{\lambda}_n, s, \bar{z}) \right]_{\bar{z}=-\bar{h}} - \frac{\bar{g} \bar{h}}{s} \bar{1}^F \quad (4.21)
\end{aligned}$$

Invoking the method of analysis by Olunloyo *et al.* (2007) for the Fourier-Laplace transform

solution of $\tilde{\Phi}^F(\bar{\lambda}_n, s, \bar{z})$ as

$$\tilde{\Phi}^F(\bar{\lambda}_n, s, \bar{z}) = \hat{\beta} s \tilde{w}^F(\bar{\lambda}_n, s) \quad (4.22)$$

where

$$\hat{\beta} = \frac{\bar{U}_w \cosh(\bar{k} \bar{z})}{\bar{k} \sinh(\bar{k} \bar{h})}; \quad \bar{k} = \frac{n\pi}{\bar{\lambda}} \quad \text{and} \quad h = \bar{h}L \quad (4.23)$$

Also,

$$\bar{\beta} = \hat{\beta} \Big|_{\bar{z}=-\bar{h}} = -\frac{\bar{U}_w}{\bar{k}} \coth \bar{k} \bar{h} \quad (4.24)$$

Therefore, equation (4.21) in view of equations (4.22 - 4.24) takes the form

$$\begin{aligned}
& n^4 \pi^4 \widetilde{W}^F(\bar{\lambda}_n, s) - \left[3\sqrt{\delta} \bar{U}^2 - \beta_o + \bar{P} \bar{A}_o \left(1 - \frac{\gamma}{2} \right) + \beta_5 \left(1 - \frac{\gamma}{2} \right) \right] n^2 \pi^2 \widetilde{W}^F(\bar{\lambda}_n, s) + s^2 \widetilde{W}^F(\bar{\lambda}_n, s) + \\
& \left[(\bar{C}_1 + \bar{C}_D) - \beta_3 \gamma - \beta_4 \left(1 - \frac{\gamma}{2} \right) - \beta_2 \bar{P} \bar{A}_o \gamma - \Delta \bar{P} \bar{A}_o \beta_2 \left(1 - \frac{\gamma}{2} \right) \right] s \widetilde{W}^F(\bar{\lambda}_n, s) + \bar{K}_b \widetilde{W}^F(\bar{\lambda}_n, s) \\
& - \mu_s \pi \bar{\delta}_s (\bar{R} - \bar{\delta}_s / 2) \mathfrak{S}_s \frac{\partial \bar{P}_s}{\partial \bar{x}}(\bar{x}, s) = \beta_8 \pi (2\bar{R} - \bar{\delta}_s) \left[s^2 \bar{\beta} \widetilde{W}^F(\bar{\lambda}_n, s, \bar{z}) \Big|_{\bar{z} = -\bar{h}} + \frac{\bar{g} \bar{h}}{s} \bar{1}^F \right]
\end{aligned} \tag{4.25}$$

Hence, it can be conveniently obtained from equation (4.25) that,

$$\widetilde{W}^F(\bar{\lambda}_n, s) = \left\{ \frac{\pi(2\bar{R} - \bar{\delta}_s) \beta_8 \bar{g} \bar{h} \bar{1}^F + \mu_s \pi \bar{\delta}_s (\bar{R} - \bar{\delta}_s / 2) \mathfrak{S}_s \frac{\partial \bar{P}_s}{\partial \bar{x}}(\bar{x}, s)}{\left[1 - \pi(2\bar{R} - \bar{\delta}_s) \beta_8 \bar{\beta} \right] s \left[s^2 + \bar{\eta}_1 s + \bar{\eta}^2 \right]} \right\} \tag{4.26}$$

where,

$$\bar{\eta}_1 = \frac{\left[(\bar{C}_1 + \bar{C}_D) - \beta_3 \gamma - \beta_4 \left(1 - \frac{\gamma}{2} \right) - \beta_2 \bar{P} \bar{A}_o \gamma - \Delta \bar{P} \bar{A}_o \beta_2 \left(1 - \frac{\gamma}{2} \right) \right]}{\left[1 - \pi(2\bar{R} - \bar{\delta}_s) \beta_8 \bar{\beta} \right]} \tag{4.27}$$

$$\bar{\eta}^2 = \frac{n^4 \pi^4 - \left[3\sqrt{\delta} \bar{U}^2 - \beta_o + \bar{P} \bar{A}_o \left(1 - \frac{\gamma}{2} \right) + \beta_5 \left(1 - \frac{\gamma}{2} \right) \right] n^2 \pi^2 + \bar{K}_b}{\left[1 - \pi(2\bar{R} - \bar{\delta}_s) \beta_8 \bar{\beta} \right]} \tag{4.28}$$

To solve equation (4.26) completely, we shall employ the method reported by Olunloyo *et al.* (2007), via the model for the rigid porous bed viz:

$$\frac{\partial \bar{P}_s}{\partial \bar{x}} = - \frac{\mu_s c_p U_s}{k_s}; \quad \forall x \in \Omega_3 \tag{4.29}$$

In the non-dimensionalised form,

$$\frac{\partial \bar{P}_s}{\partial \bar{x}} = - \frac{\mu_s \alpha^1 c_p \bar{U}_s}{k_s} \tag{4.30}$$

with the following parameters defined as:

$$x = \bar{x}L, \quad U_s = \bar{U}_s \frac{L}{\tau}, \quad \text{and} \quad \alpha^1 = \frac{L^4}{\sqrt{m_s EI}} \tag{4.31}$$

Equation (4.30) can now be rewritten by using double integral transforms as

$$\mathfrak{S}_s \frac{\partial \bar{P}_s}{\partial \bar{x}}(\bar{x}, s) = - \frac{\mu_s \alpha^1 c_p \bar{U}_s}{s k_s} \bar{1}^F \tag{4.32}$$

Using equation (4.32) in (4.26) yields,

$$\widetilde{W}^F(\bar{\lambda}_n, s) = \left\{ \frac{\pi(2\bar{R} - \bar{\delta}_s) \left[\beta_8 \bar{g} \bar{h} - \frac{\mu_s^2 \alpha^1 c_p \bar{U}_s \bar{\delta}_s}{2k_s} \right] \bar{1}^F}{\left[1 - \pi(2\bar{R} - \bar{\delta}_s) \beta_8 \bar{\beta} \right] s \left[s^2 + \bar{\eta}_1 s + \bar{\eta}^2 \right]} \right\} \tag{4.33}$$

Hence, in the Laplace domain, the transverse deflection becomes,

$$\tilde{w}(\bar{x}, s) = \left\{ \sum_{n=1}^{\infty} \left[\frac{\pi(2\bar{R}-\bar{\delta}_s) \left[\beta_8 \bar{g} \bar{h} - \frac{\mu_s^2 \alpha^1 c_p \bar{U}_s \bar{\delta}_s}{2k_s} \right]}{[1-\pi(2\bar{R}-\bar{\delta}_s) \beta_8 \bar{\beta}]} \right] \left[\frac{1+(-1)^{n+1}}{s[s^2+\bar{\eta}_1 s+\bar{\eta}^2]} \right] \frac{\sin n\pi\bar{x}}{n\pi} \right\} \quad (4.34)$$

Also, the solution of equation (4.34) from the Laplace inversion gives,

$$\bar{w}(\bar{x}, \bar{t}) = \left\{ \sum_{n=1}^{\infty} \left[\frac{\pi(2\bar{R}-\bar{\delta}_s) \left[\beta_8 \bar{g} \bar{h} - \frac{\mu_s^2 \alpha^1 c_p \bar{U}_s \bar{\delta}_s}{2k_s} \right]}{[1-\pi(2\bar{R}-\bar{\delta}_s) \beta_8 \bar{\beta}]} \right] [\bar{F}(\bar{t})(1+(-1)^{n+1})] \frac{\sin n\pi\bar{x}}{n\pi} \right\} \quad (4.35)$$

where,

$$\bar{F}(\bar{t}) = \left[\frac{1}{\bar{\alpha}_1 \bar{\alpha}_2} + \frac{1}{\bar{\alpha}_1 \bar{\alpha}_2 (\bar{\alpha}_2 - \bar{\alpha}_1)} (\bar{\alpha}_1 e^{-\bar{\alpha}_2 \bar{t}} - \bar{\alpha}_2 e^{-\bar{\alpha}_1 \bar{t}}) \right] \quad (4.36)$$

and,

$$\bar{\alpha}_1 = \frac{\bar{\eta}_1}{2} + i\sqrt{\bar{\eta}^2 - \frac{\bar{\eta}_1^2}{4}} \quad (4.37)$$

$$\bar{\alpha}_2 = \frac{\bar{\eta}_1}{2} - i\sqrt{\bar{\eta}^2 - \frac{\bar{\eta}_1^2}{4}} \quad (4.38)$$

By using closed form Fourier series representative viz:

$$\sum_{n=1}^{\infty} \frac{\sin n\bar{x}}{n} = \left(\frac{\pi - \bar{x}}{2} \right) \quad \forall (0 < \bar{x} < 2) \quad (4.39)$$

equation (4.38) is rewritten as

$$\bar{w}(\bar{x}, \bar{t}) = \left(\frac{\pi(2\bar{R}-\bar{\delta}_s) \left(\beta_8 \bar{g} \bar{h} - \frac{\mu_s^2 \alpha^1 c_p \bar{U}_s \bar{\delta}_s}{2k_s} \right)}{(1-\pi(2\bar{R}-\bar{\delta}_s) \bar{\beta} \beta_8)} \right) \bar{F}(\bar{t})(x^4 - 2x^3 + x) \quad (4.40)$$

4.4 Analysis of Longitudinal Vibration Problem

The solution for the axial displacement formulation i.e. equation (4.2) follows the same procedural methods as was done for the transverse displacement. This is done by non-dimensionalising equation (4.2) and then employs the same transform procedures invoked previously with the same boundary conditions.

Rewriting equation (4.2) yields,

$$\begin{aligned} m \frac{\partial^2 u}{\partial t^2} + [C_2 + C_D] \frac{\partial u}{\partial t} + [3m_f U^2 - EA_t] \frac{\partial^2 u}{\partial x^2} - EA_t \frac{\partial u}{\partial x} + [T_o - EA_t - PA - \alpha EA_t \theta] w' w'' \\ + [P'A + PA' + \alpha EA_t' \theta + \alpha EA_t \theta'] - [P'A + PA' + \alpha EA_t' \theta + \alpha EA_t \theta' + EA_t'] \frac{w^2}{2} \\ - EI[w'' w''' + w' w'''] = -2\mu_s \pi P_s (2R - \delta_s) \end{aligned} \quad (4.41)$$

The non-dimensionalised form of equation (4.42), following the same method above, yields,

$$\begin{aligned}
& \frac{\partial^2 \bar{u}}{\partial \bar{t}^2} + [\bar{C}_2 + \bar{C}_D] \frac{\partial \bar{u}}{\partial \bar{t}} + \left[3\sqrt{\delta} \bar{U}^2 - \beta_1 \left(1 - \frac{\gamma}{2} \right) \right] \frac{\partial^2 \bar{u}}{\partial \bar{x}^2} + \beta_1 \gamma \frac{\partial \bar{u}}{\partial \bar{x}} = \\
& \left[\frac{\partial^4 \bar{w}}{\partial \bar{x}^4} \frac{\partial \bar{w}}{\partial \bar{x}} + \frac{\partial^2 \bar{w}}{\partial \bar{x}^2} \frac{\partial^3 \bar{w}}{\partial \bar{x}^3} \right] - \left[\beta_o - \beta_1 \left(1 - \frac{\gamma}{2} \right) - \bar{P} \bar{A}_o \left(1 - \frac{\gamma}{2} \right) - \beta_5 \left(1 - \frac{\gamma}{2} \right) \right] \frac{\partial \bar{w}}{\partial \bar{x}} \frac{\partial^2 \bar{w}}{\partial \bar{x}^2} \\
& - \frac{1}{2} \left[\Delta \bar{P} \bar{A}_o \left(1 - \frac{\gamma}{2} \right) + \bar{P} \bar{A}_o \gamma + \beta_6 \left(1 - \frac{\gamma}{2} \right) + \beta_5 \gamma + \beta_1 \gamma \right] \left[\frac{\partial \bar{w}}{\partial \bar{x}} \right]^2 \\
& + \left[\Delta \bar{P} \bar{A}_o \left(1 - \frac{\gamma}{2} \right) + \bar{P} \bar{A}_o \gamma + \beta_6 \left(1 - \frac{\gamma}{2} \right) + \beta_5 \gamma \right] - 2\mu_s \pi \bar{P}_s (2\bar{R} - \bar{\delta}_s) \tag{4.42}
\end{aligned}$$

Next, we substitute the result of equation (4.35) into (4.42), to give

$$\begin{aligned}
& \frac{\partial^2 \bar{u}}{\partial \bar{t}^2} + [\bar{C}_2 + \bar{C}_D + \beta_7 \gamma] \frac{\partial \bar{u}}{\partial \bar{t}} + \left[3\sqrt{\delta} \bar{U}^2 - \beta_1 \left(1 - \frac{\gamma}{2} \right) \right] \frac{\partial^2 \bar{u}}{\partial \bar{x}^2} = \\
& \left\{ \sum_{n=1}^{\infty} \left[\frac{\pi(2\bar{R}-\bar{\delta}_s) \left[\beta_8 \bar{g} \bar{h} - \frac{\mu_s^2 \alpha^1 c_p \bar{U}_s \bar{\delta}_s}{2k_s} \right]}{[1-\pi(2\bar{R}-\bar{\delta}_s)\beta_8 \bar{\beta}]} \right]^2 \bar{\Lambda}(\bar{t}) (1 + (-1)^{n+1})^2 \sin 2n\pi \bar{x} \right\} n^3 \pi^3 \\
& + \left[\beta_o - (\beta_2 + \bar{P} \bar{A}_o + \beta_5) \left(1 - \frac{\gamma}{2} \right) \right] \left[\sum_{n=1}^{\infty} \left[\frac{\pi(2\bar{R}-\bar{\delta}_s) \left[\beta_8 \bar{g} \bar{h} - \frac{\mu_s^2 \alpha^1 c_p \bar{U}_s \bar{\delta}_s}{2k_s} \right]}{[1-\pi(2\bar{R}-\bar{\delta}_s)\beta_8 \bar{\beta}]} \right]^2 \bar{\Lambda}(\bar{t}) (1 + (-1)^{n+1})^2 \frac{\sin 2n\pi \bar{x}}{2} \right] n\pi \\
& - \frac{1}{2} \left[(\Delta \bar{P} \bar{A}_o + \beta_6) \left(1 - \frac{\gamma}{2} \right) + \right. \\
& \left. (\bar{P} \bar{A}_o + \beta_5 + \beta_1) \gamma \right] \left[\sum_{n=1}^{\infty} \left[\frac{\pi(2\bar{R}-\bar{\delta}_s) \left[\beta_8 \bar{g} \bar{h} - \frac{\mu_s^2 \alpha^1 c_p \bar{U}_s \bar{\delta}_s}{2k_s} \right]}{[1-\pi(2\bar{R}-\bar{\delta}_s)\beta_8 \bar{\beta}]} \right]^2 \bar{\Lambda}(\bar{t}) (1 + (-1)^{n+1})^2 \cos^2 n\pi \bar{x} \right] \\
& + \left[(\Delta \bar{P} \bar{A}_o + \beta_6) \left(1 - \frac{\gamma}{2} \right) + (\bar{P} \bar{A}_o + \beta_5) \gamma \right] - 2\mu_s \pi \bar{P}_s (2\bar{R} - \bar{\delta}_s) \tag{4.43}
\end{aligned}$$

where,

$$\begin{aligned}
\bar{\Lambda}(\bar{t}) &= \left(\frac{1}{\bar{\alpha}_1^2 \bar{\alpha}_2^2} + \frac{2}{\bar{\alpha}_1^2 \bar{\alpha}_2^2 (\bar{\alpha}_2 - \bar{\alpha}_1)} (\bar{\alpha}_1 e^{-\bar{\alpha}_2 \bar{t}} - \bar{\alpha}_2 e^{-\bar{\alpha}_1 \bar{t}}) \right) \\
&+ \frac{2}{\bar{\alpha}_1^2 \bar{\alpha}_2^2 (\bar{\alpha}_2 - \bar{\alpha}_1)^2} (\bar{\alpha}_2^2 e^{-2\bar{\alpha}_1 \bar{t}} - 2\bar{\alpha}_2 \bar{\alpha}_1 e^{-(\bar{\alpha}_1 + \bar{\alpha}_2) \bar{t}} + \bar{\alpha}_1^2 e^{-\bar{\alpha}_2 \bar{t}}) \tag{4.44}
\end{aligned}$$

To solve for u completely, we employed the boundary conditions in the Laplace transform plane $\bar{u}(\bar{x}, s)$ namely;

$$\tilde{u}(0, \infty) = \tilde{u}(1, \infty) = 0 \tag{4.45}$$

Hence, equation (4.45) enables us to express equation (4.43) in the Fourier-Laplace plane as,

$$\begin{aligned}
& \left[s^2 \tilde{u}^F(\bar{\lambda}_n, s) - s \tilde{u}(\bar{x}, 0) - \tilde{u}(\bar{x}, 0) \right] + \left[\bar{C}_2 + \bar{C}_D + \beta_7 \gamma \right] \left[s \tilde{u}^F(\bar{\lambda}_n, s) - \tilde{u}(\bar{x}, 0) \right] \\
& - \left[3\sqrt{\delta} \bar{U}^2 - \beta_2 \left(1 - \frac{\gamma}{2} \right) \right] n^2 \pi^2 \tilde{u}^F(\bar{\lambda}_n, s) = \\
& - \frac{1}{2} \left[(\Delta \bar{P} \bar{A}_o + \beta_6) \left(1 - \frac{\gamma}{2} \right) + (\bar{P} \bar{A}_o + \beta_5 + \beta_1) \gamma \right] \left[\frac{\pi(2\bar{R} - \bar{\delta}_s) \left[\beta_8 \bar{g} \bar{h} - \frac{\mu_s^2 \alpha^1 c_p \bar{U}_s \bar{\delta}_s}{2k_s} \right]^2}{\left[1 - \pi(2\bar{R} - \bar{\delta}_s) \beta_8 \bar{\beta} \right]} \right] \sum_{n=1}^{\infty} \left(\frac{4}{3n\pi} + \right. \\
& \left. \frac{4(-1)^{n+1}}{3n\pi} \right) \tilde{\Lambda}(s) \\
& + \left[\frac{(\Delta \bar{P} \bar{A}_o + \beta_6) \left(1 - \frac{\gamma}{2} \right) + (\bar{P} \bar{A}_o + \beta_5) \gamma - 2\mu_s \pi \bar{P}_s (2\bar{R} - \bar{\delta}_s)}{s} \right] \bar{1}^F
\end{aligned} \tag{4.46}$$

where

$$\bar{\lambda}_n = n\pi; \quad \bar{1}^F = \left(\frac{1 + (-1)^{n+1}}{n\pi} \right) \tag{4.47}$$

Applying zero initial conditions, equation (4.46) is re-written as

$$\begin{aligned}
& \tilde{u}^F(\bar{\lambda}_n, s) \left[s^2 + (\bar{C}_2 + \bar{C}_D + \beta_7 \gamma) s - \left(3\sqrt{\delta} \bar{U}^2 - \beta_2 \left(1 - \frac{\gamma}{2} \right) \right) n^2 \pi^2 \right] = \\
& - \frac{1}{2} [\Gamma + \beta_1 \gamma] \left[\frac{\pi(2\bar{R} - \bar{\delta}_s) \left[\beta_8 \bar{g} \bar{h} - \frac{\mu_s^2 \alpha^1 c_p \bar{U}_s \bar{\delta}_s}{2k_s} \right]^2}{\left[1 - \pi(2\bar{R} - \bar{\delta}_s) \beta_8 \bar{\beta} \right]} \right] \sum_{n=1}^{\infty} \left(\frac{4}{3n\pi} + \frac{4(-1)^{n+1}}{3n\pi} \right) \tilde{\Lambda}(s) + \left[\frac{\Gamma - 2\mu_s \pi \bar{P}_s (2\bar{R} - \bar{\delta}_s)}{s} \right] \bar{1}^F
\end{aligned} \tag{4.48}$$

where

$$\Gamma = (\Delta \bar{P} \bar{A}_o + \beta_6) \left(1 - \frac{\gamma}{2} \right) + (\bar{P} \bar{A}_o + \beta_5) \gamma \tag{4.49}$$

and

$$\begin{aligned}
\tilde{\Lambda}(s) = & \left(\frac{1}{\bar{\alpha}_1^2 \bar{\alpha}_2^2} + \frac{2}{\bar{\alpha}_1^2 \bar{\alpha}_2^2 (\bar{\alpha}_2 - \bar{\alpha}_1)} \left(\frac{\bar{\alpha}_1}{(s + \bar{\alpha}_2)} - \frac{\bar{\alpha}_2}{\bar{\alpha}_2 (s + \bar{\alpha}_1)} \right) \right) \\
& - \frac{1}{\bar{\alpha}_1^2 \bar{\alpha}_2^2 (\bar{\alpha}_2 - \bar{\alpha}_1)^2} \left(\frac{\bar{\alpha}_2^2}{(s + 2\bar{\alpha}_1)} - \frac{2\bar{\alpha}_1 \bar{\alpha}_2}{s + (\bar{\alpha}_1 + \bar{\alpha}_2)} + \frac{\bar{\alpha}_1^2}{(s + 2\bar{\alpha}_2)} \right)
\end{aligned} \tag{4.50}$$

Thus, it is obvious that from equation (4.48) the characteristic equation is

$$s^2 + (\bar{C}_2 + \bar{C}_D + \beta_7 \gamma) s - \left(3\sqrt{\delta} \bar{U}^2 - \beta_2 \left(1 - \frac{\gamma}{2} \right) \right) n^2 \pi^2 = 0 \tag{4.51}$$

By letting $s = -i\Omega$, the solution to this is then;

$$\bar{\Omega}^2 = \left(-\frac{\bar{c}_2 + \bar{c}_D + \beta_7 \gamma}{2}\right)^2 \pm \left[\left(-\frac{\bar{c}_2 + \bar{c}_D + \beta_7 \gamma}{2}\right)^2 + \left(3\sqrt{\delta} \bar{U}^2 - \beta_2 \left(1 - \frac{\gamma}{2}\right)\right) n^2 \pi^2 \right] \quad (4.52)$$

The roots of equation (4.52) enable us to rewrite equation (4.48) as

$$\begin{aligned} \tilde{u}^F(\bar{\lambda}_n, s) = & -\frac{1}{2} [\Gamma + \beta_1 \gamma] \left[\frac{\pi(2\bar{R} - \bar{\delta}_s) \left[\beta_8 \bar{g} \bar{h} - \frac{\mu_s^2 \alpha^1 c_p \bar{U}_s \bar{\delta}_s}{2k_s} \right]^2}{[1 - \pi(2\bar{R} - \bar{\delta}_s) \beta_8 \bar{\beta}]} \right]^2 \sum_{n=1}^{\infty} \left(\frac{4}{3n\pi} + \frac{4(-1)^{n+1}}{3n\pi} \right) \frac{\tilde{\bar{\lambda}}(s)}{(s + \bar{\chi}_1)(s + \bar{\chi}_2)} \\ & + \left[\frac{\Gamma - 2\mu_s \pi \bar{P}_s (2\bar{R} - \bar{\delta}_s)}{s(s + \bar{\chi}_1)(s + \bar{\chi}_2)} \right] \bar{1}^F \end{aligned} \quad (4.53)$$

where

$$\bar{\chi}_1 = \left(\frac{\bar{c}_2 + \bar{c}_D + \beta_7 \gamma}{2}\right) - \sqrt{\left[\left(\frac{\bar{c}_2 + \bar{c}_D + \beta_7 \gamma}{2}\right)^2 - \left(3\sqrt{\delta} \bar{U}^2 - \beta_2 \left(1 - \frac{\gamma}{2}\right)\right) n^2 \pi^2\right]} \quad (4.54)$$

and

$$\bar{\chi}_2 = \left(\frac{\bar{c}_2 + \bar{c}_D + \beta_7 \gamma}{2}\right) + \sqrt{\left[\left(-\frac{\bar{c}_2 + \bar{c}_D + \beta_7 \gamma}{2}\right)^2 - \left(3\sqrt{\delta} \bar{U}^2 - \beta_2 \left(1 - \frac{\gamma}{2}\right)\right) n^2 \pi^2\right]} \quad (4.55)$$

In equation (4.55), the axial displacement from the Fourier-Laplace inversion yields

$$\begin{aligned} \bar{u}(\bar{x}, \bar{t}) = & -\frac{1}{2} [\Gamma + \beta_1 \gamma] \left[\frac{\pi(2\bar{R} - \bar{\delta}_s) \left[\bar{\rho}_w \bar{g} \bar{h} - \frac{\mu_s^2 \alpha^1 c_p \bar{U}_s \bar{\delta}_s}{2k_s} \right]^2}{[1 - \pi(2\bar{R} - \bar{\delta}_s) \bar{\rho}_w \bar{\beta}]} \right]^2 \bar{H}_1(\bar{t}) \sum_{n=1}^{\infty} \left(\frac{4}{3n\pi} + \frac{4(-1)^{n+1}}{3n\pi} \right) \sin n\pi \bar{x} \\ & + [\Gamma - 2\mu_s \pi \bar{P}_s (2\bar{R} - \bar{\delta}_s)] \bar{H}_2(\bar{t}) \sum_{n=1}^{\infty} \frac{\sin n\pi \bar{x}}{n\pi} \end{aligned} \quad (4.56)$$

where

$$\bar{H}_1(\bar{t}) = \left[\frac{1}{\bar{\alpha}_1^2 \bar{\alpha}_2^2} - \frac{2}{\bar{\alpha}_1 (\bar{\alpha}_2 - \bar{\alpha}_1)} \bar{\Pi}_1(\bar{t}) - \frac{2}{\bar{\alpha}_1 (\bar{\alpha}_2 - \bar{\alpha}_1)} \bar{\Pi}_2(\bar{t}) + \frac{2}{\bar{\alpha}_2 (\bar{\alpha}_2 - \bar{\alpha}_1)} \bar{\Pi}_3(\bar{t}) - \frac{1}{(\bar{\alpha}_2 - \bar{\alpha}_1)^2} \bar{\Pi}_4(\bar{t}) \right] \quad (4.57)$$

$$\bar{\Pi}_1(\bar{t}) = \left[\frac{1}{\bar{\chi}_1 \bar{\chi}_2} - \frac{e^{-\bar{\chi}_1 \bar{t}}}{\bar{\chi}_1 \bar{\chi}_2 - \bar{\chi}_1^2} + \frac{e^{-\bar{\chi}_2 \bar{t}}}{\bar{\chi}_2^2 - \bar{\chi}_1 \bar{\chi}_2} \right] \quad (4.58)$$

$$\bar{\Pi}_2(\bar{t}) = \left[\frac{e^{-\bar{\alpha}_1 \bar{t}}}{\bar{\chi}_1 \bar{\chi}_2 - \bar{\alpha}_1 \bar{\chi}_2 - \bar{\alpha}_2 \bar{\chi}_1 + \bar{\alpha}_1^2} - \frac{e^{-\bar{\chi}_1 \bar{t}}}{\bar{\chi}_1 \bar{\chi}_2 - \bar{\alpha}_1 \bar{\chi}_2 - \bar{\chi}_1^2 + \bar{\alpha}_1 \bar{\chi}_1} + \frac{e^{-\bar{\chi}_2 \bar{t}}}{-\bar{\chi}_1 \bar{\chi}_2 + \bar{\alpha}_1 \bar{\chi}_1 + \bar{\chi}_2^2 - \bar{\alpha}_1 \bar{\chi}_2} \right] \quad (4.59)$$

$$\bar{\Pi}_3(\bar{t}) = \left[\frac{e^{-\bar{\alpha}_2 \bar{t}}}{\bar{\chi}_1 \bar{\chi}_2 - \bar{\alpha}_1 \bar{\chi}_2 - \bar{\alpha}_2 \bar{\chi}_1 + \bar{\chi}_1^2} - \frac{e^{-\bar{\chi}_1 \bar{t}}}{\bar{\chi}_1 \bar{\chi}_2 - \bar{\alpha}_2 \bar{\chi}_2 - \bar{\chi}_1^2 + \bar{\alpha}_2 \bar{\chi}_1} + \frac{e^{-\bar{\chi}_2 \bar{t}}}{-\bar{\chi}_1 \bar{\chi}_2 + \bar{\alpha}_1 \bar{\chi}_1 + \bar{\chi}_2^2 - \bar{\alpha}_2 \bar{\chi}_2} \right] \quad (4.60)$$

$$\begin{aligned}
\bar{H}_4(\bar{t}) = & \bar{\alpha}_2^2 \left[\frac{e^{-2\bar{\alpha}_1\bar{t}}}{\bar{\chi}_1\bar{\chi}_2 - 2\bar{\alpha}_1\bar{\chi}_2 - 2\bar{\alpha}_1\bar{\chi}_1 + 4\bar{\alpha}_1^2} - \frac{e^{-\bar{\chi}_1\bar{t}}}{\bar{\chi}_1\bar{\chi}_2 - 2\bar{\alpha}_1\bar{\chi}_2 - \bar{\chi}_1^2 + 2\bar{\alpha}_1\bar{\chi}_1} + \frac{e^{-2\bar{\alpha}_1\bar{t}}}{-\bar{\chi}_1\bar{\chi}_2 + 2\bar{\alpha}_1\bar{\chi}_1 + \bar{\chi}_2^2 - 2\bar{\alpha}_1\bar{\chi}_2} \right] \\
& - 2\bar{\alpha}_1\bar{\alpha}_2 \left[\frac{e^{-(\bar{\alpha}_1+\bar{\alpha}_2)\bar{t}}}{\bar{\chi}_1\bar{\chi}_2 - (\bar{\alpha}_1+\bar{\alpha}_2)\bar{\chi}_1 - (\bar{\alpha}_1+\bar{\alpha}_2)\bar{\chi}_2 + 4(\bar{\alpha}_1+\bar{\alpha}_2)^2} - \frac{e^{-\bar{\chi}_1\bar{t}}}{\bar{\chi}_1\bar{\chi}_2 - (\bar{\alpha}_1+\bar{\alpha}_2)\bar{\chi}_2 - \bar{\chi}_1^2 + (\bar{\alpha}_1+\bar{\alpha}_2)\bar{\chi}_1} + \right. \\
& \left. \frac{e^{-\bar{\chi}_2\bar{t}}}{-\bar{\chi}_1\bar{\chi}_2 - (\bar{\alpha}_1+\bar{\alpha}_2)\bar{\chi}_2 - \bar{\chi}_1^2 + (\bar{\alpha}_1+\bar{\alpha}_2)\bar{\chi}_1} \right] \\
& + \bar{\alpha}_1^2 \left[\frac{e^{-2\bar{\alpha}_2\bar{t}}}{\bar{\chi}_1\bar{\chi}_2 - 2\bar{\alpha}_2\bar{\chi}_2 - 2\bar{\alpha}_2\bar{\chi}_1 + 4\bar{\alpha}_2^2} - \frac{e^{-\bar{\chi}_1\bar{t}}}{\bar{\chi}_1\bar{\chi}_2 - 2\bar{\alpha}_2\bar{\chi}_2 - \bar{\chi}_2^2 + 2\bar{\alpha}_2\bar{\chi}_1} + \frac{e^{-\bar{\chi}_2\bar{t}}}{-\bar{\chi}_1\bar{\chi}_2 + 2\bar{\alpha}_2\bar{\chi}_1 + \bar{\chi}_2^2 - 2\bar{\alpha}_2\bar{\chi}_2} \right]
\end{aligned} \tag{4.61}$$

and,

$$\bar{H}_2(\bar{t}) = \left[\frac{1}{\bar{\chi}_1\bar{\chi}_2} - \frac{e^{-\bar{\chi}_1\bar{t}}}{\bar{\chi}_1\bar{\chi}_2 - \bar{\chi}_1^2} + \frac{e^{-\bar{\chi}_2\bar{t}}}{\bar{\chi}_2^2 - \bar{\chi}_1\bar{\chi}_2} \right] \tag{4.62}$$

4.5 Computation of Burst Pressure

Following Staat and Duckhoivic vu (2006), as reported in Olunloyo et al (2008) paper, the burst pressure for a thick-walled pipe, without defect is given by the expression:

$$\frac{p_b}{\sigma_u} = D \ln \frac{R_0}{R_i} = D \ln \left(1 + \frac{R_0 - R_i}{R_i} \right) = D \left(\frac{t}{R_i} - \frac{1}{2} \left(\frac{t}{R_i} \right)^2 - \frac{1}{3} \left(\frac{t}{R_i} \right)^3 - \dots \right) \tag{4.63}$$

where the constraint factor D varies for yield conditions. In particular, we recall the solutions of the derived stress formulations in Chapter 3, in the Laplace transform plane viz:

$$\tilde{\tau}_{(\bar{x}, \bar{z})1}(\bar{x}, \bar{z}, s) = \frac{\alpha'}{2} (\bar{z}^2 - \bar{R}_i \bar{z}) \frac{d^3 \tilde{w}}{d\bar{x}^3}(\bar{x}, s) - \frac{\bar{z}}{R_i} \frac{\bar{\tau}_{\max}}{s} \tag{4.64}$$

$$\tilde{\tau}_{(\bar{x}, \bar{z})2}(\bar{x}, \bar{z}, s) = \frac{\alpha'}{2} (\bar{z}^2 + \bar{R}_i \bar{z}) \frac{d^3 \tilde{w}}{d\bar{x}^3}(\bar{x}, s) - \frac{\bar{z}}{R_i} \frac{\bar{\tau}_{\max}}{s} \tag{4.65}$$

$$\tilde{\sigma}_{\bar{x}1}(\bar{x}, \bar{z}, s) = -\frac{\alpha'}{2} (2\bar{z} - \bar{R}_i) \frac{d^2 \tilde{w}}{d\bar{x}^2}(\bar{x}, s) + \frac{\bar{x}}{R_i} \frac{\bar{\tau}_{\max}}{s} + \bar{x} \beta_8 (1 + \delta) s^2 \tilde{u}(\bar{x}, s) \tag{4.66}$$

$$\tilde{\sigma}_{\bar{x}2}(\bar{x}, \bar{z}, s) = -\frac{\alpha'}{2} (2\bar{z} + \bar{R}_i) \frac{d^2 \tilde{w}}{d\bar{x}^2}(\bar{x}, s) + \frac{\bar{x}}{R_i} \frac{\bar{\tau}_{\max}}{s} + \bar{x} \beta_8 (1 + \delta) s^2 \tilde{u}(\bar{x}, s) \tag{4.67}$$

in conjunction with the following yield condition of Von-Mises viz; $D = \frac{2}{\sqrt{3}}$

for the case of pressurized pipe without defects, we can in fact compute the upper half burst pressure, as

$$\bar{p}_{b1} = \frac{2}{\sqrt{3}} \Psi(R^*) \frac{\alpha'}{2} (\bar{z}^2 - \bar{R}_i \bar{z}) \kappa^1 \bar{F}(t) (24\bar{x} - 12) - \frac{\bar{z}}{\bar{R}_i} \bar{\tau}_{\max} \quad (4.68)$$

where

$$\forall \Psi(R^*) = \left(\frac{\bar{R}_0 - \bar{R}_i}{\bar{R}_i} \right) - \frac{1}{2} \left(\frac{\bar{R}_0 - \bar{R}_i}{\bar{R}_i} \right)^2 + \frac{1}{3} \left(\frac{\bar{R}_0 - \bar{R}_i}{\bar{R}_i} \right)^3 - \dots \quad (4.69)$$

Similarly, the burst pressure for the lower half of the pipe is:

$$\bar{p}_{b2} = \frac{2}{\sqrt{3}} \Psi(R^*) \frac{\alpha'}{2} (\bar{z}^2 + \bar{R}_i \bar{z}) \kappa^1 \bar{F}(t) (24\bar{x} - 12) - \frac{\bar{z}}{\bar{R}_i} \bar{\tau}_{\max} \quad (4.70)$$

4.6 Computation of buckling pressure for the pipe

By employing similar procedural analysis, buckling pressure for the upper and lower halves can be computed as follows:

$$\bar{p}_{bu1} = \Psi(R^*) \frac{\alpha'}{2} (\bar{z}^2 - \bar{R}_i \bar{z}) \kappa^1 \bar{F}(t) (24\bar{x} - 12) - \frac{\bar{z}}{\bar{R}_i} \bar{\tau}_{\max} \quad (4.71)$$

$$\bar{p}_{bu2} = \Psi(R^*) \frac{\alpha'}{2} (\bar{z}^2 + \bar{R}_i \bar{z}) \kappa^1 \bar{F}(t) (24\bar{x} - 12) - \frac{\bar{z}}{\bar{R}_i} \bar{\tau}_{\max} \quad (4.72)$$

where,

$$\kappa^1 = \left(\frac{\pi(2\bar{R} - \bar{\delta}_s) \left(\beta_8 \bar{g} \bar{h} - \frac{\mu_s^2 \alpha^1 c_p \bar{U}_s \bar{\delta}_s}{2k_s} \right)}{(1 - \pi(2\bar{R} - \bar{\delta}_s)) \bar{\beta} \beta_8} \right) \quad (4.73)$$

$$\kappa_{11} = \frac{1}{2} [\Gamma + \beta_1 \gamma] \left(\frac{\pi(2\bar{R} - \bar{\delta}_s) \left(\beta_8 \bar{g} \bar{h} - \frac{\mu_s^2 \alpha^1 c_p \bar{U}_s \bar{\delta}_s}{2k_s} \right)}{(1 - \pi(2\bar{R} - \bar{\delta}_s)) \bar{\beta} \beta_8} \right) \quad (4.74)$$

$$\psi_1 = \Gamma - 2\mu_s \pi \bar{P}_s (2\bar{R} - \bar{\delta}_s) \quad (4.75)$$

4.7 Discussion of Results

Dynamic stress propagation, as influenced by flow induced coupled transverse and longitudinal vibrations, within the context of a vibrating offshore pipeline in deep sea environment, is investigated in this research. By employing parametric values in Table 4.1, simulated results have shown that the bursting and buckling of these conveyance media on porous rigid seabed, under hydrodynamic forces and traction are influenced by factors such as, the internal fluid transport velocity, temperature, pressurization, pre-stress etc. In particular, Figures 4.1- 4.7 illustrate the effects of accumulation of sediment layer growth (i.e. the pipe burial) and transport velocity in conjunction with geotechnical characteristics on the steady state burst and buckling pressure profiles. As can be observed in Figure 4.1, the burst pressure increases with the rate of pipe burial as the fluid moves through the pipe. In Figure 4.2, the results show that, the longer the pipe, the higher would be the burst pressure for a buried pipe.

Furthermore, the buckling pressure as demonstrated in Figures 4.3 and 4.4, with the same conditions for the burst pressure, showed that, the buckling pressure is always less than the burst pressure, which was in agreement with the results presented in Chapter 3. Also, in Figure 4.5, the effect of the pipe burial on the dynamic stress distribution is displayed, where the burst pressure increases from the middle of the buried pipe to the wall of the pipe with varying sediment growth layers.

In Figures 4.6 and 4.7, the effects of internal fluid transport velocities are shown, where it is observed that, increasing the velocity will lead to a high burst pressure. In particular, Figure 4.7 illustrates the results when the axes in Figure 4.6 are turned orthogonally. This is in conformity with the results in a well established text book of transport phenomena.

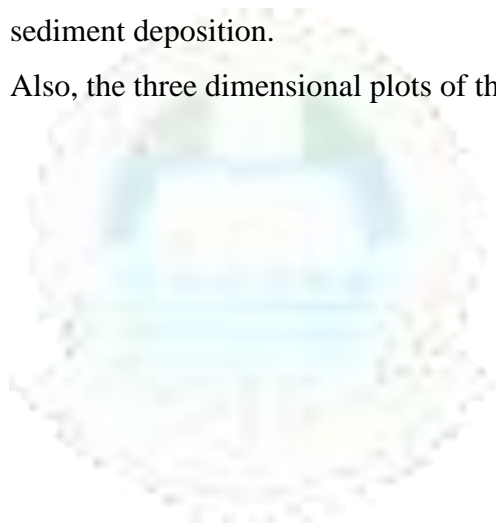
As can be seen in Figure 4.8, transient burst pressure is plotted for various seepage movement. Here, we observed the burst pressure attenuating until it reaches a minimum value before it starts to increase monotonically as the buried pipe conveys the internal fluid across.

In Figure 4.9, the profiles of the burst pressure as modulated by the level of sedimentation activities across the pipe segment is illustrated. As expected, the pressure required to burst these pipes can be significantly enhanced by increase in sedimentation activities, irrespective of the value of their diameters. We have in Figure 4.10, the plot of steady state burst pressure against the

sediment velocity for various pipe thicknesses. The results show that , the burst pressure increases with increase in the pipe thickness, hence, the thicker the pipe, the greater the burst pressure for the pipe to rupture. As can be deduced from Figure 4.11, the burst pressure is expectedly higher than the buckling pressure, regardless of whether the pipe is resting, or is partially or totally buried as a result of sedimentation activities, that are constantly reshaping the ocean floor geomorphology in endless cycles.

Besides, the modal effects are illustrated in Figure 4.12, where it is observed that the burst pressure is higher for even modes in comparison with the odd modes. While, a comparison of the steady state burst pressure profile, as computed with Barlow's equation and one of the empirical relationships reported in Saat and Duckhovic's is shown in Figure 4.13. As expected, the pressure is maximum at the walls of the pipe, which is found to be increasing with increase in the level of sediment deposition.

Also, the three dimensional plots of the burst pressure are as shown in Figures 4.14 and 4.15.



UNIVERSITY
OF LAGOS

Table 4.1: Parametric Values Used For Simulation

S/N	DESCRIPTION	SYMBOL	VALUES USED
1	Density of pipe material	ρ	7850Kg/m ³
2	Density of sea water	ρ_w	980 kg/m ³
3	Pipeline fluid relative density	ρ_f	0.977 kg/m ³
4	Wave number	k	0.1
5	Characteristic stress	T_o	5x10 ¹⁸ N/m ²
6	Modulus of elasticity of pipe material	E	200GN/m ²
7	Acceleration due to free fall	g	9.8m/s ²
8	Height (depth) of pipeline below mean sea surface	h	1500m
9	Seabed modulus of deformation	K_b	8, 800N/m
10	Length of the pipeline	L	6, 60m
11	External Diameter	D_o	0.4064m
12	Internal Diameter	D_i	0.394m
13	Inner Radius of the pipeline	R	$D_i/2$
14	Moment of inertia	I	1.17x10 ⁻⁵ m ⁴
15	Uniform fluid flow velocity through the pipe	U	3 m/s
16	Transverse pipe displacement	w	$w(x, t)$
17	Axial pipe displacement	u	$u(x, t)$
18	Temperature	θ	110°C
19	Temperature gradient	$\Delta\theta$	10°C
20	Pressure	P	1-5x10 ⁵ N/m
21	Tensile prestress	T	5x10 ¹⁸ N/m ²
22	Damping force/vel. in transverse and axial direction resp.	$C_1, C_2,$	1, 5
23	Normalised density of water	$\bar{\rho}_w$	1
24	Sediment relative density	$\bar{\rho}_s$	0.6
25	Sliding frictional coefficient at the interface of the pipe and the sediment layer	μ_s	0.2

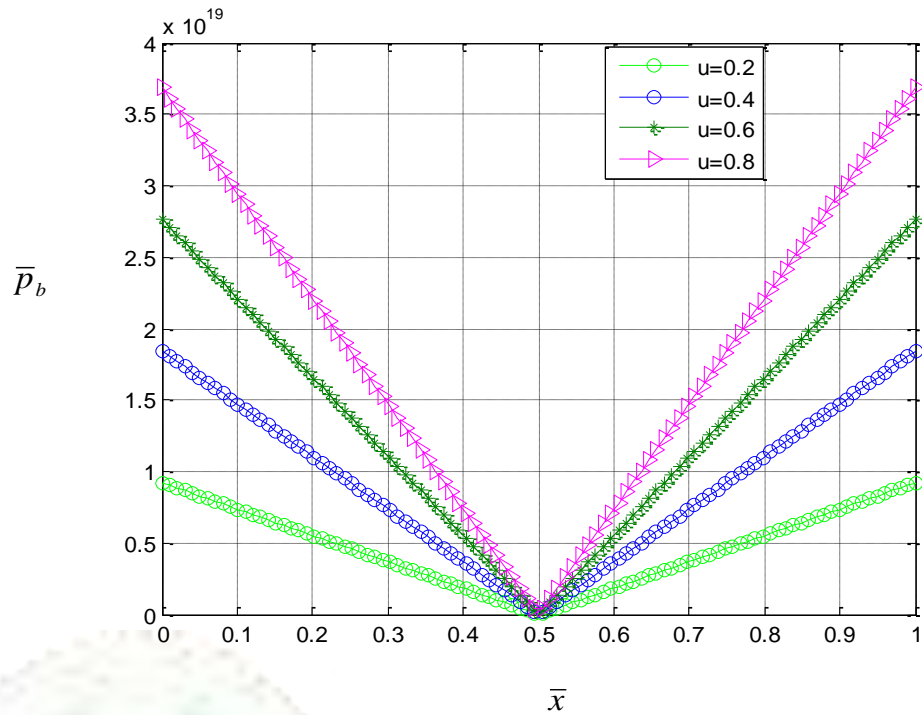


Fig.4.1 Steady state burst pressure profile of the pipe on a hard sea bed for the case $n = 1; U = 5m/s; \bar{t} = 1; \bar{z} = 1; k_b = 800; \bar{\delta}_s = 0.5; L = 6m$

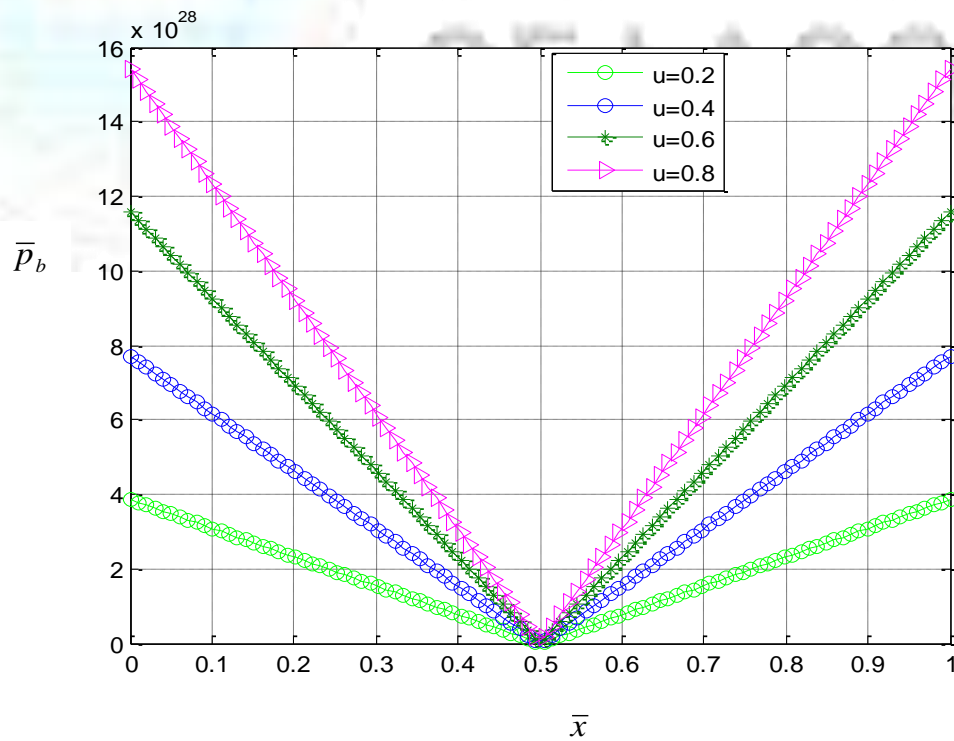


Fig.4.2: Steady state burst pressure profile of the pipe on a hard sea bed for the case $n = 1; U = 5m/s; \bar{t} = 1; \bar{z} = 1; k_b = 800; \bar{\delta}_s = 0.5; L = 60m$

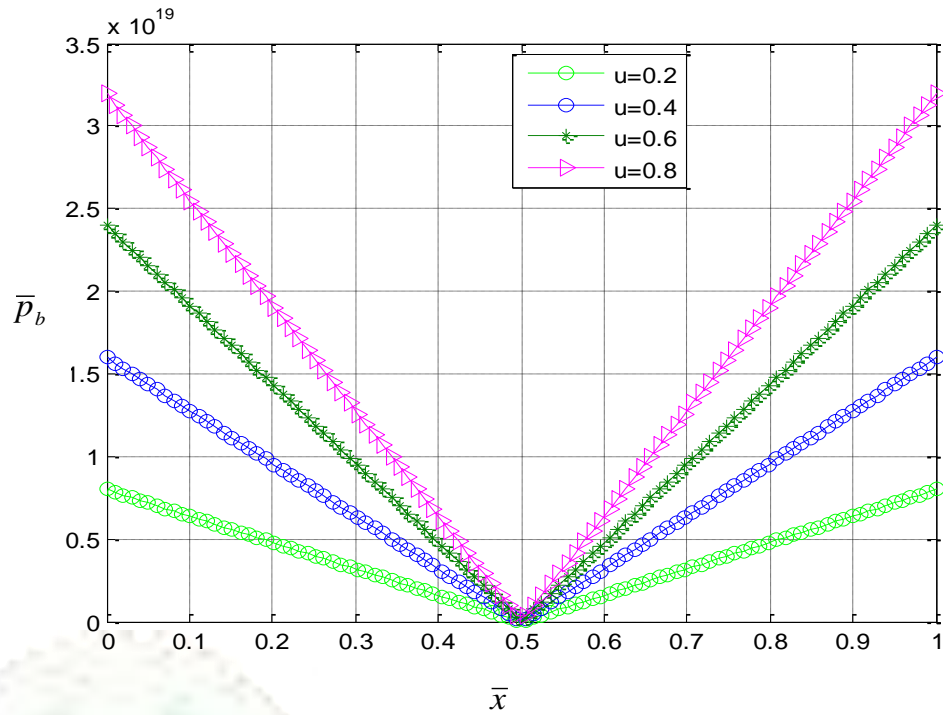


Fig.4.3: Steady state buckling pressure profile of the pipe on a hard sea bed for the case $n = 1; U = 5m/s; \bar{t} = 1; \bar{z} = 1; k_b = 800; \bar{\delta}_s = 0.5; L = 6m$

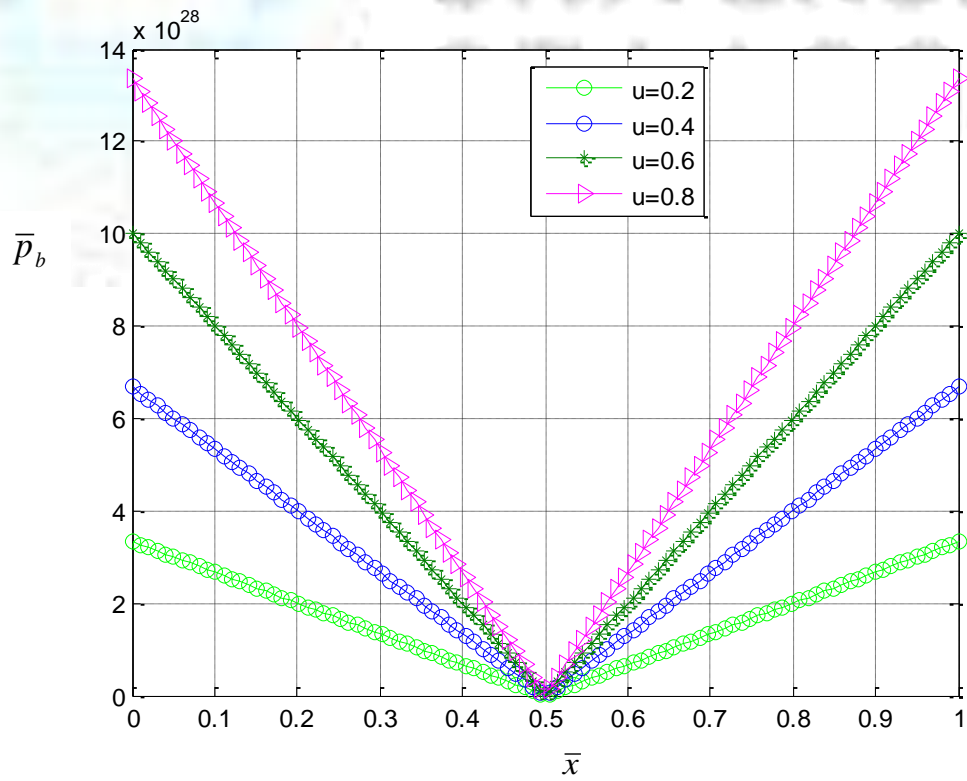


Fig.4.4: Steady state buckling pressure profile of the pipe on a hard sea bed for the case $n = 1; U = 5m/s; \bar{t} = 1; \bar{z} = 1; k_b = 800; \bar{\delta}_s = 0.5; L = 60m$

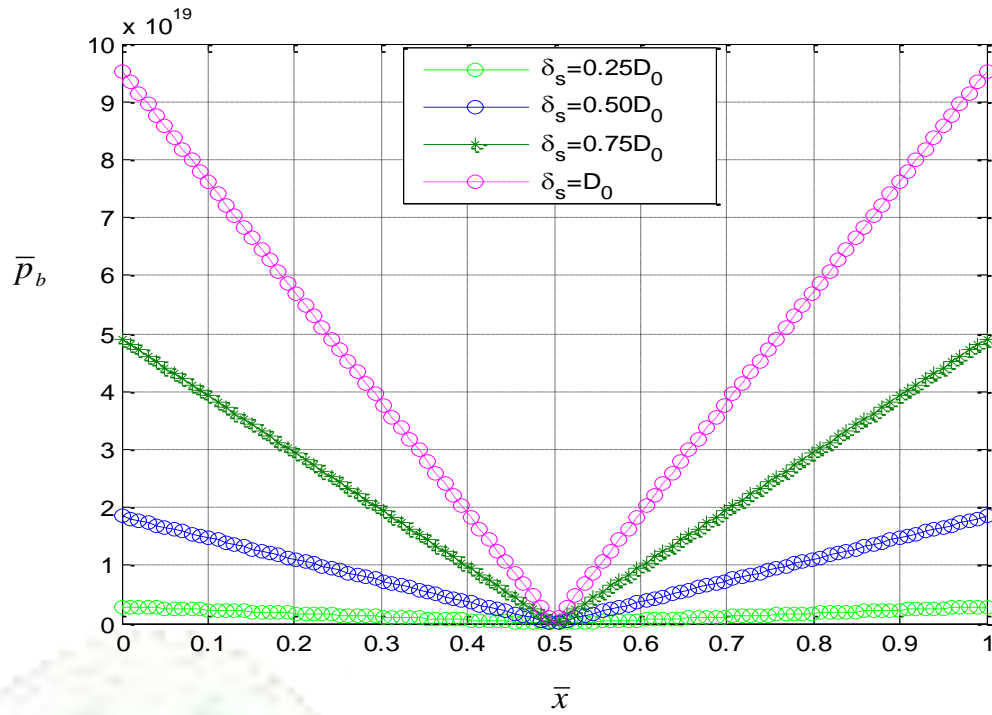


Fig.4.5: Steady state burst pressure profile of the pipe on a hard sea bed for the case
 $n = 1; U = 5m/s; \bar{t} = 1; \bar{z} = 1; k_b = 800; \bar{\delta}_s = 0.5; L = 6m$

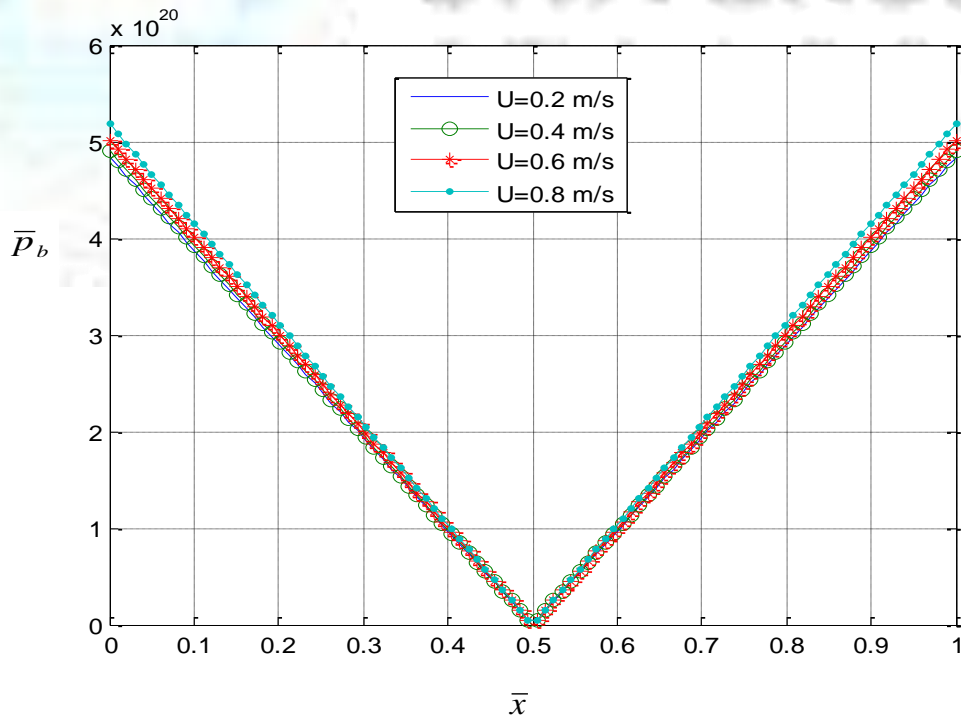


Fig.4.6: Steady state burst pressure profile of the pipe on a hard sea bed for the case
 $n = 1; \bar{t} = 1; \bar{z} = 1; k_b = 800; \bar{\delta}_s = 0.5; L = 6m$

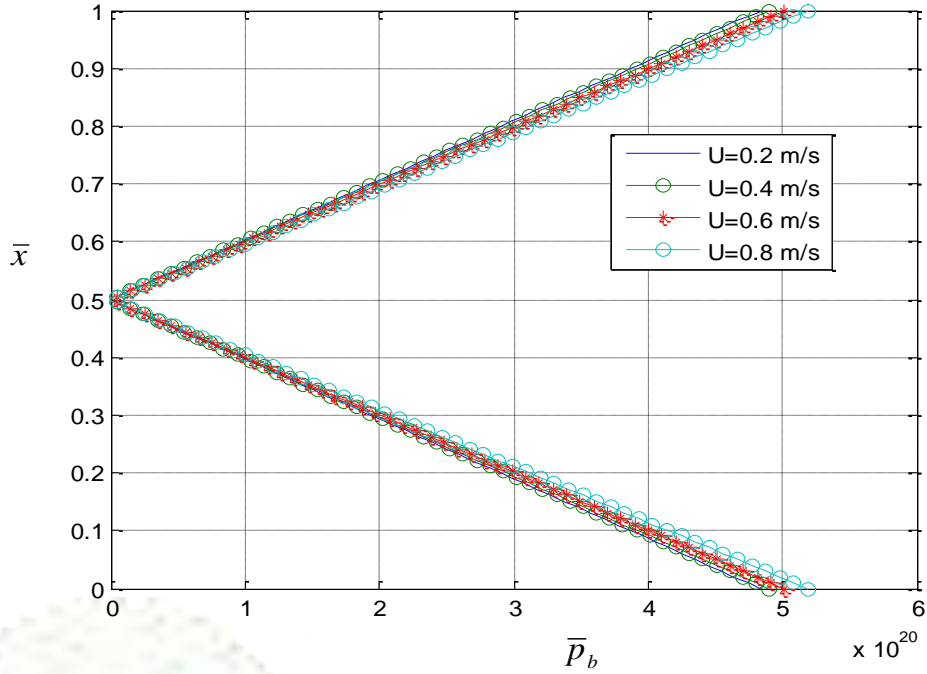


Fig.4.7: Steady state burst pressure profile of the pipe on a hard sea bed for the case (orthogonal axis)
 $n = 1; \bar{t} = 1; \bar{z} = 1; k_b = 800; \bar{\delta}_s = 0.5; L = 6m$

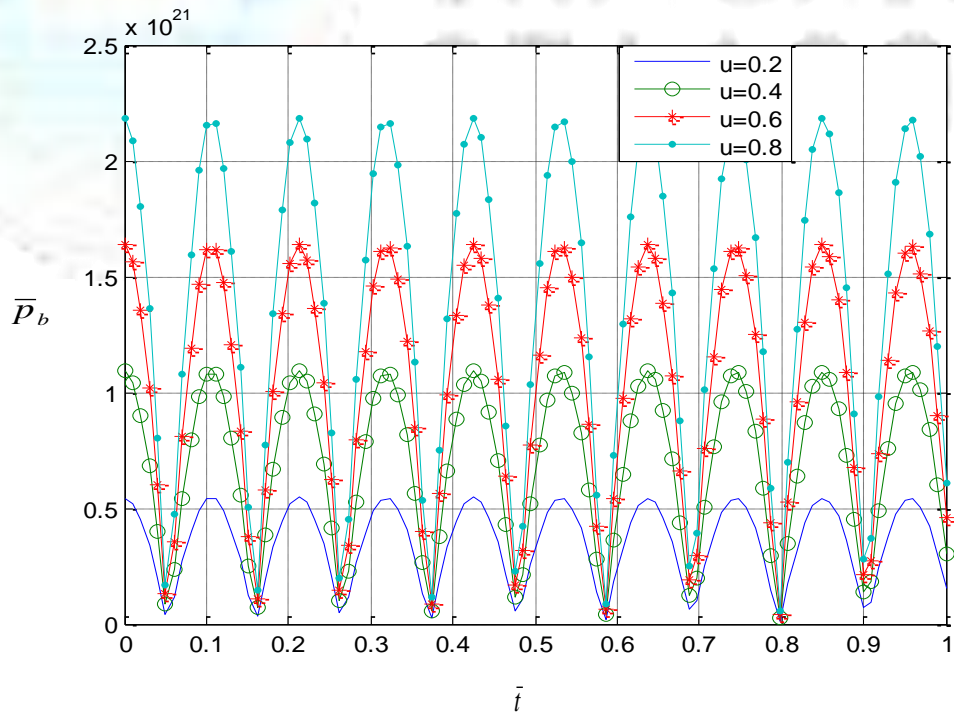


Fig.4.8: Transient burst pressure response profile of the pipe on a hard sea bed for the case
 $n = 1; U = 5m/s; \bar{x} = 1; \bar{z} = 1; k_b = 800; \bar{\delta}_s = 0.5; L = 6m$

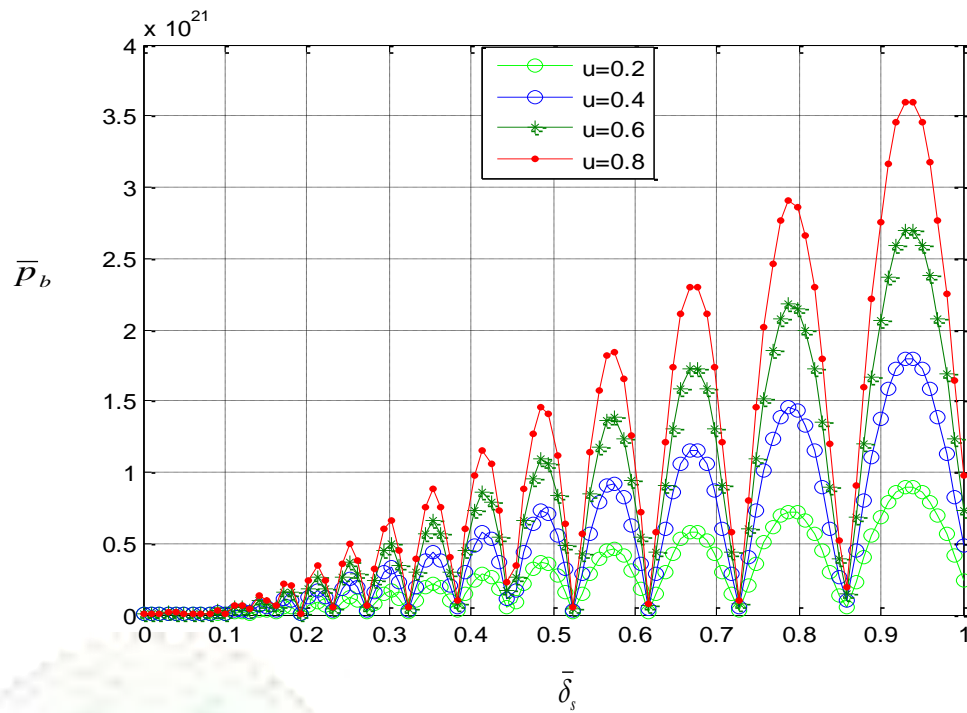


Fig.4.9: Steady state burst pressure profile of the pipe on a hard sea bed for the case

$$n = 1; U = 5m/s; \bar{t} = 1; \bar{x} = 0.5; \bar{z} = 1; k_b = 800; L = 6m$$

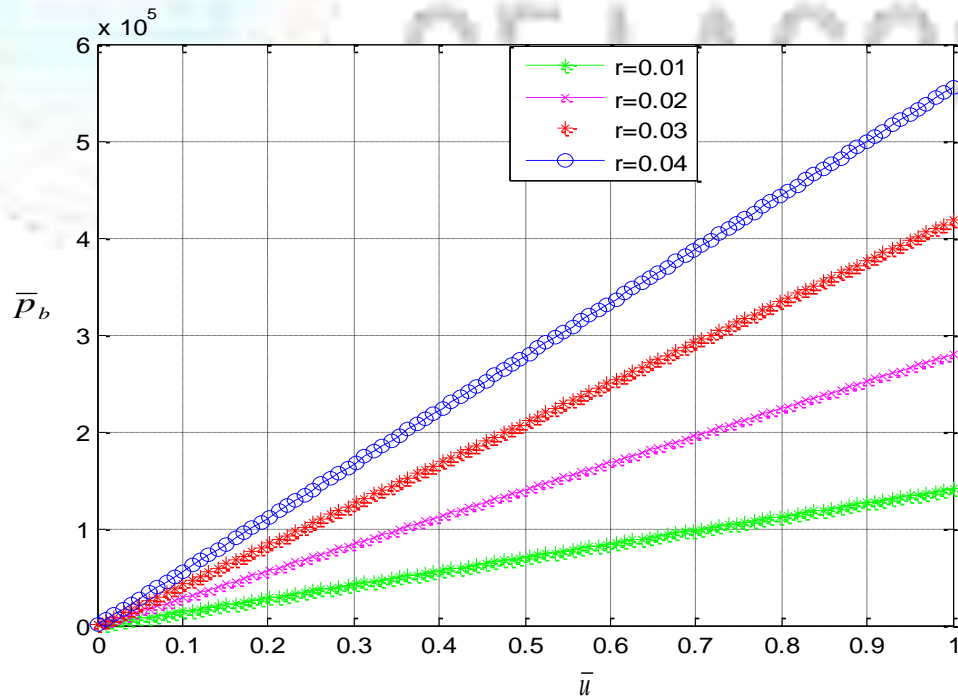


Fig.4.10: Steady state burst pressure profile of the pipe on a hard sea bed for the case

$$n = 1; U = 5m/s; \bar{t} = 1; \bar{x} = 0.5; \bar{z} = 1; k_b = 800; \bar{\delta}_s = 0.5; L = 6m$$

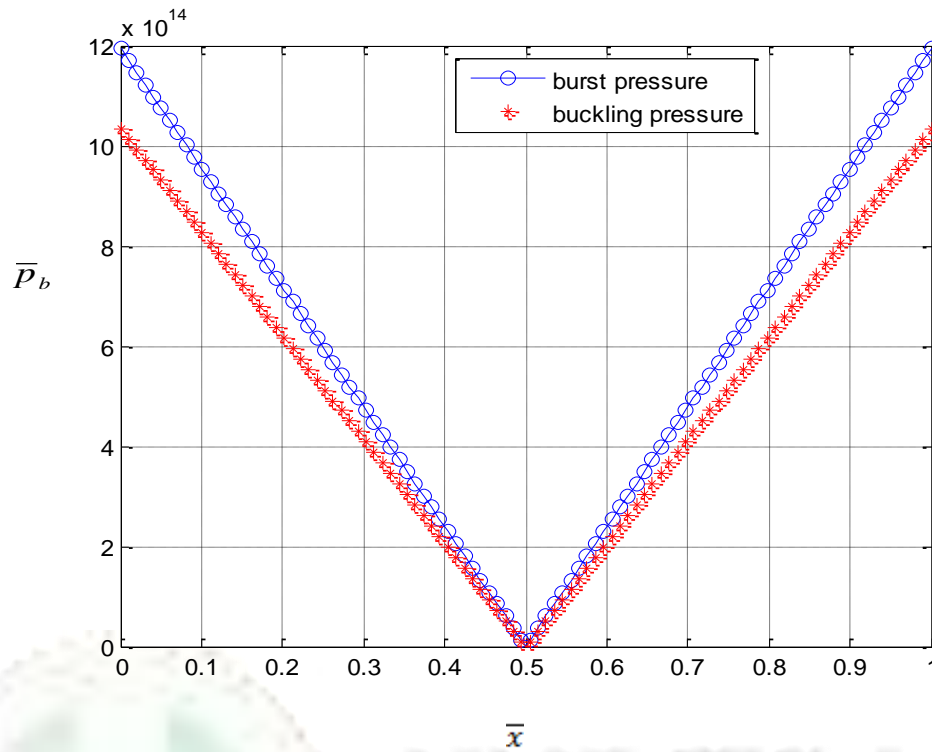


Fig.4.11: Steady state burst pressure profile of the pipe on a hard sea bed for the case

$$n = 1; U = 5m/s; \bar{t} = 1; \bar{z} = 1; k_b = 800; \bar{\delta}_s = 0.5; L = 6m$$

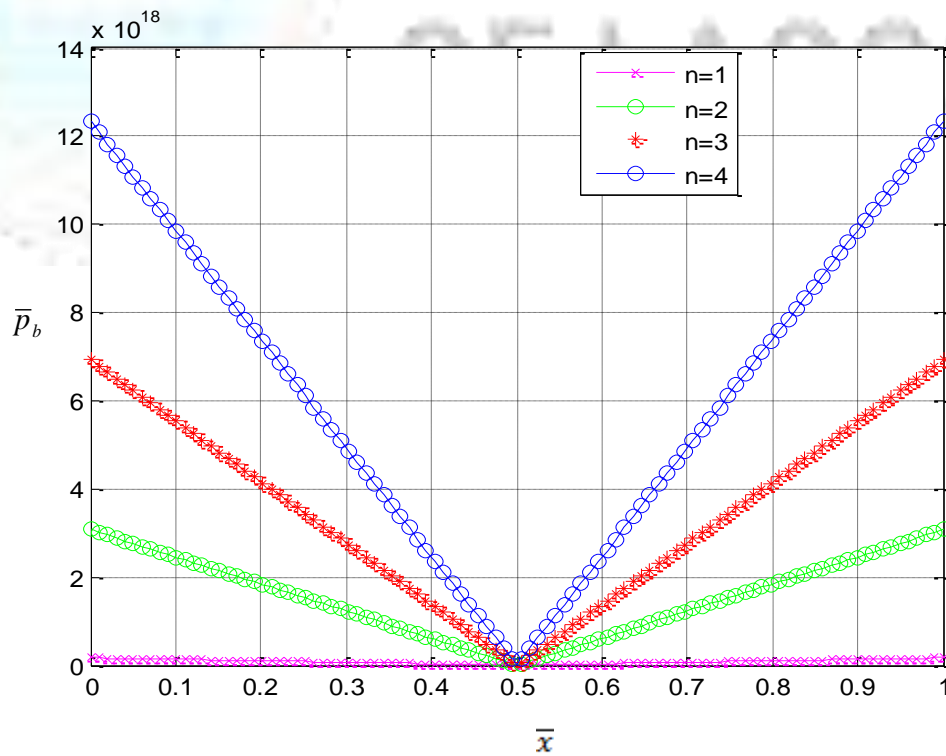


Fig. 4.12: Steady state burst pressure profile of the pipe on a hard sea bed for the case

$$U = 5m/s; \bar{t} = 1; \bar{z} = 1; k_b = 800; \bar{\delta}_s = 0.5; L = 6m$$

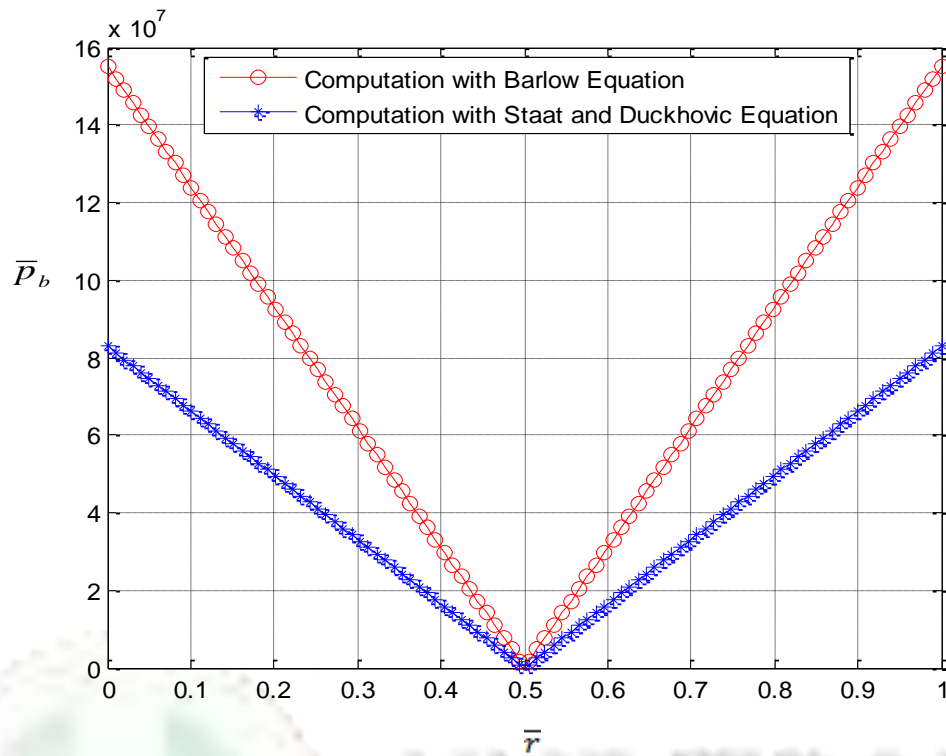


Fig.4.13: Steady state burst pressure profile of the pipe on a hard sea bed for the case
 $n = 1; U = 5m/s; \bar{t} = 1; \bar{z} = 1; k_b = 800; \bar{\delta}_s = 0.5; L = 6m$

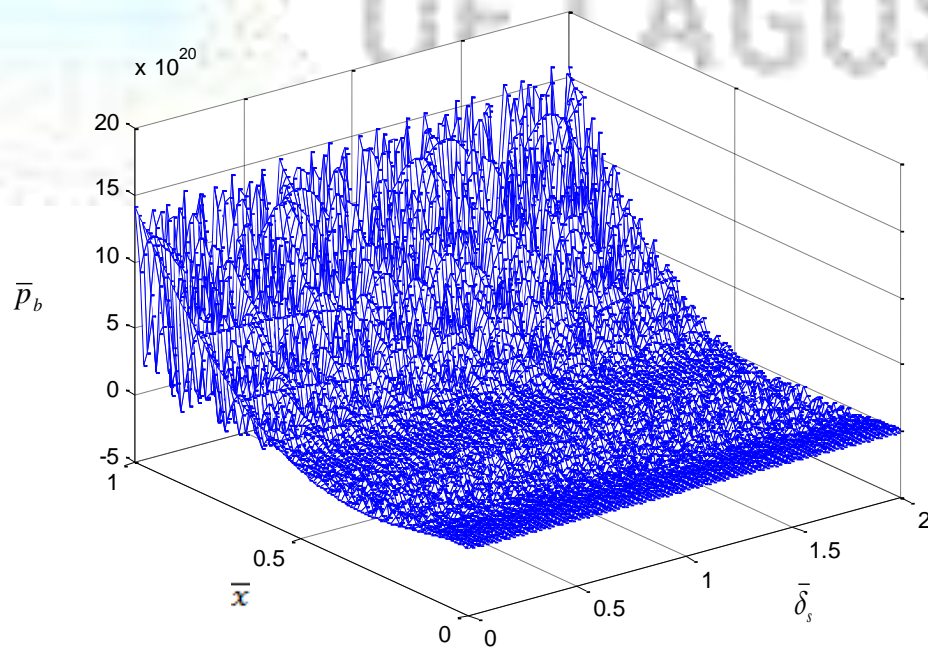


Fig.4.14: Steady state burst pressure profile of the pipe on a hard sea bed for the case
 $n = 1; \bar{U} = 5; \bar{z} = 1; k_b = 800; \bar{\delta}_s = 0.5; L = 6m$

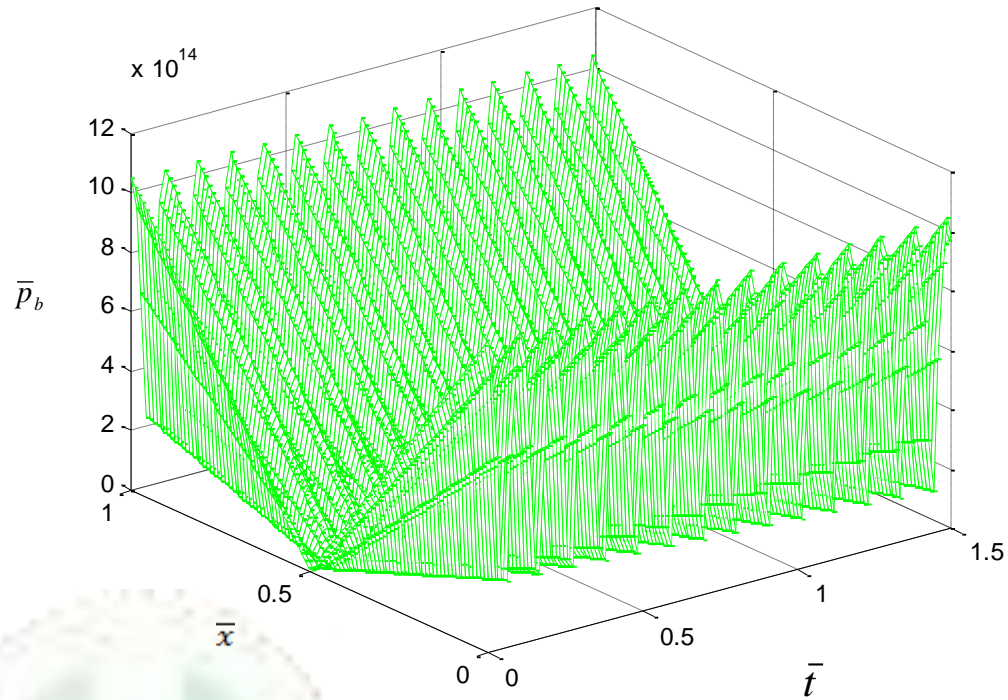


Fig.4.15: Steady state burst pressure profile of the pipe on a hard sea bed for the case

$$n = 1; \bar{U} = 5; \bar{z} = 1; k_b = 800; \bar{\delta}_s = 0.5; L = 6m$$

CHAPTER 5

CONCERNING DYNAMIC STRESS PROPAGATION IN AN OFFSHORE PIPELINE AT THE SEABED FOR DESIGN APPLICATION

5.1 Problem Fundamentals and Governing Differential Equation

This chapter attempts to present another method of dynamic stress propagation analysis concerning the vibration of a pre-stressed high pressure and high temperature subsea pipe that is transporting a fluid and resting on the seabed. For this investigation, an offshore pipeline is assumed to be sitting on an elastic foundation and the corresponding set of equations governing the transverse and longitudinal motions of the pipe are formulated. Besides, by employing integral transforms, an analytic solution for the induced stresses in polar coordinates coupled with von Mises yield criterion is reported for design analysis and applications.

The physical problem under investigation consists of a fluid pipeline sitting on an ocean floor or seabed. The investigation here entails the study of a fluid pipeline soil dynamic interaction boundary value problem, with the attendant fully fluid flow regime. The pipe and its position are as shown in Figure 5.0 below, while the necessary assumptions leading to the formulation of the well posed boundary value partial differential equations governing the dynamic interaction problem under investigation are listed viz:

- (i) The coordinate system is described appropriately by the cylindrical polar system (r, θ) ;
- (ii) The entire system is axisymmetric i.e., the geometry and the internal loading are symmetrical about the axis of the cylinder;
- (iii) Due to axial symmetry, there are no shear stresses, $\tau_{\theta r}$ and $\tau_{r\theta}$ and
- (iv) For open pipe, axial stress σ_z is negligible.

Following the above assumptions, the equations of equilibrium of forces acting on the element of material in the radial and circumferential directions have been derived in equations (C.21 & C.22) in the appendix as:

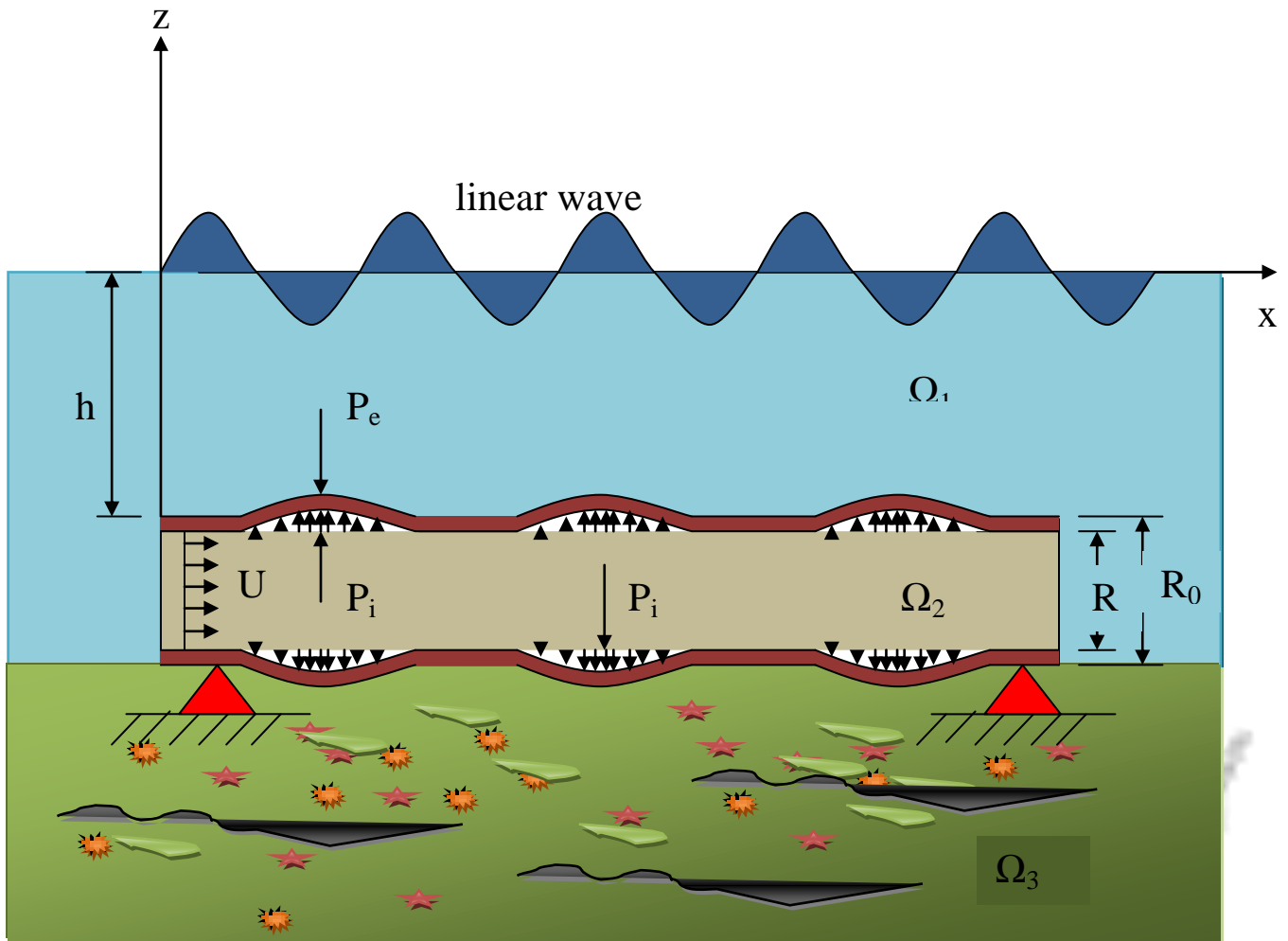


Figure 5.0. The flow geometry of the model at the seabed.

$$\sigma_r = -p_i \left(\frac{r^2 R_i^2 - R_i^2 R_0^2}{r^2 (R_i^2 - R_0^2)} \right) + \left(\frac{r^2 R_0^2 - R_i^2 R_0^2}{r^2 (R_i^2 - R_0^2)} \right) p_e$$

$$- \frac{(2-\nu)}{3(1-\nu)} (\rho \bar{a}_r) \left(\frac{r^2 (R_i + R_0) R_i + r^2 R_0^2 - R_i^2 R_0^2 - r^3 (R_i + R_0)}{r^2 (R_i + R_0)} \right) \quad (5.1)$$

$$\sigma_\theta = -p_i \left(\frac{r^2 R_i^2 + R_i^2 R_0^2}{r^2 (R_i^2 - R_0^2)} \right) + \left(\frac{r^2 R_0^2 + R_i^2 R_0^2}{r^2 (R_i^2 - R_0^2)} \right) p_e$$

$$- \frac{(2-\nu)}{3(1-\nu)} (\rho \bar{a}_r) \left(\frac{r^2 (R_i + R_0) R_i + r^2 R_0^2 + R_i^2 R_0^2 - r^3 (R_i + R_0)}{r^2 (R_i + R_0)} \right) \quad (5.2)$$

5.2 Failure Analysis

The greatest absolute values of radial and hoop stresses occur at the inner surface of the cylinder and are given below:

For σ_r , we substitute $r = R_i$ in equation (5.1) to get

$$\sigma_{r,\max} = -p_i \quad (5.3)$$

Also,

$\sigma_{\theta,\max}$ occurs at $r = R_i$, using this in equation (5.2) gives

$$\sigma_{\theta,\max} = -p_i \left(\frac{R_i^2 + R_0^2}{(R_i^2 - R_0^2)} \right) + 2 \left(\frac{R_0^2}{(R_i^2 - R_0^2)} \right) p_e - \frac{(2-\nu)}{3(1-\nu)} (\rho \bar{a}_r) 2 \left(\frac{R_0^2}{(R_i + R_0)} \right) \quad (5.4)$$

Equations (5.3 and 5.4) can be non-dimensionalised into the forms

$$\bar{\sigma}_{r,\max} = -\bar{p}_i \quad (5.5)$$

$$\bar{\sigma}_{\theta,\max} = -\bar{p}_i \left(\frac{\bar{R}_i^2 + \bar{R}_0^2}{(\bar{R}_i^2 - \bar{R}_0^2)} \right) + 2 \left(\frac{\bar{R}_0^2}{(\bar{R}_i^2 - \bar{R}_0^2)} \right) \bar{p}_e - \frac{(2-\nu)}{3(1-\nu)} (\bar{\rho} \bar{a}_r) 2 \left(\frac{\bar{R}_0^2}{(\bar{R}_i + \bar{R}_0)} \right) \quad (5.6)$$

where the followings can be expressed viz:

$$x = \bar{x}L, w = \bar{w}L, \delta = \frac{m_f}{m}, t = \tau \bar{t}, \tau = L^2 \sqrt{\frac{m}{EI}}, U = \bar{U} \frac{L}{\tau_f}, \bar{P}\bar{A} = \frac{PA_o L^2}{EI}, \Delta \bar{P}\bar{A} = \frac{\Delta PA_o L^2}{EI}, \delta_1 = \frac{m_w}{M},$$

$$R = \bar{R}L, A = \bar{A}L^2, \beta = \frac{T_0 L^2}{EI}, \beta_1 = \frac{EA_{t0} L^2}{EI}, \beta_2 = \frac{\sqrt{\delta}}{U}, \beta_3 = \alpha \beta_1 \beta_2 \Theta, \beta_4 = \alpha \beta_1 \beta_2 \Delta \Theta, \beta_5 = \alpha \beta_1 \Theta, \bar{\rho} = \frac{\rho L^5}{EI \tau^2}$$

$$\beta_6 = \alpha \beta_1 \Delta \Theta, \beta_7 = \frac{\beta_1}{U}, \beta_8 = \frac{\delta_1}{L}, \bar{C}_D = \frac{C_D L^2}{\sqrt{mEI}}, \bar{C}_s = \frac{C_s L^2}{\sqrt{mEI}}, \Phi = \frac{\bar{\Phi} L^2}{\tau^2}, \bar{g} = \frac{Mg L^3}{EI}, \bar{K}_b = \frac{K_b L^4}{EI}, \alpha' = \frac{L^4}{I}$$

For the material to yield, the hoop stress and radial stress are maxima at the inner wall of the pipe. Hence, von Mises yield criterion is applied in terms of the three principal stresses i.e., σ_1, σ_2 and σ_3 . This is written as

$$(\sigma_1 - \sigma_2)^2 + (\sigma_2 - \sigma_3)^2 + (\sigma_3 - \sigma_1)^2 = 2\sigma_y^2 \quad (5.7)$$

where σ_y is the yield stress of the pipe material.

In this case, $\sigma_1 = \bar{\sigma}_{\theta,\max}$, $\sigma_2 = \bar{\sigma}_{z,\max}$, $\sigma_3 = \bar{\sigma}_{r,\max}$. Furthermore, the pipe is open-ended, thus axial stress $\bar{\sigma}_{z,\max} = 0$.

Using the above conditions we get

$$\bar{\sigma}_{\theta,\max}^2 + \bar{\sigma}_{r,\max}^2 - \bar{\sigma}_{\theta,\max} \bar{\sigma}_{r,\max} = \bar{\sigma}_y^2 \quad (5.8)$$

Substituting equations (5.5 and 5.6) into equation (5.8), yields, after simplification,

$$\bar{p}_i^2 D + \bar{p}_i Q + M = 0 \quad (5.9)$$

where the followings are defined as

$$D = \left(1 + \frac{2\bar{R}_0^2(\bar{R}_i^2 + \bar{R}_i^2\bar{R}_0^2)}{(\bar{R}_i^2 - \bar{R}_0^2)^2} \right) \quad (5.10)$$

$$Q = \left(\frac{\bar{R}_0^2}{(\bar{R}_i^2 - \bar{R}_0^2)^2} \right) \left(\frac{2}{3} \left(\frac{2-\nu}{1-\nu} \right) \bar{\rho} \bar{a}_r \right) - \frac{2\bar{p}_e(\bar{R}_i^2 + 3\bar{R}_0^2)}{\bar{R}_i^2 - \bar{R}_0^2} \quad (5.11)$$

$$M = 4\bar{p}_e \left(\frac{\bar{R}_0^2}{\bar{R}_i^2 - \bar{R}_0^2} \right) \left(\frac{\bar{R}_0^2}{\bar{R}_i^2 - \bar{R}_0^2} - \frac{2}{3} \bar{\rho} \bar{a}_r \left(\frac{2-\nu}{1-\nu} \right) \frac{\bar{R}_0^2}{\bar{R}_i^2 + \bar{R}_0^2} \right) + \left[\left(\frac{2}{3} \left(\frac{2-\nu}{1-\nu} \right) \bar{\rho} \bar{a}_r \right) \frac{\bar{R}_0^2}{\bar{R}_i + \bar{R}_0} \right]^2 - \bar{\sigma}_y^2$$

Equation (5.9) now enables us to express

$$\bar{p}_i = \frac{-Q \pm \sqrt{Q^2 - 4DM}}{2D} \quad (5.12)$$

where

$$\bar{\rho} \bar{a}_r = \bar{\rho} \frac{\partial^2 \bar{w}}{\partial \bar{t}^2} \quad \forall \rho = \rho_p + \rho_f \quad (5.13)$$

This is obtained from the transverse response of a vibrating offshore pipeline.

Following modified Gorman et al (2000), the transverse response of a vibrating offshore pipeline in Laplace domain is given as

$$\tilde{w}(\bar{x}, s) = \sum_{n=1}^{\infty} \left(\frac{\bar{\delta}_1 \bar{g} \bar{h}}{(1 - \bar{\delta}_1 \bar{\beta})} \bar{\Gamma}^F \right) \frac{\sin n\pi\bar{x}}{s(s^2 + \bar{\eta}_1 s + \bar{\eta}^2)} \quad (5.14)$$

In the meantime, we can re-express the following in polynomial form viz:

$$\sum_{n=1}^{\infty} \bar{\Gamma}^F \sin n\pi\bar{x} = \sum_{n=1}^{\infty} \left(\frac{1 + (-1)^{n+1}}{n\pi} \right) \sin n\pi\bar{x} = \frac{n^4 \pi^4}{32} \sum_{n=1}^{\infty} \frac{\sin 2n\pi\bar{x}}{n^5 \pi^5} \quad (5.15)$$

via the following closed form Fourier series representation namely

$$\sum_{n=1}^{\infty} \frac{\sin n\bar{x}}{n^5} = \frac{\pi^4 \bar{x}}{90} - \frac{\pi^2 \bar{x}^3}{36} + \frac{\pi \bar{x}^4}{48} - \frac{\bar{x}^5}{240} \quad \forall 0 < \bar{x} < 2 \quad (5.16)$$

where

$$\Gamma(\bar{x}) = \frac{\bar{x}}{45} - \frac{2\bar{x}^3}{9} + \frac{\bar{x}^4}{3} - \frac{2\bar{x}^5}{15} \quad (5.17)$$

Consequently,

$$\bar{w}(\bar{x}, \bar{t}) = \frac{\bar{\delta}_1 \bar{g} \bar{h}}{(1 - \bar{\delta}_1 \bar{\beta})} \frac{n^4 \pi^4}{32} \Gamma(\bar{x}) F(\bar{t}) \quad (5.18)$$

where

$$\bar{\eta}_1 = \frac{\bar{C}_1 + \bar{C}_D - \beta_4(1 - \frac{\gamma}{2}) - \beta_3\gamma - \Delta\bar{P}\bar{A}_0\beta_2(1 - \frac{\gamma}{2}) - \beta_2\bar{P}\bar{A}_0\gamma}{(1 - \delta_1\bar{\beta})} \quad (5.19)$$

and,

$$\bar{\eta}^2 = \left(\frac{n^4\pi^4 - [3\sqrt{\delta}\bar{U}^2 - \beta + \beta_3(1 - \frac{\gamma}{2}) + \bar{P}\bar{A}_0(1 - \frac{\gamma}{2})]n^2\pi^2 + \bar{k}_b}{(1 - \delta_1\bar{\beta})} \right) \quad (5.20)$$

while,

$$\bar{\alpha}_1 = \frac{\bar{\eta}_1}{2} + i\sqrt{\bar{\eta}^2 - \frac{\bar{\eta}_1^2}{4}}; \bar{\alpha}_2 = \frac{\bar{\eta}_1}{2} + i\sqrt{\bar{\eta}^2 - \frac{\bar{\eta}_1^2}{4}} \quad (5.21)$$

and

$$\bar{F}(\bar{t}) = \left(\frac{1}{\bar{\alpha}_1\bar{\alpha}_2} + \frac{1}{\bar{\alpha}_1\bar{\alpha}_2(\bar{\alpha}_2 - \bar{\alpha}_1)} (\bar{\alpha}_1 e^{-\bar{\alpha}_1\bar{t}} - \bar{\alpha}_2 e^{-\bar{\alpha}_2\bar{t}}) \right) \quad (5.22)$$

Following Olunloyo et al (2007)

$$\bar{P}_{e(hyd)} = -\bar{\rho}_w \left(\frac{\partial \bar{\Phi}}{\partial \bar{t}} + \bar{h}\bar{g} \right) \quad (5.23)$$

while the velocity potential in the Laplace transform plane is given as

$$\tilde{\Phi}(s, \bar{x}, \bar{z}) = \frac{\phi(x, 0)s\tilde{w}(\bar{x}, s)}{k \sinh k\bar{h}} \cosh k\bar{z} \quad (5.24)$$

so that,

$$\tilde{\Phi}(s, x, z) = \frac{U_w Ls\tilde{w}(x, s)}{k} \coth k\bar{h} \quad (5.25)$$

Equation (5.23) can be rewritten in view of equation (5.25) as

$$\tilde{P}_{e(hyd)} = -\delta_1 \left(\bar{\beta}s^2\tilde{w}(\bar{x}, s) + \frac{\bar{h}\bar{g}}{s} \right) \quad (5.26)$$

Using equations (5.14, 5.16 and 5.18) in equation (5.26), yield

$$\bar{P}_{e(hyd)} = -\delta_1 \left(\bar{\beta} \frac{\delta_1 \bar{g} \bar{h}}{(1 - \delta_1 \bar{\beta})} \frac{n^4 \pi^4}{32} \Gamma(\bar{x}) F(\bar{t}) + \bar{h}\bar{g} \right) \quad (5.27)$$

Similarly, substituting equations. (5.16, 5.17 and 5.18) in equation (5.13) give

$$\bar{\rho} \bar{a}_r = \bar{\rho} \frac{\bar{\delta}_1 \bar{g} \bar{h}}{(1 - \bar{\delta}_1 \bar{\beta})} \frac{n^4 \pi^4}{32} \Gamma(\bar{x}) F_1(\bar{t}) \quad (5.28)$$

Here,

$$F_1(\bar{t}) = \left(\frac{(\bar{\alpha}_2 e^{-\bar{\alpha}_2 \bar{t}} - \bar{\alpha}_1 e^{-\bar{\alpha}_1 \bar{t}})}{(\bar{\alpha}_2 - \bar{\alpha}_1)} \right) \quad (5.29)$$

5.3 Discussion of the Results.

In Figure 5.1, steady state burst pressure is plotted against the normalised pipe internal radius, while Figure 5.2 shows the same result but for different modes. It is evident here that, regardless of the modes, the pressure will increase from the centre of the pipe to the inner wall of the pipe.

The next result, i.e., Figure 5.3, the pressure attenuates monotonically to a point and then rises monotonically to a maximum point before decreases to initial point while the fluid moves through the pipe. Furthermore, the result of the burst pressure against the normalised pipe thickness, where the pressure increases as the thickness increases are shown in Figure 5.4. The implication is that, high pressure will be needed to burst a thick pipe wall. Figure 5.5 shows the patterns obtained when the burst pressure is plotted against the fluid internal velocity. Here, the pressure increases steadily with the internal flow velocity until it gets to a maximum value for different thicknesses. The significant of this result is that, the maximum pressure should be avoided in order to maintain the pipeline integrity, beyond this value it could be a disastrous failure.

Interesting results were obtained in Figure 5.6 for the transient burst pressure with different fluid velocities. The results showed clearly that the burst pressure attenuates monotonically and increases monotonically with many peak values over the time of operation.

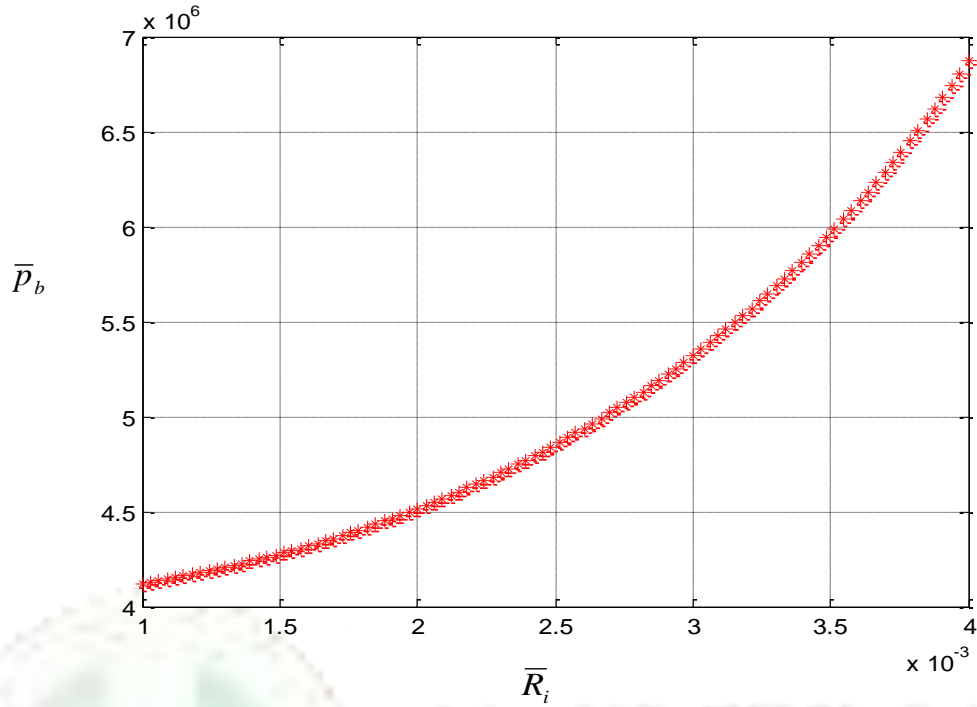


Figure 5.1: Burst pressure profile for the case;
 $n = 1; U = 5m/s; \bar{t} = 1; k_b = 8000; \bar{x} = 0.5; L = 2km; h = 1500m$

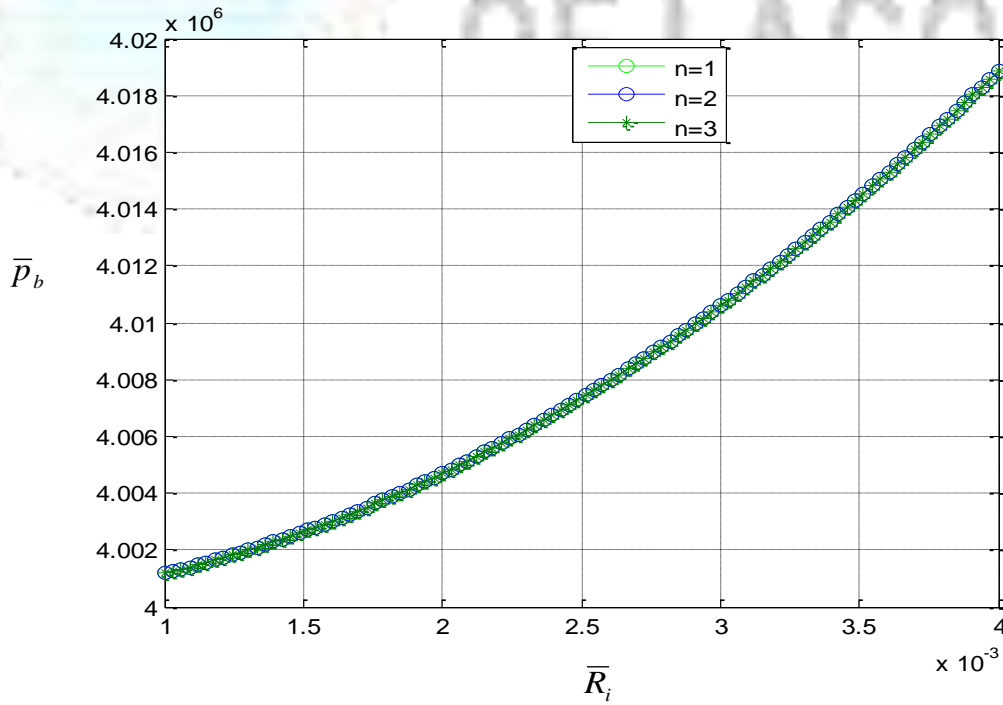


Figure 5.2: Burst pressure profile with different modes for the case;
 $U = 5m/s; \bar{t} = 1; k_b = 8000; \bar{x} = 0.5; L = 2km; h = 1500m$

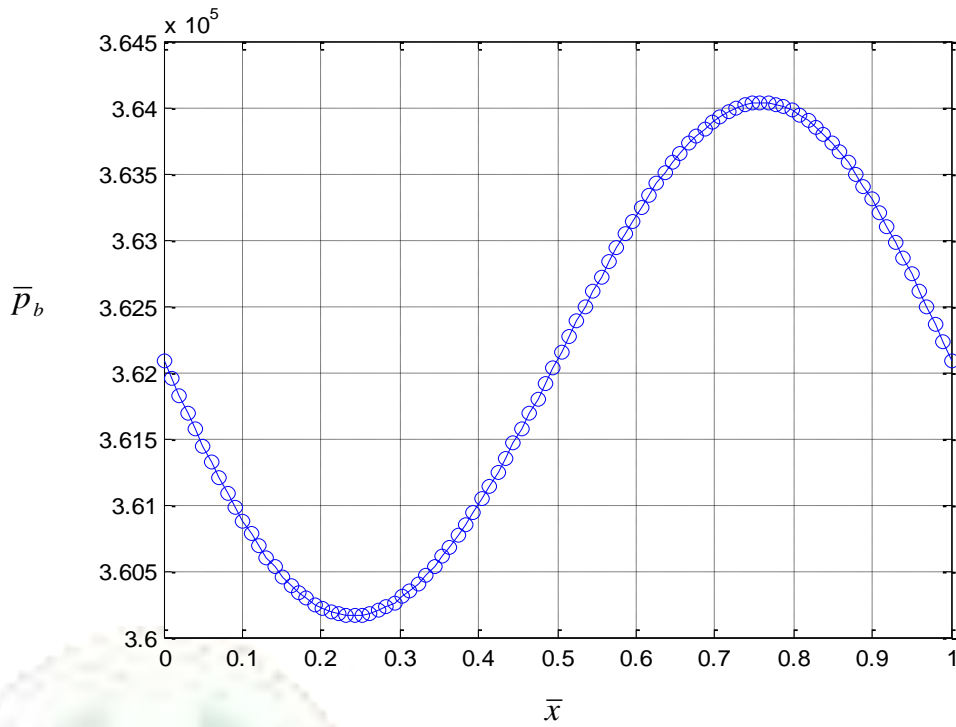


Figure 5.3: Burst pressure profile for the case;
 $n = 1; U = 5m/s; \bar{t} = 1; k_b = 8000; L = 2km; h = 1500m$

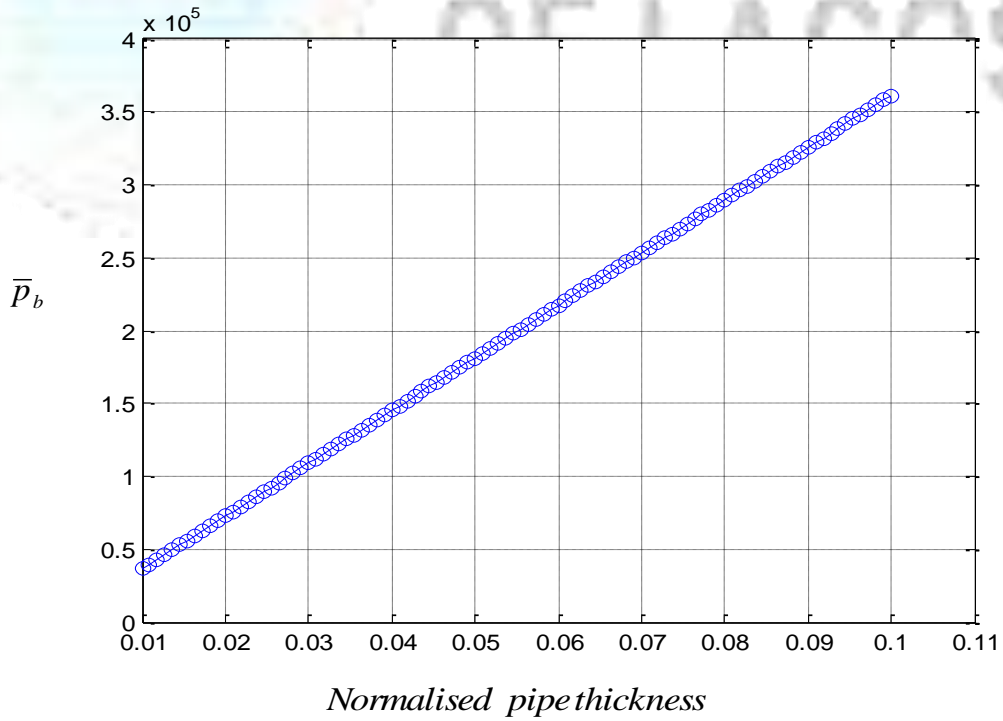


Figure 5.4: Burst pressure profile for the case;
 $n = 1; U = 5m/s; \bar{t} = 1; k_b = 8000; \bar{x} = 0.5; L = 2km; h = 1500m$

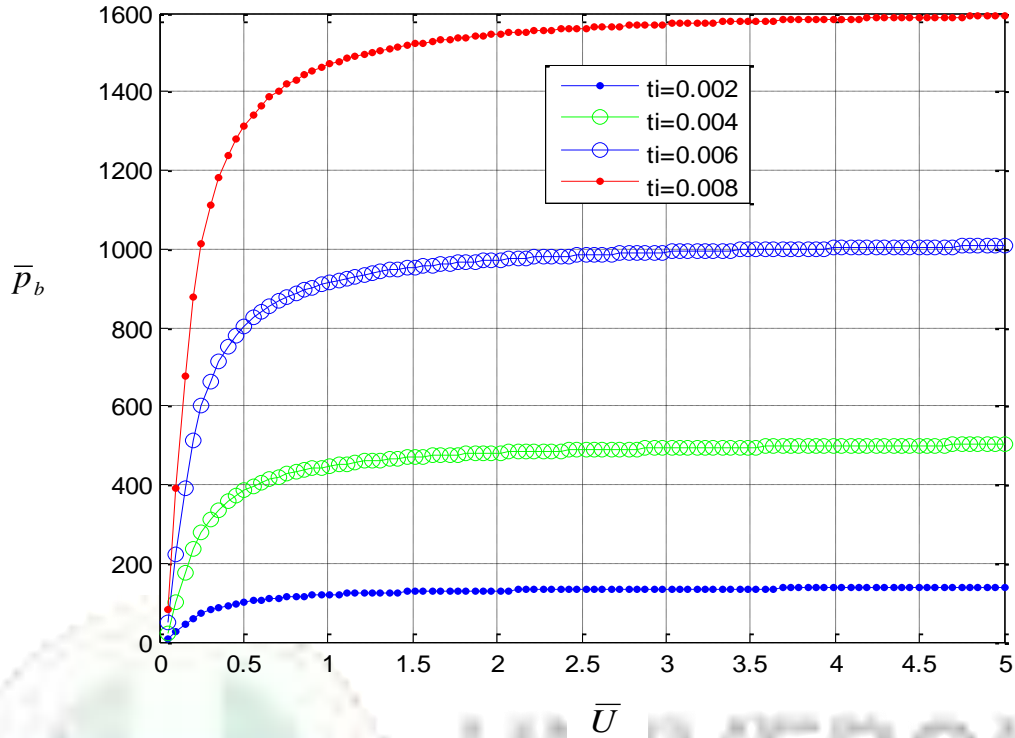


Figure 5.5: Burst pressure profile with different pipe thicknesses for the case ;
 $n = 1; \bar{t} = 1; k_b = 8000; \bar{x} = 0.5; L = 2km; h = 1500m$

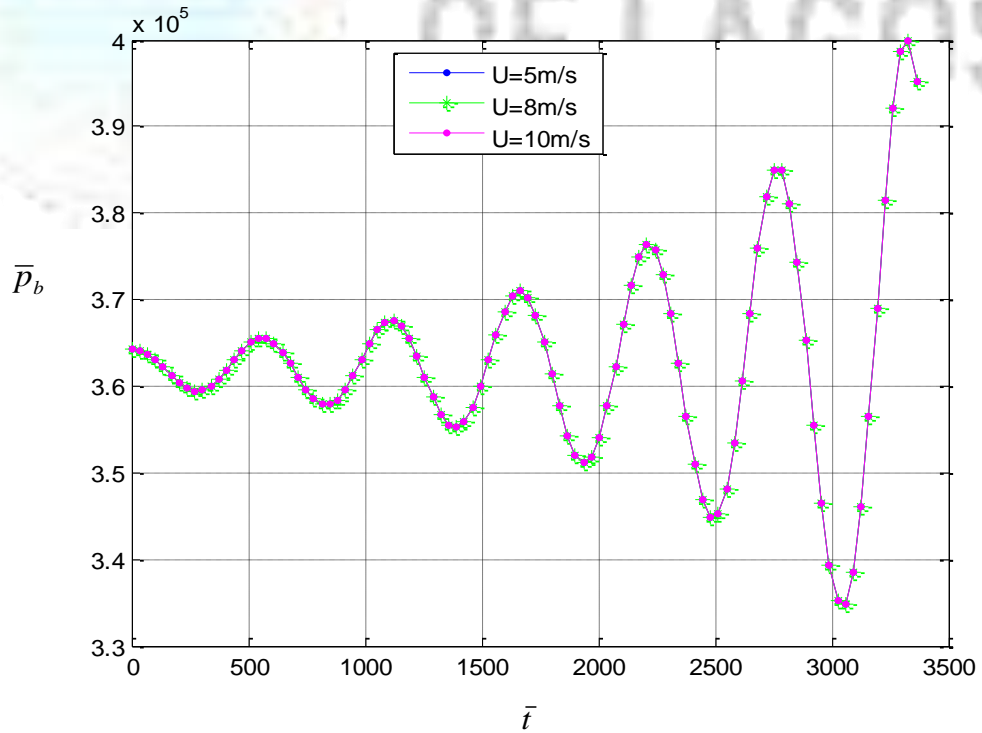


Figure 5.6 Burst pressure profile with different flow velocities for the case;
 $n = 1; k_b = 8000; \bar{x} = 0.5; L = 2km; h = 1500m$

CHAPTER 6

CONCLUSION

6.1 Summary and findings for Model Problems

In this thesis, the generalized governing differential equations for the dynamic stress propagation concerning onset of burst and buckling pressures of a subsea pipeline conveying a fluid in a pressurized environment have been established.

Here, the problem of conveyance of hot fluid in pipes laid on the sea floor within the context of dynamic stress propagation is investigated. In particular, effort have been made to examine the phenomena of pipe burst and buckling associated with pumping cycles of crude/ gas exploration in deep and ultra deep sea. In treating this problem, a set of governing differential and dynamic stresses propagation equations, that recognises the fact that pumping of such fluid sets the pipe into both transverse and longitudinal motions in conjunction with the propagation of dynamic stresses have been employed. The linearised solution of these equations enabled us to compute the nature and profiles of stress propagation. The propagation of such stresses can, in fact, trigger the phenomena of pipe burst and buckling, which have been shown to be influenced by parameters such as the nominal length of the pipe, the temperature difference between the fluid and the ambient temperature, the temperature gradient along the pipe length and the nature of the geology of the seabed. Although, several empirical relations abound in literature for design applications, closed form analytic expressions for burst and buckling pressures have not been widely reported. Nevertheless, the effect of vibrations and other operating parameters are fully captured in this investigation.

The work has equally been extended to the case of having the pipe partially/fully buried at seabed, where the sediment coverage was accounted for. It was observed that, vibration was reduced as a result of burying the pipe. However, the sediment layer increases the external load on the pipe. These results obtained can be positively exploited in oil and gas pipe and flow lines systems for deep and ultra deep waters operations.

Besides, for special cases: this work (i) recovered Ephraim (1997) results for maximum bending stress for circular hollow beam and (ii) reproduced maximum shear stress at walls of non-vibrating pipe.

6.2 Contributions to knowledge

1. The work has been able to solve the problem of conveyance of hot fluid in pipeline laid on sea floor as well as partially or completely buried at seabed within the context of dynamic stress propagation.
2. In this work, the sets of vibration induced stresses analytically for the first time to the best of my knowledge have been developed.
3. For design applications, closed form analytic expressions for burst and buckling pressures have been established (capturing the effect of vibrations and other parameters) that have not been widely reported.

6.3 Recommendations

For future work, the followings are recommended:

- Extension of the work to capture the effect of pipe sandwich and viscoelasticity.
- Consideration of non-linear equations for the pipe dynamic equations rather than the linearised version adopted in this research.
- Furthermore, this work could be extended to the areas of nuclear power plants and air-conditioning system that have arrays of piping connections.

REFERENCES

- Aitken, J. (1876): An Account of Some Experiments on Rigidity Produced by Centrifugal Force, *Philosophical magazine*, Series V, 5, 81-105.
- Amabili, M., Pellicano, F. and Paidoussis, M. P. (1998). Non-linear Vibrations of Simply Supported, Circular Shells, Coupled to Quiescent Fluid. *Journal of Fluid Structures*, vol. 12, pp 883-918.
- Amabili, M., Pellicano, F. and Paidoussis, M. P. (1999). Non-linear Dynamics and Stability of circular cylindrical Shells containing flowing fluid, Part II: Large –Amplitude Vibrations without flow, *Journal of Sound and Vibration*, vol. 228, pp 1103-1124.
- Amabili, M., Pellicano, F. and Paidoussis, M. P. (2000). Non-linear Dynamics and Stability of circular cylindrical Shells containing flowing fluid, Part III: truncation Effect without flow and Experiment, *Journal of Sound and Vibration*, vol. 237, pp 617-640.
- Andersen, J. B., Andersen, L. W., Bryndum, M., Christensen, C. J. and Nielsen, R. N. (2005). Design and Installation of Marine Pipelines, *Blackwell Science Ltd*, 1st edition.
- Andrew Cosham and Mike Kirkwood (2000). *Proceedings of IPC International Pipeline Conference; Calgary, Alberta, Canada*, pp 1-11.
- Ashley, H. and Haviland, G. (1950): Bending Vibration of a Pipeline Containing Flowing Fluid, *Journal of Applied Mechanics*, 72, 229-232.
- Benjamin, T.B (1961a): Dynamics of a System of articulated Pipes Conveying Fluid: 1. Theory 2. Experiment: *Proceedings of the Royal Society (London)*, series A, 261, 457-586.
- Benjamin, T. B. (1961b): Dynamics of a System of Articulated Pipes Conveying Fluid. II. Experiments, *Proceedings of the Royal Society (London)*, A, 261, 487-499.
- Bolotin, V. V. (1956): End Deformations of Flexible Pipelines, *Trudy Moskovskogo Instituta*, 19, 272-291.
- Bourrieres, F. J. (1939): Sur un Phenomene D' Oscillation Auto-Entretenue en Mecanique des Fluides Reels, *Publications Scientifiques et Techniques Du Ministere De L Air*, 147.
- Boyun, G., Shanhong, S., Jacob, C. and Ali, G. (2005). Offshore pipeline, *Elsevier Inc.* pp. 1-2.
- Chen, S. S. (1971): Dynamic Stability of Tube Conveying Fluid, *ASCE Journal of Engineering Mechanics Division*, 97, 1469-1485.
- Chu, C.L. and Lin, Y.H. (1995), Finite element analysis of fluid-conveying Timoshenko pipes. *Shock and Vibration*, vol. 2, pp. 247-255.

- Croll, J.G A. (1997). "A Simplified Model of Upheaval Thermal Buckling of Subsea Pipelines", *Thin Walled Structures*, vol. 29, No.1- 4, pp. 59-78.
- Damisa, O. (2002). "Dynamic Analysis of Slip Damping with Reference to Elastic Beams", *Journal of Engineering Research, University of Lagos, Nigeria*, Vol.10, Nos. 1&2 pp.1-14.
- de la Mare, R.F. (Ed.) (1985). "Advances in Offshore Oil and Gas Pipelines", *Oyez Scietific and Technical Services Ltd, London*, pp. 381.
- Ephraim, S. (1997). Applied probability for Engineers and scientists, *McGraw Hill*, pp.414.
- Evensen, D. A. (1974): Non-linear vibrations of Circular Cylindrical Shells Thin-Shell Structures: *Theory, Experiment and Design, Prentice-Hall, Englewood Cliffs, NewYork*, pp 133-155.
- Feodos'ev, V. P. (1951): Vibration and Stability of a Pipe when Liquid Flow Through it, *Inzhenernyi Sbornik*, vol. 10, pp. 169-170.
- Gorman, D. G., Reese, J. M. and Zhang, Y. L (2000): Vibration of A Flexible Pipe Conveying Viscous Pulsating Fluid Flow, *Journal of Sound and Vibration*, 230 (2), 379-392.
- Gregory, R. W. and Paidoussis, M. P (1966b): Unstable Oscillation of Tubular Cantilevers Conveying Fluid, I: Theory and II: Experiment, *Proceeding of the Royal Society (London)*, 293A, 512 – 544.
- Gregory, R. W. and Paidoussis, M. P (1966a): Unstable Oscillation of Tubular Cantilevers Conveying Fluid, I. Theory, *Proceedings of the Royal Society (London)*, A, 293, 512-527.
- Handelman, G. H. (1955): A Note on the Transverse Vibrations of a Tube Containing Flowing Fluid, *Quarterly of Applied Mathematics*, 13, 326-330.
- Haringx, J. A. (1952): Instability of Thin-Walled Cylinders Subjected to Internal Pressure, *Philips Research Report*, 7, 112-118.
- Heinrich, G. (1956): Vibrations of Tubes with Flow, *Zeitschrift fur Angewandte Machanik*, 36, 417-427.
- Henry, W.H. and Ronald, W.A. (2004). Deformable Bodies and their Material Behaviour. *John Wiley & Sons, Inc.* pp. 348.
- Herrmann, G. (1967): Stability of Equilibrium of Elastic Systems Subjected to Non-conservative Forces, *Applied Mechanics Review*, 20, 103-108.
- Herrmann, G. and Nemat-Nasser, S. (1967): Instability Modes of cantilevered Bars Induced by Fluid Flowing through Attached Pipes, *International Journal of Solids and Structures*, 3, 39-52.
- Hill, J.L. and Davis, C.G. (1974), The effect of initial forces on the hydroelastic vibration and stability of planar curved tubes. *Journal of Applied Mechanics*, pp. 355-359.

- Hobbs, R. E. (1984): In-Service Buckling of Heated Pipelines, *Journal of Transportation Engineering*, 110, 2, 175-189.
- Hobbs, R. E. and Liang, F. (1989): Thermal Buckling of Pipelines Close to Restraints, *Proceedings of OMAE*.
- Housner, G. W. (1952): Bending Vibration of a Pipeline Containing Flowing Fluid, *Journal of Applied Mechanics*, 19, 205-209.
- Hu, H. H. and Tsoon, W. S. (1957). On the Flexural Vibration of a Pipeline Containing Flowing Fluid, *Proceedings of the Theoretical and Applied Mechanics (India)*, 203-216.
- Ibrahim, R.A. (2010). “ Overview of Mechanics of Pipes Conveying Fluids, part1: Fundamental Studies” ASME Journal of Pressure Vessel Technology, Vol. 132, pp. 034001-1-034001-32.
- Jensen, J.S. (1997), Fluid transport due to nonlinear fluid-structure interaction. *Journal of Fluids and Structures*, vol. 11, pp. 327-344.
- Ju, G. T. and Kyriakides, S. (1988). “Thermal Buckling of Offshore pipelines” *Journal of Offshore Mechanics and Arctic Engineering*, vol. 110, No. 4, pp.355-364.
- Kubenko, V. D. and Koval’chuk, P. S. (2000). Non-linear problems of The Dynamics of Elastic Shells Partially Filled with a Liquid (in Russian). *Oncologica* vol. 36, No. 4, pp 3-34, (*English Version in International Applied Mechanics* vol. 36, pp 421-448).
- Lee, S. I. and Chung, J (2002): New Non-linear Modelling for Vibration Analysis of a Straight Pipe Conveying Fluid, *Journal of Sound and Vibration*, 254 (2), 313-325.
- Lee, U. and Kim, J. (1999): Dynamics of Branched Pipeline System Conveying Internal Unsteady Flow, *Journal of Vibration and Acoustics*, 121, 114 – 122.
- Lee, U. and Oh, H. (2003), The spectral element model for pipelines conveying internal steady flow. *Engineering Structures*, vol. 25, no. 23, pp. 1045-1055.
- Lee, U., Park, C. H. and Hong, S.C. (1995): The Dynamics of Piping Systems with Internal Unsteady Flow, *Journal of Sound and Vibration*, 180, 297-311.
- Lee, U., Park, J. and Kwom (2004): Spectral Element Model for the Pipelines with Internal Unsteady Flow, *45th Proceedings of AIAA Structures, Structural Dynamic and Material Conference*, 1 – 8.
- Leissa, A. W. (1973). *Vibration of Shells*. NASA SP-288, Government Printing Office, Washington DC.
- Lesmez, M.W., Wiggert, D.C. and Hatfield, F.J. (1990), Modal analysis of vibrations in liquid-filled piping systems. *Journal of Fluids Engineering*, vol. 109, no.3, pp. 311-318.

- Lin, Y.-H. and Tsai, Y.-K. (1997), Nonlinear vibration of Timoshenko pipes conveying fluid, *International Journal of Solids and Structures*, vol. 34, no. 23, pp. 2945-2956.
- Long, R.H. Jr. (1955): Experimental and Theoretical Study of Transverse Vibration of a Tube Containing Flowing Fluid, *Journal of Applied Mechanics*, 22, 65-68.
- Mouselli, A.H. (1981). "Offshore pipeline Design, Analysis and Methods". *PeenWell Publishing, Tulsa, Oklahoma*, pp. 193.
- Movchan, A. A. (1965): On the Problem of Stability of a Pipe with Fluid Flowing through it, *Journal of Applied Mathematics and Mechanics (Prikladnaia Matematika i Mekhanika)*, 29, 760-762.
- Naguleswaran, S. and Williams, C. J. H. (1968): Lateral Vibration of a Pipe Conveying Fluid, *The Journal of Mechanical Engineering Science*, 10, 228-238.
- Nemat-nasser, S, Prasad, S. N. and Hermann, G. (1966): Destabilizing Effect of Velocity-Dependent Forces in Nonconserveative Continuous Systems, *AIAA Journal*, 4 (7), 1276-1280.
- Niordson, F. I. (1953): Vibrations of a Cylinder Tube Containing Flowing Fluid: *Kungliga Tekniska Hogskolans Handlinger*, no. 73.
- Olunloyo, V. O. S., Osheku, C.A., Oyediran (2007): Dynamic Response Interaction of Vibrating Offshore Pipeline on Moving Seabed, *Journal of Offshore Mechanics and Arctic Engineering*, vol. 129, pp. 107 - 119.
- Olunloyo, V.O.S., Oyediran, A.A., Osheku, C.A., Adewale, A. and Ajayi, A.B. (2007a): Dynamics and Stability of a Fluid Conveying Vertical Beam, *Proceeding of the 26th International Conference on Offshore Mechanics and Arctic Engineering-OMAE, Vol.3, No. OMAE2007-29304*, pp 269 – 284.
- Olunloyo, V.O.S., Oyediran, A.A., Adewale, A., Adelaja, A.O. and Osheku, C.A (2007b): Concerning the Transverse and Longitudinal Vibration of a Fluid Conveying Beam and the Pipe Walking Phenomenon, *Proceeding of the 26th International Conference on Offshore Mechanics and Arctic Engineering-OMAE, Vol.3, No. OMAE2007-29299*, pp 285 – 298.
- Olunloyo, V. O. S., Osheku, C. A., and Ogunmola, B.Y. (2008) "Analysis of Dynamic Stress Propagation in Subsea Pipeline and Flow line Systems"; *27th ASME International Conference on Offshore Mechanics and Arctic Engineering, Paper No. OMAE2008- 57089, Estoril Portugal, 15th-20th, June 2008*.
- Olunloyo, V.O.S., Osheku, C.A. and Kuye, S.I. (2009): On the dynamics and stability of a viscoelastic pipe conveying a non-Newtonian fluid, *Proceeding of the 28th International Conference on Offshore Mechanics and Arctic Engineering, Paper No. OMAE2009-79588, Honolulu, Hawaii, USA, 31th May – 5th June 2009*.

Olunloyo, V.O.S., Osheku, C.A. and Adelaja, A.O. (2010a): On the Mechanics of Pipe Walking: Case of a Buried Subsea Pipeline, *Proceeding of the 29th International Conference on Offshore Mechanics and Arctic Engineering*, Paper No. OMAE2010-20094, Shanghai, China 6th – 11th June 2010.

Olunloyo, V. O. S., Osheku, C. A., and Kuye, S. I. (2010b) “Vibration and Stability Behaviour of Sandwiched Viscoelastic Pipes Conveying a Non-Newtonian Fluid”; 29th ASME International Conference on Offshore Mechanics and Arctic Engineering, Paper No. OMAE2010-20065, Shanghai, China 6th – 11th June 2010.

Osheku, C.A. (2005), Application of beam theory to machine, aero and hydro-dynamic structures in pressurized environments. Ph.D. dissertation, University of Lagos, Nigeria.

Osheku, C.A., Olunloyo, V.O.S. and Olayiwola, P.S. (2010): On the mechanics of gas pipeline vibration, *Proceeding of the 29th International Conference on Offshore Mechanics and Arctic Engineering*, Paper No. OMAE2010-20066, Shanghai, China 6th – 11th June 2010.

Öz, H. R. (2001): Non-linear Vibrations and Stability Analysis of Tensioned Pipes Conveying Fluid with Variable Velocity, *International Journal of Non-linear Mechanics*, Pergamon Press, 36, 1031-1039.

Paidoussis, M. P. (2003). Fluid-Structure Interaction: Slender Structures and Axial Flow, *Elsevier/Academic Press, London, UK*. vol. 2.

Paidoussis, M. P. (1970): Dynamics of Tubular Cantilevers Conveying Fluid, *The Journal of Mechanical Engineering Science*, 12, 85-103.

Paidoussis, M. P. and Deksnis, E. B. (1970): Articulated Models of Cantilevers Conveying Fluid: the Study of a Paradox, *The Journal of Mechanical Engineering Science*, 12, 288-300.

Paidoussis, M. P. and Denise, J. P. (1971). Flutter of cylindrical shells conveying fluid, *Journal of Sound and Vibration*, vol. 16, pp 459-461.

Paidoussis, M. P. and Denise, J. P. (1972). Flutter of thin cylindrical shells conveying fluid, *Journal of Sound and Vibration*, vol. 20, pp 9-26.

Paidoussis, M. P. and Issid, N. T. (1974): Dynamics Stability of Pipes Conveying Fluid, *Journal of Sound and Vibration*, 33, 267-294.

Paidoussis, M. P. and Laither, T. D. (1976). Dynamics of Timoshenko Beam Conveying Fluid, *Journal of Mechanical Engineering Science*, Vol. 18, pp. 210-220

Paidoussis, M. P., Luu, T. R. and Laither, B. E. (1986): Dynamics of Finite Length Tubular Beams Conveying Fluid, *Journal of Sound and Vibration*, 106 (2), 311-331.

Paidoussis, M.P. and Li, G.X (1993): Pipes Conveying Fluid; A Model Dynamic Problem, *Journal of Fluid Structure*, 7, 137-204.

- Palmer, A.C., Ellinas, C.P., Richards, D.M. and Guijt, J. (1990). “Design of Submarine pipelines Against Upheaval Buckling”, *Offshore Technology Conference*, No. OTC 6335, pp. 551- 559.
- Palmer, A.C. and King, R.A. (2004). “Subsea Pipeline Engineering”, *Peen Well*, pp. 570.
- Pedersen, P.T. and Jensen, J.J. (1988). “Upheaval Creep of Buried Heated Pipelines with Initial Imperfection”, *Marine Structures*, vol. 1, pp. 11-22.
- Pedersen, P.T. and Michelsen, J. (1988). “Large Deflection Upheaval buckling of Marine Pipelines”, *International Conference of Offshore Structures*, vol. 3 Structures, pp. 965-980.
- Pramila, A. and Laukkanen, J. (1991), Dynamics and stability of short fluid-conveying Timoshenko element pipes. *Journal of Sound and Vibration*, vol. 144, no. 3, pp. 421-425.
- Rafael, F.S., Fabio, B. A., Carlos, O. C. and Murilo, A.V. (2004). “Design and Installation of Buried Heated Pipelines at the Capixaba North Terminal Offshore Brazil”, *Proc. OMAE 2004*; Paper No. OMAE 2004-51206.
- Raouf, R.A. and Palazotto, A.N. (1991), Non-linear dynamic response of anisotropic, arbitrarily laminated shell panels: an asymptotic analysis. *Composite structure*, vol. 18, pp163-192.
- Raouf, R.A. and Palazotto, A.N. (1992), Non-linear free vibrations of symmetrically laminated, slightly compressible cylindrical shell panels, an asymptotic analysis. *Composite structure*, vol. 20, pp. 249-257.
- Raouf, R.A. (1993), A qualitative analysis of the non-linear characteristics of curved orthotropic panels, *Composite Engineering*, vol. 3, pp 1101-1110.
- Raouf, R.A. and Palazotto, A.N. (1994), On the non-linear free vibrations of curved orthotropic panels. *Int. Journal of Non-Linear Mechanics*, vol. 29, pp 507-514.
- Reddy, J. N. and Wang, C. M. (2004): Dynamics of Fluid-Conveying Beams *Centre for Offshore Research and Engineering, National University of Singapore, CORE Report*, No. 2004-03, 1-21.
- Staat, M. And Duc Khoi Vu (2006). “ Limit Analysis of Flaws in Pressurized Pipes and Cylindrical Vessels Part1: Axial Defects”, *Journal of Engineering Fracture Mechanics*. Vol.4, pp.431-450.
- Semler, C, Li, G. X and Paidoussis, M. P (1994): The Non-linear Equation of Pipes Conveying Fluid, *Journal of Sound and Vibration*, 169 (5), 577-599.
- Stein, R. A. and Trobiner, M. W. (1970): Vibration of Pipes Containing Flowing Fluids, *Journal of Applied Mechanics*, 92, 906-916.
- Taylor, N. and Gan, A.B. (1986). “Submarine Pipeline Buckling – Imperfection Studies”, *Thin Walled Structures*, vol. 4, pp. 295-323.

Thurman, A. L. and Mote, C. D. Jr. (1969): Nonlinear Oscillation of a Cylinder Containing Flowing Fluid, *Journal of Engineering for Industry, ASME*, 91, 1147-1155.

Weaver, D.S. and Unny, T.E. (1973). Dynamic stability of fluid conveying pipes, *Journal of Applied Mechanics*, vol. 40, pp 48-52.,

Wiley, J. C. and Furkert, R.E. (1972): Beam Subjected to Follower Force within the Span, *Journal of the Engineering Mechanics Division, Proceedings of the American Society of Civil Engineers*, 98, 1353-1364.

Wolbert, G. (1952). American pipelines 5.

Young Bai (2001) pipelines and Risers, *Elsevier Ocean Engineering Book Series*, Vol. 3, pp. 498.

Zhang, Y.L., Gorman, D.G. and Reese J.M. (1999), Analysis of the vibration of pipes conveying fluid. *Journal of Fluids and Structures*, vol. 11, pp. 327-344.



UNIVERSITY
OF LAGOS

APPENDIX A
GENERALIZED GOVERNING DIFFERENTIAL EQUATION FOR MODEL PROBLEM
CONCERNING DYNAMIC STRESSES OF SUBSEA PIPELINE

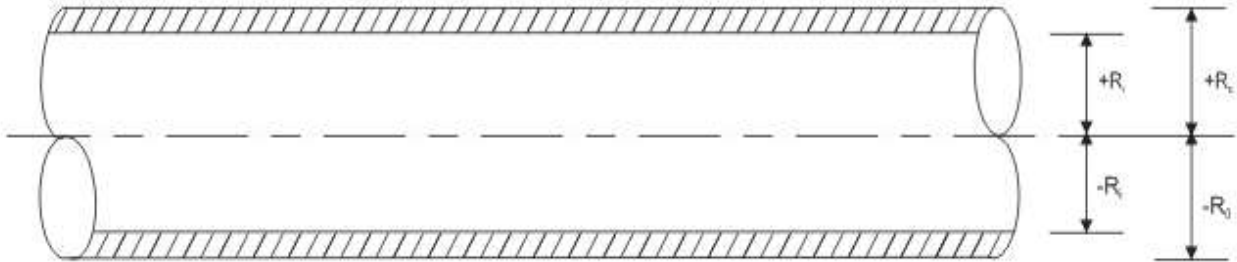


Figure A1a: Pre-deformed free body diagram



Figure A1b: free body diagram of the elastic beam approximation with upper and lower layers.

Following Damisa (2002), the longitudinal displacements in the upper and lower halves are given as

$$\left. \begin{aligned} u_1 &= -\left(z - \alpha(x) \frac{R_1}{2} \right) \frac{\partial w}{\partial x} \\ u_2 &= -\left(z - \alpha(x) \frac{R_1}{2} \right) \frac{\partial w}{\partial x} \end{aligned} \right\}$$

(A.1)

However the corresponding non-linear version will be

$$u_1(x, z, R) = u_{10} - \left(z - \alpha(x) \frac{R_i}{2} \right) \frac{\partial w}{\partial x} - \frac{\left(z - \alpha(x) \frac{R_i}{2} \right)^2 \left(\frac{\partial w}{\partial x} \right)^2}{2!} + \dots \quad (\text{A.2a})$$

$$u_2(x, z, R) = u_{20} - \left(z + \alpha(x) \frac{R_i}{2} \right) \frac{\partial w}{\partial x} - \frac{\left(z + \alpha(x) \frac{R_i}{2} \right)^2 \left(\frac{\partial w}{\partial x} \right)^2}{2!} + \quad (\text{A.2b})$$

On the other hand from theory of elasticity, the in-plane bending stresses have the forms

$$\sigma_{(x_1)} = E \frac{\partial u_1}{\partial x} = E \frac{\partial}{\partial x} \left[u_{1(0)} - \left(z - \alpha(x) \frac{R_i}{2} \right) \frac{\partial w}{\partial x} - \frac{1}{2!} \left(z - \alpha(x) \frac{R_i}{2} \right)^2 \left(\frac{\partial w}{\partial x} \right)^2 + \dots \right] \quad (\text{A.3a})$$

$$\sigma_{(x_2)} = E \frac{\partial u_2}{\partial x} = E \frac{\partial}{\partial x} \left[u_{2(0)} - \left(z + \alpha(x) \frac{R_i}{2} \right) \frac{\partial w}{\partial x} - \frac{1}{2!} \left(z + \alpha(x) \frac{R_i}{2} \right)^2 \left(\frac{\partial w}{\partial x} \right)^2 + \dots \right] \quad (\text{A.3b})$$

so that if we confine our analysis to the case of linear strain theory, equations (A.3a,b) can be shown to have the reduced forms

$$\sigma_{(x_1)} = E \frac{\partial}{\partial x} \left[u_{1(0)} - \left(z - \alpha(x) \frac{R_i}{2} \right) \frac{\partial w}{\partial x} \right] \quad (\text{A.1.4a})$$

$$\sigma_{(x_2)} = E \frac{\partial}{\partial x} \left[u_{2(0)} - \left(z + \alpha(x) \frac{R_i}{2} \right) \frac{\partial w}{\partial x} \right] \quad (\text{A.4b})$$

where $u_{1(0)}$ and $u_{2(0)}$ represent the initial displacement of the upper and lower halves at the support point. However, $u_{1(0)}$ and $u_{2(0)}$ must vanish from the support conditions. Thus

$$\sigma_{(x_1)} \approx -E \left(z - \alpha(x) \frac{R_i}{2} \right) \frac{\partial^2 w}{\partial x^2} \quad (\text{A.5a})$$

$$\sigma_{(x_2)} \approx -E \left(z + \alpha(x) \frac{R_i}{2} \right) \frac{\partial^2 w}{\partial x^2} \quad (\text{A.5b})$$

We now invoke the elastodynamic stress equations namely:

$$\frac{\partial \sigma_{x_1}}{\partial x} + \frac{\partial \tau_{(zx)_1}}{\partial z} = (\rho + \rho_f) \frac{\partial^2 u}{\partial t^2} \quad (\text{A.6a})$$

$$\frac{\partial \sigma_{z_1}}{\partial z} + \frac{\partial \tau_{(zx)_1}}{\partial x} = (\rho + \rho_f) \frac{\partial^2 w}{\partial t^2} \quad (\text{A.6b})$$

where u and w satisfy the governing differential equation for the vibrating pipeline.

Equation (A.6a) when combine with equation (A.5a) gives

$$\frac{\partial}{\partial x} \left[-E \left(z - \alpha(x) \frac{R_i}{2} \right) \frac{\partial^2 w}{\partial x^2} \right] + \frac{\partial \tau_{(zx)_1}}{\partial z} = (\rho + \rho_f) \frac{\partial^2 u}{\partial t^2}$$

or

$$-EZ \frac{\partial^3 w}{\partial x^3} + E \frac{R_i}{2} \frac{\partial}{\partial x} \left(\alpha(x) \frac{\partial^2 w}{\partial x^2} \right) + \frac{\partial \tau_{(zx)_1}}{\partial z} = (\rho + \rho_f) \frac{\partial^2 u}{\partial t^2} \quad (\text{A.7})$$

Thus

$$\frac{\partial \tau_{zx_1}}{\partial z} = EZ \frac{\partial^3 w}{\partial x^3} - E \frac{R_i}{2} \frac{\partial}{\partial x} \left(\alpha(x) \frac{\partial^2 w}{\partial x^2} \right) + (\rho + \rho_f) \frac{\partial^2 u}{\partial t^2} \quad (\text{A.8})$$

so that integrating equation (A.8) then yields

$$\tau_{(zx)_1} = \frac{EZ^2}{2} \frac{\partial^3 w}{\partial x^3} - \frac{ER_i}{2} z \frac{\partial}{\partial x} \left(\alpha(x) \frac{\partial^2 w}{\partial x^2} \right) + (\rho + \rho_f) z \frac{\partial^2 u}{\partial t^2} + f \tau_1 \quad (\text{A.9})$$

where, the constant of integration $f \tau_1$ is to be evaluated from the boundary condition at the centre of the pipe as listed below viz:

$$(i) \quad \text{At } z = 0, \tau_{(zx)_1} = 0$$

while at the inner surface of the pipe we have

$$(ii) \quad z = R_i, \tau_{(zx)_1} = -\tau_{max}$$

On invoking these conditions we can rewrite equation (A.9) as

$$\frac{EZ^2}{2} \frac{\partial^3 w}{\partial x^3} - \frac{ER_i}{2} z \frac{\partial}{\partial x} \left(\alpha(x) \frac{\partial^2 w}{\partial x^2} \right) + (\rho + \rho_f) z \frac{\partial^2 u}{\partial t^2} \quad (\text{A.10})$$

while $\tau_{(zx)_1}$ assumes the form

$$\tau_{(zx)_1} = \frac{E}{2} (Z^2 - R_i z) \frac{\partial^3 \bar{w}}{\partial x^3} - z \frac{\tau_{max}}{R_i} \quad (\text{A.11})$$

On the other hand

$$\tau_{(zx)_2} = \frac{EZ^2}{2} \frac{\partial^3 w}{\partial x^3} + \frac{ER_i z}{2} \frac{\partial}{\partial x} \left(\alpha(x) \frac{\partial^2 w}{\partial x^2} \right) + (\rho + \rho_f) \frac{\partial^2 u}{\partial t^2} + f \tau_2 \quad (\text{A.12})$$

and by carrying out a similar analysis it is found that

$$\tau_{(zx)_2} = \frac{E}{2} (Z^2 + R_i z) \frac{\partial^3 w}{\partial x^3} - z \frac{\tau_{max}}{R_i} \quad (\text{A.13})$$

The evaluation of the inplane bending stress in view of equations (A.6a) and (A.6b) now yields

$$\frac{\partial \sigma_{x_1}}{\partial x} + \frac{\partial}{\partial z} \left[\frac{E}{2} (Z^2 - z R_i) \frac{\partial^3 w}{\partial x^3} - z \frac{\tau_{max}}{R_i} \right] = (\rho + \rho_f) \frac{\partial^2 u}{\partial t^2}$$

(A.14)

which can be integrated to give

$$\sigma_{(x)_1} = -\frac{E}{2} (2Z - R_i) \frac{\partial^2 w}{\partial x^2} + x \frac{\tau_{max}}{R_i} + x (\rho + \rho_f) \frac{\partial^2 u}{\partial t^2} + f \sigma_1 \quad (\text{A.15})$$

where $f\sigma_1$ is evaluated based on the nature of the support conditions. For pinned or clamped ends

$$\begin{aligned} w(0) = w'(0) = w''(l) = 0 \\ \sigma_x(0) = 0 \\ \Rightarrow f\sigma_x = 0 \end{aligned}$$

Hence

$$\sigma_{(x)_1} = -\frac{E}{2}(2Z - R_i) \frac{\partial^2 w}{\partial x^2} + x \frac{\tau_{max}}{R_i} + x(\rho + \rho_f) \frac{\partial^2 u}{\partial t^2} \quad (\text{A.16})$$

Similarly, it is possible to derive the relation for $\sigma_{(x)_2}$ with the above procedures, as

$$\sigma_{(x)_2} = -\frac{E}{2}(2Z + R_i) \frac{\partial^2 w}{\partial x^2} + x \frac{\tau_{max}}{R_i} + x(\rho + \rho_f) \frac{\partial^2 u}{\partial t^2} \quad (\text{A.17})$$

Also σ_z can be expressed from (A.6b) via (A.13) and (A.16), thus

$$\frac{\partial \sigma_{z_1}}{\partial z} + \frac{\partial}{\partial x} \left[\frac{E}{2} (Z^2 - zR_i) \frac{\partial^3 w}{\partial x^3} - z \frac{\tau_{max}}{R_i} \right] = (\rho + \rho_f) \frac{\partial^2 w}{\partial t^2} \quad (\text{A.18})$$

which simplifies to

$$\sigma_{z_1} = -\frac{E}{2} \left(\frac{z^3}{3} - \frac{R_i z^2}{2} \right) \frac{\partial^4 w}{\partial x^4} + z(\rho + \rho_f) \frac{\partial^2 w}{\partial t^2} + f\sigma_{z_1} \quad (\text{A.19})$$

In this case $f\sigma_z$ is evaluated based on the support condition viz

at $z = +R_o$ (the upper outer pipe wall)

By invoking this, σ_{z_1} is expressed as

$$\sigma_{z_1} = \frac{F_{im} - c_{st} \frac{\partial w}{\partial t}}{2\pi R_o L} - P_f - \frac{E}{2} \left[\frac{1}{3} (Z^3 - R_o^3) - \frac{1}{2} (R_i Z^2 - R_i R_o^2) \right] \frac{\partial^4 w}{\partial x^4} + (Z - R_o)(\rho + \rho_f) \frac{\partial^2 w}{\partial t^2} \quad (\text{A.20})$$

Similarly,

at $z = -R_o$ (the lower outer pipe wall)

$$\begin{aligned} \sigma_{z_2} = \frac{1}{2\pi R_o L} \left(F_{in} - (c_{st} - c_o) \frac{\partial w}{\partial t} - K_{soil} w - c_{soil} \frac{\partial w}{\partial t} \right) + P_f \\ + (Z + R_o)(\rho + \rho_f) \frac{\partial^2 \bar{w}}{\partial t^2} - \frac{E}{2} \left[\frac{1}{3} (Z^3 + R_o^3) + \frac{1}{2} (R_i Z^2 + R_i R_o^2) \right] \frac{\partial^4 w}{\partial x^4} \end{aligned} \quad (\text{A.21})$$

APPENDIX B

GENERALIZED GOVERNING DIFFERENTIAL EQUATION FOR MODEL PROBLEM CONCERNING VIBRATION OF SUBSEA PIPELINE

B.1 Model formulation

Here we consider one-dimensional pulsating flow of a Newtonian viscous incompressible fluid in a pipe conveying fluid as shown in figure B1 below. The pipe has length L , cross-sectional area A_p , mass per unit length m_p , initial axial tension T_0 , transporting a fluid of mass m_f per unit length with axial velocity U and pressure p , that is space and time dependent. Also, this pipe conveying fluid is simply supported at both ends, and experiences external forces such as tangential force $F_t = m_f \dot{v}$ due to bending and centripetal force of $m_f \frac{v^2}{R}$.

In general, the pipeline is inclined at an angle of ϕ to the ground. Besides, the pipe material is considered to be linear, homogeneous and isotropic elastic medium. In figure B1, the system is decomposed into fluid and pipe element. The fluid is acted upon by a normal force $f_n \delta x$ and a tangential force $f_t \delta x$ due to the fluid-pipe interaction. On the other hand, the pipe element is acted upon by shearing force Q , bending moment M as well as $f_t \delta x$ and $f_n \delta x$ that are as a result of fluid pipe interaction. As a result of deflection, let θ be the angle between the pipe element position and the x -axis. Furthermore, $w(x, t)$ and $u(x, t)$ represent transverse and longitudinal displacements of the element, while U is the fluid velocity before pipe deformation.

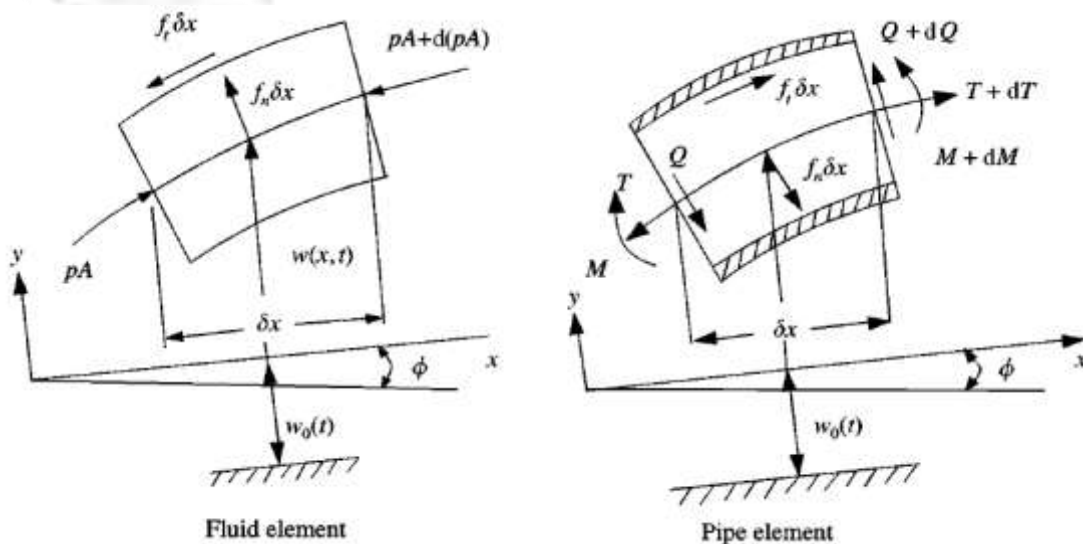


Figure B1. Fluid and pipe elements together with an indication of forces.

Force balance on the fluid and empty pipe elements are given respectively below by taking a small fluid and pipe element of length δx in the x and y directions. For the fluid element the longitudinal and transverse equations of motion are:

In the x-direction (longitudinal)

$$-f_t \delta x \cos \theta - f_n \delta x \sin \theta - (pA \cos \theta)' \delta x - m_f g \delta x \sin \phi = m_f \delta x \frac{D^2(x+u)}{Dt^2} \quad (\text{B.1})$$

Similarly, resolving forces in the y-direction (transverse) after simplification

$$-f_t \delta x \sin \theta + f_n \delta x \cos \theta - (pA \sin \theta)' \delta x - m_f g \delta x \cos \phi = m_f \delta x \frac{D^2(w+w_0)}{Dt^2} \quad (\text{B.2})$$

where the terms in the equations have been defined in the nomenclature

For the pipe element, the equation of motion in the x-axis (longitudinally) is:

$$(T \cos \theta)' \delta x - (Q \sin \theta)' \delta x + f_t \delta x \cos \theta + f_n \delta x \sin \theta - m_p g \delta x \sin \phi = m_p \delta x \ddot{u} \quad (\text{B.3})$$

In the y-axis (transversely) the equation of motion assumes:

$$(T \sin \theta)' \delta x + (Q \cos \theta)' \delta x + f_t \delta x \sin \theta - f_n \delta x \cos \theta - m_t g \cos \phi \delta x - c \delta x \dot{w} = m_p \delta x (\ddot{w} + \ddot{w}_0) \quad (\text{B.4})$$

Next, we add equations (B.1) and (B.3) to obtain:

$$(T \cos \theta)' \delta x - (Q \sin \theta)' \delta x - (pA \cos \theta)' \delta x - m g \delta x \sin \phi = m_p \delta x \ddot{u} + m_f \delta x \frac{D^2(x+u)}{Dt^2} \quad (\text{B.5})$$

Also, addition of equations (B.2) and (B.4) yields:

$$(T \sin \theta)' \delta x + (Q \cos \theta)' \delta x - (pA \sin \theta)' \delta x - c \delta x \dot{w} - m_f g \delta x \cos \phi = m_p \delta x (\ddot{w} + \ddot{w}_0) + m_f \delta x \frac{D^2(w+w_0)}{Dt^2} \quad (\text{B.6})$$

where $m = m_p + m_f$

Further simplification of equations (B.5) and (B.6) leads to

$$(T \cos \theta)' - (Q \sin \theta)' - (pA \cos \theta)' - m g \sin \phi = m_p \ddot{u} + m_f \frac{D^2(x+u)}{Dt^2} \quad (\text{B.7})$$

$$(T \sin \theta)' + (Q \cos \theta)' - (pA \sin \theta)' - c \dot{w} - m_f g \cos \phi = m_p (\ddot{w} + \ddot{w}_0) + m_f \frac{D^2(w+w_0)}{Dt^2} \quad (\text{B.8})$$

Furthermore, in Gorman et al (2000), the strain was considered as comprising two components viz: a steady state strain due to T_0 and oscillatory strain ϵ , due to pipe vibration i.e

$$T = T_0 + EA\epsilon \quad (\text{B.9})$$

where

$$\epsilon = u' + \frac{1}{2}w'^2 \quad (\text{B.10})$$

However, in this work, thermal strain due to temperature effect is introduced. Thus, the new expression for T has the form:

$$T = T_0 + EA\epsilon - \alpha EA_p \theta \quad (\text{B.11})$$

Here, the following are defined as

$E =$ the young modulus of the pipe, $\alpha =$ the coefficient of expansion of the pipe, $\theta =$ the temperature effect, $T_0 =$ the pre – stress

B.2 Procedural analysis

There are some preliminaries needed to express certain terms such as $(T \sin \theta)'$, $(T \cos \theta)'$, $\cos \theta$, $\sin \theta$, etc. in equations (B.7) and (B.8) respectively.

Using Semler *et al.* (1994), it was assumed that (X, Y, Z) be the position of a material point p at the initial state and (x,y,z) to denote the position of p in the new state, such that $x = X + u$ and $y = Y + w$ while z is considered to be zero

If an element of initial length δx (*undeformed*) be deformed to a new length δs , then δs is given by:

$$(\delta s)^2 - (\delta X)^2 = \left[\left(\frac{dx}{dX} \right)^2 + \left(\frac{dy}{dX} \right)^2 - 1 \right] (\delta x)^2 \quad (\text{B.12})$$

Now $dY = Y = 0$ when the initial length lies on the X-axis so that, $x = x(X, Y)$ and $y = (X, Y)$

Therefore,

$$\frac{dx}{dX} = 1 + \frac{\partial u}{\partial X}, \quad \frac{dy}{dX} = \frac{\partial w}{\partial X} \quad (\text{B.13})$$

or

$$\frac{dx}{dX} = 1 + u', \quad \frac{dy}{dX} = w' \quad (\text{B.14})$$

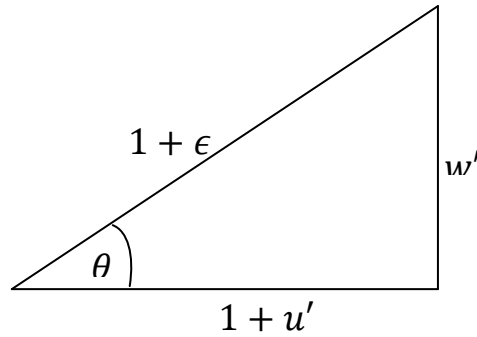


Figure B2: Right angle triangle for the Strain

The right angle triangle represents the strain according to Semler *et al.* (1994) and Thurman and Mote Jr (1969) in x and y axes.

Next the followings are written as

$$ds = (1 + \epsilon)dX, \quad \frac{\partial X}{\partial s} = \frac{1}{1+\epsilon} \quad (\text{B.15})$$

and the curvature k as

$$k = \frac{\partial \theta}{\partial s} \quad (\text{B.16})$$

Equation (B.16) in terms of the X-coordinate assumes the form

$$k = \frac{\partial \theta}{\partial X} \frac{\partial X}{\partial s} = \frac{1}{1+\epsilon} \frac{\partial \theta}{\partial X} \quad (\text{B.17})$$

while $\frac{\partial \theta}{\partial X}$ can be obtained by differentiating $\sin \theta$.

From figure B2,

$$\sin \theta = \frac{w'}{1+\epsilon}, \quad \cos \theta = \frac{1+u'}{1+\epsilon} \quad (\text{B.18})$$

Now,

$$\frac{\partial}{\partial X} (\sin \theta) = \frac{\partial \theta}{\partial X} \cos \theta = \frac{w''(1+\epsilon) - w'(1+\epsilon)'}{(1+\epsilon)^2} \quad (\text{B.19})$$

where

$$1 + \epsilon = \sqrt{(1 + u')^2 + w'^2} \Rightarrow (1 + \epsilon)' = \frac{(1+u)u'' + w'w''}{1+\epsilon} \quad (\text{B.20})$$

Substituting equation (B.19) in (B.20) gives

$$\frac{\partial \theta}{\partial X} = \frac{w''(1+\epsilon)^2 - w'[(1+u)u'' + w'w'']}{(1+\epsilon)^2(1+u')} \quad (\text{B.21})$$

From figure B2

$$(1 + \epsilon)^2 = [(1 + u')^2 + w'^2] \quad (\text{B.22})$$

Thus, equation (B.21) becomes

$$\frac{\partial \theta}{\partial X} = \frac{w''(1+u') - w'u''}{(1+\epsilon)^2} \quad (\text{B.23})$$

The next exercise is to consider term by term equation (B.7) and (B.8).

Expression for Q:

$$Q = -\frac{\partial M}{\partial s} = -\frac{\partial M}{\partial X} \frac{\partial X}{\partial s} = -\frac{\partial M}{\partial X} \frac{1}{1+\epsilon} \quad (\text{B.24})$$

where M is related to the curvature of a beam as:

$$M = EI(1 + \epsilon) \frac{\partial \theta}{\partial s} = EI(1 + \epsilon) \frac{\partial \theta}{\partial X} \frac{\partial X}{\partial s} = EI \frac{\partial \theta}{\partial X} \quad (\text{B.25})$$

hence

$$Q = -\frac{EI}{1+\epsilon} \frac{\partial^2 \theta}{\partial X^2} \quad (\text{B.26})$$

Expressions for $\sin \theta$ and $\cos \theta$:

From equation (B.18)

$$\sin \theta = \frac{w'}{1+\epsilon}, \text{ and } \cos \theta = \frac{1+u'}{1+\epsilon}$$

but from equation (B.22)

$$1 + \epsilon = [(1 + u')^2 + w'^2]^{\frac{1}{2}} \quad (\text{B.27})$$

By using binomial expansion

$$\epsilon \approx u' + \frac{1}{2}w'^2 \text{ for small strain}$$

Thus,

$$\sin \theta = w'(1 - \epsilon) = w' \left(1 - u' - \frac{1}{2}w'^2\right) \quad (\text{B.28})$$

also

$$\cos \theta = (1 + u')(1 - \epsilon) = 1 - u'^2 - \frac{1}{2}w'^2 - \frac{1}{2}u'w'^2 \quad (\text{B.29})$$

If we use order of magnitude, with $u' = o(\epsilon^2)$, it then applies that $u'^2 = o(\epsilon^4)$, $w' = o(\epsilon)$ Then only terms of $o(\epsilon^3)$ are needed.

Hence

$$\cos \theta = 1 - \frac{1}{2}w'^2 \quad (\text{B.30})$$

Expressions for T are now being considered

From equation (B.11)

$$T = T_0 + EA_p \epsilon - \alpha EA_p \theta$$

Thus,

$$T \cos \theta = \left[T_0 + EA_p \left(u' + \frac{1}{2} w'^2 \right) - \alpha EA_p \theta \right] \left[1 - \frac{1}{2} w'^2 \right] + o(\epsilon^4)$$

simplifying this,

$$T \cos \theta = T_0 + EA_p \left(u' + \frac{1}{2} w'^2 \right) - \alpha EA_p \theta - T_0 \frac{w'^2}{2} + \alpha EA_p \theta \frac{w'^2}{2} \quad (\text{B.31})$$

while

$$(T \cos \theta)' = -(T_0 - EA_p - \alpha EA_p \theta) w' w'' + EA_p u'' + EA_p' \left(u' + \frac{w'^2}{2} \right) - \alpha EA_p' \theta - \alpha EA_p \theta' + \alpha EA_p' \frac{w'^2}{2} + \alpha EA_p \theta' \frac{w'^2}{2} \quad (\text{B.32})$$

Also for $T \sin \theta$ the expression assumes

$$\begin{aligned} T \sin \theta &= \left[T_0 + EA_p \left(u' + \frac{1}{2} w'^2 \right) - \alpha EA_p \theta \right] w' \left[1 - u' - \frac{w'^2}{2} \right] \\ &= T_0 \left[w' - w' u' - \frac{w'^2}{2} \right] + EA_p \left[u' w' + \frac{w'^3}{2} \right] - \alpha EA_p \theta \left[w' - w' u' - \frac{w'^2}{2} \right] + o(\epsilon^5) \end{aligned} \quad (\text{B.33})$$

Hence combining equations (B.11) and (B.33) yields

$$\begin{aligned} (T \sin \theta)' &= (T_0 - \alpha EA_p \theta) w'' - (T_0 - EA_p - \alpha EA_p \theta) \left(w u' + w' u + \frac{3}{2} w'^2 w'' \right) + \\ &EA_p' \left[u' w' + \frac{w'^3}{2} \right] - [\alpha EA_p' \theta + \alpha EA_p \theta'] \left[w' - w' u' - \frac{w'^2}{2} \right] + \end{aligned} \quad (\text{B.34})$$

Likewise there is need for $(pA \cos \theta)'$ and $(pA \sin \theta)'$ terms.

$$\begin{aligned} (pA \cos \theta)' &= \left(pA \left(1 - \frac{w'^2}{2} \right) \right)' \\ &= PA' + P'A - (PA' + P'A) \frac{w'^2}{2} - PA w' w'' \end{aligned} \quad (\text{B.34})$$

and

$$\begin{aligned}
(PASin\theta)' &= (PA' + P'A) \left(w' - u'w' - \frac{w'^3}{2} \right) + PA \left(w'' - u''w' - u'w'' - \frac{3}{2}w'^2w'' \right) \\
&= (PA)' \left(w' - u'w' - \frac{w'^3}{2} \right) + PAw'' - PA \left(u''w' + u'w'' + \frac{3}{2}w'^2w'' \right)
\end{aligned} \tag{B.35}$$

The expressions for velocity and acceleration terms are as follows:

$$\frac{D}{Dt}(w + w_0) = \left(\frac{\partial}{\partial t} + U \frac{\partial}{\partial x} \right) (w + w_0) = \dot{w} + \dot{w}_0 + U(w' + w_0) \tag{B.36}$$

while

$$\frac{D^2}{Dt^2}(w + w_0) = \left(\frac{\partial}{\partial t} + U \frac{\partial}{\partial x} \right) (\dot{w} + \dot{w}_0 + U(w' + w_0)) \tag{B.37}$$

Now, $w_0 \neq w_0(x)$

Then

$$\frac{D^2}{Dt^2}(w + w_0) = \ddot{w} + \ddot{w}_0 + 2U\dot{w}' + \dot{U}w' + UU'w' + U^2w'' \tag{B.38}$$

Also

$$\frac{D}{Dt}(x + u) = \left(\frac{\partial}{\partial t} + U \frac{\partial}{\partial x} \right) (x + u)$$

where $x \neq x(t)$

Therefore,

$$\frac{D}{Dt}(x + u) = \dot{x} + U(1 + u') \tag{B.39}$$

Hence

$$\frac{D^2}{Dt^2}(x + u) = \ddot{x} + \dot{U}u' + 2U\dot{u}' + \dot{U}u' + \dot{U} + UU'u' + U^2u'' \tag{B.40}$$

Using equations (B.26, B.21)

$$Q = -\frac{EI}{1 + \varepsilon} \frac{\partial^2 \theta}{\partial x^2} \quad \text{and} \quad \frac{\partial \theta}{\partial x} = \frac{w''(1 + u') - w'u''}{(1 + \varepsilon)^2}$$

For small strain, $\varepsilon = u' + \frac{w'^2}{2}$

$$(1 + \varepsilon)^2 \approx 1 - 2u' - w'^2$$

Then

$$\frac{\partial \theta}{\partial x} = w'' - w''u' - w'u'' - w'^2w'' \quad (\text{B.41})$$

$$\Rightarrow \frac{\partial^2 \theta}{\partial x^2} = w''' - w'''u' - 2w''u'' - w'u''' - w'^2w''' - 2w'w''^2 \quad (\text{B.42})$$

Thus,

$$\frac{1}{(1 + \varepsilon)} \frac{\partial^2 \theta}{\partial x^2} = -EI \left[w''' - w'''u' - 2w''u'' - w'u''' - w'^2w''' - 2w'w''^2 \right] \left[1 - u' - \frac{w'^2}{2} \right]$$

so that

$$Q = -EI \left(w''' - 2w'''u' - 2w''u'' - w'u''' - 2w'w''^2 - \frac{3w''w'^2}{2} \right) \quad (\text{B.43})$$

Using equations (B.28, B.29 and B.43), $(Q \sin \theta)'$ and $(Q \cos \theta)'$ can be equally written as

$$Q \sin \theta = -EI(w'w''' - 2w'w''u'') + 0(\varepsilon^4)$$

hence

$$(Q \sin \theta)' = -EI(w'w'''' + w''w''') \quad (\text{B.44})$$

similarly

$$Q \cos \theta = -EI(w''' - 2w''u'' - 2w''u' - w'u''' - 2w'^2w''' - 2w'w''^2)$$

then

$$(Q \cos \theta)' = -EI(w'''' - 4w''''u'' - 3w''''u' - 2w''''u' - w'u'''' - 8w''w''w'''' - 2w''^2w'''' - 2w''^3) \quad (\text{B.45})$$

Governing Differential Equations

w- equation

Substitution of equations (B.34), (B.45), (B.35) and (B.38) into equation (B.8) yields

$$\begin{aligned}
& m\ddot{w} + c\dot{w} + m_f \dot{U}w' + 2m_f U\dot{w}' + m_f UU'w' + m_f U^2 w'' \\
& - (T_0 - pA - EA_p \alpha \Theta)w'' + (T_0 - EA_p - pA - EA_p \alpha \Theta) \left(w''u' + w'u'' + \frac{3}{2} w'^2 w'' \right) \\
& - EI \left(w'^v + 4w'''u'' + 3w''u''' + 2w'^v u' + w'u'^v \right) + EIw'^v \\
& + \left((PA)' + (EA_p \alpha \Theta)' \right) \left(w' - u'w' - \frac{w'^3}{2} \right) + EA_p' \left(u'w' + \frac{3}{2} w'^3 \right) \\
& + mg \cos \phi + m\ddot{w}_o = F_1(t)
\end{aligned} \tag{B.46}$$

Using Olunloyo *et al.* (2007)

$$F_1(t) = \mu_s \pi \delta_s \left(R - \frac{\delta_s}{2} \right) \frac{\partial p_s}{\partial x} + P_h \pi (2R - \delta_s) - c_D \dot{w} \tag{B.47}$$

When the pipe is laid horizontally, the reaction force of the seabed cancels the weight of the pipe and fluid. The generalized governing differential equation in transverse direction then admits the form in equation (B.48)

$$\begin{aligned}
& EI \frac{\partial^4 w}{\partial x^4} + m \frac{\partial^2 w}{\partial t^2} + (C_1 + C_D) \frac{\partial w}{\partial t} + K_b w + 2m_f U \frac{\partial^2 w}{\partial t \partial x} - (T_0 - PA - m_f U^2 - \alpha EA \Theta) \frac{\partial^2 w}{\partial x^2} \\
& + (P'A + PA' - \alpha EA' \Theta - \alpha EA \Theta') \frac{\partial w}{\partial x} = \mu_s \pi \delta_s \left(R - \frac{\delta_s}{2} \right) \frac{\partial p_s}{\partial x} + P_h \pi (2R - \delta_s)
\end{aligned} \tag{B.48}$$

If the pipe is sitting on the seabed without sediment covering, equation (B.47) then becomes

$$\begin{aligned}
& EI \frac{\partial^4 w}{\partial x^4} + m \frac{\partial^2 w}{\partial t^2} + (C_1 + C_D) \frac{\partial w}{\partial t} + K_b w + 2m_f U \frac{\partial^2 w}{\partial t \partial x} - (T_0 - PA - m_f U^2 - \alpha EA \Theta) \frac{\partial^2 w}{\partial x^2} \\
& + (P'A + PA' - \alpha EA' \Theta - \alpha EA \Theta') \frac{\partial w}{\partial x} = P_h A_p
\end{aligned} \tag{B.49}$$

u- equation

Combining equations (B.31), (B.44), (B.34) and (B.40) with equation (B.7) gives

$$\begin{aligned}
& m\ddot{u} + m_f \dot{U}u' + 2m_f U\dot{u}' + m_f \dot{U}u' + m_f \dot{U} + m_f UU'u' + m_f U^2u'' \\
& - EA_p u'' - EA_p' \left(u' + \frac{w'^2}{2} \right) + \left(T_o - (EA_p + \alpha EA_p \Theta) \right) w' w'' \\
& + \alpha EA_p' \Theta + \alpha EA_p \Theta' - (\alpha EA_p' \Theta + \alpha EA_p \Theta') \alpha \theta' \frac{w'^2}{2} \\
& + (PA)' - (PA)' \frac{w'^2}{2} - PAw'w'' - EI(w''w''' + w'w''') + mg \sin \phi = F_2(t)
\end{aligned} \tag{B.50}$$

where

$$F_2(t) = \mu_s P_s \pi (2R - \delta_s) - c_D \dot{w}$$

Thus

$$\begin{aligned}
& (m_f U^2 - EA) \frac{\partial^2 u}{\partial x^2} + m \frac{\partial^2 u}{\partial t^2} + (C_2 + C_D) \frac{\partial u}{\partial t} + 2m_f U \frac{\partial^2 u}{\partial t \partial x} - EA' \frac{\partial u}{\partial x} \\
& + P'A + PA' + \alpha EA' \Theta + \alpha EA \Theta' - (P'A + PA' + \alpha EA' \Theta + \alpha EA \Theta' + EA') \frac{1}{2} \left(\frac{\partial w}{\partial x} \right)^2 \\
& + (T_o - EA - PA - \alpha EA \Theta) \frac{\partial W}{\partial x} \cdot \frac{\partial^2 W}{\partial x^2} - EI \left(\frac{\partial^2 w}{\partial x^2} \cdot \frac{\partial^3 w}{\partial x^3} + \frac{\partial w}{\partial x} \cdot \frac{\partial^4 w}{\partial x^4} \right) = -2\mu_s P_s \pi (2R - \delta_s)
\end{aligned} \tag{B.51}$$

APPENDIX C

BURST PRESSURE FORMULATION IN CYLINDRICAL POLAR COORDINATES

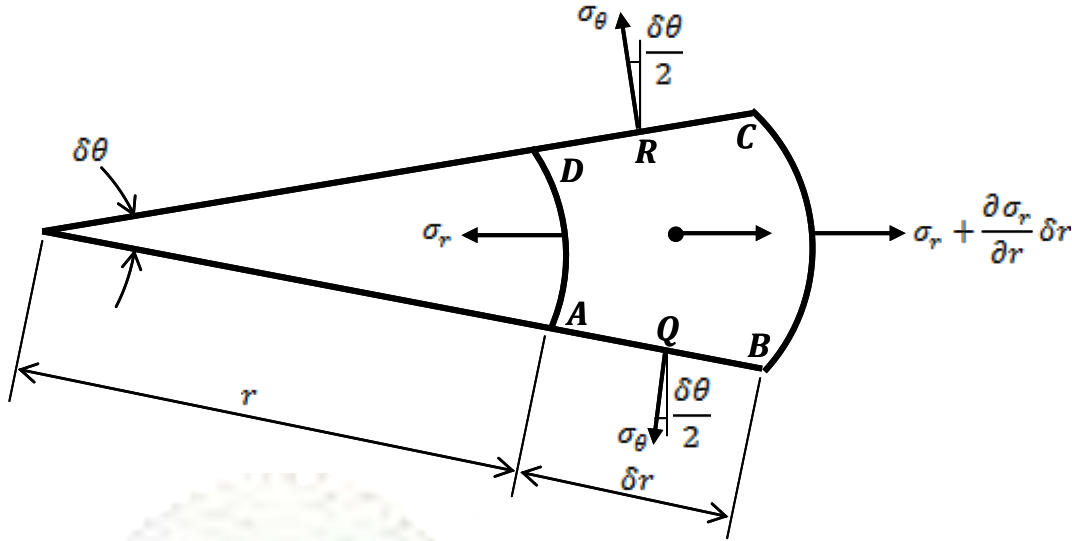


Figure C1. Stress Components on a sector-shaped element ABCD of an axisymmetric pipe.

The in-plane stresses acting on the element are as shown in Figure C1. The derivation of the stresses follows assumptions in chapter 5, thus an equation of equilibrium of forces acting on the element of material in the radial direction is written as

$$\left(\sigma_r + \frac{\partial \sigma_r}{\partial r} \delta r \right) (r + \delta r) \delta \theta \delta z - \sigma_r r \delta \theta \delta z - 2 \sigma_\theta \delta r \delta z \sin \frac{\delta \theta}{2} + B_r \delta r \left(r + \frac{\delta r}{2} \right) \delta \theta \delta z = \rho \bar{a}_r r \delta \theta \delta r \delta z \quad (C.1)$$

where

B_r = the body force in the r direction,

\bar{a}_r = the acceleration in the r direction

By simplifying equation (C.1) and neglecting small quantities and replacing sine of the small angle $\frac{\delta \theta}{2}$ with $\frac{\delta \theta}{2}$, equation (C.2) is obtained as

$$\left(\sigma_r + \frac{\partial \sigma_r}{\partial r} \delta r \right) (r + \delta r) \delta \theta \delta z - \sigma_r r \delta \theta \delta z - 2 \sigma_\theta \delta r \delta z \frac{\delta \theta}{2} + B_r \delta r \left(r + \frac{\delta r}{2} \right) \delta \theta \delta z = \rho \bar{a}_r r \delta \theta \delta r \delta z \quad (C.2)$$

Dividing equation (C.2) by $r \delta \theta \delta r \delta z$, and taking $\delta r \rightarrow 0$, yields

$$\frac{d\sigma_r}{dr} + \frac{1}{r}(\sigma_r - \sigma_\theta) + B_r = \rho \bar{a}_r \quad (\text{C.3})$$

Neglecting body force, equation (C.3) becomes

$$\frac{d\sigma_r}{dr} + \frac{1}{r}(\sigma_r - \sigma_\theta) = \rho \bar{a}_r \quad \forall \rho = \rho_p + \rho_f \quad (\text{C.4})$$

We note that, the partial derivative becomes a total derivative because, r is now the only independent variable, Roger (1989).

Also, the strain compatibility equations are written as

$$e_r = \frac{du_r}{dr}, \quad e_\theta = \frac{u_r}{r} \quad (\text{C.5a})$$

$$e_r = \frac{du_r}{dr} = \frac{d}{dr}(re_\theta) \quad (\text{C.5b})$$

From Hooke's law, we have the stress-strain relations

$$e_r = \frac{1}{E}[\sigma_r - \nu(\sigma_\theta + \sigma_z)] \quad (\text{C.6a})$$

$$e_\theta = \frac{1}{E}[\sigma_\theta - \nu(\sigma_z + \sigma_r)] \quad (\text{C.6b})$$

$$e_z = \frac{1}{E}[\sigma_z - \nu(\sigma_r + \sigma_\theta)] \quad (\text{C.6c})$$

Internally pressurized thick-walled pipe

Figure C2 illustrates the cross section of a long thick-walled cylinder of internal radius R_1 and external radius R_2 , subjected to fluid pressure p at its inner surface. The variations of radial and hoop stresses with radius through the thickness of the pipe wall are expressed below.

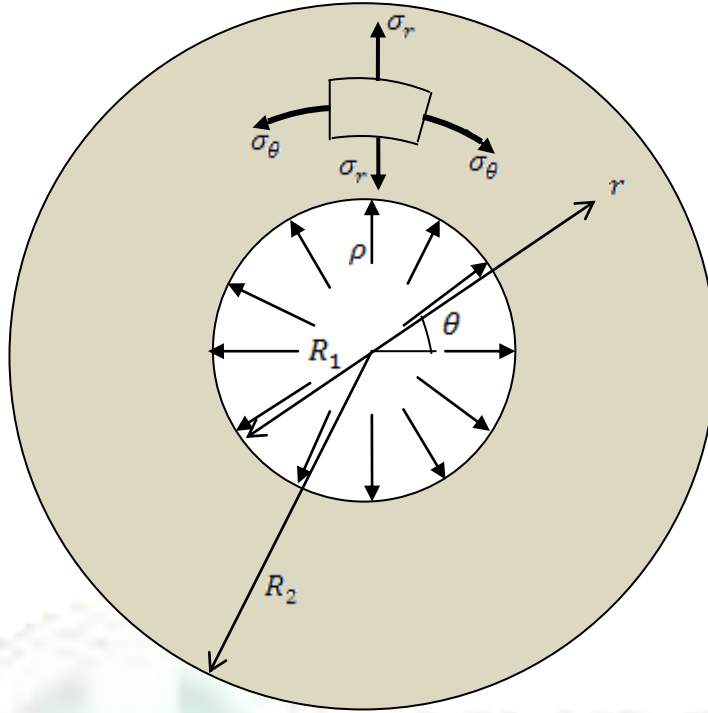


Figure C2. Cross section of a long thick-walled pipe

Substituting equations (C.6a and 6b) into equation (C.5b) gives

$$\sigma_r - \nu(\sigma_\theta + \sigma_z) = \frac{d}{dr} \{r(\sigma_\theta - \nu(\sigma_z + \sigma_r))\} \quad (C.7)$$

Differentiating the right-hand side of equation (C.7) and make some rearrangement yields

$$(\sigma_r - \sigma_\theta)(1 + \nu) = r \frac{d}{dr} (\sigma_\theta - \nu(\sigma_z + \sigma_r)) \quad (C.8)$$

Assuming plane strain condition, since the length of the pipe is large compared to its diameter, hence, the axial strain is independent of radius. We can then differentiate equation (C.6c) with respect to radius and setting the derivative of e_z to zero, to get

$$\frac{d\sigma_z}{dr} = \frac{d}{dr} [\nu(\sigma_r + \sigma_\theta)] \quad (C.9)$$

Using equation (C.9) in equation (C.8), we obtain

$$(\sigma_r - \sigma_\theta) = r \frac{d}{dr} (\sigma_\theta(1 - \nu) - \nu\sigma_r) \quad (C.10)$$

Rearranging equation (C.4), we get

$$(\sigma_r - \sigma_\theta) = r \left(\rho \bar{a}_r - \frac{d\sigma_r}{dr} \right) \quad (C.11)$$

Comparing these two expressions for the difference between the radial and hoop stresses, it can be deduced that

$$\frac{d\sigma_r}{dr} = -\frac{d}{dr} (\sigma_\theta (1-\nu) - \nu \sigma_r) + \rho \bar{a}_r$$

integrating this to give

$$(\sigma_r + \sigma_\theta)(1-\nu) = \rho \bar{a}_r r + 2C \quad (C.12)$$

where for convenience, $2C$ is used as constant of integration.

From equation (C.12),

$$\sigma_\theta = \frac{1}{(1-\nu)} (\rho \bar{a}_r r + 2C) - \sigma_r \quad (C.13)$$

Putting equation (C.13) into equation (C.11) yields

$$2Ar + \frac{\rho \bar{a}_r r^2 (2-\nu)}{(1-\nu)} = \frac{d}{dr} (r^2 \sigma_r) \quad (C.14)$$

where $2A = \frac{2C}{(1-\nu)}$

Integrating equation (C.14) gives

$$\sigma_r = A - \frac{B}{r^2} + \frac{(2-\nu)}{3(1-\nu)} (\rho \bar{a}_r r) \quad (C.15)$$

Substituting equation (C.14) into equation (C.13) to obtain

$$\sigma_\theta = A + \frac{B}{r^2} + \frac{(1+\nu)}{3(1-\nu)} (\rho \bar{a}_r r) \quad (C.16)$$

Further analysis of the foregoing equations is subject to the following boundary conditions viz:

$$\sigma_r = -p_i \quad \text{at} \quad r = R_i \quad (\text{internal radius}) \quad (C.17a)$$

$$\sigma_r = -p_{e(\text{total})} \quad \text{at} \quad r = R_0 \quad (\text{external radius}) \quad (C.17b)$$

Equations. (C.17) enable us to rewrite equations (C.15 & C.16) respectively as

$$-p_i = A - \frac{B}{R_i^2} + \frac{(2-\nu)}{3(1-\nu)}(\rho\bar{\alpha}_r R_i) \quad (\text{C.18a})$$

$$-p_e = A - \frac{B}{R_0^2} + \frac{(2-\nu)}{3(1-\nu)}(\rho\bar{\alpha}_r R_0) \quad (\text{C.18b})$$

Subtracting equation (C.18b) from equation (C.18a) gives

$$B = \frac{R_0^2 R_i^2}{R_i^2 - R_0^2} \left[p_e - p_i - \frac{(2-\nu)}{3(1-\nu)} \rho\bar{\alpha}_r (R_i - R_0) \right] \quad (\text{C.19})$$

Using equation (C.19) in equation (C.18a), we obtain

$$A = -p_i \left(1 + \frac{R_0^2}{R_i^2 - R_0^2} \right) + \frac{R_0^2}{R_i^2 - R_0^2} p_e - \frac{(2-\nu)}{3(1-\nu)} \rho\bar{\alpha}_r \left(R_i + \frac{R_0^2}{R_i + R_0} \right) \quad (\text{C.20})$$

Substituting equations (C.19 and C.20) into equations (C.15 and C.16) yields

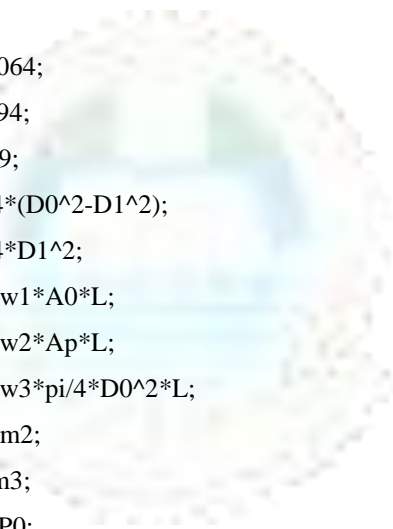
$$\begin{aligned} \sigma_r = & -p_i \left(\frac{r^2 R_i^2 + R_i^2 R_0^2}{r^2 (R_i^2 - R_0^2)} \right) + \left(\frac{r^2 R_0^2 + R_i^2 R_0^2}{r^2 (R_i^2 - R_0^2)} \right) p_e \\ & - \frac{(2-\nu)}{3(1-\nu)} (\rho\bar{\alpha}_r) \left(\frac{r^2 (R_i + R_0) R_i + r^2 R_0^2 - R_i^2 R_0^2 - r^3 (R_i + R_0)}{r^2 (R_i + R_0)} \right) \end{aligned} \quad (\text{C.21})$$

$$\begin{aligned} \sigma_\theta = & -p_i \left(\frac{r^2 R_i^2 + R_i^2 R_0^2}{r^2 (R_i^2 - R_0^2)} \right) + \left(\frac{r^2 R_0^2 + R_i^2 R_0^2}{r^2 (R_i^2 - R_0^2)} \right) p_e \\ & - \frac{(2-\nu)}{3(1-\nu)} (\rho\bar{\alpha}_r) \left(\frac{r^2 (R_i + R_0) R_i + r^2 R_0^2 + R_i^2 R_0^2 - r^3 (R_i + R_0)}{r^2 (R_i + R_0)} \right) \end{aligned} \quad (\text{C.22})$$

APPENDIX D
MATLAB PROGRAMS

D.1 Matlab Program for Pipe Sitting on the Seabed (Chapter 3)

```
P0=1.5e8;
T0=5e8;
L=600;
h0=1500;
c1=1;
rhow1=0.977;
rhow2=7850;
rhow3=980;
c2=5;
D0=0.4064;
D1=0.394;
E=200e9;
Ap=pi/4*(D0^2-D1^2);
A0=pi/4*D1^2;
m1=rhow1*A0*L;
m2=rhow2*Ap*L;
m3=rhow3*pi/4*D0^2*L;
m=m1+m2;
M=m+m3;
P1=10*P0;
P2=10*P0;
K0=400;
I=1.17*10^-5;
teta0=110;
teta1=10;
alpha=1.7e-5;
u=linspace(0,5,100);
delta=m1/m;
delta0=m3/M;
beta=((T0*L^2)/E*I);
beta1=((E*A0*L^2)/E*I);
beta2=sqrt(delta)./u;
beta3=alpha*beta1*beta2*teta0;
```



UNIVERSITY
OF LAGOS

```

beta4=alpha*beta1*beta2*teta1;
beta5=(alpha*beta1*teta0);
beta6=(alpha*beta1*teta1);
U=3;
beta7=beta1./u;
beta8=delta0/L;
C1=(c1*L^2/m*E*I);
C2=(c2*L^2/m*E*I);
g0=9.8;
g=M*g0*L^3/E*I;
gama=0.2;
gama1=(P1*A0*L^2/E*I);
gama2=((P1-P2)*A0*L^2/E*I);
rho=1;
U_w=3;
k=1;
h=h0/L;
beta=(-U_w*coth(k*h)/k)
delтта=0.25*D0;% not actual
kb=8;
Kb=((kb*L^4)/E*I);
alpha0=(L^4/I);
u=linspace(0,5,100);
u1=.5;
K=pi*(2*(D0/(2*L))-delтта)*(beta8*g*h/L-0.2^2*alpha0*0.03*delтта/2*0.02)*u1;
KK=K./(1-pi*(2*(D0/(2*L))-delтта)*beta8*beta);
n=1;
eta1=(C1+C2-beta4*(1-0.5*gama)-beta3*gama-gama2*beta2*(1-0.5*gama)-beta4*(1-0.5*gama));
Eta1=eta1/(1-pi*(2*(D0/(2*L))-delтта)*beta8*beta);
eta2=((n^4*pi^4)-((3*sqrt(delta)*u.^2-beta+gama1*(1-0.5*gama))+beta5*(1-0.5*gama))*(n^2*pi^2) + Kb);
Eta2=eta2/(1-pi*(2*(D0/(2*L))-delтта)*beta8*beta);
alpha1=(Eta1/2+i*sqrt(Eta2-Eta1.^2./4));
alpha2=(Eta1/2-i*sqrt(Eta2-Eta1.^2./4));
F1=(1./(alpha1.*alpha2));
n1=1;
n2=2;
n3=3;
n4=4;
n5=5;

```



$z=1;$
 $x=0.5;$
 $R1=(D1/(2*L));$
 $\eta1=(C1+C2-\beta4*(1-0.5*\gamma)-\beta3*\gamma-\gamma2*\beta2*(1-0.5*\gamma)-\beta4*(1-0.5*\gamma));$
 $\text{Eta1}=\eta1/(1-\pi*(2*(D0/(2*L))-\text{del}t\tau)*\beta8*\beta\tau);$
 $\eta2=((n1^4*\pi^4)-((3*\sqrt{\text{delta}}*u.^2-\beta+\gamma1*(1-0.5*\gamma))+\beta5*(1-0.5*\gamma))*(n1^2*\pi^2) + K\beta);$
 $\text{Eta2}=\eta2/(1-\pi*(2*(D0/(2*L))-\text{del}t\tau)*\beta8*\beta\tau);$
 $\alpha1=(\text{Eta1}/2+i*\sqrt{\text{Eta2}-\text{Eta1}.^2./4});$
 $\alpha2=(\text{Eta1}/2-i*\sqrt{\text{Eta2}-\text{Eta1}.^2./4});$
 $F1=(1./(\alpha1.*\alpha2));$
 $\eta1=(C1+C2-\beta4*(1-0.5*\gamma)-\beta3*\gamma-\gamma2*\beta2*(1-0.5*\gamma)-\beta4*(1-0.5*\gamma));$
 $\text{Eta1}=\eta1/(1-\pi*(2*(D0/(2*L))-\text{del}t\tau)*\beta8*\beta\tau);$
 $\eta2=((n2^4*\pi^4)-((3*\sqrt{\text{delta}}*u.^2-\beta+\gamma1*(1-0.5*\gamma))+\beta5*(1-0.5*\gamma))*(n2^2*\pi^2) + K\beta);$
 $\text{Eta2}=\eta2/(1-\pi*(2*(D0/(2*L))-\text{del}t\tau)*\beta8*\beta\tau);$
 $\alpha1=(\text{Eta1}/2+i*\sqrt{\text{Eta2}-\text{Eta1}.^2./4});$
 $\alpha2=(\text{Eta1}/2-i*\sqrt{\text{Eta2}-\text{Eta1}.^2./4});$
 $F2=(1./(\alpha1.*\alpha2));$
 $\eta1=(C1+C2-\beta4*(1-0.5*\gamma)-\beta3*\gamma-\gamma2*\beta2*(1-0.5*\gamma)-\beta4*(1-0.5*\gamma));$
 $\text{Eta1}=\eta1/(1-\pi*(2*(D0/(2*L))-\text{del}t\tau)*\beta8*\beta\tau);$
 $\eta2=((n3^4*\pi^4)-((3*\sqrt{\text{delta}}*u.^2-\beta+\gamma1*(1-0.5*\gamma))+\beta5*(1-0.5*\gamma))*(n3^2*\pi^2) + K\beta);$
 $\text{Eta2}=\eta2/(1-\pi*(2*(D0/(2*L))-\text{del}t\tau)*\beta8*\beta\tau);$
 $\alpha1=(\text{Eta1}/2+i*\sqrt{\text{Eta2}-\text{Eta1}.^2./4});$
 $\alpha2=(\text{Eta1}/2-i*\sqrt{\text{Eta2}-\text{Eta1}.^2./4});$
 $F3=(1./(\alpha1.*\alpha2));$
 $\eta1=(C1+C2-\beta4*(1-0.5*\gamma)-\beta3*\gamma-\gamma2*\beta2*(1-0.5*\gamma)-\beta4*(1-0.5*\gamma));$
 $\text{Eta1}=\eta1/(1-\pi*(2*(D0/(2*L))-\text{del}t\tau)*\beta8*\beta\tau);$
 $\eta2=((n4^4*\pi^4)-((3*\sqrt{\text{delta}}*u.^2-\beta+\gamma1*(1-0.5*\gamma))+\beta5*(1-0.5*\gamma))*(n4^2*\pi^2) + K\beta);$
 $\text{Eta2}=\eta2/(1-\pi*(2*(D0/(2*L))-\text{del}t\tau)*\beta8*\beta\tau);$
 $\alpha1=(\text{Eta1}/2+i*\sqrt{\text{Eta2}-\text{Eta1}.^2./4});$
 $\alpha2=(\text{Eta1}/2-i*\sqrt{\text{Eta2}-\text{Eta1}.^2./4});$
 $F4=(1./(\alpha1.*\alpha2));$
 $\eta1=(C1+C2-\beta4*(1-0.5*\gamma)-\beta3*\gamma-\gamma2*\beta2*(1-0.5*\gamma)-\beta4*(1-0.5*\gamma));$
 $\text{Eta1}=\eta1/(1-\pi*(2*(D0/(2*L))-\text{del}t\tau)*\beta8*\beta\tau);$
 $\eta2=((n5^4*\pi^4)-((3*\sqrt{\text{delta}}*u.^2-\beta+\gamma1*(1-0.5*\gamma))+\beta5*(1-0.5*\gamma))*(n5^2*\pi^2) + K\beta);$
 $\text{Eta2}=\eta2/(1-\pi*(2*(D0/(2*L))-\text{del}t\tau)*\beta8*\beta\tau);$
 $\alpha1=(\text{Eta1}/2+i*\sqrt{\text{Eta2}-\text{Eta1}.^2./4});$
 $\alpha2=(\text{Eta1}/2-i*\sqrt{\text{Eta2}-\text{Eta1}.^2./4});$
 $F5=(1./(\alpha1.*\alpha2));$

```

R1=(D1/2*L);
r1=0.01;
r2=0.02;
r3=0.04;
r4=0.06;
r5=0.09;
u=linspace (0, 5,100);
Y1=abs((2/sqrt(3))*alpha0*((z^2-(D1/(2*L))*z)*n1^2*pi^2*(1+(-1)^n1+1)*KK*F1*cos(n1*pi*x))-3.1e-6*z*u)*(r1/R1-1/2*r1^2/R1^2+1/3*r1^3/R1^3));
Y2=abs((2/sqrt(3))*alpha0*((z^2-(D1/(2*L))*z)*n1^2*pi^2*(1+(-1)^n1+1)*KK*F1*cos(n1*pi*x))-3.1e-6*z*u)*(r2/R1-1/2*r1^2/R1^2+1/3*r2^3/R1^3));
Y3=abs((2/sqrt(3))*alpha0*((z^2-(D1/(2*L))*z)*n1^2*pi^2*(1+(-1)^n1+1)*KK*F1*cos(n1*pi*x))-3.1e-6*z*u)*(r3/R1-1/2*r1^2/R1^2+1/3*r3^3/R1^3));
Y4=abs((2/sqrt(3))*alpha0*((z^2-(D1/(2*L))*z)*n1^2*pi^2*(1+(-1)^n1+1)*KK*F1*cos(n1*pi*x))-3.1e-6*z*u)*(r4/R1-1/2*r1^2/R1^2+1/3*r4^3/R1^3));
Y5=abs((2/sqrt(3))*alpha0*((z^2-(D1/(2*L))*z)*n1^2*pi^2*(1+(-1)^n1+1)*KK*F1*cos(n1*pi*x))-3.1e-6*z*u)*(r5/R1-1/2*r1^2/R1^2+1/3*r5^3/R1^3));
figure(1),plot(u,Y1,u,Y2,'m-',u,Y3,'r*',u,Y4,'bo-',u,Y5,'k*-')
grid on
legend('r=0.01','r=0.02','r=0.03','r=0.04','r=0.09')
n1=2;
Y1=abs((2/sqrt(3))*alpha0*((z^2-(D1/(2*L))*z)*n1^2*pi^2*(1+(-1)^n1+1)*KK*F1*cos(n1*pi*x))-3.1e-6*z*u)*(r1/R1-1/2*r1^2/R1^2+1/3*r1^3/R1^3));
Y2=abs((2/sqrt(3))*alpha0*((z^2-(D1/(2*L))*z)*n1^2*pi^2*(1+(-1)^n1+1)*KK*F1*cos(n1*pi*x))-3.1e-6*z*u)*(r2/R1-1/2*r1^2/R1^2+1/3*r2^3/R1^3));
Y3=abs((2/sqrt(3))*alpha0*((z^2-(D1/(2*L))*z)*n1^2*pi^2*(1+(-1)^n1+1)*KK*F1*cos(n1*pi*x))-3.1e-6*z*u)*(r3/R1-1/2*r1^2/R1^2+1/3*r3^3/R1^3));
Y4=abs((2/sqrt(3))*alpha0*((z^2-(D1/(2*L))*z)*n1^2*pi^2*(1+(-1)^n1+1)*KK*F1*cos(n1*pi*x))-3.1e-6*z*u)*(r4/R1-1/2*r1^2/R1^2+1/3*r4^3/R1^3));
Y5=abs((2/sqrt(3))*alpha0*((z^2-(D1/(2*L))*z)*n1^2*pi^2*(1+(-1)^n1+1)*KK*F1*cos(n1*pi*x))-3.1e-6*z*u)*(r5/R1-1/2*r1^2/R1^2+1/3*r5^3/R1^3));
figure(2),plot(u,Y1,u,Y2,'m-',u,Y3,'r*',u,Y4,'bo-',u,Y5,'k*-')
grid on
legend ('r=0.01','r=0.02','r=0.03','r=0.04','r=0.09')
u=.5;
beta=((T0*L^2)/E*I);
beta1= ((E*A0*L^2)/E*I);
beta2=sqrt (delta)./u;

```

```

beta3=alpha*beta1*beta2*teta0;
beta4=alpha*beta1*beta2*teta1;
beta5=(alpha*beta1*teta0);
beta6=(alpha*beta1*teta1);
beta7=beta1./u;
beta8=delta0/L;
z=linspace(-1,0,100);
eta1=(C1+C2-beta4*(1-0.5*gama)-beta3*gama-gama2*beta2*(1-0.5*gama)-beta4*(1-0.5*gama));
Eta1=eta1/(1-pi*(2*(D0/(2*L))-delтта)*beta8*beta);
eta2=((n1^4*pi^4)-((3*sqrt(delta)*u.^2-beta+gama1*(1-0.5*gama))+beta5*(1-0.5*gama))*(n1^2*pi^2) + Kb);
Eta2=eta2/(1-pi*(2*(D0/(2*L))-delтта)*beta8*beta);
alpha1=(Eta1/2+i*sqrt(Eta2-Eta1.^2./4));
alpha2=(Eta1/2-i*sqrt(Eta2-Eta1.^2./4));
F1=(1./(alpha1.*alpha2));
eta1=(C1+C2-beta4*(1-0.5*gama)-beta3*gama-gama2*beta2*(1-0.5*gama)-beta4*(1-0.5*gama));
Eta1=eta1/(1-pi*(2*(D0/(2*L))-delтта)*beta8*beta);
eta2=((n2^4*pi^4)-((3*sqrt(delta)*u.^2-beta+gama1*(1-0.5*gama))+beta5*(1-0.5*gama))*(n2^2*pi^2) + Kb);
Eta2=eta2/(1-pi*(2*(D0/(2*L))-delтта)*beta8*beta);
alpha1=(Eta1/2+i*sqrt(Eta2-Eta1.^2./4));
alpha2=(Eta1/2-i*sqrt(Eta2-Eta1.^2./4));
F2=(1./(alpha1.*alpha2));
eta1=(C1+C2-beta4*(1-0.5*gama)-beta3*gama-gama2*beta2*(1-0.5*gama)-beta4*(1-0.5*gama));
Eta1=eta1/(1-pi*(2*(D0/(2*L))-delтта)*beta8*beta);
eta2=((n3^4*pi^4)-((3*sqrt(delta)*u.^2-beta+gama1*(1-0.5*gama))+beta5*(1-0.5*gama))*(n3^2*pi^2) + Kb);
Eta2=eta2/(1-pi*(2*(D0/(2*L))-delтта)*beta8*beta);
alpha1=(Eta1/2+i*sqrt(Eta2-Eta1.^2./4));
alpha2=(Eta1/2-i*sqrt(Eta2-Eta1.^2./4));
F3=(1./(alpha1.*alpha2));
eta1=(C1+C2-beta4*(1-0.5*gama)-beta3*gama-gama2*beta2*(1-0.5*gama)-beta4*(1-0.5*gama));
Eta1=eta1/(1-pi*(2*(D0/(2*L))-delтта)*beta8*beta);
eta2=((n4^4*pi^4)-((3*sqrt(delta)*u.^2-beta+gama1*(1-0.5*gama))+beta5*(1-0.5*gama))*(n4^2*pi^2) + Kb);
Eta2=eta2/(1-pi*(2*(D0/(2*L))-delтта)*beta8*beta);
alpha1=(Eta1/2+i*sqrt(Eta2-Eta1.^2./4));
alpha2=(Eta1/2-i*sqrt(Eta2-Eta1.^2./4));
F4=(1./(alpha1.*alpha2));
eta1=(C1+C2-beta4*(1-0.5*gama)-beta3*gama-gama2*beta2*(1-0.5*gama)-beta4*(1-0.5*gama));
Eta1=eta1/(1-pi*(2*(D0/(2*L))-delтта)*beta8*beta);
eta2=((n5^4*pi^4)-((3*sqrt(delta)*u.^2-beta+gama1*(1-0.5*gama))+beta5*(1-0.5*gama))*(n5^2*pi^2) + Kb);
Eta2=eta2/(1-pi*(2*(D0/(2*L))-delтта)*beta8*beta);

```

```

alpha1=(Eta1/2+i*sqrt(Eta2-Eta1.^2./4));
alpha2=(Eta1/2-i*sqrt(Eta2-Eta1.^2./4));
F5=(1./(alpha1.*alpha2));
U=5;
x=0
Y1=abs((2/sqrt(3)*alpha0*((z.^2-(D1/(2*L)))*z).^n1^2*pi^2*(1+(-1)^n1+1).*KK.*F1*cos(n1*pi*x))-3.1e-6*z*U)*(r1/R1-1/2*r1^2/R1^2+1/3*r1^3/R1^3));
Y2=abs((2/sqrt(3)*alpha0*((z.^2-(D1/(2*L)))*z).^n1^2*pi^2*(1+(-1)^n1+1).*KK.*F2*cos(n1*pi*x))-3.1e-6*z*U)*(r2/R1-1/2*r2^2/R1^2+1/3*r2^3/R1^3));
Y3=abs((2/sqrt(3)*alpha0*((z.^2-(D1/(2*L)))*z).^n1^2*pi^2*(1+(-1)^n1+1).*KK.*F3*cos(n1*pi*x))-3.1e-6*z*U)*(r3/R1-1/2*r3^2/R1^2+1/3*r3^3/R1^3));
Y4=abs((2/sqrt(3)*alpha0*((z.^2-(D1/(2*L)))*z).^n1^2*pi^2*(1+(-1)^n1+1).*KK.*F4*cos(n1*pi*x))-3.1e-6*z*U)*(r4/R1-1/2*r4^2/R1^2+1/3*r4^3/R1^3));
Y5=abs((2/sqrt(3)*alpha0*((z.^2-(D1/(2*L)))*z).^n1^2*pi^2*(1+(-1)^n1+1).*KK.*F5*cos(n1*pi*x))-3.1e-6*z*U)*(r5/R1-1/2*r5^2/R1^2+1/3*r5^3/R1^3));
figure(3),plot(z,Y1,z,Y2,'m-',z,Y3,'r*',z,Y4,'bo-',z,Y5,'k*-')
grid on
legend('r=0.1','r=0.2','r=0.3','r=0.4','r=0.9')
z=linspace(-1,1,100);
Y1=abs((2/sqrt(3)*alpha0*((z.^2-(D1/(2*L)))*z).^n1^2*pi^2*(1+(-1)^n1+1).*KK.*F1*cos(n1*pi*x))-3.1e-6*z*U)*(r1/R1-1/2*r1^2/R1^2+1/3*r1^3/R1^3));
Y2=abs((2/sqrt(3)*alpha0*((z.^2-(D1/(2*L)))*z).^n1^2*pi^2*(1+(-1)^n1+1).*KK.*F2*cos(n1*pi*x))-3.1e-6*z*U)*(r2/R1-1/2*r2^2/R1^2+1/3*r2^3/R1^3));
Y3=abs((2/sqrt(3)*alpha0*((z.^2-(D1/(2*L)))*z).^n1^2*pi^2*(1+(-1)^n1+1).*KK.*F3*cos(n1*pi*x))-3.1e-6*z*U)*(r3/R1-1/2*r3^2/R1^2+1/3*r3^3/R1^3));
Y4=abs((2/sqrt(3)*alpha0*((z.^2-(D1/(2*L)))*z).^n1^2*pi^2*(1+(-1)^n1+1).*KK.*F4*cos(n1*pi*x))-3.1e-6*z*U)*(r4/R1-1/2*r4^2/R1^2+1/3*r4^3/R1^3));
Y5=abs((2/sqrt(3)*alpha0*((z.^2-(D1/(2*L)))*z).^n1^2*pi^2*(1+(-1)^n1+1).*KK.*F5*cos(n1*pi*x))-3.1e-6*z*U)*(r5/R1-1/2*r5^2/R1^2+1/3*r5^3/R1^3));
figure(4),plot(z,Y1,z,Y2,'m-',z,Y3,'r*',z,Y4,'bo-',z,Y5,'k*-')
grid on
legend('r=0.1','r=0.2','r=0.3','r=0.4','r=0.9')
z=1;
x=linspace(0,1,100);
Y1=abs((2/sqrt(3)*alpha0*((z.^2+(D1/(2*L)))*z).^n1^2*pi^2*(1+(-1)^n1+1).*KK.*F1*cos(n1*pi*x))-3.1e-6*z*U)*(r1/R1-1/2*r1^2/R1^2+1/3*r1^3/R1^3));
Y2=abs((2/sqrt(3)*alpha0*((z.^2+(D1/(2*L)))*z).^n2^2*pi^2*(1+(-1)^n2+1).*KK.*F2*cos(n2*pi*x))-3.1e-6*z*U)*(r2/R1-1/2*r2^2/R1^2+1/3*r2^3/R1^3));

```

```

Y3=abs((2/sqrt(3))*alpha0*((z.^2+(D1/(2*L))*z).^n3^2*pi^2*(1+(-1)^n3+1)*KK*F3*cos(n3*pi*x))-3.1e-
6*z*U)*(r3/R1-1/2*r3^2/R1^2+1/3*r3^3/R1^3));
Y4=abs((2/sqrt(3))*alpha0*((z.^2+(D1/(2*L))*z).^n4^2*pi^2*(1+(-1)^n4+1)*KK*F4*cos(n4*pi*x))-3.1e-
6*z*U)*(r4/R1-1/2*r4^2/R1^2+1/3*r4^3/R1^3));
Y5=abs((2/sqrt(3))*alpha0*((z.^2+(D1/(2*L))*z).^n5^2*pi^2*(1+(-1)^n5+1)*KK*F5*cos(n5*pi*x))-3.1e-
6*z*U)*(r5/R1-1/2*r5^2/R1^2+1/3*r5^3/R1^3));
figure(5),plot(x,Y1,x,Y2,'m-',x,Y3,'r*',x,Y4,'bo-',x,Y5,'k*-')
grid on
legend('r=0.1','r=0.2','r=0.3','r=0.4','r=0.9')
U=5;
n1=2;
n2=4;
n3=6;
n4=8;
n5=10;
z=1;
K=pi*(2*(D0/(2*L))-delta)*(beta8*g*h/L-0.2^2*alpha0*0.03*delta/2*0.02)*u1;
KK=K./(1-pi*(2*(D0/(2*L))-delta)*beta8*beta);
x=linspace(0,1,100);
Y1=abs((2/sqrt(3))*alpha0*((z.^2+(D1/(2*L))*z).^n1^2*pi^2*(1+(-1)^n1+1)*KK.*F1*cos(n1*pi*x))-3.1e-
6*z*U)*(r1/R1-1/2*r1^2/R1^2+1/3*r1^3/R1^3));
Y2=abs((2/sqrt(3))*alpha0*((z.^2+(D1/(2*L))*z).^n2^2*pi^2*(1+(-1)^n2+1)*KK.*F2*cos(n2*pi*x))-3.1e-
6*z*U)*(r1/R1-1/2*r1^2/R1^2+1/3*r1^3/R1^3));
Y3=abs((2/sqrt(3))*alpha0*((z.^2+(D1/(2*L))*z).^n3^2*pi^2*(1+(-1)^n3+1)*KK.*F3*cos(n3*pi*x))-3.1e-
6*z*U)*(r1/R1-1/2*r1^2/R1^2+1/3*r1^3/R1^3));
Y4=abs((2/sqrt(3))*alpha0*((z.^2+(D1/(2*L))*z).^n4^2*pi^2*(1+(-1)^n4+1)*KK.*F4*cos(n4*pi*x))-3.1e-
6*z*U)*(r1/R1-1/2*r1^2/R1^2+1/3*r1^3/R1^3));
Y5=abs((2/sqrt(3))*alpha0*((z.^2+(D1/(2*L))*z).^n5^2*pi^2*(1+(-1)^n5+1)*KK.*F5*cos(n5*pi*x))-3.1e-
6*z*U)*(r1/R1-1/2*r1^2/R1^2+1/3*r1^3/R1^3));
figure(55),plot(x,Y1,x,Y2,'m-',x,Y3,'r*',x,Y4,'bo-',x,Y5,'k*-')
grid on
legend('n=1','n=3','n=5','n=7','n=9')
U=5;
n1=1;
n2=4;
n3=6;
n4=8;
n5=10;
z=1;

```

```

x=linspace(0,1,100);
Y1=abs((2/sqrt(3))*alpha0*((z.^2+(D1/(2*L))*z).*n1^2*pi^2*(1+(-1)^n1+1).*KK*F1*cos(n1*pi*x))-3.1e-6*z*U)*(r1/R1-1/2*r1^2/R1^2+1/3*r1^3/R1^3));
Y2=abs((2/sqrt(3))*alpha0*((z.^2+(D1/(2*L))*z).*n2^2*pi^2*(1+(-1)^n2+1).*KK*F2*cos(n2*pi*x))-3.1e-6*z*U)*(r1/R1-1/2*r2^2/R1^2+1/3*r1^3/R1^3));
Y3=abs((2/sqrt(3))*alpha0*((z.^2+(D1/(2*L))*z).*n3^2*pi^2*(1+(-1)^n3+1).*KK*F3*cos(n3*pi*x))-3.1e-6*z*U)*(r1/R1-1/2*r3^2/R1^2+1/3*r1^3/R1^3));
Y4=abs((2/sqrt(3))*alpha0*((z.^2+(D1/(2*L))*z).*n4^2*pi^2*(1+(-1)^n4+1).*KK*F4*cos(n4*pi*x))-3.1e-6*z*U)*(r1/R1-1/2*r4^2/R1^2+1/3*r1^3/R1^3));
Y5=abs((2/sqrt(3))*alpha0*((z.^2+(D1/(2*L))*z).*n5^2*pi^2*(1+(-1)^n5+1).*KK*F5*cos(n5*pi*x))-3.1e-6*z*U)*(r1/R1-1/2*r5^2/R1^2+1/3*r1^3/R1^3));
figure(66),plot(x,Y1,x,Y2,'m-',x,Y3,'r*',x,Y4,'bo-',x,Y5,'k*-')

```

```
grid on
```

```
legend('n=2','n=4','n=6','n=8','n=10'),axis([0,1,0,30])
```

```
Y1=abs((2/sqrt(3))*alpha0*((z.^2+(D1/(2*L))*z).*n1^2*pi^2*(1+(-1)^n1+1).*KK*F1*cos(n1*pi*x))-3.1e-6*z*u)*(r1/R1));
```

```
Y2=abs((alpha0*((z.^2+(D1/(2*L))*z).*n1^2*pi^2*(1+(-1)^n1+1).*KK*F2*cos(n1*pi*x))-3.1e-6*z*u)*(r1/R1));
```

```
figure(77),plot(x,Y1,x,Y2,'r-o')
```

```
grid on
```

```
legend('burst pressure','buckling pressure')
```

```
n1=2;
```

```
x=0.5;
```

```
u=5;
```

```
z=linspace(-1,1,100);
```

```
alpha0=(L^4/I);
```

```
xi=linspace(0,1,100);
```

```
yi=linspace(0,1,100);
```

```
eta1=(C1+C2-beta4*(1-0.5*gama)-beta3*gama-gama2*beta2*(1-0.5*gama)-beta4*(1-0.5*gama));
```

```
Eta1=eta1/(1-pi*(2*(D0/(2*L))-delтта)*beta8*beta);
```

```
eta2=((n1^4*pi^4)-((3*sqrt(delta)*u.^2-beta+gama1*(1-0.5*gama))+beta5*(1-0.5*gama))*(n1^2*pi^2) + Kb);
```

```
Eta2=eta2/(1-pi*(2*(D0/(2*L))-delтта)*beta8*beta);
```

```
alpha1=(Eta1/2+i*sqrt(Eta2-Eta1.^2./4));
```

```
alpha2=(Eta1/2-i*sqrt(Eta2-Eta1.^2./4));
```

```
F1=(1./(alpha1.*alpha2));
```

```
[xxi,yyi]=meshgrid(xi,yi)
```

```
zzi=4*((2/sqrt(3))*alpha0*((xxi.^2+(D1/(2*L))))*xxi)*n1^2*pi^2*(1+(-1)^n1+1).*KK*F1.*cos(n1*pi*yyi)
```

```
figure(6),mesh(xxi,yyi,zzi)
```

```
u=5;
```

```
delta1=0.1;
```

```

delta2=0.2;
delta3=0.3;
delta4=0.4;
delta5=0.5;
eta1=(C1+C2-beta4*(1-0.5*gama)-beta3*gama-gama2*beta2*(1-0.5*gama)-beta4*(1-0.5*gama));
Eta21=eta1/(1-pi*(2*(D0/(2*L))-delтта)*beta8*beta);
eta22=(C1+C2-beta4*(1-0.5*gama)-beta3*gama-gama2*beta2*(1-0.5*gama)-beta4*(1-0.5*gama));
eta32=(C1+C2-beta4*(1-0.5*gama)-beta3*gama-gama2*beta2*(1-0.5*gama)-beta4*(1-0.5*gama));
eta42=(C1+C2-beta4*(1-0.5*gama)-beta3*gama-gama2*beta2*(1-0.5*gama)-beta4*(1-0.5*gama));
eta52=(C1+C2-beta4*(1-0.5*gama)-beta3*gama-gama2*beta2*(1-0.5*gama)-beta4*(1-0.5*gama));
eta62=(C1+C2-beta4*(1-0.5*gama)-beta3*gama-gama2*beta2*(1-0.5*gama)-beta4*(1-0.5*gama));
Eta22=eta22/(1-pi*(2*(D0/(2*L))-delтта)*beta8*beta);
Eta32=eta32/(1-pi*(2*(D0/(2*L))-delтта)*beta8*beta);
Eta42=eta42/(1-pi*(2*(D0/(2*L))-delтта)*beta8*beta);
Eta52=eta52/(1-pi*(2*(D0/(2*L))-delтта)*beta8*beta);
Eta62=eta62/(1-pi*(2*(D0/(2*L))-delтта)*beta8*beta);
alpha11=(Eta21/2+i*sqrt(Eta22-Eta21.^2./4));
alpha12=(Eta21/2+i*sqrt(Eta32-Eta21.^2./4));
alpha13=(Eta21/2+i*sqrt(Eta42-Eta21.^2./4));
alpha14=(Eta21/2+i*sqrt(Eta52-Eta21.^2./4));
alpha15=(Eta21/2+i*sqrt(Eta62-Eta21.^2./4));
alpha21=(Eta21/2-i*sqrt(Eta22-Eta21.^2./4));
alpha22=(Eta21/2-i*sqrt(Eta32-Eta21.^2./4));
alpha23=(Eta21/2-i*sqrt(Eta42-Eta21.^2./4));
alpha24=(Eta21/2-i*sqrt(Eta52-Eta21.^2./4));
alpha25=(Eta21/2-i*sqrt(Eta62-Eta21.^2./4));
F11=(1./(alpha11.*alpha21));
F21=(1./(alpha12.*alpha22));
F31=(1./(alpha13.*alpha23));
F41=(1./(alpha14.*alpha24));
F51=(1./(alpha15.*alpha25));
z=linspace(0,1,100);
x=0;
Y1=abs((2/sqrt(3))*alpha0*((z.^2-(D1/(2*L)))*z).^n5^2*pi^2*(1+(-1)^n5+1).*KK.*F11*cos(n5*pi*x))-3.1e-6*z*u*(r1/R1-1/2*r1^2/R1^2+1/3*r1^3/R1^3));
Y2=abs((2/sqrt(3))*alpha0*((z.^2-(D1/(2*L)))*z).^n5^2*pi^2*(1+(-1)^n5+1).*KK.*F21*cos(n5*pi*x))-3.1e-6*z*u*(r1/R1-1/2*r1^2/R1^2+1/3*r1^3/R1^3));
Y3=abs((2/sqrt(3))*alpha0*((z.^2-(D1/(2*L)))*z).^n5^2*pi^2*(1+(-1)^n5+1).*KK.*F31*cos(n5*pi*x))-3.1e-6*z*u*(r1/R1-1/2*r1^2/R1^2+1/3*r1^3/R1^3));

```



```

Y4=abs((2/sqrt(3)*alpha0*((z.^2-(D1/(2*L))*z). *n5^2*pi^2*(1+(-1)^n5+1). *KK. *F41*cos(n5*pi*x))-3.1e-
6*z*u)*(r1/R1-1/2*r1^2/R1^2+1/3*r1^3/R1^3));
Y5=abs((2/sqrt(3)*alpha0*((z.^2-(D1/(2*L))*z). *n5^2*pi^2*(1+(-1)^n5+1). *KK. *F51*cos(n5*pi*x))-3.1e-
6*z*u)*(r1/R1-1/2*r1^2/R1^2+1/3*r1^3/R1^3));
figure(7),plot(z,Y1,z,Y2,'m-',z,Y3,'r*',z,Y4,'bo-',z,Y5,'k*-' )
grid on
legend('\delta=0.1','\delta=0.2','\delta=0.3','\delta=0.4','\delta=0.5')
x=.5;
u=5;
z=linspace(-1,1,100);
Y1=abs((2/sqrt(3)*alpha0*((z.^2-(D1/(2*L))*z). *n5^2*pi^2*(1+(-1)^n5+1). *KK. *F11*cos(n5*pi*x))-3.1e-
6*z*u)*(r1/R1-1/2*r1^2/R1^2+1/3*r1^3/R1^3));
Y2=abs((2/sqrt(3)*alpha0*((z.^2-(D1/(2*L))*z). *n5^2*pi^2*(1+(-1)^n5+1). *KK. *F21*cos(n5*pi*x))-3.1e-
6*z*u)*(r1/R1-1/2*r1^2/R1^2+1/3*r1^3/R1^3));
Y3=abs((2/sqrt(3)*alpha0*((z.^2-(D1/(2*L))*z). *n5^2*pi^2*(1+(-1)^n5+1). *KK. *F31*cos(n5*pi*x))-3.1e-
6*z*u)*(r1/R1-1/2*r1^2/R1^2+1/3*r1^3/R1^3));
Y4=abs((2/sqrt(3)*alpha0*((z.^2-(D1/(2*L))*z). *n5^2*pi^2*(1+(-1)^n5+1). *KK. *F41*cos(n5*pi*x))-3.1e-
6*z*u)*(r1/R1-1/2*r1^2/R1^2+1/3*r1^3/R1^3));
Y5=abs((2/sqrt(3)*alpha0*((z.^2-(D1/(2*L))*z). *n5^2*pi^2*(1+(-1)^n5+1). *KK. *F51*cos(n5*pi*x))-3.1e-
6*z*u)*(r1/R1-1/2*r1^2/R1^2+1/3*r1^3/R1^3));
figure(8),plot(z,Y1,z,Y2,'m-',z,Y3,'r*',z,Y4,'bo-',z,Y5,'k*-' )
grid on
legend('\delta=0.1','\delta=0.2','\delta=0.3','\delta=0.4','\delta=0.5')
Y1=abs((2/sqrt(3)*alpha0*((z.^2+(D1/(2*L))*z). *n5^2*pi^2*(1+(-1)^n5+1). *KK. *F11*cos(n5*pi*x))-3.1e-
6*z*u)*(r1/R1-1/2*r1^2/R1^2+1/3*r1^3/R1^3));
Y2=abs((2/sqrt(3)*alpha0*((z.^2+(D1/(2*L))*z). *n5^2*pi^2*(1+(-1)^n5+1). *KK. *F21*cos(n5*pi*x))-3.1e-
6*z*u)*(r1/R1-1/2*r1^2/R1^2+1/3*r1^3/R1^3));
Y3=abs((2/sqrt(3)*alpha0*((z.^2+(D1/(2*L))*z). *n5^2*pi^2*(1+(-1)^n5+1). *KK. *F31*cos(n5*pi*x))-3.1e-
6*z*u)*(r1/R1-1/2*r1^2/R1^2+1/3*r1^3/R1^3));
Y4=abs((2/sqrt(3)*alpha0*((z.^2+(D1/(2*L))*z). *n5^2*pi^2*(1+(-1)^n5+1). *KK. *F41*cos(n5*pi*x))-3.1e-
6*z*u)*(r1/R1-1/2*r1^2/R1^2+1/3*r1^3/R1^3));
Y5=abs((2/sqrt(3)*alpha0*((z.^2+(D1/(2*L))*z). *n5^2*pi^2*(1+(-1)^n5+1). *KK. *F51*cos(n5*pi*x))-3.1e-
6*z*u)*(r1/R1-1/2*r1^2/R1^2+1/3*r1^3/R1^3));
figure(9),plot(z,Y1,z,Y2,'m-',z,Y3,'r*',z,Y4,'bo-',z,Y5,'k*-' )
grid on
legend('\delta=0.1','\delta=0.2','\delta=0.3','\delta=0.4','\delta=0.5')
z=1;
x=0;
r=linspace(0.1,.9,100);

```

Y1=abs((2/sqrt(3)*alpha0*((z^2+(D1/(2*L))*z)*n5^2*pi^2*(1+(-1)^n5+1)*KK*F11*cos(n5*pi*x))-3.1e-6*z*u)*(r./R1-1/2*r.^2/R1^2+1/3*r.^3/R1^3));

Y2=abs((2/sqrt(3)*alpha0*((z^2+(D1/(2*L))*z)*n5^2*pi^2*(1+(-1)^n5+1)*KK*F21*cos(n5*pi*x))-3.1e-6*z*u)*(r./R1-1/2*r.^2/R1^2+1/3*r.^3/R1^3));

Y3=abs((2/sqrt(3)*alpha0*((z^2+(D1/(2*L))*z)*n5^2*pi^2*(1+(-1)^n5+1)*KK*F31*cos(n5*pi*x))-3.1e-6*z*u)*(r./R1-1/2*r.^2/R1^2+1/3*r.^3/R1^3));

Y4=abs((2/sqrt(3)*alpha0*((z^2+(D1/(2*L))*z)*n5^2*pi^2*(1+(-1)^n5+1)*KK*F41*cos(n5*pi*x))-3.1e-6*z*u)*(r./R1-1/2*r.^2/R1^2+1/3*r.^3/R1^3));

Y5=abs((2/sqrt(3)*alpha0*((z^2+(D1/(2*L))*z)*n5^2*pi^2*(1+(-1)^n5+1)*KK*F51*cos(n5*pi*x))-3.1e-6*z*u)*(r./R1-1/2*r.^2/R1^2+1/3*r.^3/R1^3));

figure(10),plot(r,Y1,r,Y2,'p',r,Y3,'r',r,Y4,'bo-',r,Y5,'k*-')

grid on

legend('\delta=0.1','\delta=0.2','\delta=0.3','\delta=0.4','\delta=0.5')

Y1=abs((2/sqrt(3)*alpha0*((z^2-(D1/(2*L))*z)*n5^2*pi^2*(1+(-1)^n5+1)*KK*F11*cos(n5*pi*x))-3.1e-6*z*u)*(r./R1-1/2*r.^2/R1^2+1/3*r.^3/R1^3));

Y2=abs((2/sqrt(3)*alpha0*((z^2-(D1/(2*L))*z)*n5^2*pi^2*(1+(-1)^n5+1)*KK*F21*cos(n5*pi*x))-3.1e-6*z*u)*(r./R1-1/2*r.^2/R1^2+1/3*r.^3/R1^3));

Y3=abs((2/sqrt(3)*alpha0*((z^2-(D1/(2*L))*z)*n5^2*pi^2*(1+(-1)^n5+1)*KK*F31*cos(n5*pi*x))-3.1e-6*z*u)*(r./R1-1/2*r.^2/R1^2+1/3*r.^3/R1^3));

Y4=abs((2/sqrt(3)*alpha0*((z^2-(D1/(2*L))*z)*n5^2*pi^2*(1+(-1)^n5+1)*KK*F41*cos(n5*pi*x))-3.1e-6*z*u)*(r./R1-1/2*r.^2/R1^2+1/3*r.^3/R1^3));

Y5=abs((2/sqrt(3)*alpha0*((z^2-(D1/(2*L))*z)*n5^2*pi^2*(1+(-1)^n5+1)*KK*F51*cos(n5*pi*x))-3.1e-6*z*u)*(r./R1-1/2*r.^2/R1^2+1/3*r.^3/R1^3));

figure(11),plot(r,Y1,r,Y2,'p',r,Y3,'r',r,Y4,'bo-',r,Y5,'k*-')

grid on

legend('\delta=0.1','\delta=0.2','\delta=0.3','\delta=0.4','\delta=0.5')

n1=1;

n2=2;

n3=3;

n4=4;

alpha0=(L^4/I);

Y1=(abs((2/sqrt(3)*alpha0*((z.^2-(D1/(2*L))*z).*n1^2*pi^2*(1+(-1)^n1+1).*KK*F11*cos(n1*pi*x))-3.1e-6*z*u)*(r./R1-1/2*r.^2./R1^2+1/3*r.^3./R1^3));

Y21=(abs((alpha0*((z.^2-(D1/(2*L))*z).*n1^2*pi^2*(1+(-1)^n1+1).*KK*F11*cos(n1*pi*x))-3.1e-6*z*u)*(r./R1-1/2*r.^2./R1^2+1/3*r.^3./R1^3));

Y22=(abs((alpha0*((z.^2-(D1/(2*L))*z).*n2^2*pi^2*(1+(-1)^n2+1).*KK*F11*cos(n2*pi*x))-3.1e-6*z*u)*(r./R1-1/2*r.^2./R1^2+1/3*r.^3./R1^3));

Y23=(abs((alpha0*((z.^2-(D1/(2*L))*z).*n3^2*pi^2*(1+(-1)^n3+1).*KK*F11*cos(n3*pi*x))-3.1e-6*z*u)*(r./R1-1/2*r.^2./R1^2+1/3*r.^3./R1^3));


```

figure(14),plot(u,Y1,u,Y2,'ro-')
grid on
legend('buckling pressure','burst pressure ')
x=[0 2 6 10 ];
y=[0.038/0.0325 0.0382/0.0327 0.0384/0.0329 0.042/0.0325 ]
xx=linspace(0,5,100);
yy1=spline(x, y, xx)
figure(15),plot(xx,yy1)
grid on
x=[0 2 6 10 ];
y=[4.22/3.68 4.25/3.69 4.38/3.78 4.65/4.08 ]
xx=linspace(0,10,100);
yy2=spline(x, y, xx)
figure(16),plot(xx,yy2)
grid on
figure(17),plot(xx,yy1,xx,yy2,'r*-')
legend('pipe thickness =0.9','pipe thickness =0.1 ')
grid on
xlabel( 'Normalised flow velocity')
ylabel ( 'Ratio of burst to buckling pressure')
x=0;
z=1;
u=5;
n1=1;
r=linspace(0,0.9,100);
eta1=(C1+C2-beta4*(1-0.5*gama)-beta3*gama-gama2*beta2*(1-0.5*gama)-beta4*(1-0.5*gama));
Eta1=eta1/(1-pi*(2*(D0/(2*L))-delтта)*beta8*beta);
eta2=((n4^4*pi^4)-((3*sqrt(delta)*u.^2-beta+gama1*(1-0.5*gama))+beta5*(1-0.5*gama))*(n4^2*pi^2) + Kb);
Eta2=eta2/(1-pi*(2*(D0/(2*L))-delтта)*beta8*beta);
alpha1=(Eta1/2+i*sqrt(Eta2-Eta1.^2./4));
alpha2=(Eta1/2-i*sqrt(Eta2-Eta1.^2./4));
F1=(1./(alpha1.*alpha2));
Y1=abs((alpha0*((z^2-(D1/(2*L))*z)*n1^2*pi^2*(1+(-1)^n1+1)*KK*F1*cos(n1*pi*x))-3.1e-6*z*u)*(r./R1-1/2*r.^2./R1^2+1/3*r.^3./R1^3));
Y2=abs((2/sqrt(3))*alpha0*((z^2-(D1/(2*L))*z)*n1^2*pi^2*(1+(-1)^n1+1)*KK*F1*cos(n1*pi*x))-3.1e-6*z*u)*(r./R1-1/2*r.^2./R1^2+1/3*r.^3./R1^3));
figure(18),plot(r,Y1,'ro-',r,Y2,'k*-')
grid on

```

```

legend('buckling pressure','burst pressure')
x=[0.1 0.3 0.5 0.7 ];
y=[0.0098/0.095 0.025/0.024 0.048/0.04 0.065/0.058 ]
xx=linspace(0.1,0.88,100);
yy1=spline(x, y, xx)
figure(19),plot(xx,yy1)
grid on
x=0;
z=1;
u=8;
n1=1;
r=linspace(0,0.9,100);
eta1=(C1+C2-beta4*(1-0.5*gama)-beta3*gama-gama2*beta2*(1-0.5*gama)-beta4*(1-0.5*gama));
Eta1=eta1/(1-pi*(2*(D0/(2*L))-delтта)*beta8*beta);
eta2=((n4^4*pi^4)-((3*sqrt(delta)*u.^2-beta+gama1*(1-0.5*gama))+beta5*(1-0.5*gama))*(n4^2*pi^2) + Kb);
Eta2=eta2/(1-pi*(2*(D0/(2*L))-delтта)*beta8*beta);
alpha1=(Eta1/2+i*sqrt(Eta2-Eta1.^2./4));
alpha2=(Eta1/2-i*sqrt(Eta2-Eta1.^2./4));
F1=(1./(alpha1.*alpha2));
Y1=abs((alpha0*((z^2-(D1/(2*L))*z)*n1^2*pi^2*(1+(-1)^n1+1)*KK*F1*cos(n1*pi*x))-3.1e-6*z*u)*(r./R1-1/2*r.^2./R1^2+1/3*r.^3./R1^3));
Y2=abs((2/sqrt(3))*alpha0*((z^2-(D1/(2*L))*z)*n1^2*pi^2*(1+(-1)^n1+1)*KK*F1*cos(n1*pi*x))-3.1e-6*z*u)*(r./R1-1/2*r.^2./R1^2+1/3*r.^3./R1^3));
figure(20),plot(r,Y1,'ro-',r,Y2,'k*-')
grid on
legend('buckling pressure','burst pressure')
x=[0.1 0.3 0.5 0.7 ];
y=[0.011/0.01 0.032/0.029 0.058/0.048 0.078/0.068 ]
xx=linspace(0.1,0.88,100);
yy2=spline(x, y, xx)
figure(21),plot(xx,yy2)
x=0;
z=1;
u=10;
n1=1;
r=linspace(0,0.9,100);
eta1=(C1+C2-beta4*(1-0.5*gama)-beta3*gama-gama2*beta2*(1-0.5*gama)-beta4*(1-0.5*gama));
Eta1=eta1/(1-pi*(2*(D0/(2*L))-delтта)*beta8*beta);
eta2=((n4^4*pi^4)-((3*sqrt(delta)*u.^2-beta+gama1*(1-0.5*gama))+beta5*(1-0.5*gama))*(n4^2*pi^2) + Kb);

```

```

Eta2=eta2/(1-pi*(2*(D0/(2*L))-delta)*beta8*beta);
alpha1=(Eta1/2+i*sqrt(Eta2-Eta1.^2./4));
alpha2=(Eta1/2-i*sqrt(Eta2-Eta1.^2./4));
F1=(1./(alpha1.*alpha2));
Y1=abs((alpha0*((z^2-(D1/(2*L))*z)*n1^2*pi^2*(1+(-1)^n1+1)*KK*F1*cos(n1*pi*x))-3.1e-6*z*u)*(r./R1-
1/2*r.^2./R1^2+1/3*r.^3./R1^3));
Y2=abs((2/sqrt(3)*alpha0*((z^2-(D1/(2*L))*z)*n1^2*pi^2*(1+(-1)^n1+1)*KK*F1*cos(n1*pi*x))-3.1e-
6*z*u)*(r./R1-1/2*r.^2./R1^2+1/3*r.^3./R1^3));
figure(22),plot(r,Y1,'ro-',r,Y2,'k*-')
grid on
legend('buckling pressure','burst pressure')
x=[0.1 0.3 0.5 0.7 ];
y=[0.016/0.015 0.04/0.038 0.064/0.05 0.088/0.068 ]
xx=linspace(0.1,0.88,100);
yy3=spline(x, y, xx)
figure(23),plot(xx,yy3)
figure(24),plot(xx,yy2,xx,yy3,'ro-')
grid on
xlabel( 'Normalised pipe thickness')
ylabel ( 'Ratio of burst to buckling pressure')
legend('normalised flow velocity=8','normalised flow velocity=10')
x=[0.1 0.3 0.5 0.7 ];
y=[0.045/0.043 0.14/0.12 0.23/0.18 0.29/0.252 ]
xx=linspace(0.1,0.88,100);
yy4=spline(x, y, xx)
x=[0.1 0.3 0.5 0.7 ];
y=[0.05101/0.048 0.058/0.051 0.125/0.120 0.167/0.135 ]
xx=linspace(0.1,0.88,100);
yy5=spline(x, y, xx)
figure(25),plot(xx,yy4,xx,yy5,'ro-')
grid on
xlabel( 'Normalised pipe thickness')
ylabel ( 'Ratio of burst to buckling pressure')
legend('normalised flow velocity=8','normalised flow velocity=10')
u=10;
beta=((T0*L^2)/E*I);
beta1=((E*A0*L^2)/E*I);
beta2=sqrt(delta)./u;
beta3=alpha*beta1*beta2*teta0;

```

$\beta_4 = \alpha \beta_1 \beta_2 \tau_1$;
 $\beta_5 = (\alpha \beta_1 \tau_0)$;
 $\beta_6 = (\alpha \beta_1 \tau_1)$;
 $\beta_7 = \beta_1 / u$;
 $\beta_8 = \delta_0 / L$;
 $\eta_1 = (C_1 + C_2 - \beta_4 (1 - 0.5 \gamma) - \beta_3 \gamma - \gamma_2 \beta_2 (1 - 0.5 \gamma) - \beta_4 (1 - 0.5 \gamma))$;
 $\eta_1 = \eta_1 / (1 - \pi (2 (D_0 / (2L)) - \delta_{lta}) \beta_8 \beta_2)$;
 $\eta_2 = ((n^4 \pi^4) - (3 \sqrt{\delta} u^2 - \beta + \gamma_1 (1 - 0.5 \gamma) + \beta_5 (1 - 0.5 \gamma)) (n^2 \pi^2) + K_b)$;
 $\eta_2 = \eta_2 / (1 - \pi (2 (D_0 / (2L)) - \delta_{lta}) \beta_8 \beta_2)$;
 $\alpha_1 = (\eta_1 / 2 + i \sqrt{(\eta_2 - \eta_1^2 / 4)})$;
 $\alpha_2 = (\eta_1 / 2 - i \sqrt{(\eta_2 - \eta_1^2 / 4)})$;
 $F_1 = (1 / (\alpha_1 \alpha_2))$;
 $\eta_1 = (C_1 + C_2 - \beta_4 (1 - 0.5 \gamma) - \beta_3 \gamma - \gamma_2 \beta_2 (1 - 0.5 \gamma) - \beta_4 (1 - 0.5 \gamma))$;
 $\eta_1 = \eta_1 / (1 - \pi (2 (D_0 / (2L)) - \delta_{lta}) \beta_8 \beta_2)$;
 $\eta_2 = ((n^4 \pi^4) - (3 \sqrt{\delta} u^2 - \beta + \gamma_1 (1 - 0.5 \gamma) + \beta_5 (1 - 0.5 \gamma)) (n^2 \pi^2) + K_b)$;
 $\eta_2 = \eta_2 / (1 - \pi (2 (D_0 / (2L)) - \delta_{lta}) \beta_8 \beta_2)$;
 $\alpha_1 = (\eta_1 / 2 + i \sqrt{(\eta_2 - \eta_1^2 / 4)})$;
 $\alpha_2 = (\eta_1 / 2 - i \sqrt{(\eta_2 - \eta_1^2 / 4)})$;
 $F_2 = (1 / (\alpha_1 \alpha_2))$;
 $\eta_1 = (C_1 + C_2 - \beta_4 (1 - 0.5 \gamma) - \beta_3 \gamma - \gamma_2 \beta_2 (1 - 0.5 \gamma) - \beta_4 (1 - 0.5 \gamma))$;
 $\eta_1 = \eta_1 / (1 - \pi (2 (D_0 / (2L)) - \delta_{lta}) \beta_8 \beta_2)$;
 $\eta_2 = ((n^4 \pi^4) - (3 \sqrt{\delta} u^2 - \beta + \gamma_1 (1 - 0.5 \gamma) + \beta_5 (1 - 0.5 \gamma)) (n^2 \pi^2) + K_b)$;
 $\eta_2 = \eta_2 / (1 - \pi (2 (D_0 / (2L)) - \delta_{lta}) \beta_8 \beta_2)$;
 $\alpha_1 = (\eta_1 / 2 + i \sqrt{(\eta_2 - \eta_1^2 / 4)})$;
 $\alpha_2 = (\eta_1 / 2 - i \sqrt{(\eta_2 - \eta_1^2 / 4)})$;
 $F_3 = (1 / (\alpha_1 \alpha_2))$;
 $\eta_1 = (C_1 + C_2 - \beta_4 (1 - 0.5 \gamma) - \beta_3 \gamma - \gamma_2 \beta_2 (1 - 0.5 \gamma) - \beta_4 (1 - 0.5 \gamma))$;
 $\eta_1 = \eta_1 / (1 - \pi (2 (D_0 / (2L)) - \delta_{lta}) \beta_8 \beta_2)$;
 $\eta_2 = ((n^4 \pi^4) - (3 \sqrt{\delta} u^2 - \beta + \gamma_1 (1 - 0.5 \gamma) + \beta_5 (1 - 0.5 \gamma)) (n^2 \pi^2) + K_b)$;
 $\eta_2 = \eta_2 / (1 - \pi (2 (D_0 / (2L)) - \delta_{lta}) \beta_8 \beta_2)$;
 $\alpha_2 = (\eta_1 / 2 - i \sqrt{(\eta_2 - \eta_1^2 / 4)})$;
 $F_4 = (1 / (\alpha_1 \alpha_2))$;
 $\eta_1 = (C_1 + C_2 - \beta_4 (1 - 0.5 \gamma) - \beta_3 \gamma - \gamma_2 \beta_2 (1 - 0.5 \gamma) - \beta_4 (1 - 0.5 \gamma))$;
 $\eta_1 = \eta_1 / (1 - \pi (2 (D_0 / (2L)) - \delta_{lta}) \beta_8 \beta_2)$;
 $\eta_2 = ((n^4 \pi^4) - (3 \sqrt{\delta} u^2 - \beta + \gamma_1 (1 - 0.5 \gamma) + \beta_5 (1 - 0.5 \gamma)) (n^2 \pi^2) + K_b)$;
 $\eta_2 = \eta_2 / (1 - \pi (2 (D_0 / (2L)) - \delta_{lta}) \beta_8 \beta_2)$;
 $\alpha_1 = (\eta_1 / 2 + i \sqrt{(\eta_2 - \eta_1^2 / 4)})$;
 $\alpha_2 = (\eta_1 / 2 - i \sqrt{(\eta_2 - \eta_1^2 / 4)})$;
 $F_5 = (1 / (\alpha_1 \alpha_2))$;

```

z=-1;
x=0.5;
u=.5;
u2=u;
t=linspace(0,01,100)
R1=(D1/(2*L))
Y1=abs((4/sqrt(3)*t./R1*alpha0.*((z^2-R1*z)*pi^2*KK*F1*cos(-pi*x)))-(-3.1e-6*u2*z*t./R1.^2));
YY1=abs((-2*z*t./R1.^2))
figure(26),plot(t,Y1,t,YY1,'-o')
grid on
n1=1;
n2=3;
n3=5;
n4=7;
n5=9;
beta=((T0*L^2)/E*I);
beta1=((E*A0*L^2)/E*I);
beta2=sqrt(delta)./u;
beta3=alpha*beta1*beta2*teta0;
beta4=alpha*beta1*beta2*teta1;
beta5=(alpha*beta1*teta0);
beta6=(alpha*beta1*teta1);
beta7=beta1./u;
beta8=delta0/L;
eta1=(C1+C2-beta4*(1-0.5*gama)-beta3*gama-gama2*beta2*(1-0.5*gama)-beta4*(1-0.5*gama));
Eta1=eta1/(1-pi*(2*(D0/(2*L))-delтта)*beta8*beta);
eta2=((n^4*pi^4)-((3*sqrt(delta)*u.^2-beta+gama1*(1-0.5*gama))+beta5*(1-0.5*gama))*(n^2*pi^2) + Kb);
Eta2=eta2/(1-pi*(2*(D0/(2*L))-delтта)*beta8*beta);
alpha1=(Eta1/2+i*sqrt(Eta2-Eta1.^2./4));
alpha2=(Eta1/2-i*sqrt(Eta2-Eta1.^2./4));
F1=(1./(alpha1.*alpha2));
eta1=(C1+C2-beta4*(1-0.5*gama)-beta3*gama-gama2*beta2*(1-0.5*gama)-beta4*(1-0.5*gama));
Eta1=eta1/(1-pi*(2*(D0/(2*L))-delтта)*beta8*beta);
eta2=((n^4*pi^4)-((3*sqrt(delta)*u.^2-beta+gama1*(1-0.5*gama))+beta5*(1-0.5*gama))*(n^2*pi^2) + Kb);
Eta2=eta2/(1-pi*(2*(D0/(2*L))-delтта)*beta8*beta);
alpha1=(Eta1/2+i*sqrt(Eta2-Eta1.^2./4));
alpha2=(Eta1/2-i*sqrt(Eta2-Eta1.^2./4));
F2=(1./(alpha1.*alpha2));
eta1=(C1+C2-beta4*(1-0.5*gama)-beta3*gama-gama2*beta2*(1-0.5*gama)-beta4*(1-0.5*gama));

```



```

Eta1=eta1/(1-pi*(2*(D0/(2*L))-delтта)*beta8*beta);
eta2=((n^4*pi^4)-((3*sqrt(delta)*u.^2-beta+gama1*(1-0.5*gama))+beta5*(1-0.5*gama))*(n^2*pi^2) + Kb);
Eta2=eta2/(1-pi*(2*(D0/(2*L))-delтта)*beta8*beta);
alpha1=(Eta1/2+i*sqrt(Eta2-Eta1.^2./4));
alpha2=(Eta1/2-i*sqrt(Eta2-Eta1.^2./4));
F3=(1./(alpha1.*alpha2));
eta1=(C1+C2-beta4*(1-0.5*gama)-beta3*gama-gama2*beta2*(1-0.5*gama)-beta4*(1-0.5*gama));
Eta1=eta1/(1-pi*(2*(D0/(2*L))-delтта)*beta8*beta);
eta2=((n^4*pi^4)-((3*sqrt(delta)*u.^2-beta+gama1*(1-0.5*gama))+beta5*(1-0.5*gama))*(n^2*pi^2) + Kb);
Eta2=eta2/(1-pi*(2*(D0/(2*L))-delтта)*beta8*beta);
alpha1=(Eta1/2+i*sqrt(Eta2-Eta1.^2./4));
alpha2=(Eta1/2-i*sqrt(Eta2-Eta1.^2./4));
F4=(1./(alpha1.*alpha2));
eta1=(C1+C2-beta4*(1-0.5*gama)-beta3*gama-gama2*beta2*(1-0.5*gama)-beta4*(1-0.5*gama));
Eta1=eta1/(1-pi*(2*(D0/(2*L))-delтта)*beta8*beta);
eta2=((n^4*pi^4)-((3*sqrt(delta)*u.^2-beta+gama1*(1-0.5*gama))+beta5*(1-0.5*gama))*(n^2*pi^2) + Kb);
Eta2=eta2/(1-pi*(2*(D0/(2*L))-delтта)*beta8*beta);
alpha1=(Eta1/2+i*sqrt(Eta2-Eta1.^2./4));
alpha2=(Eta1/2-i*sqrt(Eta2-Eta1.^2./4));
F5=(1./(alpha1.*alpha2));
YZ1=abs(((4/sqrt(3))*t./R1*alpha0.*((z^2-R1*z)*n1^2*pi^2*(1+(-1)^n1+1)*KK*F1*cos(n1*pi*x)))-(3.1e-6*u2*z*t./R1^2));
YZ2=abs(((4/sqrt(3))*t./R1*alpha0.*((z^2-R1*z)*n2^2*pi^2*(1+(-1)^n2+1)*KK*F2*cos(n2*pi*x)))-(3.1e-6*u2*z*t./R1^2));
YZ3=abs(((4/sqrt(3))*t./R1*alpha0.*((z^2-R1*z)*n3^2*pi^2*(1+(-1)^n3+1)*KK*F3*cos(n3*pi*x)))-(3.1e-6*u2*z*t./R1^2));
YZ4=abs(((4/sqrt(3))*t./R1*alpha0.*((z^2-R1*z)*n4^2*pi^2*(1+(-1)^n4+1)*KK*F4*cos(n4*pi*x)))-(3.1e-6*u2*z*t./R1^2));
YZ5=abs(((4/sqrt(3))*t./R1*alpha0.*((z^2-R1*z)*n5^2*pi^2*(1+(-1)^n5+1)*KK*F5*cos(n5*pi*x)))-(3.1e-6*u2*z*t./R1^2));
figure(27),plot(t,YZ1,t,YZ2,'- ',t,YZ3,'-',t,YZ4,'k--',t,YZ5,'b*',t,YY1,'r-o')
legend('n=1','n=3','n=5','n=7','n=9','Barlow Equation')
grid on
n1=2;
n2=4;
n3=6;
n4=8;
n5=10;
beta=((T0*L^2)/E*I);

```

$\beta_1 = (E \cdot A_0 \cdot L^2) / E \cdot I;$
 $\beta_2 = \sqrt{\delta} / u;$
 $\beta_3 = \alpha \cdot \beta_1 \cdot \beta_2 \cdot \tau_0;$
 $\beta_4 = \alpha \cdot \beta_1 \cdot \beta_2 \cdot \tau_1;$
 $\beta_5 = (\alpha \cdot \beta_1 \cdot \tau_0);$
 $\beta_6 = (\alpha \cdot \beta_1 \cdot \tau_1);$
 $\beta_7 = \beta_1 / u;$
 $\beta_8 = \delta / L;$
 $\eta_1 = (C_1 + C_2 - \beta_4 \cdot (1 - 0.5 \cdot \gamma) - \beta_3 \cdot \gamma - \gamma_2 \cdot \beta_2 \cdot (1 - 0.5 \cdot \gamma) - \beta_4 \cdot (1 - 0.5 \cdot \gamma));$
 $\text{Eta}_1 = \eta_1 / (1 - \pi \cdot (2 \cdot (D_0 / (2 \cdot L)) - \delta) \cdot \beta_8 \cdot \beta_2);$
 $\eta_2 = ((n^4 \cdot \pi^4) - (3 \cdot \sqrt{\delta} \cdot u \cdot \beta_2 - \beta_4 \cdot \gamma + \gamma_1 \cdot (1 - 0.5 \cdot \gamma)) + \beta_5 \cdot (1 - 0.5 \cdot \gamma)) \cdot (n^2 \cdot \pi^2) + K_b);$
 $\text{Eta}_2 = \eta_2 / (1 - \pi \cdot (2 \cdot (D_0 / (2 \cdot L)) - \delta) \cdot \beta_8 \cdot \beta_2);$
 $\alpha_1 = (\text{Eta}_1 / 2 + i \cdot \sqrt{(\text{Eta}_2 - \text{Eta}_1^2 / 4)});$
 $\alpha_2 = (\text{Eta}_1 / 2 - i \cdot \sqrt{(\text{Eta}_2 - \text{Eta}_1^2 / 4)});$
 $F_1 = (1 / (\alpha_1 \cdot \alpha_2));$
 $\eta_1 = (C_1 + C_2 - \beta_4 \cdot (1 - 0.5 \cdot \gamma) - \beta_3 \cdot \gamma - \gamma_2 \cdot \beta_2 \cdot (1 - 0.5 \cdot \gamma) - \beta_4 \cdot (1 - 0.5 \cdot \gamma));$
 $\text{Eta}_1 = \eta_1 / (1 - \pi \cdot (2 \cdot (D_0 / (2 \cdot L)) - \delta) \cdot \beta_8 \cdot \beta_2);$
 $\eta_2 = ((n^4 \cdot \pi^4) - (3 \cdot \sqrt{\delta} \cdot u \cdot \beta_2 - \beta_4 \cdot \gamma + \gamma_1 \cdot (1 - 0.5 \cdot \gamma)) + \beta_5 \cdot (1 - 0.5 \cdot \gamma)) \cdot (n^2 \cdot \pi^2) + K_b);$
 $\text{Eta}_2 = \eta_2 / (1 - \pi \cdot (2 \cdot (D_0 / (2 \cdot L)) - \delta) \cdot \beta_8 \cdot \beta_2);$
 $\alpha_1 = (\text{Eta}_1 / 2 + i \cdot \sqrt{(\text{Eta}_2 - \text{Eta}_1^2 / 4)});$
 $\alpha_2 = (\text{Eta}_1 / 2 - i \cdot \sqrt{(\text{Eta}_2 - \text{Eta}_1^2 / 4)});$
 $F_2 = (1 / (\alpha_1 \cdot \alpha_2));$
 $\eta_1 = (C_1 + C_2 - \beta_4 \cdot (1 - 0.5 \cdot \gamma) - \beta_3 \cdot \gamma - \gamma_2 \cdot \beta_2 \cdot (1 - 0.5 \cdot \gamma) - \beta_4 \cdot (1 - 0.5 \cdot \gamma));$
 $\text{Eta}_1 = \eta_1 / (1 - \pi \cdot (2 \cdot (D_0 / (2 \cdot L)) - \delta) \cdot \beta_8 \cdot \beta_2);$
 $\eta_2 = ((n^4 \cdot \pi^4) - (3 \cdot \sqrt{\delta} \cdot u \cdot \beta_2 - \beta_4 \cdot \gamma + \gamma_1 \cdot (1 - 0.5 \cdot \gamma)) + \beta_5 \cdot (1 - 0.5 \cdot \gamma)) \cdot (n^2 \cdot \pi^2) + K_b);$
 $\text{Eta}_2 = \eta_2 / (1 - \pi \cdot (2 \cdot (D_0 / (2 \cdot L)) - \delta) \cdot \beta_8 \cdot \beta_2);$
 $\alpha_1 = (\text{Eta}_1 / 2 + i \cdot \sqrt{(\text{Eta}_2 - \text{Eta}_1^2 / 4)});$
 $\alpha_2 = (\text{Eta}_1 / 2 - i \cdot \sqrt{(\text{Eta}_2 - \text{Eta}_1^2 / 4)});$
 $F_3 = (1 / (\alpha_1 \cdot \alpha_2));$
 $\eta_1 = (C_1 + C_2 - \beta_4 \cdot (1 - 0.5 \cdot \gamma) - \beta_3 \cdot \gamma - \gamma_2 \cdot \beta_2 \cdot (1 - 0.5 \cdot \gamma) - \beta_4 \cdot (1 - 0.5 \cdot \gamma));$
 $\text{Eta}_1 = \eta_1 / (1 - \pi \cdot (2 \cdot (D_0 / (2 \cdot L)) - \delta) \cdot \beta_8 \cdot \beta_2);$
 $\eta_2 = ((n^4 \cdot \pi^4) - (3 \cdot \sqrt{\delta} \cdot u \cdot \beta_2 - \beta_4 \cdot \gamma + \gamma_1 \cdot (1 - 0.5 \cdot \gamma)) + \beta_5 \cdot (1 - 0.5 \cdot \gamma)) \cdot (n^2 \cdot \pi^2) + K_b);$
 $\text{Eta}_2 = \eta_2 / (1 - \pi \cdot (2 \cdot (D_0 / (2 \cdot L)) - \delta) \cdot \beta_8 \cdot \beta_2);$
 $\alpha_1 = (\text{Eta}_1 / 2 + i \cdot \sqrt{(\text{Eta}_2 - \text{Eta}_1^2 / 4)});$
 $\alpha_2 = (\text{Eta}_1 / 2 - i \cdot \sqrt{(\text{Eta}_2 - \text{Eta}_1^2 / 4)});$
 $F_4 = (1 / (\alpha_1 \cdot \alpha_2));$
 $\eta_1 = (C_1 + C_2 - \beta_4 \cdot (1 - 0.5 \cdot \gamma) - \beta_3 \cdot \gamma - \gamma_2 \cdot \beta_2 \cdot (1 - 0.5 \cdot \gamma) - \beta_4 \cdot (1 - 0.5 \cdot \gamma));$
 $\text{Eta}_1 = \eta_1 / (1 - \pi \cdot (2 \cdot (D_0 / (2 \cdot L)) - \delta) \cdot \beta_8 \cdot \beta_2);$
 $\eta_2 = ((n^4 \cdot \pi^4) - (3 \cdot \sqrt{\delta} \cdot u \cdot \beta_2 - \beta_4 \cdot \gamma + \gamma_1 \cdot (1 - 0.5 \cdot \gamma)) + \beta_5 \cdot (1 - 0.5 \cdot \gamma)) \cdot (n^2 \cdot \pi^2) + K_b);$

```

Eta2=eta2/(1-pi*(2*(D0/(2*L))-delтта)*beta8*beta);
alpha1=(Eta1/2+i*sqrt(Eta2-Eta1.^2./4));
alpha2=(Eta1/2-i*sqrt(Eta2-Eta1.^2./4));
F5=(1./(alpha1.*alpha2));
YZ1=abs(((4/sqrt(3))*t./R1*alpha0.*((z^2-R1*z)*n1^2*pi^2*(1+(-1)^n1+1)*KK*F1*cos(n1*pi*x)))-3.1e-6*u2*z*t./R1^2);
YZ2=abs(((4/sqrt(3))*t./R1*alpha0.*((z^2-R1*z)*n2^2*pi^2*(1+(-1)^n2+1)*KK*F2*cos(n2*pi*x)))-3.1e-6*u2*z*t./R1^2);
YZ3=abs(((4/sqrt(3))*t./R1*alpha0.*((z^2-R1*z)*n3^2*pi^2*(1+(-1)^n3+1)*KK*F3*cos(n3*pi*x)))-3.1e-6*u2*z*t./R1^2);
YZ4=abs(((4/sqrt(3))*t./R1*alpha0.*((z^2-R1*z)*n4^2*pi^2*(1+(-1)^n4+1)*KK*F4*cos(n4*pi*x)))-3.1e-6*u2*z*t./R1^2);
YZ5=abs(((4/sqrt(3))*t./R1*alpha0.*((z^2-R1*z)*n5^2*pi^2*(1+(-1)^n5+1)*KK*F5*cos(n5*pi*x)))-3.1e-6*u2*z*t./R1^2);
figure(28),plot(t,YZ1,t,YZ2,'-v',t,YZ3,'-.',t,YZ4,'k--',t,YZ5,'b-*',t,YY1,'r-o')
legend('n=2','n=4','n=6','n=8','n=10','Barlow Equation')
grid on
n1=1;
t=0.01;
x=linspace(0,1,100);
YZ1=abs(((4/sqrt(3))*t./R1*alpha0.*((z^2-R1*z)*n1^2*pi^2*(1+(-1)^n1+1)*KK*F1*cos(n1*pi*x)))-3.1e-6*u2*z*t./R1^2);
Y1=abs((2/sqrt(3))*alpha0*((z^2+(D1/(2*L))*z)*n1^2*pi^2*(1+(-1)^n1+1)*KK*F1*cos(n1*pi*x))-3.1e-6*z*u2)*(t/R1);
figure(29),plot(x,YZ1,'r-o',x,Y1,'b-*')
legend('Computation with Barlow Equation', 'Computation with Staat and Duckhovic Equation')
grid on
n1=1;
n2=3;
n3=5;
beta=((T0*L^2)/E*I);
beta1=((E*A0*L^2)/E*I);
beta2=sqrt(delta)./u;
beta3=alpha*beta1*beta2*teta0;
beta4=alpha*beta1*beta2*teta1;
beta5=(alpha*beta1*teta0);
beta6=(alpha*beta1*teta1);
beta7=beta1./u;
beta8=delta0/L;

```

$\eta_1 = (C_1 + C_2 - \beta_4 * (1 - 0.5 * \gamma) - \beta_3 * \gamma - \gamma_2 * \beta_2 * (1 - 0.5 * \gamma) - \beta_4 * (1 - 0.5 * \gamma));$
 $\text{Eta1} = \eta_1 / (1 - \pi * (2 * (D_0 / (2 * L)) - \text{del}t) * \beta_8 * \beta);$
 $\eta_2 = ((n^4 * \pi^4) - ((3 * \sqrt{\text{delta}} * u.^2 - \beta + \gamma_1 * (1 - 0.5 * \gamma)) + \beta_5 * (1 - 0.5 * \gamma)) * (n^2 * \pi^2) + K_b);$
 $\text{Eta2} = \eta_2 / (1 - \pi * (2 * (D_0 / (2 * L)) - \text{del}t) * \beta_8 * \beta);$
 $\alpha_1 = (\text{Eta1} / 2 + i * \sqrt{\text{Eta2} - \text{Eta1}.^2 / 4});$
 $\alpha_2 = (\text{Eta1} / 2 - i * \sqrt{\text{Eta2} - \text{Eta1}.^2 / 4});$
 $F_1 = (1 / (\alpha_1 * \alpha_2));$
 $\eta_1 = (C_1 + C_2 - \beta_4 * (1 - 0.5 * \gamma) - \beta_3 * \gamma - \gamma_2 * \beta_2 * (1 - 0.5 * \gamma) - \beta_4 * (1 - 0.5 * \gamma));$
 $\text{Eta1} = \eta_1 / (1 - \pi * (2 * (D_0 / (2 * L)) - \text{del}t) * \beta_8 * \beta);$
 $\eta_2 = ((n^4 * \pi^4) - ((3 * \sqrt{\text{delta}} * u.^2 - \beta + \gamma_1 * (1 - 0.5 * \gamma)) + \beta_5 * (1 - 0.5 * \gamma)) * (n^2 * \pi^2) + K_b);$
 $\text{Eta2} = \eta_2 / (1 - \pi * (2 * (D_0 / (2 * L)) - \text{del}t) * \beta_8 * \beta);$
 $\alpha_1 = (\text{Eta1} / 2 + i * \sqrt{\text{Eta2} - \text{Eta1}.^2 / 4});$
 $\alpha_2 = (\text{Eta1} / 2 - i * \sqrt{\text{Eta2} - \text{Eta1}.^2 / 4});$
 $F_2 = (1 / (\alpha_1 * \alpha_2));$
 $\eta_1 = (C_1 + C_2 - \beta_4 * (1 - 0.5 * \gamma) - \beta_3 * \gamma - \gamma_2 * \beta_2 * (1 - 0.5 * \gamma) - \beta_4 * (1 - 0.5 * \gamma));$
 $\text{Eta1} = \eta_1 / (1 - \pi * (2 * (D_0 / (2 * L)) - \text{del}t) * \beta_8 * \beta);$
 $\eta_2 = ((n^4 * \pi^4) - ((3 * \sqrt{\text{delta}} * u.^2 - \beta + \gamma_1 * (1 - 0.5 * \gamma)) + \beta_5 * (1 - 0.5 * \gamma)) * (n^2 * \pi^2) + K_b);$
 $\text{Eta2} = \eta_2 / (1 - \pi * (2 * (D_0 / (2 * L)) - \text{del}t) * \beta_8 * \beta);$
 $\alpha_1 = (\text{Eta1} / 2 + i * \sqrt{\text{Eta2} - \text{Eta1}.^2 / 4});$
 $\alpha_2 = (\text{Eta1} / 2 - i * \sqrt{\text{Eta2} - \text{Eta1}.^2 / 4});$
 $F_3 = (1 / (\alpha_1 * \alpha_2));$
 $\eta_1 = (C_1 + C_2 - \beta_4 * (1 - 0.5 * \gamma) - \beta_3 * \gamma - \gamma_2 * \beta_2 * (1 - 0.5 * \gamma) - \beta_4 * (1 - 0.5 * \gamma));$
 $\text{Eta1} = \eta_1 / (1 - \pi * (2 * (D_0 / (2 * L)) - \text{del}t) * \beta_8 * \beta);$
 $\eta_2 = ((n^4 * \pi^4) - ((3 * \sqrt{\text{delta}} * u.^2 - \beta + \gamma_1 * (1 - 0.5 * \gamma)) + \beta_5 * (1 - 0.5 * \gamma)) * (n^2 * \pi^2) + K_b);$
 $\text{Eta2} = \eta_2 / (1 - \pi * (2 * (D_0 / (2 * L)) - \text{del}t) * \beta_8 * \beta);$
 $\alpha_1 = (\text{Eta1} / 2 + i * \sqrt{\text{Eta2} - \text{Eta1}.^2 / 4});$
 $\alpha_2 = (\text{Eta1} / 2 - i * \sqrt{\text{Eta2} - \text{Eta1}.^2 / 4});$
 $F_4 = (1 / (\alpha_1 * \alpha_2));$
 $\eta_1 = (C_1 + C_2 - \beta_4 * (1 - 0.5 * \gamma) - \beta_3 * \gamma - \gamma_2 * \beta_2 * (1 - 0.5 * \gamma) - \beta_4 * (1 - 0.5 * \gamma));$
 $\text{Eta1} = \eta_1 / (1 - \pi * (2 * (D_0 / (2 * L)) - \text{del}t) * \beta_8 * \beta);$
 $\eta_2 = ((n^4 * \pi^4) - ((3 * \sqrt{\text{delta}} * u.^2 - \beta + \gamma_1 * (1 - 0.5 * \gamma)) + \beta_5 * (1 - 0.5 * \gamma)) * (n^2 * \pi^2) + K_b);$
 $\text{Eta2} = \eta_2 / (1 - \pi * (2 * (D_0 / (2 * L)) - \text{del}t) * \beta_8 * \beta);$
 $\alpha_1 = (\text{Eta1} / 2 + i * \sqrt{\text{Eta2} - \text{Eta1}.^2 / 4});$
 $\alpha_2 = (\text{Eta1} / 2 - i * \sqrt{\text{Eta2} - \text{Eta1}.^2 / 4});$
 $F_5 = (1 / (\alpha_1 * \alpha_2));$
 $\text{YZ1} = \text{abs}(((4 / \sqrt{3}) * t / R_1 * \alpha_0 * ((z^2 - R_1 * z) * n_1^2 * \pi^2 * (1 + (-1)^{n_1 + 1}) * K * F_1 * \cos(n_1 * \pi * x))) - (3.1e-6 * u^2 * z * t / R_1^2));$
 $\text{YZ2} = \text{abs}(((4 / \sqrt{3}) * t / R_1 * \alpha_0 * ((z^2 - R_1 * z) * n_2^2 * \pi^2 * (1 + (-1)^{n_2 + 1}) * K * F_2 * \cos(n_2 * \pi * x))) - (3.1e-6 * u^2 * z * t / R_1^2));$

```

YZ3=abs(((4/sqrt(3))*t./R1*alpha0.*((z^2-R1*z)*n3^2*pi^2*(1+(-1)^n3+1)*KK*F3*cos(n3*pi*x)))-(3.1e-
6*u2*z*t./R1^2));
YZ4=abs(((4/sqrt(3))*t./R1*alpha0.*((z^2-R1*z)*n4^2*pi^2*(1+(-1)^n4+1)*KK*F4*cos(n4*pi*x)))-(3.1e-
6*u2*z*t./R1^2));
YZ5=abs(((4/sqrt(3))*t./R1*alpha0.*((z^2-R1*z)*n5^2*pi^2*(1+(-1)^n5+1)*KK*F5*cos(n5*pi*x)))-(3.1e-
6*u2*z*t./R1^2));
figure(30),plot(x,YZ1,x,YZ2,'-v',x,YZ3,'r-')
legend('n=1','n=3','n=5')
grid on
n1=2;
n2=4;
n3=6;
beta=((T0*L^2)/E*I);
beta1=((E*A0*L^2)/E*I);
beta2=sqrt(delta)./u;
beta3=alpha*beta1*beta2*teta0;
beta4=alpha*beta1*beta2*teta1;
beta5=(alpha*beta1*teta0);
beta6=(alpha*beta1*teta1);
beta7=beta1./u;
beta8=delta0/L;
eta1=(C1+C2-beta4*(1-0.5*gama)-beta3*gama-gama2*beta2*(1-0.5*gama)-beta4*(1-0.5*gama));
Eta1=eta1/(1-pi*(2*(D0/(2*L))-delтта)*beta8*beta);
eta2=((n^4*pi^4)-((3*sqrt(delta)*u.^2-beta+gama1*(1-0.5*gama))+beta5*(1-0.5*gama))*(n^2*pi^2) + Kb);
Eta2=eta2/(1-pi*(2*(D0/(2*L))-delтта)*beta8*beta);
alpha1=(Eta1/2+i*sqrt(Eta2-Eta1.^2./4));
alpha2=(Eta1/2-i*sqrt(Eta2-Eta1.^2./4));
F1=(1./(alpha1.*alpha2));
eta1=(C1+C2-beta4*(1-0.5*gama)-beta3*gama-gama2*beta2*(1-0.5*gama)-beta4*(1-0.5*gama));
Eta1=eta1/(1-pi*(2*(D0/(2*L))-delтта)*beta8*beta);
eta2=((n^4*pi^4)-((3*sqrt(delta)*u.^2-beta+gama1*(1-0.5*gama))+beta5*(1-0.5*gama))*(n^2*pi^2) + Kb);
Eta2=eta2/(1-pi*(2*(D0/(2*L))-delтта)*beta8*beta);
alpha1=(Eta1/2+i*sqrt(Eta2-Eta1.^2./4));
alpha2=(Eta1/2-i*sqrt(Eta2-Eta1.^2./4));
F2=(1./(alpha1.*alpha2));
eta1=(C1+C2-beta4*(1-0.5*gama)-beta3*gama-gama2*beta2*(1-0.5*gama)-beta4*(1-0.5*gama));
Eta1=eta1/(1-pi*(2*(D0/(2*L))-delтта)*beta8*beta);
eta2=((n^4*pi^4)-((3*sqrt(delta)*u.^2-beta+gama1*(1-0.5*gama))+beta5*(1-0.5*gama))*(n^2*pi^2) + Kb);
Eta2=eta2/(1-pi*(2*(D0/(2*L))-delтта)*beta8*beta);

```

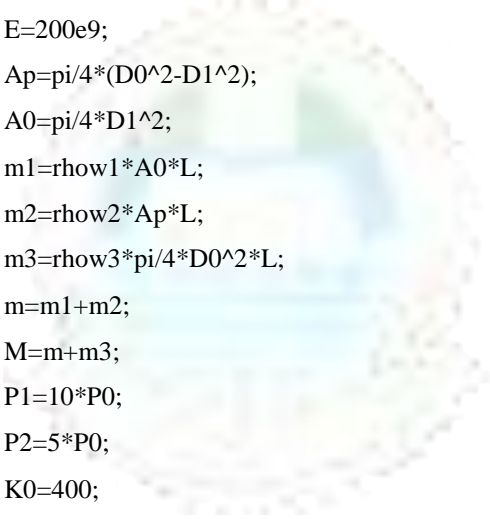
```

alpha1=(Eta1/2+i*sqrt(Eta2-Eta1.^2./4));
alpha2=(Eta1/2-i*sqrt(Eta2-Eta1.^2./4));
F3=(1./(alpha1.*alpha2));
eta1=(C1+C2-beta4*(1-0.5*gama)-beta3*gama-gama2*beta2*(1-0.5*gama)-beta4*(1-0.5*gama));
Eta1=eta1/(1-pi*(2*(D0/(2*L))-delтта)*beta8*beta);
eta2=((n^4*pi^4)-((3*sqrt(delta)*u.^2-beta+gama1*(1-0.5*gama))+beta5*(1-0.5*gama))*(n^2*pi^2) + Kb);
Eta2=eta2/(1-pi*(2*(D0/(2*L))-delтта)*beta8*beta);
alpha1=(Eta1/2+i*sqrt(Eta2-Eta1.^2./4));
alpha2=(Eta1/2-i*sqrt(Eta2-Eta1.^2./4));
F4=(1./(alpha1.*alpha2));
eta1=(C1+C2-beta4*(1-0.5*gama)-beta3*gama-gama2*beta2*(1-0.5*gama)-beta4*(1-0.5*gama));
Eta1=eta1/(1-pi*(2*(D0/(2*L))-delтта)*beta8*beta);
eta2=((n^4*pi^4)-((3*sqrt(delta)*u.^2-beta+gama1*(1-0.5*gama))+beta5*(1-0.5*gama))*(n^2*pi^2) + Kb);
Eta2=eta2/(1-pi*(2*(D0/(2*L))-delтта)*beta8*beta);
alpha1=(Eta1/2+i*sqrt(Eta2-Eta1.^2./4));
alpha2=(Eta1/2-i*sqrt(Eta2-Eta1.^2./4));
F5=(1./(alpha1.*alpha2));
YZ1=abs(((4/sqrt(3))*t./R1*alpha0.*((z^2-R1*z)*n1^2*pi^2*(1+(-1)^n1+1)*KK*F1*cos(n1*pi*x)))-(3.1e-6*u2*z*t./R1^2));
YZ2=abs(((4/sqrt(3))*t./R1*alpha0.*((z^2-R1*z)*n2^2*pi^2*(1+(-1)^n2+1)*KK*F2*cos(n2*pi*x)))-(3.1e-6*u2*z*t./R1^2));
YZ3=abs(((4/sqrt(3))*t./R1*alpha0.*((z^2-R1*z)*n3^2*pi^2*(1+(-1)^n3+1)*KK*F3*cos(n3*pi*x)))-(3.1e-6*u2*z*t./R1^2));
YZ4=abs(((4/sqrt(3))*t./R1*alpha0.*((z^2-R1*z)*n4^2*pi^2*(1+(-1)^n4+1)*KK*F4*cos(n4*pi*x)))-(3.1e-6*u2*z*t./R1^2));
YZ5=abs(((4/sqrt(3))*t./R1*alpha0.*((z^2-R1*z)*n5^2*pi^2*(1+(-1)^n5+1)*KK*F5*cos(n5*pi*x)))-(3.1e-6*u2*z*t./R1^2));
figure(31),plot(x,YZ1,x,YZ2,'-v',x,YZ3,'r-*')
legend('n=2','n=4','n=6')
grid on

```

D.2 Matlab Program for Pipe Partially/Fully Buried on the Seabed (Chapter 4)

```
P=1.5e7;
P0=1.25e4;
T0=5e8;
L=6;
h0=1500;
c1=1;
rhow1=977;
rhow2=7850;
rhow3=980;
c2=5;
D0=0.4064;
D1=0.394;
E=200e9;
Ap=pi/4*(D0^2-D1^2);
A0=pi/4*D1^2;
m1=rhow1*A0*L;
m2=rhow2*Ap*L;
m3=rhow3*pi/4*D0^2*L;
m=m1+m2;
M=m+m3;
P1=10*P0;
P2=5*P0;
K0=400;
I=1.561*10^-4;
teta0=110;
teta1=10;
alpha=1.7e-5;
u=5;
delta=m1/m;
delta0=m3/M;
beta=((T0*L^2)/E*I);
beta1=((E*A0*L^2)/E*I);
beta2=sqrt(delta)/u;
beta3=alpha*beta1*beta2*teta0;
beta4=alpha*beta1*beta2*teta1;
beta5=(alpha*beta1*teta0);
beta6=(alpha*beta1*teta1);
```

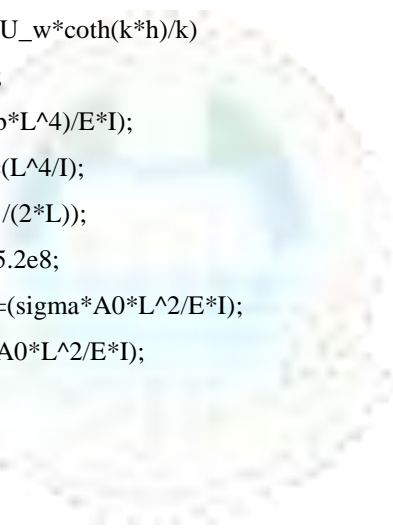


UNIVERSITY
OF LAGOS

```

U=3;
beta7=beta1/u;
beta8=delta0/L;
C1=(c1*L^2/sqrt(m*E*I));
C2=(c2*L^2/sqrt(m*E*I));
g0=9.8;
g=M*g0*L^3/E*I;
gama=0.2;
gama1=(P1*A0*L^2/E*I);
gama2=((P1-P2)*A0*L^2/E*I);
rhow=1;
U_w=3;
k=1;
h=h0/L;
betta=(-U_w*coth(k*h)/k)
kb=8e6;
Kb=((kb*L^4)/E*I);
alpha0=(L^4/I);
R2=(D1/(2*L));
sigma=5.2e8;
sigma0=(sigma*A0*L^2/E*I);
Pb=(P*A0*L^2/E*I);
r1=0.2;
n3=1;
z=1;
u=0;
u1=.2;
u2=.4;
u3=.6;
u4=.8;
u5=10;
deltt1=.5;
delta=.5;
t=1;
eta1=(C1+C2-beta4*(1-0.5*gama)-beta3*gama-gama2*beta2*(1-0.5*gama)-beta4*(1-0.5*gama));
Eta1=eta1./([1-pi*([(D0/L)-deltt1]])*(beta8*betta));
eta2=[((n3^4*pi^4)-((3*sqrt(delta)*u.^2-beta+gama1*(1-0.5*gama))+beta5*(1-0.5*gama))*(n3^2*pi^2) + Kb)];
Eta2=eta2./([1-pi*([(D0/L)-deltt1]])*(beta8*betta));
alpha1=[(Eta1./2+i*sqrt(Eta2-Eta1.^2./4))];

```



UNIVERSITY
OF LAGOS

```

alpha2=[(Eta1./2-i*sqrt(Eta2-Eta1.^2./4))];
H31=(1./(alpha1.*alpha2));
HH31=((alpha1*exp(-alpha2*t))-(alpha2*exp(-alpha1*t)));
F3=(1./((alpha1.*alpha2)).*(alpha2-alpha1))
K1=((pi*[(D0/L)-delтта1]).*([(beta8*g*(h/L))-((0.2^2*alpha0*0.03*delтта1*u1)/(2*0.02))]);
K2=((pi*[(D0/L)-delтта1]).*([(beta8*g*(h/L))-((0.2^2*alpha0*0.03*delтта1*u2)/(2*0.02))]);
K3=((pi*[(D0/L)-delтта1]).*([(beta8*g*(h/L))-((0.2^2*alpha0*0.03*delтта1*u3)/(2*0.02))]);
K4=((pi*[(D0/L)-delтта1]).*([(beta8*g*(h/L))-((0.2^2*alpha0*0.03*delтта1*u4)/(2*0.02))]);
K1=K1./([1-pi*([(D0/L)-delтта1])*(beta8*beta));
KK2=K2./([1-pi*([(D0/L)-delтта1])*(beta8*beta));
KK3=K3./([1-pi*([(D0/L)-delтта1])*(beta8*beta));
KK4=K4./([1-pi*([(D0/L)-delтта1])*(beta8*beta));
tau1=-3.1e-6*z*u;
tau2=-3.1e-6*z*u;
tau3=-3.1e-6*z*u;
tau4=-3.1e-6*z*u;
x=linspace(0,1,100);
g=(r1/R2);
H=(g-(1/2*g^2)+(1/3*g^3));
Y1=abs((-2/sqrt(3)*H*((alpha0/2)*(z^2-R2*z)*KK1.*F3)*(24*x-12)-(z/R2)*tau1));
Y2=abs((-2/sqrt(3)*H*((alpha0/2)*(z^2-R2*z)*KK2.*F3)*(24*x-12)-(z/R2)*tau2));
Y3=abs((-2/sqrt(3)*H*((alpha0/2)*(z^2-R2*z)*KK3.*F3)*(24*x-12)-(z/R2)*tau3));
Y4=abs((-2/sqrt(3)*H*((alpha0/2)*(z^2-R2*z)*KK4.*F3)*(24*x-12)-(z/R2)*tau4));
YY1=1+Y1./sigma0;
YY2=1+Y2./sigma0;
YY3=1+Y3./sigma0;
YY4=1+Y4./sigma0;
figure(1),plot(x,YY1,'go-',x,YY2,'o-',x,YY3,'-',x,YY4,'>-m')
grid on
legend('u=0.2','u=0.4','u=0.6','u=0.8')
figure(2),plot(YY1,x,YY2,x,YY3,x,YY4,x)
grid on
legend('u=0.2','u=0.4','u=0.6','u=0.8')
D0=0.4064;
delтта1=0.25;
eta1=(C1+C2-beta4*(1-0.5*gama)-beta3*gama-gama2*beta2*(1-0.5*gama)-beta4*(1-0.5*gama));
Eta1=eta1./([1-pi*([(D0/L)-delтта1])*(beta8*beta));
eta2=[((n3^4*pi^4)-((3*sqrt(delta)*u.^2-beta+gama1*(1-0.5*gama))+beta5*(1-0.5*gama))*(n3^2*pi^2)+Kb)];
Eta2=eta2./([1-pi*([(D0/L)-delтта1])*(beta8*beta));

```

$\alpha_1 = [(\text{Eta}_1 / 2 + i \sqrt{\text{Eta}_2 - \text{Eta}_1.^2 / 4})];$
 $\alpha_2 = [(\text{Eta}_1 / 2 - i \sqrt{\text{Eta}_2 - \text{Eta}_1.^2 / 4})];$
 $H_{31} = (1 / (\alpha_1 * \alpha_2));$
 $HH_{31} = ((\alpha_1 * \exp(-\alpha_2 * t)) - (\alpha_2 * \exp(-\alpha_1 * t)));$
 $FF_{31} = (1 / ((\alpha_1 * \alpha_2)) * (\alpha_2 - \alpha_1));$
 $\text{del}t_2 = 0.50;$
 $\text{eta}_1 = (C_1 + C_2 - \beta_4 * (1 - 0.5 * \gamma) - \beta_3 * \gamma - \gamma_2 * \beta_2 * (1 - 0.5 * \gamma) - \beta_4 * (1 - 0.5 * \gamma));$
 $\text{Eta}_1 = \text{eta}_1 / ([1 - \pi * ((D_0 / L) - \text{del}t_2)]) * (\beta_8 * \beta);$
 $\text{eta}_2 = [((n_3^4 * \pi^4) - (3 * \sqrt{\text{delta}} * u.^2 - \beta + \gamma_1 * (1 - 0.5 * \gamma)) + \beta_5 * (1 - 0.5 * \gamma)) * (n_3^2 * \pi^2 + K_b)];$
 $\text{Eta}_2 = \text{eta}_2 / ([1 - \pi * ((D_0 / L) - \text{del}t_2)]) * (\beta_8 * \beta);$
 $\alpha_1 = [(\text{Eta}_1 / 2 + i \sqrt{\text{Eta}_2 - \text{Eta}_1.^2 / 4})];$
 $\alpha_2 = [(\text{Eta}_1 / 2 - i \sqrt{\text{Eta}_2 - \text{Eta}_1.^2 / 4})];$
 $H_{31} = (1 / (\alpha_1 * \alpha_2));$
 $HH_{31} = ((\alpha_1 * \exp(-\alpha_2 * t)) - (\alpha_2 * \exp(-\alpha_1 * t)));$
 $FF_{32} = (1 / ((\alpha_1 * \alpha_2)) * (\alpha_2 - \alpha_1));$
 $\text{del}t_3 = 0.75;$
 $\text{eta}_1 = (C_1 + C_2 - \beta_4 * (1 - 0.5 * \gamma) - \beta_3 * \gamma - \gamma_2 * \beta_2 * (1 - 0.5 * \gamma) - \beta_4 * (1 - 0.5 * \gamma));$
 $\text{Eta}_1 = \text{eta}_1 / ([1 - \pi * ((D_0 / L) - \text{del}t_3)]) * (\beta_8 * \beta);$
 $\text{eta}_2 = [((n_3^4 * \pi^4) - (3 * \sqrt{\text{delta}} * u.^2 - \beta + \gamma_1 * (1 - 0.5 * \gamma)) + \beta_5 * (1 - 0.5 * \gamma)) * (n_3^2 * \pi^2 + K_b)];$
 $\text{Eta}_2 = \text{eta}_2 / ([1 - \pi * ((D_0 / L) - \text{del}t_3)]) * (\beta_8 * \beta);$
 $\alpha_1 = [(\text{Eta}_1 / 2 + i \sqrt{\text{Eta}_2 - \text{Eta}_1.^2 / 4})];$
 $\alpha_2 = [(\text{Eta}_1 / 2 - i \sqrt{\text{Eta}_2 - \text{Eta}_1.^2 / 4})];$
 $H_{31} = (1 / (\alpha_1 * \alpha_2));$
 $HH_{31} = ((\alpha_1 * \exp(-\alpha_2 * t)) - (\alpha_2 * \exp(-\alpha_1 * t)));$
 $FF_{33} = (1 / ((\alpha_1 * \alpha_2)) * (\alpha_2 - \alpha_1));$
 $\text{del}t_4 = 0.999;$
 $\text{eta}_1 = (C_1 + C_2 - \beta_4 * (1 - 0.5 * \gamma) - \beta_3 * \gamma - \gamma_2 * \beta_2 * (1 - 0.5 * \gamma) - \beta_4 * (1 - 0.5 * \gamma));$
 $\text{Eta}_1 = \text{eta}_1 / ([1 - \pi * ((D_0 / L) - \text{del}t_4)]) * (\beta_8 * \beta);$
 $\text{eta}_2 = [((n_3^4 * \pi^4) - (3 * \sqrt{\text{delta}} * u.^2 - \beta + \gamma_1 * (1 - 0.5 * \gamma)) + \beta_5 * (1 - 0.5 * \gamma)) * (n_3^2 * \pi^2 + K_b)];$
 $\text{Eta}_2 = \text{eta}_2 / ([1 - \pi * ((D_0 / L) - \text{del}t_4)]) * (\beta_8 * \beta);$
 $\alpha_1 = [(\text{Eta}_1 / 2 + i \sqrt{\text{Eta}_2 - \text{Eta}_1.^2 / 4})];$
 $\alpha_2 = [(\text{Eta}_1 / 2 - i \sqrt{\text{Eta}_2 - \text{Eta}_1.^2 / 4})];$
 $H_{31} = (1 / (\alpha_1 * \alpha_2));$
 $HH_{31} = ((\alpha_1 * \exp(-\alpha_2 * t)) - (\alpha_2 * \exp(-\alpha_1 * t)));$
 $FF_{33} = (1 / ((\alpha_1 * \alpha_2)) * (\alpha_2 - \alpha_1));$
 $K_1 = (\pi * [(D_0 / L) - \text{del}t_1]) * [(\beta_8 * g * (h / L)) - ((0.2^2 * \alpha_0 * 0.03 * \text{del}t_1 * u_1) / (2 * 0.02))];$
 $K_2 = (\pi * [(D_0 / L) - \text{del}t_2]) * [(\beta_8 * g * (h / L)) - ((0.2^2 * \alpha_0 * 0.03 * \text{del}t_2 * u_2) / (2 * 0.02))];$
 $K_3 = (\pi * [(D_0 / L) - \text{del}t_3]) * [(\beta_8 * g * (h / L)) - ((0.2^2 * \alpha_0 * 0.03 * \text{del}t_3 * u_3) / (2 * 0.02))];$
 $K_4 = (\pi * [(D_0 / L) - \text{del}t_4]) * [(\beta_8 * g * (h / L)) - ((0.2^2 * \alpha_0 * 0.03 * \text{del}t_4 * u_4) / (2 * 0.02))];$

```

KK1=K1./([1-pi*([(D0/L)-deltta1]])*(beta8*beta));
KK2=K2./([1-pi*([(D0/L)-deltta2]])*(beta8*beta));
KK3=K3./([1-pi*([(D0/L)-deltta3]])*(beta8*beta));
KK4=K4./([1-pi*([(D0/L)-deltta4]])*(beta8*beta));
tau1=-3.1e-6*z*u;
tau2=-3.1e-6*z*u;
tau3=-3.1e-6*z*u;
tau4=-3.1e-6*z*u;
x=linspace(0,1,100);
g=(r1/R2);
H=(g-(1/2*g^2)+(1/3*g^3));
Y1=abs((-2/sqrt(3)*H*((alpha0/2)*(z^2-R2*z)*KK1.*F3)*(24*x-12)-(z/R2)*tau1));
Y2=abs((-2/sqrt(3)*H*((alpha0/2)*(z^2-R2*z)*KK2.*F3)*(24*x-12)-(z/R2)*tau2));
Y3=abs((-2/sqrt(3)*H*((alpha0/2)*(z^2-R2*z)*KK3.*F3)*(24*x-12)-(z/R2)*tau3));
Y4=abs((-2/sqrt(3)*H*((alpha0/2)*(z^2-R2*z)*KK4.*F3)*(24*x-12)-(z/R2)*tau3));
YY1=1+Y1./sigma0;
YY2=1+Y2./sigma0;
YY3=1+Y3./sigma0;
YY4=1+Y4./sigma0;
figure(3),plot(x,YY1,'go-',x,YY2,'o-',x,YY3,'-',x,YY4,'mo-.')
grid on
legend('\delta_s=0.25D_0','\delta_s=0.50D_0','\delta_s=0.75D_0','\delta_s=D_0')
U1=.2;
U2=.4;
U3=.6;
U4=.8;
deltta1=.5;
deltta=.5;
eta1=(C1+C2-beta4*(1-0.5*gama)-beta3*gama-gama2*beta2*(1-0.5*gama)-beta4*(1-0.5*gama));
Eta1=eta1./([1-pi*([(D0/L)-deltta1]])*(beta8*beta));
eta2=[((n3^4*pi^4)-((3*sqrt(delta)*U1.^2-beta+gama1*(1-0.5*gama))+beta5*(1-0.5*gama))*(n3^2*pi^2) + Kb)];
Eta2=eta2./([1-pi*([(D0/L)-deltta1]])*(beta8*beta));
alpha1=[(Eta1./2+i*sqrt(Eta2-Eta1.^2./4))];
alpha2=[(Eta1./2-i*sqrt(Eta2-Eta1.^2./4))];
H31=(1./(alpha1.*alpha2));
HH31=((alpha1*exp(-alpha2*t))-alpha2*exp(-alpha1*t));
FF31=(1./((alpha1.*alpha2)).*(alpha2-alpha1))
U1=U2;

```

$$\text{eta1}=(C1+C2-\text{beta4}*(1-0.5*\text{gama})-\text{beta3}*\text{gama}-\text{gama2}*\text{beta2}*(1-0.5*\text{gama})-\text{beta4}*(1-0.5*\text{gama}));$$

$$\text{Eta1}=\text{eta1}/([1-\text{pi}*((D0/L)-\text{del}t\text{ta1})])*(\text{beta8}*\text{beta});$$

$$\text{eta2}=[((n3^4*\text{pi}^4)-((3*\text{sqrt}(\text{delta})*U1.^2-\text{beta}+\text{gama1}*(1-0.5*\text{gama}))+\text{beta5}*(1-0.5*\text{gama}))*(\text{n3}^2*\text{pi}^2) + \text{Kb})];$$

$$\text{Eta2}=\text{eta2}/([1-\text{pi}*((D0/L)-\text{del}t\text{ta1})])*(\text{beta8}*\text{beta});$$

$$\text{alpha1}=[(\text{Eta1}/2+i*\text{sqrt}(\text{Eta2}-\text{Eta1}.^2./4))];$$

$$\text{alpha2}=[(\text{Eta1}/2-i*\text{sqrt}(\text{Eta2}-\text{Eta1}.^2./4))];$$

$$\text{H31}=(1./(\text{alpha1}.*\text{alpha2}));$$

$$\text{HH31}=(\text{alpha1}*\text{exp}(-\text{alpha2}*t)-(\text{alpha2}*\text{exp}(-\text{alpha1}*t)));$$

$$\text{FF32}=(1./((\text{alpha1}.*\text{alpha2})).*(\text{alpha2}-\text{alpha1}))$$

$$U1=U3;$$

$$\text{eta1}=(C1+C2-\text{beta4}*(1-0.5*\text{gama})-\text{beta3}*\text{gama}-\text{gama2}*\text{beta2}*(1-0.5*\text{gama})-\text{beta4}*(1-0.5*\text{gama}));$$

$$\text{Eta1}=\text{eta1}/([1-\text{pi}*((D0/L)-\text{del}t\text{ta1})])*(\text{beta8}*\text{beta});$$

$$\text{eta2}=[((n3^4*\text{pi}^4)-((3*\text{sqrt}(\text{delta})*U1.^2-\text{beta}+\text{gama1}*(1-0.5*\text{gama}))+\text{beta5}*(1-0.5*\text{gama}))*(\text{n3}^2*\text{pi}^2) + \text{Kb})];$$

$$\text{Eta2}=\text{eta2}/([1-\text{pi}*((D0/L)-\text{del}t\text{ta1})])*(\text{beta8}*\text{beta});$$

$$\text{alpha1}=[(\text{Eta1}/2+i*\text{sqrt}(\text{Eta2}-\text{Eta1}.^2./4))];$$

$$\text{alpha2}=[(\text{Eta1}/2-i*\text{sqrt}(\text{Eta2}-\text{Eta1}.^2./4))];$$

$$\text{H31}=(1./(\text{alpha1}.*\text{alpha2}));$$

$$\text{HH31}=(\text{alpha1}*\text{exp}(-\text{alpha2}*t)-(\text{alpha2}*\text{exp}(-\text{alpha1}*t)));$$

$$\text{FF33}=(1./((\text{alpha1}.*\text{alpha2})).*(\text{alpha2}-\text{alpha1}));$$

$$U1=U4;$$

$$\text{eta1}=(C1+C2-\text{beta4}*(1-0.5*\text{gama})-\text{beta3}*\text{gama}-\text{gama2}*\text{beta2}*(1-0.5*\text{gama})-\text{beta4}*(1-0.5*\text{gama}));$$

$$\text{Eta1}=\text{eta1}/([1-\text{pi}*((D0/L)-\text{del}t\text{ta1})])*(\text{beta8}*\text{beta});$$

$$\text{eta2}=[((n3^4*\text{pi}^4)-((3*\text{sqrt}(\text{delta})*U1.^2-\text{beta}+\text{gama1}*(1-0.5*\text{gama}))+\text{beta5}*(1-0.5*\text{gama}))*(\text{n3}^2*\text{pi}^2) + \text{Kb})];$$

$$\text{Eta2}=\text{eta2}/([1-\text{pi}*((D0/L)-\text{del}t\text{ta1})])*(\text{beta8}*\text{beta});$$

$$\text{alpha1}=[(\text{Eta1}/2+i*\text{sqrt}(\text{Eta2}-\text{Eta1}.^2./4))];$$

$$\text{alpha2}=[(\text{Eta1}/2-i*\text{sqrt}(\text{Eta2}-\text{Eta1}.^2./4))];$$

$$\text{H31}=(1./(\text{alpha1}.*\text{alpha2}));$$

$$\text{HH31}=(\text{alpha1}*\text{exp}(-\text{alpha2}*t)-(\text{alpha2}*\text{exp}(-\text{alpha1}*t)));$$

$$\text{FF34}=(1./((\text{alpha1}.*\text{alpha2})).*(\text{alpha2}-\text{alpha1}))$$

$$u1=5;$$

$$K1=((\text{pi}*((D0/L)-\text{del}t\text{ta1})).*([\text{beta8}*\text{g}*(\text{h}/L)-((0.2^2*\text{alpha0}*\text{beta8}*\text{del}t\text{ta1})*u1)/(2*0.02)]));$$

$$K2=((\text{pi}*((D0/L)-\text{del}t\text{ta1})).*([\text{beta8}*\text{g}*(\text{h}/L)-((0.2^2*\text{alpha0}*\text{beta8}*\text{del}t\text{ta1})*u1)/(2*0.02)]));$$

$$K3=((\text{pi}*((D0/L)-\text{del}t\text{ta1})).*([\text{beta8}*\text{g}*(\text{h}/L)-((0.2^2*\text{alpha0}*\text{beta8}*\text{del}t\text{ta1})*u1)/(2*0.02)]));$$

$$K4=((\text{pi}*((D0/L)-\text{del}t\text{ta1})).*([\text{beta8}*\text{g}*(\text{h}/L)-((0.2^2*\text{alpha0}*\text{beta8}*\text{del}t\text{ta1})*u1)/(2*0.02)]));$$

$$\text{KK1}=K1./([1-\text{pi}*((D0/L)-\text{del}t\text{ta1})])*(\text{beta8}*\text{beta});$$

$$\text{KK2}=K2./([1-\text{pi}*((D0/L)-\text{del}t\text{ta1})])*(\text{beta8}*\text{beta});$$

$$\text{KK3}=K3./([1-\text{pi}*((D0/L)-\text{del}t\text{ta1})])*(\text{beta8}*\text{beta});$$

$$\text{KK4}=K4./([1-\text{pi}*((D0/L)-\text{del}t\text{ta1})])*(\text{beta8}*\text{beta});$$

$$\text{tau1}=-3.1\text{e-}6*\text{z}*U1;$$

```

tau2=-3.1e-6*z*U2;
tau3=-3.1e-6*z*U3;
tau4=-3.1e-6*z*U4;
x=linspace(0,1,100);
g=(r1/R2);
H=(g-(1/2*g^2)+(1/3*g^3));
Y1=abs((-2/sqrt(3))*H*((alpha0/2)*(z^2-R2*z)*KK1.*FF31)*(24*x-12)-(z/R2)*tau1));
Y2=abs((-2/sqrt(3))*H*((alpha0/2)*(z^2-R2*z)*KK2.*FF32)*(24*x-12)-(z/R2)*tau2));
Y3=abs((-2/sqrt(3))*H*((alpha0/2)*(z^2-R2*z)*KK3.*FF33)*(24*x-12)-(z/R2)*tau3));
Y4=abs((-2/sqrt(3))*H*((alpha0/2)*(z^2-R2*z)*KK4.*FF34)*(24*x-12)-(z/R2)*tau4));
YY1=1+Y1./sigma0;
YY2=1+Y2./sigma0;
YY3=1+Y3./sigma0;
YY4=1+Y4./sigma0;
figure(4),plot(YY1,x,YY2,x,'o-',YY3,x,'- ',YY4,x,'-')
grid on
legend('U=0.2 m/s','U=0.4 m/s','U=0.6 m/s','U=0.8 m/s')
figure(5),plot(x,YY1,x,YY2,'o-',x,YY3,'- ',x,YY4,'-')
grid on
legend('U=0.2 m/s','U=0.4 m/s','U=0.6 m/s','U=0.8 m/s')
u1=.2;
u2=.4;
u3=.6;
u4=.8;
delтта1=.5;
delтта= .5;
u=5;
t=linspace(0,1,100);
eta1=(C1+C2-beta4*(1-0.5*gama)-beta3*gama-gama2*beta2*(1-0.5*gama)-beta4*(1-0.5*gama));
Eta1=eta1./([1-pi*([(D0/L)-delтта1]])*(beta8*beta));
eta2=[((n3^4*pi^4)-(3*sqrt(delta)*u.^2-beta+gama1*(1-0.5*gama))+beta5*(1-0.5*gama))*(n3^2*pi^2 + Kb)];
Eta2=eta2./([1-pi*([(D0/L)-delтта1]])*(beta8*beta));
alpha1=[(Eta1./2+i*sqrt(Eta2-Eta1.^2./4))]
alpha2=[(Eta1./2-i*sqrt(Eta2-Eta1.^2./4))];
H31=(1./(alpha1.*alpha2));
HH31=((alpha1.*exp(-alpha2*t))-(alpha2.*exp(-alpha1*t)));
GG3=(1./(alpha1.*alpha2)).*(alpha2-alpha1));
F3=(H31+(GG3.*HH31));

```

```

K1=((pi*[(D0/L)-deltta1]).*([(beta8*g*(h/L))-((0.2^2*alpha0*0.03*deltta1*u1)/(2*0.02))]);
K2=((pi*[(D0/L)-deltta1]).*([(beta8*g*(h/L))-((0.2^2*alpha0*0.03*deltta1*u2)/(2*0.02))]);
K3=((pi*[(D0/L)-deltta1]).*([(beta8*g*(h/L))-((0.2^2*alpha0*0.03*deltta1*u3)/(2*0.02))]);
K4=((pi*[(D0/L)-deltta1]).*([(beta8*g*(h/L))-((0.2^2*alpha0*0.03*deltta1*u4)/(2*0.02))]);
KK1=K1./([1-pi*[(D0/L)-deltta1]]*(beta8*beta));
KK2=K2./([1-pi*[(D0/L)-deltta1]]*(beta8*beta));
KK3=K3./([1-pi*[(D0/L)-deltta1]]*(beta8*beta));
KK4=K4./([1-pi*[(D0/L)-deltta1]]*(beta8*beta));
tau1=-3.1e-6*z*u;
tau2=-3.1e-6*z*u;
tau3=-3.1e-6*z*u;
tau4=-3.1e-6*z*u;
x=1;
g=(r1/R2);
H=(g-(1/2*g^2)+(1/3*g^3));
Y1=abs((-2/sqrt(3)*H*((alpha0/2)*(z^2-R2*z)*KK1.*F3)*(24*x-12)-(z/R2)*tau1));
Y2=abs((-2/sqrt(3)*H*((alpha0/2)*(z^2-R2*z)*KK2.*F3)*(24*x-12)-(z/R2)*tau2));
Y3=abs((-2/sqrt(3)*H*((alpha0/2)*(z^2-R2*z)*KK3.*F3)*(24*x-12)-(z/R2)*tau3));
Y4=abs((-2/sqrt(3)*H*((alpha0/2)*(z^2-R2*z)*KK4.*F3)*(24*x-12)-(z/R2)*tau4));
YY1=1+Y1./sigma0;
YY2=1+Y2./sigma0;
YY3=1+Y3./sigma0;
YY4=1+Y4./sigma0;
figure(7),plot(t,YY1,t,YY2,'o-',t,YY3,'-.*',t,YY4,'.-')
grid on
legend('u=0.2','u=0.4','u=0.6','u=0.8')
n1=1;
u1=.2;
deltta1=.5;
deltta= .5;
t=linspace(0,1.5,100);
xi=t;
yi=linspace(0,1,100);
[xxi,yyi]=meshgrid(xi,yi);
eta1=(C1+C2-beta4*(1-0.5*gama)-beta3*gama-gama2*beta2*(1-0.5*gama)-beta4*(1-0.5*gama));
Eta1=eta1./([1-pi*[(D0/L)-deltta1]]*(beta8*beta));
eta2=[((n3^4*pi^4)-((3*sqrt(delta)*u.^2-beta+gama1*(1-0.5*gama))+beta5*(1-0.5*gama))*(n3^2*pi^2) + Kb)];
Eta2=eta2./([1-pi*[(D0/L)-deltta1]]*(beta8*beta));
alpha1=[(Eta1./2+i*sqrt(Eta2-Eta1.^2./4))]

```

```

alpha2=[(Eta1./2-i*sqrt(Eta2-Eta1.^2./4))];
H31=(1./(alpha1.*alpha2));
HH31=((alpha1.*exp(-alpha2*xxi))-(alpha2.*exp(-alpha1 *xxi)));
GG3=(1./((alpha1.*alpha2)).*(alpha2-alpha1));
F3=(H31+(GG3.*HH31));
K1=((pi*[D0/L]-delтта1).*((beta8*g*(h/L))-((0.2^2*alpha0*0.03*delтта1 *u1)/(2*0.02))));
KK1=K1./([1-pi*([D0/L]-delтта1)]*(beta8*beta));
tau1=-3.1e-6*z*u1;
g=(r1/R2);
H=(g-(1/2*g^2)+(1/3*g^3));
Z1=abs((-2/sqrt(3)*H*((alpha0/2)*(z^2+R2*z)*n1^4*pi^4*KK1.*F3).*((([1-2*yyi])./8))-z/R2*tau1));
figure(8),mesh(xxi,yyi,Z1,'Facecolor','white','Edgecolor','green','Facelighting','none','Edgelighting','flat')
delтта1=linspace(0,1,100);
u1=.2;
u2=.4;
u3=.6;
u4=.8;
t=2;
eta1=(C1+C2-beta4*(1-0.5*gama)-beta3*gama-gama2*beta2*(1-0.5*gama)-beta4*(1-0.5*gama));
Eta1=eta1./([1-pi*([D0/L]-delтта1)]*(beta8*beta));
eta2=[((n3^4*pi^4)-((3*sqrt(delta)*u.^2-beta+gama1*(1-0.5*gama))+beta5*(1-0.5*gama))*(n3^2*pi^2) + Kb)];
Eta2=eta2./([1-pi*([D0/L]-delтта1)]*(beta8*beta));
alpha1=[(Eta1./2+i*sqrt(Eta2-Eta1.^2./4))]
alpha2=[(Eta1./2-i*sqrt(Eta2-Eta1.^2./4))];
H31=(1./(alpha1.*alpha2));
HH31=((alpha1.*exp(-alpha2*t))-(alpha2.*exp(-alpha1 *t)));
GG3=(1./((alpha1.*alpha2)).*(alpha2-alpha1));
F3=(H31+(GG3.*HH31));
K1=((pi*[D0/L]-delтта1).*((beta8*g*(h/L))-((0.2^2*alpha0*0.03*delтта1 *u1)/(2*0.02))));
K2=((pi*[D0/L]-delтта1).*((beta8*g*(h/L))-((0.2^2*alpha0*0.03*delтта1 *u2)/(2*0.02))));
K3=((pi*[D0/L]-delтта1).*((beta8*g*(h/L))-((0.2^2*alpha0*0.03*delтта1 *u3)/(2*0.02))));
K4=((pi*[D0/L]-delтта1).*((beta8*g*(h/L))-((0.2^2*alpha0*0.03*delтта1 *u4)/(2*0.02))));
KK1=K1./([1-pi*([D0/L]-delтта1)]*(beta8*beta));
KK2=K2./([1-pi*([D0/L]-delтта1)]*(beta8*beta));
KK3=K3./([1-pi*([D0/L]-delтта1)]*(beta8*beta));
KK4=K4./([1-pi*([D0/L]-delтта1)]*(beta8*beta));
n1=2;
tau1=-3.1e-6*z*u;
tau2=-3.1e-6*z*u;

```

```

tau3=-3.1e-6*z*u;
tau4=-3.1e-6*z*u;
x=.85;
g=(r1/R2);
H=(g-(1/2*g^2)+(1/3*g^3));
Y1=abs((-2/sqrt(3)*H*((alpha0/2)*(z^2-R2*z)*KK1.*F3)*(24*x-12)-(z/R2)*tau1));
Y2=abs((-2/sqrt(3)*H*((alpha0/2)*(z^2-R2*z)*KK2.*F3)*(24*x-12)-(z/R2)*tau2));
Y3=abs((-2/sqrt(3)*H*((alpha0/2)*(z^2-R2*z)*KK3.*F3)*(24*x-12)-(z/R2)*tau3));
Y4=abs((-2/sqrt(3)*H*((alpha0/2)*(z^2-R2*z)*KK4.*F3)*(24*x-12)-(z/R2)*tau4));
YY1=1+Y1./sigma0;
YY2=1+Y2./sigma0;
YY3=1+Y3./sigma0;
YY4=1+Y4./sigma0;
figure(9),plot(delta1,YY1,'go-',delta1,YY2,'o-',delta1,YY3,'-* ',delta1,YY4,'.-')
grid on
legend('u=0.2','u=0.4','u=0.6','u=0.8')
u1=0.2;
t=linspace(0,2,100);
xi=t;
yi=linspace(0,1,100);
[xxi,yyi]=meshgrid(xi,yi);
eta1=(C1+C2-beta4*(1-0.5*gama)-beta3*gama-gama2*beta2*(1-0.5*gama)-beta4*(1-0.5*gama));
Eta1=eta1./([1-pi*([(D0/L)-yyi]])*(beta8*beta));
eta2=[((n3^4*pi^4)-(3*sqrt(delta)*u.^2-beta+gama1*(1-0.5*gama))+beta5*(1-0.5*gama))*(n3^2*pi^2 + Kb)];
Eta2=eta2./([1-pi*([(D0/L)-yyi]])*(beta8*beta));
alpha1=[(Eta1./2+i*sqrt(Eta2-Eta1.^2./4))]
alpha2=[(Eta1./2-i*sqrt(Eta2-Eta1.^2./4))];
H31=(1./(alpha1.*alpha2));
HH31=((alpha1.*exp(-alpha2*xxi))-(alpha2.*exp(-alpha1*xxi)));
GG3=(1./((alpha1.*alpha2)).*(alpha2-alpha1));
F3=abs(H31+(GG3.*HH31));
K1=((pi*[(D0/L)-yyi]).*([(beta8*g*(h/L))-((0.2^2*alpha0*0.03*yyi*u1)/(2*0.02))]);
KK1=K1./([1-pi*([(D0/L)-yyi]])*(beta8*beta));
tau1=-3.1e-6*z*u1;
g=(r1/R2);
H=(g-(1/2*g^2)+(1/3*g^3));
Y1=(-2/sqrt(3)*H*((alpha0/2)*(z^2-R2*z)*KK1.*F3).*(24*yyi-12)-z/R2*tau1);
Z1=1+Y1./sigma0;
figure(10),mesh(xxi,yyi,Z1,'Facecolor','white','Edgecolor','blue','Facelighting','none','Edgelighting','flat')

```

```

n3=1;
r1=0.2;
z=1;
u=5;
delta=.5;
t=1;
D0=0.4064;
D1=0.394;
R2=(D1/(2*L));
delтта1=0.25;
eta1=(C1+C2-beta4*(1-0.5*gama)-beta3*gama-gama2*beta2*(1-0.5*gama)-beta4*(1-0.5*gama));
Eta1=eta1./([1-pi*([(D0/L)-delтта1]])*(beta8*beta));
eta2=[((n3^4*pi^4)-((3*sqrt(delta)*u.^2-beta+gama1*(1-0.5*gama))+beta5*(1-0.5*gama))*(n3^2*pi^2) + Kb)];
Eta2=eta2./([1-pi*([(D0/L)-delтта1]])*(beta8*beta));
alpha1=[(Eta1./2+i*sqrt(Eta2-Eta1.^2./4))];
alpha2=[(Eta1./2-i*sqrt(Eta2-Eta1.^2./4))];
H31=(1./(alpha1.*alpha2));
HH31=((alpha1*exp(-alpha2*t))-(alpha2*exp(-alpha1*t)));
FF31=(1./((alpha1.*alpha2)).*(alpha2-alpha1));
delтта2=0.50;
eta1=(C1+C2-beta4*(1-0.5*gama)-beta3*gama-gama2*beta2*(1-0.5*gama)-beta4*(1-0.5*gama));
Eta1=eta1./([1-pi*([(D0/L)-delтта2]])*(beta8*beta));
eta2=[((n3^4*pi^4)-((3*sqrt(delta)*u.^2-beta+gama1*(1-0.5*gama))+beta5*(1-0.5*gama))*(n3^2*pi^2) + Kb)];
Eta2=eta2./([1-pi*([(D0/L)-delтта2]])*(beta8*beta));
alpha1=[(Eta1./2+i*sqrt(Eta2-Eta1.^2./4))];
alpha2=[(Eta1./2-i*sqrt(Eta2-Eta1.^2./4))];
H31=(1./(alpha1.*alpha2));
HH31=((alpha1*exp(-alpha2*t))-(alpha2*exp(-alpha1*t)));
FF32=(1./((alpha1.*alpha2)).*(alpha2-alpha1))
delтта3=0.75;
eta1=(C1+C2-beta4*(1-0.5*gama)-beta3*gama-gama2*beta2*(1-0.5*gama)-beta4*(1-0.5*gama));
Eta1=eta1./([1-pi*([(D0/L)-delтта3]])*(beta8*beta));
eta2=[((n3^4*pi^4)-((3*sqrt(delta)*u.^2-beta+gama1*(1-0.5*gama))+beta5*(1-0.5*gama))*(n3^2*pi^2) + Kb)];
Eta2=eta2./([1-pi*([(D0/L)-delтта3]])*(beta8*beta));
alpha1=[(Eta1./2+i*sqrt(Eta2-Eta1.^2./4))];
alpha2=[(Eta1./2-i*sqrt(Eta2-Eta1.^2./4))];
H31=(1./(alpha1.*alpha2));
HH31=((alpha1*exp(-alpha2*t))-(alpha2*exp(-alpha1*t)));

```

```

FF33=(1./((alpha1.*alpha2)).*(alpha2-alpha1));
deltta4=0.999;
eta1=(C1+C2-beta4*(1-0.5*gama)-beta3*gama-gama2*beta2*(1-0.5*gama)-beta4*(1-0.5*gama));
Eta1=eta1./([1-pi*[(D0/L)-deltta4]]*(beta8*beta));
eta2=[((n3^4*pi^4)-((3*sqrt(delta)*u.^2-beta+gama1*(1-0.5*gama))+beta5*(1-0.5*gama))*(n3^2*pi^2) + Kb)];
Eta2=eta2./([1-pi*[(D0/L)-deltta4]]*(beta8*beta));
alpha1=[(Eta1./2+i*sqrt(Eta2-Eta1.^2./4))];
alpha2=[(Eta1./2-i*sqrt(Eta2-Eta1.^2./4))];
H31=(1./(alpha1.*alpha2));
HH31=((alpha1*exp(-alpha2*t))-(alpha2*exp(-alpha1*t)));
FF33=(1./((alpha1.*alpha2)).*(alpha2-alpha1));
K1=((pi*[(D0/L)-deltta1]).*([(beta8*g*(h/L))-((0.2^2*alpha0*0.03*deltta1*u1)/(2*0.02))]);
K2=((pi*[(D0/L)-deltta2]).*([(beta8*g*(h/L))-((0.2^2*alpha0*0.03*deltta2*u2)/(2*0.02))]);
K3=((pi*[(D0/L)-deltta3]).*([(beta8*g*(h/L))-((0.2^2*alpha0*0.03*deltta3*u3)/(2*0.02))]);
K4=((pi*[(D0/L)-deltta4]).*([(beta8*g*(h/L))-((0.2^2*alpha0*0.03*deltta4*u4)/(2*0.02))]);
KK1=K1./([1-pi*[(D0/L)-deltta1]]*(beta8*beta));
KK2=K2./([1-pi*[(D0/L)-deltta2]]*(beta8*beta));
KK3=K3./([1-pi*[(D0/L)-deltta3]]*(beta8*beta));
KK4=K4./([1-pi*[(D0/L)-deltta4]]*(beta8*beta));
tau1=-3.1e-6*z*u;
tau2=-3.1e-6*z*u;
tau3=-3.1e-6*z*u;
tau4=-3.1e-6*z*u;
L=linspace(0,10,100);
g=(r1/R2);
H31=(1./(alpha1.*alpha2));
HH31=((alpha1.*exp(-alpha2*t))-(alpha2.*exp(-alpha1*t)));
GG3=(1./((alpha1.*alpha2)).*(alpha2-alpha1));
F3=(H31+(GG3.*HH31));
H=(g-(1/2*g^2)+(1/3*g^3));
Y1=abs((-2/sqrt(3)*H*((alpha0/2)*(z^2-R2*z)*KK1.*F3)*(24*L-12)-(z/R2)*tau1));
Y2=abs((-2/sqrt(3)*H*((alpha0/2)*(z^2-R2*z)*KK2.*F3)*(24*L-12)-(z/R2)*tau2));
Y3=abs((-2/sqrt(3)*H*((alpha0/2)*(z^2-R2*z)*KK3.*F3)*(24*L-12)-(z/R2)*tau3));
Y4=abs((-2/sqrt(3)*H*((alpha0/2)*(z^2-R2*z)*KK4.*F3)*(24*L-12)-(z/R2)*tau3));
YY1=1+Y1./sigma0;
YY2=1+Y2./sigma0;
YY3=1+Y3./sigma0;
YY4=1+Y4./sigma0;
figure(11),plot(L,YY1,'go-',L,YY2,'o-',L,YY3,'- ',L,YY4,'mo-.')

```

```

grid on
legend('\delta_s=0.25D_0','\delta_s=0.50D_0','\delta_s=0.75D_0','\delta_s=D_0')
delttal=linspace(0,1,100);
L=6;
u=3;
u1=.2;
u2=.4;
u3=.6;
u4=.8;
t=1;
z=1;
n3=1;
x=1;
delta=0.5;
D0=0.4064;
D1=0.394;
R2=(D1/(2*L));
eta1=(C1+C2-beta4*(1-0.5*gama)-beta3*gama-gama2*beta2*(1-0.5*gama)-beta4*(1-0.5*gama));
Eta1=eta1./([1-pi*([(D0/L)-delttal]])*(beta8*beta));
eta2=[((n3^4*pi^4)-((3*sqrt(delta)*u.^2-beta+gama1*(1-0.5*gama))+beta5*(1-0.5*gama))*(n3^2*pi^2 + Kb)];
Eta2=eta2./([1-pi*([(D0/L)-delttal]])*(beta8*beta));
alpha1=[(Eta1./2+i*sqrt(Eta2-Eta1.^2./4))]
alpha2=[(Eta1./2-i*sqrt(Eta2-Eta1.^2./4))];
H31=(1./(alpha1.*alpha2));
HH31=((alpha1.*exp(-alpha2*t))-(alpha2.*exp(-alpha1*t)));
GG3=(1./((alpha1.*alpha2)).*(alpha2-alpha1));
F3=(H31+(GG3.*HH31));
K1=((pi*[(D0/L)-delttal]).*([(beta8*g*(h/L))-((0.2^2*alpha0*0.03*delttal*u1)/(2*0.02))]);
K2=((pi*[(D0/L)-delttal]).*([(beta8*g*(h/L))-((0.2^2*alpha0*0.03*delttal*u2)/(2*0.02))]);
K3=((pi*[(D0/L)-delttal]).*([(beta8*g*(h/L))-((0.2^2*alpha0*0.03*delttal*u3)/(2*0.02))]);
K4=((pi*[(D0/L)-delttal]).*([(beta8*g*(h/L))-((0.2^2*alpha0*0.03*delttal*u4)/(2*0.02))]);
KK1=K1./([1-pi*([(D0/L)-delttal]])*(beta8*beta));
KK2=K2./([1-pi*([(D0/L)-delttal]])*(beta8*beta));
KK3=K3./([1-pi*([(D0/L)-delttal]])*(beta8*beta));
KK4=K4./([1-pi*([(D0/L)-delttal]])*(beta8*beta));
n1=2;
tau1=-3.1e-6*z*u;
tau2=-3.1e-6*z*u;
tau3=-3.1e-6*z*u;

```

```

tau4=-3.1e-6*z*u;
g=(r1/R2);
H=(g-(1/2*g^2)+(1/3*g^3));
Y1=abs((-2/sqrt(3)*H*((alpha0/2)*(z^2-R2*z)*KK1.*F3)*(24*x-12)-(z/R2)*tau1));
Y2=abs((-H*((alpha0/2)*(z^2-R2*z)*KK1.*F3)*(24*x-12)-(z/R2)*tau1));
YY1=1+Y1./sigma0;
YY2=1+Y2./sigma0;
Z1=YY1./YY2;
figure(12),plot(delta1,Z1,'go-')
grid on

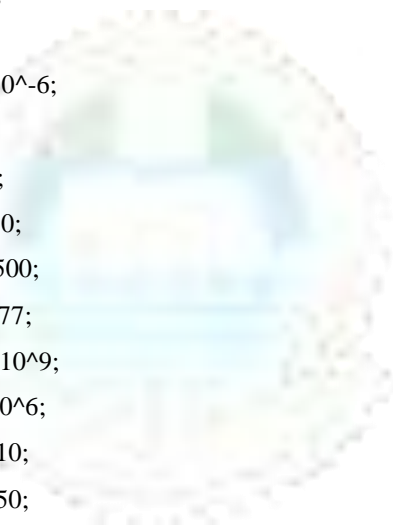
```



UNIVERSITY
OF LAGOS

D.3 Matlab Program for Pipe Sitting on the Seabed (Chapter 5)

```
clc
clear
format long
ti=0.02;
L=2000;
R=0.197;
R1=R/L;
j=0.1*R1;
R0=R1+j;
n=1;
C1=0.2;
Cd=0.1;
y=0.1;
a=1.1*10^-6;
g=10;
h=1000;
rhof=980;
rhop=7500;
rhow=977;
E=207*10^9;
T0=1*10^6;
theta=110;
dtheta=50;
p=1.5e7;
dp=(1/6)*p;
K=10;
k=0.1;
Uw=0.5;
t=50;
v=0.3;
SIGy=4000000;
U=5;
A1=pi*R1^2;
A0=pi*R0^2;
I=1.17e-5;
mf=rhof*A1;
mp=rhop*(A0-A1);
```



UNIVERSITY
OF LAGOS

```

mw=rhow*A0;
m=mp+mf;
M=m+mw;
hb=h/L;
tau=L^2/sqrt(m/E*I);
tb=t/tau;
Ub=U*L*sqrt(mf/(E*I));
R1b=R1/L;
R0b=R0/L;
d=mf/m;
d1=mw/M;
b=T0*L^2/(E*I);
b1=A0*L^2/I;
b2=sqrt(d)/Ub;
b3=a*b1*b2*theta;
b4=a*b1*b2*dtheta;
b5=a*b1*theta;
b6=a*b1*dtheta;
b7=b1/Ub;
b8=d1/L;
C1b=C1*L^2/sqrt(m*E*I);
Cdb=Cd*L^2/sqrt(m*E*I);
gb=M*g*L^3/(E*I);
apr=L^4/I;
rhob=rhof*L^5/(E*I*tau);
Kb=K*L^4/(E*I);
B1=-Uw*coth(k*hb)/k;
x=0.6;
gam=(x/45)-(2*x.^3/9)+(x.^4/3)-(2*x.^5/15);
et1=((C1b+Cdb-b4*(1-y/2)-b3*y-dp*A0*(1-y/2)-b2*p*A0*y)/(1-d1*B1));
et2=((n^4*pi^4-(3*sqrt(d)*Ub.^2-b+b5*(1-y/2)+p*A0*(1-y/2))*n^2*pi^2+Kb)/(1-d1*B1));
a1=((et1/2)-i*sqrt(et2.^2-et1.^2/4));
a2=((et1/2)+i*sqrt(et2.^2-et1.^2/4));
tb=linspace (0,0.01,100);
Ft=(1./(a1.*a2)+(1./(a1.*a2.*(a2-a1))).*(a1.*exp(-a2.*tb)-a2.*exp(-a1.*tb)));
F1t=(a2.*exp(-a2.*tb)-a1.*exp(-a1.*tb))./(a2-a1);
pe=-d1*(((B1*d1*gb*hb)/(1-d1*B1))*n^4*pi^4*gam.*Ft+hb*gb);
rhoar=rhof*((d1*gb*hb)/(1-d1*B1))*n^4*pi^4*gam.*F1t;

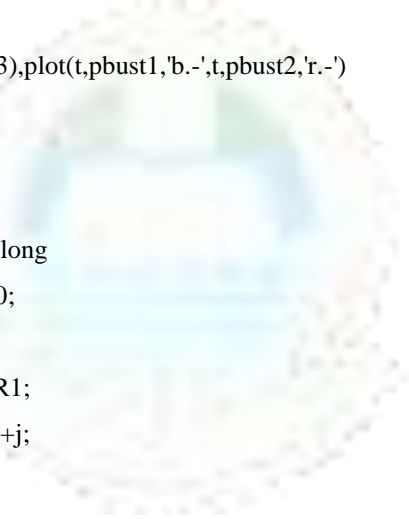
```



```

%D=(1+((2*R0.^2.*(R1.^2+R1.^2*R0.^2))/(R1.^2-R0.^2).^2));
D=(1+((2*R0.^2.*(R1.^2+R1.^2*R0.^2))/(ti.^2*(R1+R0).^2));
%Q=(R0.^2./(R1.^2-R0.^2).^2).*((2/3)*rhoar*((2-v)/(1-v)))-(2*pe.*(R1.^2+3*R0.^2)/(R1.^2-R0.^2));
Q=(R0.^2./(ti.^2*(R1+R0).^2)).*((2/3)*rhoar*((2-v)/(1-v)))-(2*pe.*(R1.^2+3*R0.^2)/(ti*(R1+R0)));
M1=4*pe.*(R0.^2./(-ti*(R1+R0)));
M2=(R0.^2./(R1.^2+R0.^2).^2).*((2/3)*rhoar*((2-v)/(1-v)));
M3=R0.^2./(ti*(R1+R0));
M=M1.*(M3-M2)+M2-SIGy^2;
pbust1=(-Q+sqrt(Q.^2-4*D*M))/(2*D);
pbust2=(-Q-sqrt(Q.^2-4*D*M))/(2*D);
t=tb*tau;
figure(1),plot(t,pbust1,'b.-')
grid
figure(2),plot(t,pbust2,'r.-')
grid
figure(3),plot(t,pbust1,'b.-',t,pbust2,'r.-')
%grid
clc
clear
format long
L=2000;
R1=1;
j=0.1*R1;
R0=R1+j;
n=1;
C1=0.2;
Cd=0.1;
y=0.1;
a=1.1*10^-6;
g=10;
h=1000;
rhof=980;
rhop=7500;
rhow=977;
E=207*10^9;
T0=1*10^6;
theta=110;
dtheta=50;
p=1.5e7;

```

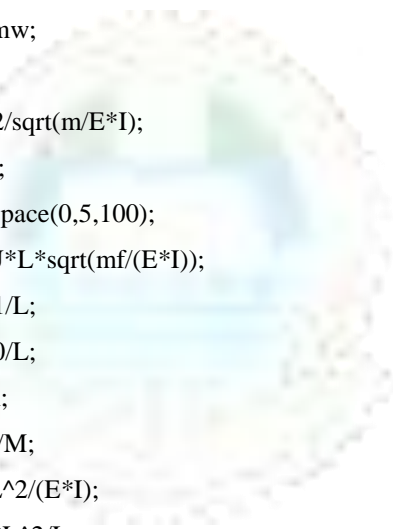


UNIVERSITY
OF LAGOS

```

dp=(1/6)*p;
K=10;
k=0.1;
Uw=0.5;
t=50;
v=0.3;
SIGy=4000000;
A1=pi*R1^2;
A0=pi*R0^2;
I=pi*((2*R0)^4-(2*R1)^4)/64;
mf=rhof*A1;
mp=rhop*(A0-A1);
mw=rhow*A0;
m=mp+mf;
M=m+mw;
hb=h/L;
tau=L^2/sqrt(m/E*I);
tb=t/tau;
Ub=linspace(0.5,100);
%Ub=U*L*sqrt(mf/(E*I));
R1b=R1/L;
R0b=R0/L;
d=mf/m;
d1=mw/M;
b=T0*L^2/(E*I);
b1=A0*L^2/I;
b2=sqrt(d)./Ub;
b3=a*b1*b2*theta;
b4=a*b1*b2*dtheta;
b5=a*b1*theta;
b6=a*b1*dtheta;
b7=b1./Ub;
b8=d1/L;
C1b=C1*L^2/sqrt(m*E*I);
Cdb=Cd*L^2/sqrt(m*E*I);
gb=M*g*L^3/(E*I);
apr=L^4/I;
rhob=rhof*L^5/(E*I*tau);
Kb=K*L^4/(E*I);

```



UNIVERSITY
OF LAGOS

```

B1=-Uw*coth(k*hb)/k;
x=.6; % good results obtained at x= 0.1, 0.2, 0.3, 0.4, 0.6, 0.7, 0.8, 0.9
ti=0.0002;
ti=0.0004;
ti=0.0006;
ti=0.0002;
gam=(x/45)-(2*x.^3/9)+(x.^4/3)-(2*x.^5/15);
et1=((C1b+Cdb-b4*(1-y/2)-b3*y-dp*A0*(1-y/2)-b2*p*A0*y)/(1-d1*B1));
%et1=((C1b+Cdb-b4*(1-y/2)-b3*y)/(1-d1*B1));
et2=(n^4*pi^4-(3*sqrt(d)*Ub.^2-b+b5*(1-y/2)+p*A0*(1-y/2))*n^2*pi^2+Kb)/(1-d1*B1);
%et2=(n^4*pi^4-(3*sqrt(d)*Ub.^2-b+b5*(1-y/2))*n^2*pi^2+Kb)/(1-d1*B1);
a1=(et1/2)-i*sqrt(et2.^2-et1.^2/4);
a2=(et1/2)+i*sqrt(et2.^2-et1.^2/4);
Ft=(1./(a1.*a2)+(1./(a1.*a2.*(a2-a1))).*(a1.*exp(-a2.*tb)-a2.*exp(-a1.*tb)));
F1t=(a2.*exp(-a2.*tb)-a1.*exp(-a1.*tb))./(a2-a1);
pe=-d1*(((B1*d1*gb*hb)/(1-d1*B1))*n^4*pi^4*gam.*Ft+hb*gb);
rhoar=rhof*((d1*gb*hb)/(1-d1*B1))*n^4*pi^4*gam.*F1t;
%D=(1+((2*R0.^2.*(R1.^2+R1.^2*R0.^2))/(R1.^2-R0.^2).^2));
D=(1+((2*R0.^2.*(R1.^2+R1.^2*R0.^2))./(ti.^2*(R1+R0).^2));
%Q=(R0.^2./(R1.^2-R0.^2).^2).*((2/3)*rhoar*((2-v)/(1-v)))-(2*pe.*(R1.^2+3*R0.^2)./(R1.^2-R0.^2));
Q=(R0.^2./(ti.^2*(R1+R0).^2)).*((2/3)*rhoar*((2-v)/(1-v)))-(2*pe.*(R1.^2+3*R0.^2)./(ti*(R1+R0)));
M1=4*pe.*(R0.^2./(-ti*(R1+R0)));
M2=(R0.^2./(R1.^2+R0.^2).^2).*((2/3)*rhoar*((2-v)/(1-v)));
M3=R0.^2./(-ti*(R1+R0));
M=M1.*(M3-M2)+M2-SIGy^2;
pbust1=(-Q+sqrt(Q.^2-4*D.*M))./(2*D));
ti=0.0004;
gam=(x/45)-(2*x.^3/9)+(x.^4/3)-(2*x.^5/15);
et1=((C1b+Cdb-b4*(1-y/2)-b3*y-dp*A0*(1-y/2)-b2*p*A0*y)/(1-d1*B1));
%et1=((C1b+Cdb-b4*(1-y/2)-b3*y)/(1-d1*B1));
et2=(n^4*pi^4-(3*sqrt(d)*Ub.^2-b+b5*(1-y/2)+p*A0*(1-y/2))*n^2*pi^2+Kb)/(1-d1*B1);
%et2=(n^4*pi^4-(3*sqrt(d)*Ub.^2-b+b5*(1-y/2))*n^2*pi^2+Kb)/(1-d1*B1);
a1=(et1/2)-i*sqrt(et2.^2-et1.^2/4);
a2=(et1/2)+i*sqrt(et2.^2-et1.^2/4);
Ft=(1./(a1.*a2)+(1./(a1.*a2.*(a2-a1))).*(a1.*exp(-a2.*tb)-a2.*exp(-a1.*tb)));
F1t=(a2.*exp(-a2.*tb)-a1.*exp(-a1.*tb))./(a2-a1);
pe=-d1*(((B1*d1*gb*hb)/(1-d1*B1))*n^4*pi^4*gam.*Ft+hb*gb);
rhoar=rhof*((d1*gb*hb)/(1-d1*B1))*n^4*pi^4*gam.*F1t;

```

```

%D=(1+((2*R0.^2.*(R1.^2+R1.^2*R0.^2))/(R1.^2-R0.^2).^2));
D1=(1+((2*R0.^2.*(R1.^2+R1.^2*R0.^2))/(ti.^2*(R1+R0).^2));
%Q=(R0.^2./(R1.^2-R0.^2).^2).*((2/3)*rhoar*((2-v)/(1-v)))-(2*pe.*(R1.^2+3*R0.^2)/(R1.^2-R0.^2));
Q1=(R0.^2./(ti.^2*(R1+R0).^2)).*((2/3)*rhoar*((2-v)/(1-v)))-(2*pe.*(R1.^2+3*R0.^2)/(ti*(R1+R0)));
M11=4*pe.*(R0.^2./(-ti*(R1+R0)));
M21=(R0.^2./(R1.^2+R0.^2).^2).*((2/3)*rhoar*((2-v)/(1-v)));
M31=R0.^2./(ti*(R1+R0));
M1=M11.*(M31-M21)+M21-SIGy^2;
pbust2=(-Q1+sqrt(Q1.^2-4*D1.*M1))./(2*D1);
ti=0.0006;
gam=(x/45)-(2*x.^3/9)+(x.^4/3)-(2*x.^5/15);
et1=((C1b+Cdb-b4*(1-y/2)-b3*y-dp*A0*(1-y/2)-b2*p*A0*y)/(1-d1*B1));
%et1=((C1b+Cdb-b4*(1-y/2)-b3*y)/(1-d1*B1));
et2=(n^4*pi^4-(3*sqrt(d)*Ub.^2-b+b5*(1-y/2)+p*A0*(1-y/2))*n^2*pi^2+Kb)/(1-d1*B1);
%et2=(n^4*pi^4-(3*sqrt(d)*Ub.^2-b+b5*(1-y/2))*n^2*pi^2+Kb)/(1-d1*B1);
a1=(et1/2)-i*sqrt(et2.^2-et1.^2/4);
a2=(et1/2)+i*sqrt(et2.^2-et1.^2/4);
Ft=(1./(a1.*a2)+(1./(a1.*a2.*(a2-a1))).*(a1.*exp(-a2.*tb)-a2.*exp(-a1.*tb)));
F1t=(a2.*exp(-a2.*tb)-a1.*exp(-a1.*tb))./(a2-a1);
pe=-d1*(((B1*d1*gb*hb)/(1-d1*B1))*n^4*pi^4*gam.*Ft+hb*gb);
rhoar=rhof*((d1*gb*hb)/(1-d1*B1))*n^4*pi^4*gam.*F1t;
%D=(1+((2*R0.^2.*(R1.^2+R1.^2*R0.^2))/(R1.^2-R0.^2).^2));
D2=(1+((2*R0.^2.*(R1.^2+R1.^2*R0.^2))/(ti.^2*(R1+R0).^2));
%Q=(R0.^2./(R1.^2-R0.^2).^2).*((2/3)*rhoar*((2-v)/(1-v)))-(2*pe.*(R1.^2+3*R0.^2)/(R1.^2-R0.^2));
Q2=(R0.^2./(ti.^2*(R1+R0).^2)).*((2/3)*rhoar*((2-v)/(1-v)))-(2*pe.*(R1.^2+3*R0.^2)/(ti*(R1+R0)));
M12=4*pe.*(R0.^2./(-ti*(R1+R0)));
M22=(R0.^2./(R1.^2+R0.^2).^2).*((2/3)*rhoar*((2-v)/(1-v)));
M32=R0.^2./(ti*(R1+R0));
M2=M12.*(M32-M22)+M22-SIGy^2;
pbust3=(-Q2+sqrt(Q2.^2-4*D2.*M2))./(2*D2);
ti=0.0008;
gam=(x/45)-(2*x.^3/9)+(x.^4/3)-(2*x.^5/15);
et1=((C1b+Cdb-b4*(1-y/2)-b3*y-dp*A0*(1-y/2)-b2*p*A0*y)/(1-d1*B1));
%et1=((C1b+Cdb-b4*(1-y/2)-b3*y)/(1-d1*B1));
et2=(n^4*pi^4-(3*sqrt(d)*Ub.^2-b+b5*(1-y/2)+p*A0*(1-y/2))*n^2*pi^2+Kb)/(1-d1*B1);
%et2=(n^4*pi^4-(3*sqrt(d)*Ub.^2-b+b5*(1-y/2))*n^2*pi^2+Kb)/(1-d1*B1);
a1=(et1/2)-i*sqrt(et2.^2-et1.^2/4);
a2=(et1/2)+i*sqrt(et2.^2-et1.^2/4);
Ft=(1./(a1.*a2)+(1./(a1.*a2.*(a2-a1))).*(a1.*exp(-a2.*tb)-a2.*exp(-a1.*tb)));

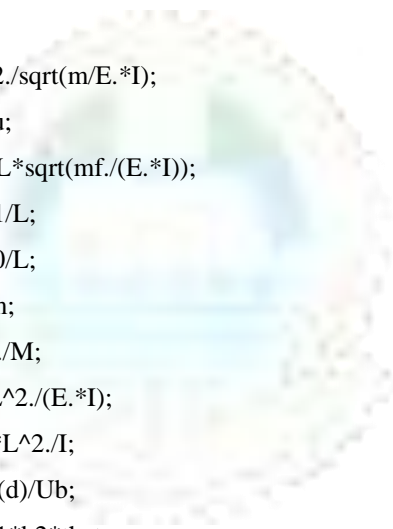
```

```

F1t=(a2.*exp(-a2.*tb)-a1.*exp(-a1.*tb))./(a2-a1);
pe=-d1*(((B1*d1*gb*hb)/(1-d1*B1))*n^4*pi^4*gam.*Ft+hb*gb);
rhoar=rhof*((d1*gb*hb)/(1-d1*B1))*n^4*pi^4*gam.*F1t;
%D=(1+((2*R0.^2.*(R1.^2+R1.^2*R0.^2))/(R1.^2-R0.^2).^2));
D3=(1+((2*R0.^2.*(R1.^2+R1.^2*R0.^2))./(ti.^2*(R1+R0).^2)));
%Q=(R0.^2./(R1.^2-R0.^2).^2).*((2/3)*rhoar*((2-v)/(1-v)))-(2*pe.*(R1.^2+3*R0.^2)./(R1.^2-R0.^2));
Q3=(R0.^2./(ti.^2*(R1+R0).^2)).*((2/3)*rhoar*((2-v)/(1-v)))-(2*pe.*(R1.^2+3*R0.^2)./(ti*(R1+R0)));
M13=4*pe.*(R0.^2./(-ti*(R1+R0)));
M23=(R0.^2./(R1.^2+R0.^2).^2).*((2/3)*rhoar*((2-v)/(1-v)));
M33=R0.^2./(ti*(R1+R0));
M3=M13.*(M33-M23)+M23-SIGy^2;
pbust4=(-Q3+sqrt(Q3.^2-4*D3.*M3))./(2*D3);
figure(4),plot(Ub,pbust1,'b.-',Ub,pbust2,'go-',Ub,pbust3,'o-',Ub,pbust4,'r.-')
grid
legend('ti=0.002','ti=0.004','ti=0.006','ti=0.008')
%figure(5),plot(x,YY1,'go-',x,YY2,'o-',x,YY3,'- ',x,YY4,'mo.-')
clc
clear
L=2000;
ti=0.002;
R1=1;
R0=1.1*R1;
n=1;
C1=0.2;
Cd=0.1;
y=0.1;
a=1.1*10^-6;
g=10;
h=1000;
rhof=980;
rhop=7500;
rhow=977;
E=207*10^9;
T0=1*10^6;
theta=110;
dtheta=50;
p=1.5e7;
dp=(1/6)*p;
U=5;

```

$K=10;$
 $k=0.1;$
 $U_w=0.5;$
 $t=5;$
 $v=0.3;$
 $SIG_y=4000000;$
 $A_1=\pi*R_1.^2;$
 $A_0=\pi*R_0.^2;$
 $I=\pi*((2*R_0).^4-(2*R_1).^4)/64;$
 $mf=rhof*A_1;$
 $mp=rhop*(A_0-A_1);$
 $mw=rhow*A_0;$
 $m=mp+mf;$
 $M=m+mw;$
 $hb=h/L;$
 $\tau=L^2./\sqrt{m/E.*I};$
 $tb=t./\tau;$
 $U_b=U*L*\sqrt{mf./(E.*I)};$
 $R_{1b}=R_1/L;$
 $R_{0b}=R_0/L;$
 $d=mf/m;$
 $d_1=mw./M;$
 $b=T_0*L^2./(E.*I);$
 $b_1=A_0*L^2./I;$
 $b_2=\sqrt{d}/U_b;$
 $b_3=a*b_1*b_2*\theta;$
 $b_4=a*b_1*b_2*d\theta;$
 $b_5=a*b_1*\theta;$
 $b_6=a*b_1*d\theta;$
 $b_7=b_1./U_b;$
 $b_8=d_1/L;$
 $C_{1b}=C_1*L^2./\sqrt{m.*E.*I};$
 $C_{db}=C_d*L^2./\sqrt{m.*E.*I};$
 $g_b=M*g*L^3/(E*I);$
 $apr=L^4./I;$
 $\rho_{hb}=rhof*L^5./(E.*I.*\tau);$
 $K_b=K*L^4./(E.*I);$
 $B_1=-U_w*\coth(k*hb)/k;$



UNIVERSITY
OF LAGOS

```

x=linspace(0,5,100);
gam=(x/45)-(2*x.^3/9)+(x.^4/3)-(2*x.^5/15);
et1=((C1b+Cdb-b4*(1-y/2)-b3*y-dp*A0*(1-y/2)-b2*p*A0*y)/(1-d1*B1));
et2=(n^4*pi^4-(3*sqrt(d).*Ub.^2-b+b5*(1-y/2)+p*A0*(1-y/2))*n^2*pi^2+Kb)/(1-d1*B1);
a1=(et1/2)-i*sqrt(et2.^2-et1.^2/4);
a2=(et1/2)+i*sqrt(et2.^2-et1.^2/4);
Ft=(1./(a1.*a2)+(1./(a1.*a2.*(a2-a1))).*(a1.*exp(-a2.*tb)-a2.*exp(-a1.*tb)));
F1t=(a2.*exp(-a2.*tb)-a1.*exp(-a1.*tb))/(a2-a1);
pe=-d1.*(((B1*d1*gb*hb)/(1-d1*B1))*n^4*pi^4*gam*Ft+hb*gb);
rhoar=rhof*((d1*gb*hb)/(1-d1*B1))*n^4*pi^4*gam*F1t;
%D=(1+((2*R0.^2.*(R1.^2+R1.^2*R0.^2))/(R1.^2-R0.^2).^2));
D=(1+((2*R0.^2.*(R1.^2+R1.^2*R0.^2))./(ti.^2*(R1+R0).^2));
%Q=(R0.^2./(R1.^2-R0.^2).^2).*((2/3)*rhoar*((2-v)/(1-v)))-(2*pe.*(R1.^2+3*R0.^2)./(R1.^2-R0.^2));
Q=(R0.^2./(ti.^2*(R1+R0).^2)).*((2/3)*rhoar*((2-v)/(1-v)))-(2*pe.*(R1.^2+3*R0.^2)./(ti*(R1+R0)));
M1=4*pe.*(R0.^2./(-ti*(R1+R0)));
M2=(R0.^2./(R1.^2+R0.^2).^2).*((2/3)*rhoar*((2-v)/(1-v)));
M3=R0.^2./(-ti*(R1+R0));
M=M1.*(M3-M2)+M2-SIGy^2;
pbust1=(-Q+sqrt(Q.^2-4*D.*M))./(2*D));
pbust2=(-Q-sqrt(Q.^2-4*D.*M))./(2*D));
figure(6),plot(x,pbust1,'bo-')
%axis[0.01 0.1 0 4e5]

```

